BERICHTE
aus dem Fachbereich Geowissenschaften
der Universität Bremen

No. 189

Esper, O.

RECONSTRUCTION OF RECENT AND LATE QUATERNARY OCEANOGRAPHIC CONDITIONS IN THE EASTERN SOUTH ATLANTIC OCEAN BASED ON CALCAREOUS- AND ORGANIC-WALLED DINOFLAGELLATE CYSTS

Berichte, Fachbereich Geowissenschaften, Universität Bremen, No. 189,
130 pages, Bremen 2001

ISSN 0931-0800

Summary

In the last decades it has become apparent that climatic change is greatly influenced by changes in the global ocean circulation. One of the most important current systems is the thermohaline circulation of the Atlantic Ocean, responsible for the interhemispheric heat exchange. This current system transports cold, higher saline deep water from the northern Atlantic Ocean to the southern hemisphere and in return warmer waters of the South Atlantic Ocean to the north, positively influencing the northern continental climate. To understand the fluctuations in the heat transport through glacial/interglacial cycles in the Late Quaternary, it is necessary to study several key areas. One of such areas is the south-eastern South Atlantic Ocean, where warmer Indian Ocean (sub)surface water is carried around the cape of South Africa via the Agulhas Current into the Atlantic Ocean. Other important regions along the warm water return path of the Atlantic Ocean are the Benguela upwelling area off south-western Africa and the Equatorial Divergence Zone, were colder, nutrient-rich intermediate water is converted to (sub)surface water by wind driven upwelling, causing high bioproductivity. The main aim of the present study is to reconstruct the palaeoceanographic conditions of this regions for the Late Quaternary. The work is focused on the detection of steering mechanism for the (sub)surface water influx to the Atlantic Ocean, taking place in the region off South Africa, as well as on the main driving forces of northward warm water transport.

Oceanographic and environmental changes can be discovered through the analysis of different constituents of the seafloor sediments. Useful tools are calcareous- and organic-walled dinoflagellate cysts (dinocysts). These proxies are capable of reflecting palaeoecological and palaeoceanographical changes at their time of deposition, in the course of which organic-walled dinocysts are sensitive for other environmental changes than calcareous-walled dinocysts are, complementing one another.

Information on modern organic-walled dinocyst distribution of the South Atlantic Ocean was restricted to the western tropical and eastern subtropical regions, and no information was available so far for the Atlantic sector of the Southern Ocean. To use organic-walled cysts for the detection of Late Quaternary changes in the current system off South Africa, their modern distribution in the central South Atlantic Ocean was analysed in 32 surface sediment samples and brought into relation with the location of the Antarctic Circumpolar Current frontal system. This study revealed a high surface water temperature dependency of the organic-walled dinocyst distribution as well as a strong affinity of some species to frontal environments.

To understand Late Quaternary changes in the complex nexus of three major current systems off South Africa, influencing the warm water transfer from the Indian Ocean to the Atlantic Ocean, a sediment core derived from the south-eastern Cape Basin (GeoB 3603-2) was analysed for its variation in organic- and calcareous-walled dinocyst associations during the last 160,000 years. This study shows strong orbital forcing on the interbasin heat exchange during the Late Quaternary. A dominant precessional forcing on palaeoproductivity with high productivity at times of high seasonal contrast as

well as the establishment of stratified, oligo- to mesotrophic environmental conditions at times of low seasonal contrast, notably during the glacial Terminations, is assumed. In addition, periodicities on a sub-Milankovitch scale as well as modulations of the primary frequencies suggest complex interactions between the subtropical region around Africa and the high latitudes.

To use calcareous dinoflagellate cysts in reconstructing orbital and sub-orbital changes in the eastern subtropical and equatorial South Atlantic Ocean palaeoceanography during the last two glacial/interglacial-cycles (the past 150,000 years), several cores were analysed in detail for their calcareous-walled dinocyst content. The results were compared with other known proxies of the respective cores and regions. This study reconstructs generally weakened surface currents along the warm water path of the thermohaline circulation at the Terminations. Additionally, reduced upwelling in the Benguela and Equator Divergence regions due to a dominant meridional component of the south-eastern trade winds at times of minimum precession is assumed. Under the assumption of reduced or blocked cross-equatorial heat transport at the Terminations, this would have led to the build-up of a heat depot in the South Atlantic Ocean subtropical regions.

Although a lot of research has to be done on the development of dinocysts as reliable palaeoceanographic proxy, especially concerning the preservation of calcareous-walled dinocysts, this work shows the good applicability of both dinocyst groups for detecting orbital forcing on palaeoenvironmental and palaeoceanographical changes.

Zusammenfassung

In den letzten Jahrzehnten wurde der Einfluss von Veränderungen in der globalen Ozeanzirkulation auf Klimaschwankungen immer offensichtlicher. Eines der bedeutendsten Strömungssysteme ist die Thermohaline Zirkulation des Atlantiks, welche für den Wärmeaustausch zwischen den Hemisphären sorgt. Dieses Strömungssystem transportiert kaltes, hochsalines Tiefenwasser vom Nordatlantik zur südlichen Hemisphäre, um im Gegenzug warme Südatlantik-Wässer nach Norden zu führen und so das Klima der Nordkontinente positiv zu beeinflussen. Um die Schwankungen im Wärmetransport während spätquartärer Glazial-/Interglazial-Zyklen zu verstehen, ist es notwendig, ausgesuchte Schlüsselgebiete zu untersuchen. Eines jener Gebiete ist der südöstliche Südatlantik, wo warme Oberflächenwässer des Indischen Ozeans über den Agulhas-Strom um das Kap von Südafrika herum in den Atlantik gleitet werden. Weitere wichtige Gebiete entlang der atlantischen Rückfluss-Route des warmen Wassers sind das Benguela-Auftriebsgebiet vor dem südwestlichen Afrika und die äquatoriale Divergenzzone, in welchen kalte, nährstoffreiche Zwischenwassermassen durch windinduzierten Auftrieb in Oberflächenwässer konvertiert werden und zu hoher Bioproduktion in diesen Gebieten führen. Hauptziel der vorliegenden Arbeit ist die Rekonstruktion spätquartärer paläozeanographischer Bedingungen in diesen Gebieten. Die Arbeit konzentriert sich auf die Feststellung von Steuerungsmechanismen des Oberflächenwasser-Einstroms in den Atlantik im Gebiet südlich vor Afrika, sowie der antreibenden Kräften des Warmwassertransports nordwärts.

Änderungen in Ozeanographie und Umweltbedingungen können durch die Analyse verschiedenster Sedimentpartikel des Meeresbodens angezeigt werden. Als hilfreiche Werkzeuge haben sich organisch-wandige und kalkwandige Dinoflagellatenzysten (Dinozysten) herausgestellt. Diese Hilfsmittel sind dazu in der Lage, Veränderungen der Palökologie und Paläozeanographie zum Zeitpunkt ihrer Ablagerung widerzuspiegeln, wobei organisch-wandige und kalkwandige Dinozysten unterschiedliche Sensibilität gegenüber verschiedenen Milieuänderungen besitzen, sich dabei aber ergänzen.

Informationen über die Verteilung moderner organisch-wandiger Dinozysten des Südatlantiks waren bisher auf Gebiete der westlichen Tropen und der östlichen Subtropen beschränkt, für den Atlantiksektor des Südozeans lagen jedoch keine Informationen vor. Um dennoch organisch-wandige Dinozysten zum Aufspüren spätquartärer Veränderungen im Strömungssystem vor Südafrika zu nutzen, wurde deren Verteilung in 32 Sedimentoberflächenproben des zentralen Südatlantiks bearbeitet und in Beziehung zur heutigen Position des Frontensystems im antarktischen Zirkumpolarstrom gesetzt. Diese Studie zeigte eine hohe Temperaturabhängigkeit der Zystenverteilung, sowie eine starke Affinität einiger Arten zu Frontmilieus auf.

Um spätquartäre Veränderungen am komplexen Nexus der drei großen Strömungssysteme vor Südafrika zu verstehen, welche den Warmwassertransfer vom Indischen Ozean zum Südatlantik beeinflussen, wurde ein Sedimentkern aus dem südöstlichen Kapbecken (GeoB 3603-2) auf

Veränderungen der organisch-wandigen und kalkigen Dinozysten-Assoziationen während der letzten 160.000 Jahre hin untersucht. Diese Studie zeigte einen starken orbitalen Einfluss auf den spätquartären Wärmeaustausch zwischen den Ozeanbecken. Es wird ein dominanter Einfluss der Präzession auf die Paläoproduktivität, mit Hochproduktion in Zeiten starken saisonalen Kontrastes und der Ausbildung stratifizierter, oligo- bis mesotropher Milieubedingungen in Zeiten geringen saisonalen Kontrastes, speziell während der glazialen Terminationen, angenommen. Zusätzlich deuten Periodizitäten im sub-Milankovitch-Bereich, ebenso wie Modulationen der Primärfrequenzen, auf komplexe Beziehungen zwischen den Subtropen und den hohen Breiten hin.

Um mittels kalkiger Dinozysten orbital und sub-orbital gesteuerte Veränderungen der Paläozeanographie in den östlichen Subtropen und im äquatorialen Atlantik während der letzten beiden Glazial-/Interglazial-Zyklen (die letzten 150.000 Jahre) zu rekonstruieren, wurden mehrere Sedimentkerne detailliert auf ihren Dinozysten-Inhalt hin untersucht. Die Ergebnisse wurden mit Resultaten anderer bekannter paläozeanographischer Hilfsmitteln aus den gleichen Kernen oder der gleichen Region verglichen. Die Ergebnisse dieser Studie deuten auf generell schwächere Oberflächenströmungen entlang der Warmwasserroute der thermohaline Zirkulation an den Terminationen hin. Zusätzlich wird reduzierter Auftrieb in den Gebieten des Benguela und der äquatorialen Divergenz angenommen, was auf eine Dominanz der meridionalen Komponente der Südost-Passate zu Zeiten minimaler Präzession zurückzuführen ist. Unter der Annahme reduzierten oder gar verebbten Wärmetransports über den Äquator, würde solch eine Situation zum Aufbau eines Wärmedepots in den Subtropen des Südatlantiks geführt haben.

Obwohl noch einiges zur Entwicklung der Dinozysten als zuverlässigem Hilfsmittel in der Paläozeanographie getan werden muss, speziell in Hinsicht auf die Erhaltung kalkiger Dinozysten, zeigt die vorliegende Arbeit eine gute Anwendbarkeit beider Dinozysten-Gruppen zum Nachweis orbitaler Einflüsse auf Veränderungen im Paläomilieu und der Paläozeanographie.

Contents

1. Introduction

1.1. Motivation and main objectives

Since the Early Pleistocene, earth's climate is characterised by cyclic changes of cold (glacial) and warm (interglacial) periods (e.g. Wefer et al., 1996a). To understand global climatic changes in the Late Pleistocene, one main field of interest is focused on the interaction between atmosphere and hydrosphere. The Atlantic Ocean nowadays is an area of inter-ocean heat exchange and, therefore, a major factor in global climate control (e.g. Wefer et al., 1996a). Within the so called thermohaline circulation a deep and upper-level current system transports cold, high saline deep water from the northern hemisphere to the southern hemisphere and in return carries warm (sub)surface water from the southern hemisphere back to the North Atlantic Ocean (Fig. 1; Gordon, 1986). In the North Atlantic Ocean the entrained heat energy is transferred to the atmosphere by evaporation, thereby positively influencing the climate of the northern continents. Although the heat-transfer seems to be of major impact on the global climate, recent studies have shown the carbon cycle as well to be a major driving force on global glacial/interglacial changes via carbon dioxide exchange between the oceans and the atmosphere (e.g. Broecker and Henderson, 1998).

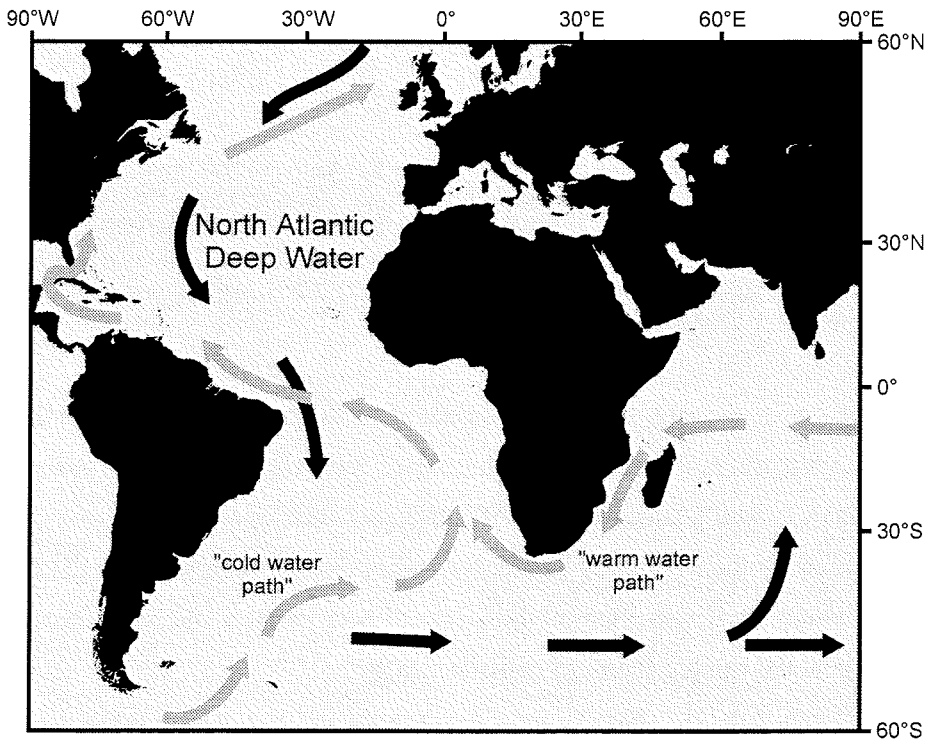

Fig. 1. The global thermohaline circulation (modified after Gordon, 1986; black arrows indicate deep water circulation, grey arrows indicate (sub)surface currents).

Several regions of the Atlantic Ocean are especially sensitive to monitor changes in the thermohaline circulation. For instance the Atlantic sector of the Southern Ocean and the eastern South Atlantic Ocean form key areas within the global circulation system. In the Atlantic sector of the Southern Ocean upwelling and northward Ekman transport of deep water (Toggweiler and Samuels, 1995) as well as bottom water production in the Weddell Sea (Orsi et al., 1999) form one of the motors of the thermohaline circulation (Fig. 2). The main feature of this region is the strictly eastward circulating, west wind driven Antarctic Circumpolar Current (ACC), subdivided into jet streams from north to south by the Subtropical Front, the Subantarctic Front, the Antarctic Polar Front and the Southern ACC Front, and bound to the south by the ACC-Weddell Gyre Boundary.

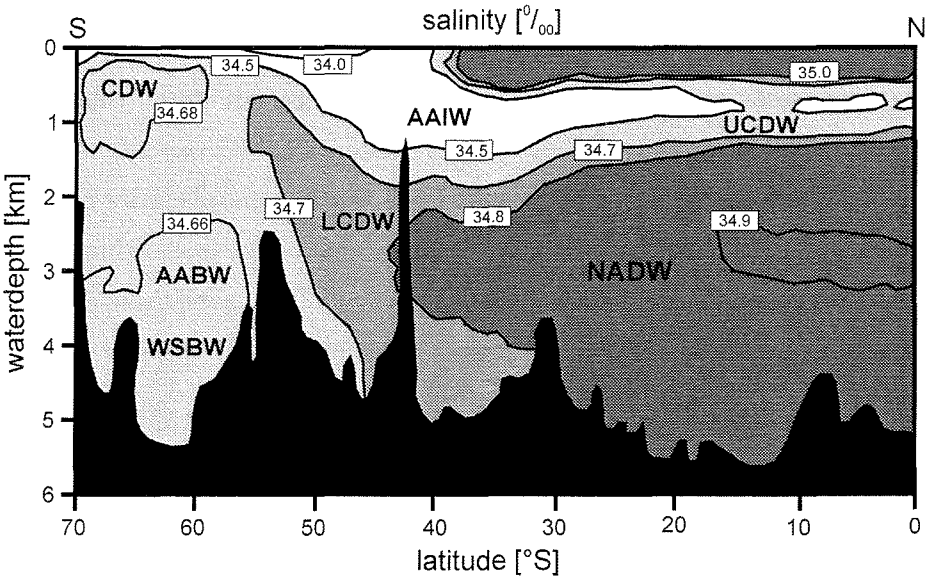

Fig. 2. Deep and bottom water masses of the South Atlantic Ocean based on salinity: a hydrographic section through the South Atlantic Ocean along the Greenwich Meridian (after Reid, 1989; AABW: Antarctic Bottom Water; AAIW: Antarctic Intermediate Water; CDW: Circumpolar Deep Water; LCDW: Lower Circumpolar Deep Water; NADW: North Atlantic Deep Water; UCDW: Upper Circumpolar Deep Water; WSBW: Weddell Sea Bottom Water).

Besides its role as deep water source, the influence of the Southern Ocean on the global carbon cycle by enormous bioproduction, caused by high nutrient concentrations in the upper water column of the ACC, is important as well (Bakker et al., 1997). The so called opal belt acts as a CO_2-sink through high amounts of photosynthetic primary producers within the photic zone and, therefore, is directly linked to global climate. Studies focused on the causes of heat transfer and productivity changes, thus, can help to understand the driving forces of climatic change.

The eastern South Atlantic Ocean forms a key area for the warm water return path of the thermohaline circulation. Within the Agulhas Current in the south-eastern Cape Basin warm (sub)surface waters enter the South Atlantic Ocean to be transported further northward via the Benguela Current and the South Equatorial Current, finally crossing the equator in the western tropical Atlantic Ocean. Besides this so called "warm water path" a return flow occurs via colder water influx

into the Atlantic Ocean at the Drake Passage, further transported with the South Atlantic Current to the Cape Basin; the so called "cold water path" (Fig. 1). The dominance of either the "cold water path" or the "warm water path" as return flow appears to be important to understand the glacial/interglacial variations in the thermohaline circulation.

Main driving force of the deep water flow to the southern hemisphere is the production of extremely cold, high saline water in the North Atlantic Ocean (North Atlantic Deep Water), whereas the warm water return flow is mainly wind driven (Gordon, 1986). These driving wind forces, the westerlies, the south-east trade winds and the monsoon winds, responding linear to the solar radiation, which influences the continental pressure field and the subtropical anticyclones of the Indian and South Atlantic oceans (McIntyre et al., 1989). After Imbrie et al. (1992) the variations in Late Quaternary South Atlantic Ocean time series records reflect these insolation changes controlled by the three main Milankovitch periodicities of precession (19-kyr and 23-kyr), obliquity (41-kyr) and eccentricity (100-kyr). From time series analyses in the tropical and eastern South Atlantic Ocean, there is evidence for the precessional component to be the main driving force for environmental changes due to trade wind intensity and direction changes (McIntyre et al., 1989; Schneider, 1991). On the other hand, the subtropical South Atlantic interacts with the Southern Ocean at the Subtropical Front. As high latitude insolation is rather obliquity then precessional influenced, complex interferences may result out of interocean exchange. There is increasing evidence for environmental changes occurring on a sub-Milankovitch period level (Little et al., 1997). Thus, information on the periodicities of the main driving forces may be important to understand the interaction between different parts of the thermohaline circulation.

Variations in the abundance of environmental sensitive micro-organisms in the water column and in the sediments, such as e.g. coccoliths, diatoms, radiolarians and foraminifers, may detect and reflect environmental and hydrographic changes in the upper water column and, therefore, be useful palaeoceanographic tools (e.g. Zielinski and Gersonde, 1997; Niebler and Gersonde, 1998; Abelmann et al., 1999; Flores et al., 1999). In addition to these groups of fossilisable marine phyto- and microplankton, well preserving dinoflagellate cysts are useful proxies especially in marine environments were the other groups do not preserve well or experience harsh life conditions. During the last decades, it has become more and more apparent that dinoflagellates are highly sensitive to environmental changes. This sensitivity is expressed through changes in the species composition of dinoflagellate cyst assemblages in relation to environmental variability. As such, variations in the cyst assemblage can reflect variation in environmental parameters such as temperature, salinity, nutrient concentrations and water stratification (e.g. Rochon et al., 1999; Devillers and de Vernal, 2000; Vink et al., 2000; Zonneveld et al., 2000; Vink et al., 2001; Zonneveld et al., 2001). Therefore, we can use fossil dinoflagellate cysts as tools for reconstructing palaeoenvironment, palaeoclimate, palaeoecology and palaeoceanography. To provide additional information on Later Quaternary variations of the

thermohaline circulation in the South Atlantic Ocean major emphasis has been placed on the following research questions:

- Besides a few studies on organic-walled dinoflagellate cyst distribution in sediments of the southern Indian Ocean (Marret and de Vernal, 1997) and the western Atlantic sector of the Southern Ocean (Harland et al., 1998), little is known on dinocysts assemblage composition as well as species diversity in vicinity of the major fronts of the Antarctic Circumpolar Current and the sea-ice boundary in the Weddell Sea. How do organic-walled cyst assemblages change in a transect from the oligotrophic subtropics of the central South Atlantic Ocean southward across the nutrient-rich opal belt? Is the dinocyst assemblage composition controlled only by environmental changes or do transport and organic matter decay caused by oxygen-rich bottom currents have major influence on the assemblage as well?
- The wind driven surface currents of the thermohaline circulation are linear forced by changes in the insolation controlled by orbital Milankovitch parameters. How do dinoflagellate cyst assemblages reflect environmental changes caused by insolation variation? Can the dinocyst analysis provide additional information to reconstructions based on calcareous and silicious plankton due to the different preservation of organic-walled dinocysts?
- The nexus of Indian Ocean, South Atlantic Ocean and Southern Ocean surface water off South Africa is influenced by insolation components of the tropics, the subtropics and the high latitudes, resulting in complex interferences. Can these interferences on a sub-Milankovitch level be tracked by dinoflagellate cyst analysis? Can dinoflagellates add information to the reconstruction of non-linear forcing of the surface currents?
- The Agulhas Retroflection off South Africa is the main gateway for warm water transport from the tropics and subtropics into the Atlantic Ocean. Former studies assumed a periodicity related to glacial/interglacial change on the volume transport (Flores et al. 1999). Is the warm water influx coupled to the global glacial/interglacial cycles or does local changes in the hydrography influence this system as well? Which process forces these local mechanisms? How do transitional times between glacials and interglacial play an important role on the path of the thermohaline circulation in the South Atlantic Ocean? Can information be provided on the importance of either the "warm water path" or the "cold water path" as return flow of the thermohaline circulation during glacial/interglacial cycles?

Questions on organic-walled cyst distribution in the Southern Ocean in relation to the main hydrographic features will be answered in **Chapter 2**. Many of the palaeoceanographic questions mentioned above have been answered through the analysis of organic-walled and calcareous dinoflagellate cyst assemblages in Late Quaternary time series of the eastern South Atlantic Ocean, and are dealt with in **Chapter 3.**, **Chapter 4**. and **Chapter 5**. These Chapters will answer questions

focused on periodic environmental changes in the Cape Basin as well as on orbital forcing of the thermohaline circulation.

1.2. Dinoflagellates and their life cycle

Dinoflagellates are generally unicellular algae with a complex life cycle, living in most aquatic environments (full marine to limnic). They are found in all climatic and biogeographic zones from the tropics to polar regions. This highly variable group of protists includes planktic, benthic, parasitic and symbiotic life-styles with autotrophic, mixotrophic and/or heterotrophic metabolisms. They are generally found as free-living forms (motile) in the upper water column, which provides enough sunlight and nutrients for the photosynthetic forms or, in the case of heterotrophic form, enough prey organisms or organic detritus (e.g. Dale, 1983). The major part of dinoflagellate species is represented by marine planktic forms (~90 %) with its highest diversity in tropical regions (Taylor and Pollingher, 1987).

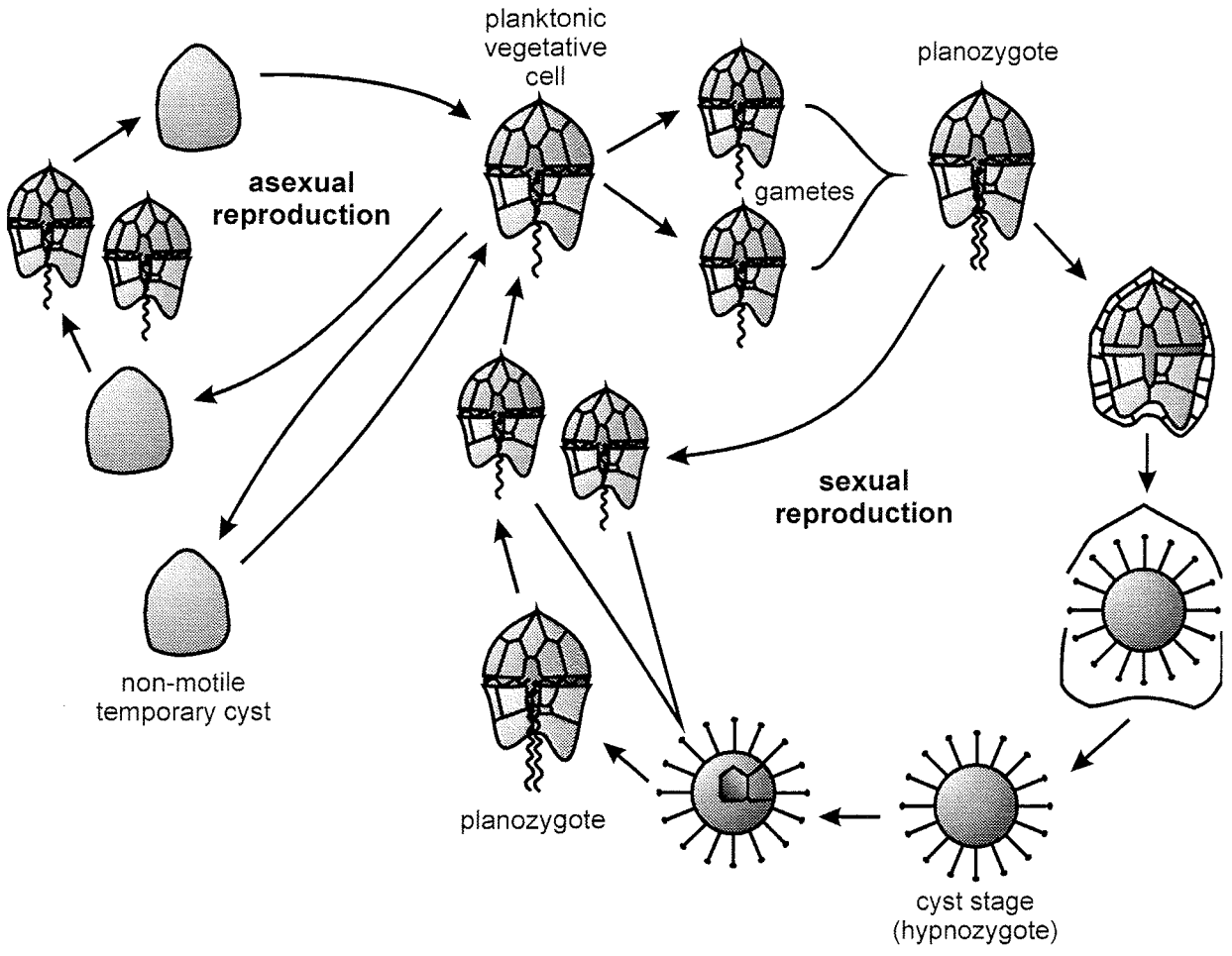

Fig. 3. Simplified dinoflagellate life cycle (modified after Dale, 1986).

Depending on the dinoflagellate group, asexual and sexual reproduction can take place to a varying extent (Fig. 3). Asexual reproduction occurs mainly through the fission of a haploid motile

dinoflagellate cell. During sexual reproduction, the motile cell produces gametes, which merge into a planozygote stage. After fusion, the resulting diploid cell might build a resting cyst composed of a sporopollenin-like material, or calcite (depending on the species), which is more resistant to chemical corrosion and/or digestion. Having completed a dormancy period (a period in which the cyst is unable to hatch), the protoplast leaves the fossilisable cyst (dinocyst) and builds a new vegetative cell of non-fossilisable material (theca). As dinocysts are generally species-specific, organic-walled and calcareous dinocyst assemblages preserved in sediments reflect the motile dinoflagellate association in the upper water column at the time of deposition. A cyst stage is assumed to be produced only by around 75 of the nearly 2000 known dinoflagellate species (Taylor, 1987). Asexual reproduction is observed by the calcareous dinoflagellate *Thoracosphaera heimii*, which occurs most of its life time in a vegetative, coccoid, calcified stage.

The organic-walled cyst producing dinoflagellates used in this study belong to the orders Gonyaulacales, Peridiniales and Gymnodiniales, with mainly autotrophic life-style in the case of the Gonyaulacales and mainly heterotrophic life-style in the case of the two other orders. The calcareous cysts found in oceanic sediments are produced by dinoflagellates of the subfamily Calciodinelloidea of the order Peridiniales with the exception of *Thoracosphaera heimii*, belonging to the order Thoracosphaerales (see Appendix A of **Chapter 3** for additional taxonomical information). These calcareous dinoflagellates are mainly autotrophic (e.g. Tangen et al., 1982; Pfiester and Anderson, 1987; Lewis, 1991; Montresor et al., 1993).

Progress in Modern dinoflagellate research

Since the first comprehensive studies on Modern distribution and ecological affinities of dinoflagellates carried out in the seventies of the twentieth century (e.g. Wall and Dale, 1973; Wall et al., 1977), the interest in ecological and oceanographic applicabilities of this organism group has increased rapidly (e.g. Dale, 1983; Dale and Dale, 1992; Edwards & Andrle, 1992; Dale, 1996). In the last few years many research programs focused on organic-walled dinocyst distribution related to marine environmental conditions were established in the North Atlantic Ocean (e.g. de Vernal et al., 1994; Matthiessen, 1995; de Vernal et al., 1997; Rochon et al., 1999; de Vernal and Hillaire-Marcel, 2000; Devillers and de Vernal, 2000), in the South Atlantic Ocean (Vink et al., 2000; Zonneveld et al., 2001) and in the Southern Ocean (Marret and de Vernal, 1997; Harland et al., 1998). These studies proved the organic-walled dinocysts to be useful proxies, sensitive to environmental and hydrographic changes.

The research on Modern calcareous dinocyst distribution and its ecological relationship on the other hand is relatively young. Since early studies carried out by Dale (1992), the research nowadays is mainly focused on the Equatorial and South Atlantic Ocean (Kerntopf, 1997; Karwath, 2000; Vink et al., 2000; Zonneveld et al., 2000). These studies revealed a high dependence of calcareous dinocyst distribution to stratified, oligotrophic conditions of the (sub)surface water layer.

Outgoing from these base studies, organic-walled and calcareous dinoflagellate cysts were used as palaeoceanographic proxies on Later Quaternary times series in the western tropical Atlantic Ocean to reveal Heinrich events (Vink, 2000), and in the equatorial South Atlantic Ocean to show changes in surface water productivity and thermocline depth variations in relation to glacial/interglacial cycles (Höll et al, 1998; Höll et al., 1999, Höll and Kemle von Mücke, 2000).

1.3. Synopsis

The main objectives of this dissertation are to provide additional information on the common knowledge of organic-walled dinocyst distribution in Southern Ocean sea floor sediments as well as to use this knowledge to interpret the dinoflagellate cyst distribution in time series of the eastern South Atlantic Ocean. Here, variations in the dinocyst associations shall be used to reveal the relation between orbitally forced climatic change and variations in the thermohaline circulation. This study is centred on four articles published, submitted or to be submitted in international journals of geosciences:

To use organic-walled dinoflagellate cysts as palaeoceanographic proxies on a time series in the eastern South Atlantic Ocean, the dinocyst abundances in the surrounding areas as well as their relationship to environmental parameters have to be known. Relatively little information is available on the organic-walled dinocysts distribution at the Subtropical Front, boundary between the subtropical South Atlantic Ocean and the Southern Ocean, as well as the dinocyst distribution in the Antarctic Circumpolar Current. Therefore, 32 surface sediment samples more or less located on a north-south transect across the main fronts of the ACC were quantitatively analysed for their organic-walled dinocyst content in **Chapter 2**. Multivariate statistical analyses (detrended canonical analysis and canonical correspondence analysis) were used to determine possible relationships between cyst distributions and environmental parameter such as sea surface summer and winter temperatures and salinities, and mean annual nutrient concentrations. Substantial differences in cyst distribution patterns are observed which appear to be related to surface water mass changes at the oceanic fronts. As such, organic-walled dinocysts can potentially be used to track hydrographic changes and to distinguish between different water masses of the Southern Ocean.

In **Chapter 3.**, the information obtained from **Chapter 2.** was used in addition to information on Modern organic-walled and calcareous dinocyst distribution of the South Atlantic Ocean already available (Zonneveld et al., 2000; Zonneveld et al., 2001) to detect palaeoceanographic changes in the Agulhas Current region. The study on this key area of the thermohaline circulation was an attempt to reveal palaeoenvironmental changes on Milankovitch and sub-Milankovitch scales. Therefore, the content of organic-walled and calcareous dinocysts of a well-dated gravity core (GeoB 3603-2) from the eastern Cape Basin was investigated for the last 162 kyr. The dinocyst accumulation rates and the various indices of specific dinocyst groups were analysed with frequency analysis for their power

spectra to detect periodicities. Changes in cyst association and accumulation occur, which appear to be controlled by (1) global glacial/interglacial change, (2) variations in insolation forced in first order by the precession of the equinoxes and (3) frequency modulation of the first order variations caused by interferences of the subtropical Agulhas Current and the obliquity controlled Southern Ocean at the Subtropical Front. Prominent peaks in organic-walled dinocyst accumulation reflect times of high seasonal contrast, times of increased ocean current velocities and upwelling of trophic subsurface water due to Ekman transport. These peaks are in phase with maxima in the precipitation record of South Africa, suggesting times of dynamic ocean and atmosphere circulation. In contrast, high accumulation rates of calcareous dinocysts occur at the Terminations 2 and 1, reflecting stable, stratified, oligotrophic, warm water conditions in the eastern Cape Basin during times of low seasonal contrast and a large overturn in the global ocean circulation.

In **Chapter 4.**, the local reconstruction made in **Chapter 3** on the base of the calcareous dinocysts is compared to local reconstructions of two originally investigated sediment cores of the Walvis Ridge (GeoB 1214-1) and the eastern Brazil Basin south of the Equatorial Divergence (GeoB 1117-2), and to previously published results of sediment cores from the Guinea Basin at the Equatorial Divergence (GeoB 1105-4) and the western tropical Brazil Basin (GeoB 2204-2). This study reveals the extremely high calcareous dinocyst accumulation rates not only to appear in the eastern Cape Basin alone but to occur in the entire eastern South Atlantic Ocean along the surface water path of the thermohaline circulation as well. The mechanism responsible for the high calcareous dinocyst accumulation rates seems to be a combination of increased production due to stratified, oligotrophic, warm surface water conditions and extremely good carbonate preservation during the Terminations. The suggestion made by Vink (2000) is supported, that oligotrophy secondarily influences the rate of calcareous cyst production within a well-stratified environment.

In **Chapter 5.**, the local reconstruction made in **Chapter 3** on the base of the calcareous dinocysts is compared to the calcareous dinocysts analysis of a further sediment core (GeoB 1710-3) in the vicinity of the Benguela upwelling area. The results are used in addition to results of previous studies carried out on calcareous dinocysts (**Chapter 4**), planktic foraminifera and palaeotemperature proxies to suggest reduced productivity and stratified, warm water conditions during the last two major Terminations in the South Atlantic Ocean along the warm water return path of the thermohaline circulation.

2. Distribution of organic-walled dinoflagellate cysts in surface sediments of the Southern Ocean (eastern Atlantic sector) between the Subtropical Front and the Weddell Gyre

Oliver Esper and Karin A.F. Zonneveld
Universität Bremen, Fachbereich 5 - Geowissenschaften, Postfach 330 440, 28334 Bremen, Germany

Abstract

32 surface sediment samples from the Southern Ocean (eastern Atlantic sector), between the Subtropical Front and the Weddell Gyre, were investigated to provide information on the distribution of modern organic-walled dinoflagellate cysts in relation to the oceanic fronts of the Antarctic Circumpolar Current. A clearly distinguishable distribution pattern was observed in relation to the water masses and fronts of the Antarctic Circumpolar Current. The dinoflagellate cysts of species characteristic of open oceanic environments, such as *Impagidinium* species, are highly abundant around the Subtropical Front, whereas South of this front, cosmopolitan species such as *Nematosphaeropsis labyrinthus* and the cysts of *Protoceratium reticulatum* characterise the transition from Subtropical to Subantarctic surface waters. The Subantarctic surface waters are dominated by the cysts of heterotrophic dinoflagellates, such as *Protoperidinium* spp. and *Selenopemphix antarctica.* The cysts of *Protoperidinium* spp. form the dominant part of the assemblages around the Antarctic Polar Front, whereas *Selenopemphix antarctica* concentrations increase further to the south. The presence of *S. antarctica* in sediments of the Maud Rise, a region of seasonal sea-ice cover, reflects its tolerance for low temperatures and sea-ice cover. A previously undescribed species, *Cryodinium meridianum* gen. nov. sp. nov., has a restricted distribution pattern between the Antarctic Polar Front and the Antarctic Circumpolar Current –Weddell Gyre Boundary.

Keywords: dinoflagellate cysts; modern; ecology; South Atlantic; Southern Ocean

Introduction

The Southern Ocean forms a key area within the global ocean thermohaline circulation. Here, southward flowing North Atlantic Deep Water mixes with cold, dense endemic water masses generated from the Weddell and Ross shelf seas and forms generally northward flowing Antarctic Bottom Water (e.g. Orsi et al., 1999). Changes in the oceanographic setting of the Antarctic Circumpolar Current (ACC) can affect the volume of cold endemic water generated and hence the global thermohaline circulation system.

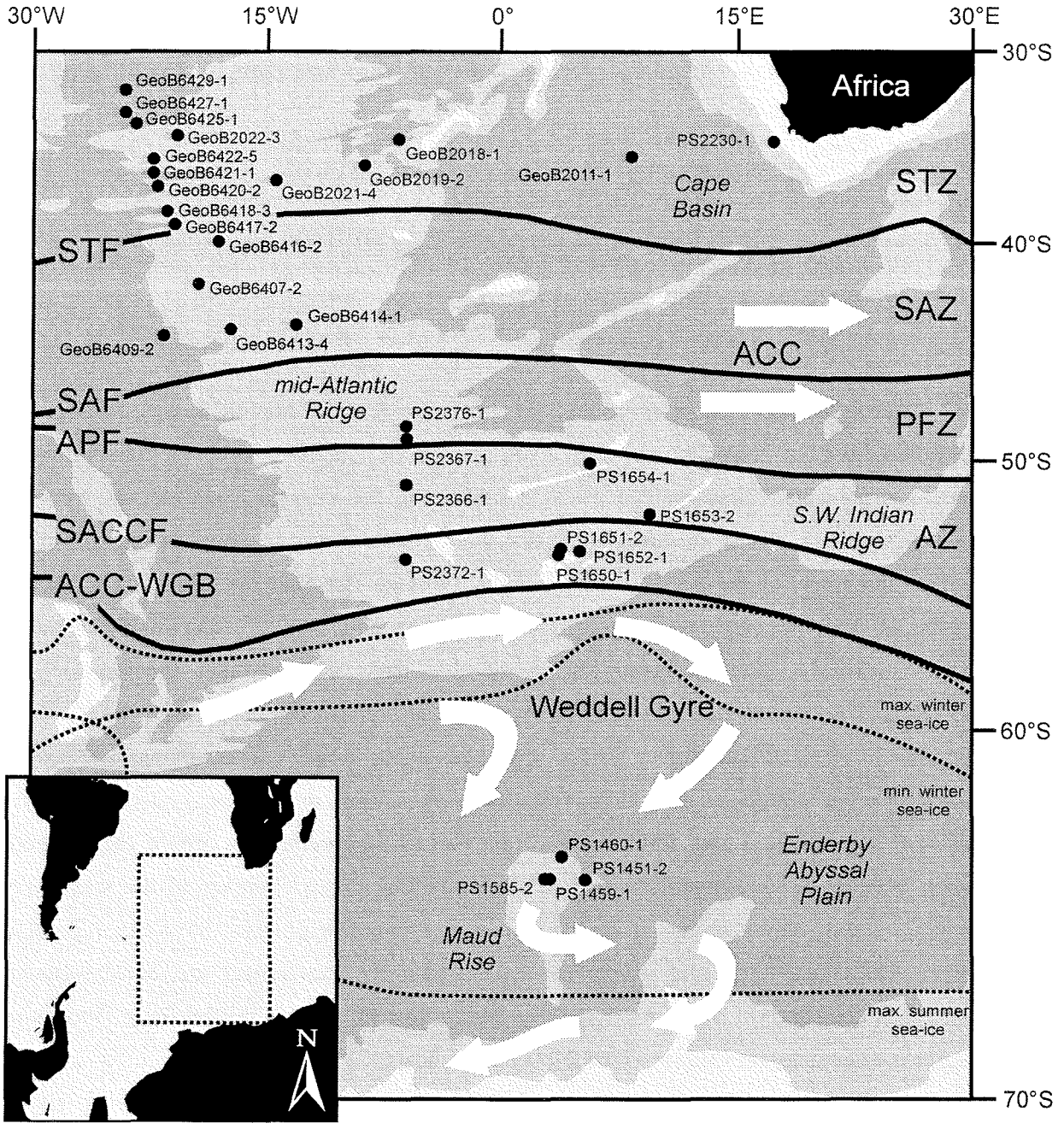

Fig. 1. Present-day oceanography in the Atlantic sector of the Southern Ocean between South Africa and Antarctica with the positions of the oceanic fronts (after Peterson and Stramma, 1992; Fahrbach, 1993; Orsi et al., 1993; Orsi et al., 1995; ACC: Antarctic Circumpolar Current; ACC-WGB: ACC-Weddell Gyre Boundary; APF: Antarctic Polar Front; AZ: Antarctic Zone; PFZ: Polar Frontal Zone; SACCF: Southern ACC Front; SAF: Subantarctic Front; SAZ: Subantarctic Zone; STF Subtropical Front; STZ: Subtropical Zone), the sea ice distribution (after Sea Ice Climatic Atlas, 1985), the bathymetry of the observed area (light grey: <2000 m, medium grey: 2000-4000 m, dark grey: >4000 m) and the 32 sample positions.

Besides its role in the global ocean circulation, the ACC is an important contributor to the biogenic primary production of the worlds oceans. High Chlorophyll *a* values related to high nutrient concentrations (Froneman and Perissinotto, 1996; Klaas, 1997) and increased concentrations of primary production-limiting trace metals, especially iron (Bathmann et al., 1997; Löscher et al., 1997), can be found especially in the vicinity of the Polar Front, whereas the lack of trace metals restricts the

primary production at the Antarctic Divergence south of the ACC (de Baar, 1995; Wiebinga and de Baar, 1998). Due to the high primary production at the fronts, the Southern Ocean is thought to influence the global carbon cycle via the carbon dioxide exchange at the air/water interface (Bakker et al., 1997). Recent studies suggest that productivity variations and/or changes in circulation and alkalinity of the Southern Ocean water masses might be important factors in influencing the global changes in atmospheric carbon dioxide concentrations during glacial/interglacial cycles (e.g. Howard and Prell, 1994; Broecker and Henderson, 1998). An enhanced knowledge of the driving forces of deep water production and possible factors influencing the biological productivity is, therefore, of great importance.

To gain such knowledge, it is essential to apply methods that can provide data on temporal changes in the oceanic system. In recent years, transfer fuctions based on foraminiferal, diatom, and radiolarian associations have allowed the reconstruction of surface water conditions of the circumantarctic current system in the Atlantic sector of the Southern Ocean (Niebler and Gersonde, 1998; Zielinski et al., 1998; Abelmann et al., 1999; Brathauer and Abelmann, 1999). However, the results of these studies often conflict with each other, which can partly be explained by the ecological and statistical limitations of these tools. Especially species-selective dissolution of calcareous and silicious tests can inflict relative abundances and, thus, alter statistic analyses. Organic-walled dinoflagellate cysts (dinocysts) have been successfully used for (palaeo-) oceanographic reconstructions in high northern latitudes (e.g. Rochon et al., 1999; de Vernal and Hillaire-Marcel, 2000; Devillers and de Vernal, 2000). Dinoflagellates are planktonic microorganisms living in nearly all aquatic environments worldwide and comprise different life strategies (e.g. photoautotrophic or heterotrophic species). Beneath unarmoured and armoured species without a fossilisable cell wall, a few taxa are capable of producing fossilisable resting cysts of organic material, which easily can be extracted out of the sediments. The distribution patterns of dinocysts depend on production rates, transport, dilution and preservation. Recent studies of the western Atlantic sector of the Southern Ocean (Harland et al., 1998; Harland et al., 1999) and the southern Indian Ocean (Marret and de Vernal, 1997) show that organic-walled dinocyst species have clearly restricted distribution patterns in sea surface sediments, which can be related to oceanic features of the upper water masses. In surface waters of the eastern Atlantic sector of the Southern Ocean, up to nine different motile dinoflagellate taxa were found across the Subtropical Front (Barange et al., 1998), in the ACC (Eynaud et al., 1999) and at the ACC-Weddell Gyre Boundary (Klaas, 1997). However, there are no data on the modern distribution of dinocysts in surface sediments is present for this area.

The aim of this study is to provide information on the modern dinocyst distribution in relation to the oceanic fronts of the ACC in the eastern Atlantic sector of the Southern Ocean. For this purpose, 32 surface sediment samples from the ACC, focused on the Subtropical Front over the mid-Atlantic Ridge, areas north and south of the Antarctic Polar Front and the Weddell Gyre, were analysed (Fig. 1). As autotrophic dinoflagellate distribution is favoured by oligotrophic environments

with less competition (Harland et al., 1998), an affinity of autotrophic species to frontal proximity in oligotrophic areas can be expected. On the contrary, we expect high numbers of cysts related to heterotrophic species in the high-nutrient environment of the ACC (Marret and de Vernal, 1997; Harland et al., 1998). Furthermore, the ratio between individual heterotrophic species with dissimilar environmental affinities might be characteristic for different regions of the subpolar and polar regimes. This information might be useful in further studies to reconstruct the Late Quaternary dynamics of the Antarctic Ocean frontal system.

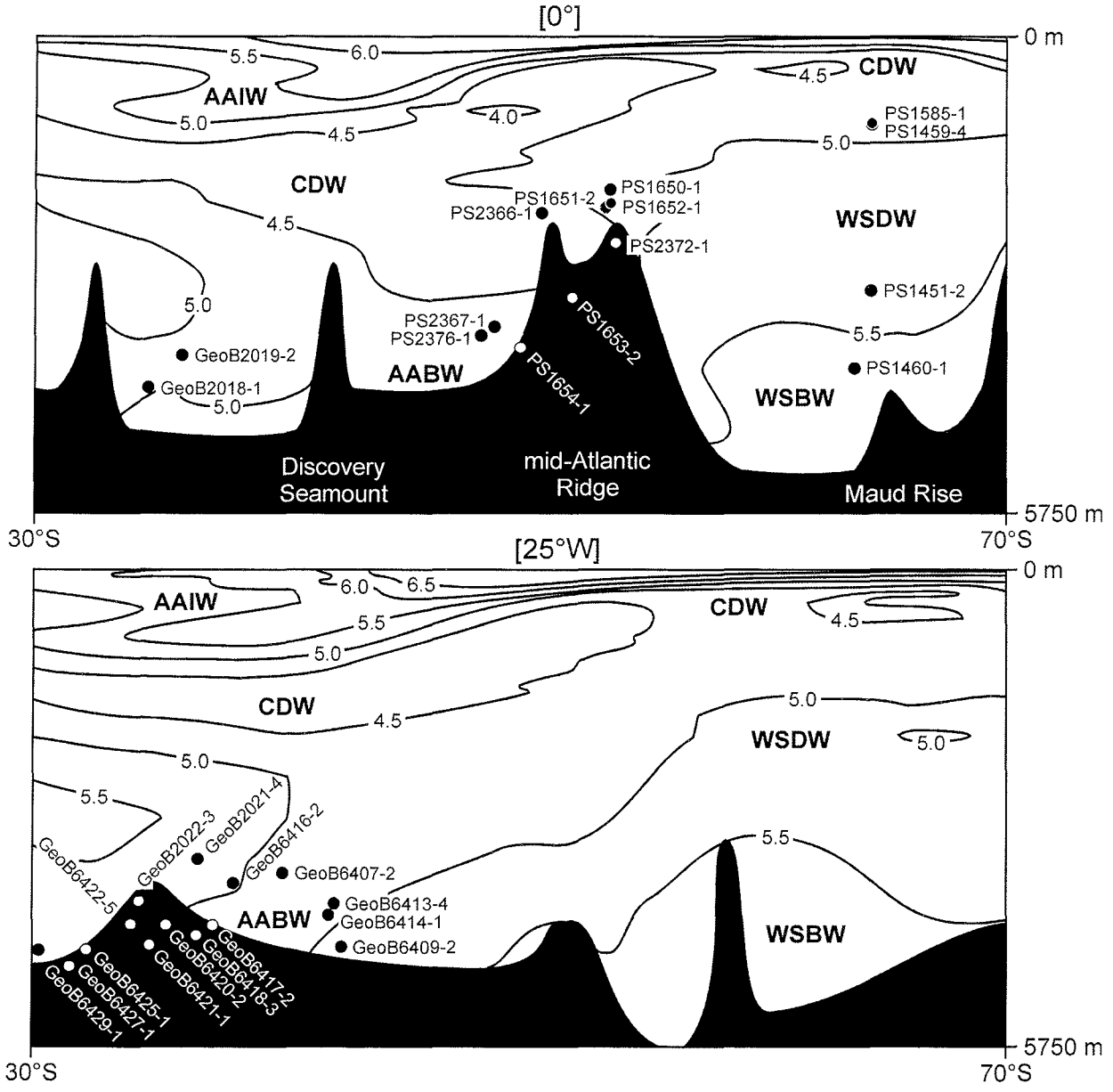

Fig. 2. Two meridional sections across the Southern Ocean from 30°S to 70°S along the Greenwich Meridian [0°] and the 25°W meridian, showing the sample positions (without the two Cape Basin samples) in relation to the dissolved oxygen concentrations [micromolar] and distinguished water masses (AABW: Antarctic Bottom Water; AAIW: Antarctic Intermediate Water; CDW: Circumpolar Deep Water; WSBW: Weddell Sea Bottom Water; WSDW: Weddell Sea Deep Water).

Present-day oceanography

The most prominent feature of the Atlantic sector of the Southern Ocean is the multi-banded nature of the Antarctic Circumpolar Current (Fig. 1; Peterson and Stramma, 1991). This eastward flowing current, driven by strong Westerlies, is bound to the north by the Subtropical Front (STF), which represents a northward descending temperature and salinity discontinuity characterised by a 4-5°C temperature and ~0.5‰ salinity difference. At the STF, cold, nutrient-rich Subantarctic Surface Water is subducted below the warmer, nutrient-depleted Subtropical Surface Water of the Subtropical Gyre, separating the Subtropical Zone from the Subantarctic Zone (Lutjeharms and Valentine, 1984; Eynaud et al., 1999). Within the ACC three circumpolar frontal systems can be recognised from north to south; the Subantarctic Front (SAF), the Antarctic Polar Front (APF) and the recently observed Southern ACC Front. These fronts are characterised by bands of large horizontal density gradients associated with high velocity surface currents (Orsi et al., 1995; Holliday and Read, 1998). The SAF divides the nutrient-rich Subantarctic Surface Water into the Subantarctic Zone (SAZ) and the Polar Frontal Zone (PFZ). At the APF, Antarctic Surface Water is subducted below the less dense Subantarctic Surface Water, separating the Polar Frontal Zone from the Antarctic Zone (AZ) (Lutjeharms and Valentine, 1984; Lutjeharms, 1985). Unlike other ACC fronts, the Southern ACC Front does not separate distinct surface water masses. The ACC-Weddell Gyre Boundary, a front-like feature, bounds the ACC to the south.

Below the surface waters flows eastwardly circulating Circumpolar Deep Water, which is formed by a mixture of North Atlantic Deep Water and deep and bottom waters of the ACC (Fig. 2). The deepest layers of the ACC are characterised by generally northward flowing Antarctic Bottom Water, originally a mixture of Circumpolar Deep Water and Antarctic Shelf Water (Pudsey, 1992; Orsi et al., 1999).

The Southern Ocean between the ACC-Weddell Gyre Boundary and the Antarctic continent is characterised by the Weddell Gyre, a subpolar cyclone located above the Weddell Abyssal Plain, where the main production of Antarctic Bottom Water takes place. The Weddell Gyre incorporates heat and salinity of the ACC and transports it to the continental shelf (Orsi et al., 1993). The water masses of the Weddell Gyre consist of very cold, oxygen-enriched Antarctic Surface Water down to a depth of about 200 m, less oxygenated Circumpolar Deep Water between 200 m and 800 m, and oxygen-enriched Weddell Sea Deep- and Bottom waters below 800 m (Fig. 2). Dense Weddell Sea Bottom Water is formed by the mixing of Circumpolar Deep Water with shelf waters whose temperatures are near freezing point. The Weddell Sea Deep Water, in turn, represents a less dense mixture of Circumpolar Deep Water and Weddell Sea Bottom Water, enabling it to leave the Gyre and spread into the Scotia Sea, the Georgia Basin and the Enderby Abyssal Plain. At the northern border of the Weddell Gyre, Weddell Sea Deep Water incorporates more Circumpolar Deep Water and

eventually spreads into the basins north of the Southern Ocean as Antarctic Bottom Water (Orsi et al., 1993; Orsi et al., 1999).

Table 1. Station list, characteristics of the analysed sediment samples and sea surface water parameters.

sample no.	ship	cruise	sampling gear [a]	latitude	longitude	water depth [m]	sediment type [b]	dinocyst counts	dinocyst concentration [cysts/g]	SSST [°C] [c]	SSWT [°C] [c]	SSSS [p.s.u] [c]	SSWS [p.s.u] [c]	nitrate [micromol] [c]	phosphate [micromol] [c]
GeoB2011-1	METEOR	M23/1	bc	35°35.0'S	8°16.2'E	5067	pc	581	1277	19.19	17.45	35.38	35.38	2.5150	0.2956
GeoB2018-1	METEOR	M23/1	muc	34°40.2'S	6°33.1'W	4237	nfo	79	79	20.48	15.65	35.34	35.52	0.8809	0.1712
GeoB2019-2	METEOR	M23/1	muc	36°03.2'S	8°46.0'W	3836	fno	221	221	18.71	14.46	34.98	35.25	1.1300	0.2505
GeoB2021-4	METEOR	M23/1	muc	36°50.1'S	14°24.3'W	3576	nfo	119	119	19.16	13.77	35.10	35.07	1.5268	0.3315
GeoB2022-3	METEOR	M23/1	muc	34°26.1'S	20°54.5'W	4016	nfo	128	128	21.71	14.72	35.62	35.25	0.5996	0.2537
GeoB6407-2	METEOR	M46/4	muc	42°02.7'S	19°30.0'W	3354	fno	399	200	13.37	10.39	34.56	34.71	9.0772	0.8082
GeoB6409-2	METEOR	M46/4	muc	44°30.4'S	21°43.0'W	4283	nfo	1208	2220	11.21	8.70	34.26	34.42	13.0129	1.0182
GeoB6413-4	METEOR	M46/4	bc	44°12.4'S	17°20.4'W	3768	fno	1369	1368	11.30	8.37	34.28	34.42	13.3597	1.0478
GeoB6414-1	METEOR	M46/4	bc	43°59.9'S	13°04.2'W	3830	fno	354	708	12.19	8.63	34.57	34.60	9.9839	0.8732
GeoB6416-2	METEOR	M46/4	bc	39°57.3'S	18°09.8'W	3525	fno	391	98	16.42	12.17	34.95	35.01	3.3320	0.5204
GeoB6417-2	METEOR	M46/4	bc	39°05.6'S	21°02.5'W	4024	nfo	452	90	16.53	12.59	35.02	35.07	2.9318	0.4523
GeoB6419-1	METEOR	M46/4	bc	37°46.4'S	21°51.8'W	3568	fno	713	143	17.57	13.05	35.14	35.14	1.7553	0.3461
GeoB6420-2	METEOR	M46/4	bc	37°09.5'S	22°08.8'W	3998	fno	656	131	18.62	13.54	35.25	35.22	0.7885	0.2965
GeoB6421-1	METEOR	M46/4	bc	36°26.9'S	22°26.7'W	4216	fno	302	151	19.64	13.99	35.36	35.25	0.4051	0.2544
GeoB6422-5	METEOR	M46/4	bc	35°42.4'S	22°26.4'W	3972	fno	560	112	20.62	14.45	35.45	35.29	0.2101	0.2198
GeoB6425-1	METEOR	M46/4	bc	33°49.5'S	23°35.3'W	4352	nfo	277	141	22.20	16.07	35.63	35.48	0.0404	0.1516
GeoB6427-1	METEOR	M46/4	muc	33°10.9'S	24°14.9'W	4491	nfo	407	117	22.04	16.28	35.61	35.53	0.0201	0.1387
GeoB6429-1	METEOR	M46/4	bc	31°57.0'S	24°14.9'W	4335	nfo	297	74	23.52	18.13	35.87	35.78	0.0346	0.0961
PS1451-2	POLARSTERN	ANT-IV/4	bc	64°33.6'S	5°27.6'E	3593	do	7	11	0.79	-1.94	34.10	34.36	23.3774	1.6001
PS1459-4	POLARSTERN	ANT-IV/4	bc	64°30.6'S	3°11.4'E	2083	do	80	117	0.78	-2.00	34.10	34.38	23.1058	1.5796
PS1460-1	POLARSTERN	ANT-IV/4	bc	63°52.8'S	3°59.4'E	4005	do	1	2	0.83	-1.82	34.08	34.35	23.2923	1.5543
PS1585-1	POLARSTERN	ANT-VI/3	bc	64°31.2'S	3°05.4'E	2078	do	60	97	0.78	-2.00	34.10	34.38	23.3774	1.5796
PS1650-1	POLARSTERN	ANT-VI/3	bc	53°45.6'S	3°48.0'E	1859	do	141	647	1.97	-0.46	33.91	34.00	23.4010	1.7903
PS1651-2	POLARSTERN	ANT-VI/3	bc	53°37.8'S	3°51.6'E	2071	do	130	489	1.97	-0.46	33.91	34.00	23.4010	1.7903
PS1652-1	POLARSTERN	ANT-VI/3	bc	53°39.6'S	6°06.0'E	1949	do	33	171	2.03	-0.63	33.96	34.03	22.4570	1.7949
PS1653-2	POLARSTERN	ANT-VI/3	bc	52°13.2'S	9°30.6'E	3163	do	29	69	2.47	0.05	33.99	34.00	21.1774	1.7492
PS1654-1	POLARSTERN	ANT-VI/3	bc	50°09.6'S	5°43.2'E	3769	do	321	1605	4.44	2.11	33.85	33.89	19.9327	1.6701
PS2230-1	POLARSTERN	ANT-X/4	muc	34°45.0'S	17°21.6'E	2575	fno	1740	8714	19.70	15.94	35.39	35.36	3.1015	0.4335
PS2366-1	POLARSTERN	ANT-X/6	muc	51°00.0'S	5°57.0'W	2114	do	335	1678	2.12	0.56	33.87	33.88	22.8370	1.5600
PS2367-1	POLARSTERN	ANT-X/6	muc	49°07.2'S	6°00.0'W	3525	do	225	1125	3.24	1.78	33.91	33.94	21.0775	1.4413
PS2372-1	POLARSTERN	ANT-X/6	muc	53°58.8'S	6°00.0'W	2415	do	234	585	1.52	-0.50	33.81	33.87	23.4358	1.5960
PS2376-2	POLARSTERN	ANT-X/6	muc	48°34.2'S	6°00.0'W	3657	do	449	2245	4.08	2.54	33.94	33.98	19.9672	1.3657

[a] bc = boxcorer; muc = multicorer

[b] do = diatomaceous ooze; fno = foraminiferal-nannofossil ooze; nfo = nannofossil-foraminiferal ooze; pc = pelagic clay

[c] values obtained from the LEVITUS World Ocean Atlas 1994 via the Internet (http://ingrid.ldgo.columbia.edu/SOURCES/.LEVITUS94/); SSSS = sea surface summer salinity; SSST = sea surface summer temperature; SSWS = sea surface winter salinity; SSWT = sea surface winter temperature

Material

32 samples were obtained from the upper centimetre of box- or multicorer sediments (Fig. 1; Tab. 1) collected during cruises M38/2 and M46/4 of the RV METEOR (Spieß et al., 1994, Wefer et al., internal report) and cruises ANT-IV/4, ANT-VI/3, ANT-X/4 and ANT-X/6 of the RV POLARSTERN (Fütterer, 1987; Fütterer, 1988; Bathmann et al., 1994; Lemke, 1994). Based on the comparison with seven adjacent, well-dated sediment core tops in the vicinity of the studied sites, we assume sub-Recent to Recent ages for the analysed sediment samples (Tab. 2).

Table 2. Seven well-dated sediment cores of different regions of the Antarctic Circumpolar Current close to the analysed surface sediments.

Core	latitude	longitude	sample depth [cm]	age [kyr]	estimated age of upper cm	reference
GeoB3603-2	35°08.0′S	17°33.0′E	8	2.32	Recent to sub-Recent	**Chapter 4**
PS1754-1	46°46.2′S	7°36.7′E	5	2.23	Recent to sub-Recent	Frank et al., 1996
PS1756-5	48°43.9′S	6°42.8′E	7	7.80	Recent to sub-Recent	Frank et al., 1996
PS1768-8	52°35.6′S	4°28.6′E	2	3.25	Recent to sub-Recent	Frank et al., 1996
PS1772-8	55°27.5′S	1°09.8′E	6	3.81	Recent to sub-Recent	Frank et al., 1996
PS2498-1	44°09.2′S	14°13.7′W	9	2.13	Recent to sub-Recent	Asmus et al., 1999
PS2499-5	46°30.7′S	15°20.0′W	4	3.01	Recent to sub-Recent	Asmus et al., 1999

Methods

Laboratory preparation and taxonomy

Wet sediment was dried overnight at 75°C, weighed and treated with 10% hydrochloric acid (HCl) to dissolve the carbonate content. After the material was carefully neutralised with 10% potassium hydroxide solution (KOH), decanted and washed twice with demineralised water. 40% cold hydrofluoric acid (HF) was then added to dissolve the siliceous content. After two days of reaction and settling time the solution was neutralised with 40% KOH and washed twice with demineralised water. Care was taken that the solution did not become alkaline at any time to prevent dinocyst dissolution. After ultrasonic treatment for 1-2 h, the material was sieved over a 20 µm mesh sieve and concentrated to 500 or 1000 µl of sample in an eppendorf tube. The extensive use of ultrasound will not harm any dinocyst (Funkhouser and Evitt, 1959). A fraction varying from 50 µl to 1000 µl,

depending on the dinocyst concentration, was brought onto a slide, embedded in glycerine jelly and sealed with paraffin wax.

The dinocyst content of a whole slide was counted with a light microscope at x400 magnification. Taxonomic information on the cyst species encountered is provided in Appendix A and the counting results are given in Appendix B. The nomenclature of the identified cysts follows Williams et al. (1998) and Fensome et al. (1993). In principal, the motile dinoflagellate taxonomy is used, except when the application of motile names is not sufficient to differentiate the different cyst types. Cyst-theca relationships are discussed and listed in Head (1996).

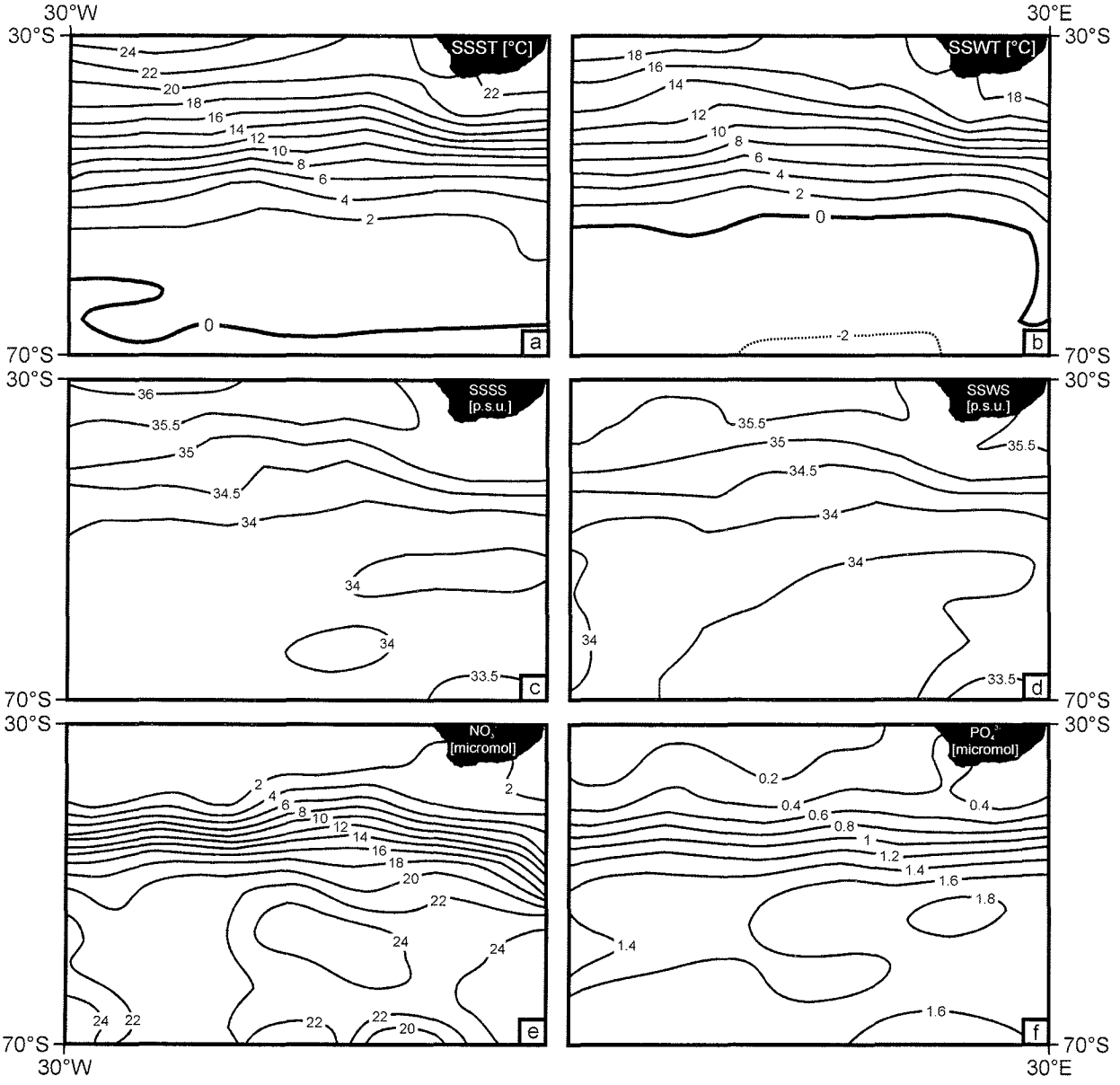

Fig. 3. Sea surface distribution of summer temperature (SSST), winter temperature (SSWT), summer salinity (SSSS), winter salinity (SSWS), nitrate (NO_3^-) and phosphate (PO_4^{3-}) in the Atlantic sector of the Southern Ocean (after Conkright et al., 1994; Levitus et al., 1994; Levitus and Boyer, 1994b).

Statistical methods

The relationship between dinocyst species distribution and environmental parameters has been determined using the multivariate ordination techniques of Detrended Correspondence Analysis (DCA) and Canonical Correspondence Analysis (CCA) of the CANOCO software (Ter Braak and Smilauer, 1998). DCA uses the variation in assemblage composition between the samples to determine the underlying environmental gradients influencing the data. The basic assumption of this method is that the most prominent environmental gradient causes the largest variation in assemblage composition. By means of a two way weighted averaging algorithm, the direction of this variation is calculated and represented as the first DCA axis. The second DCA axis represents the second most important direction of variation. In order to prevent a quadratic relation between the first and higher axes, the method of detrending (by segments) is applied (Hill and Gauch, 1980). The perpendicular projection of a species or sample point to the axis gives the position of the abundance optimum of that species or sample on that axis. The position of a species and sample on an axis is given in standard deviations (sd) in such way that species plotted more than 4 sd apart do not occur in similar samples. If the length of the first axis is less than 2 sd, the assumption of a unimodal response of species abundance in relation to environmental parameters does not hold. In such cases, the use of an ordination method based on linear relations between the species abundance and environmental gradients is preferable.

The variation represented by a DCA axis can be interpreted as caused by one or more environmental parameters. Interpretation of the DCA axes can be facilitated by including environmental information of the upper water column at the sample positions in the statistical analyses. In this study, the species distributions (relative abundances) have been compared to the sea surface temperatures (SST) and salinities (SSS) of austral summer and winter (Tab. 1; Fig. 3a-d), and with the mean annual concentrations of the prime nutrients nitrate and phosphate in the surface waters (Tab. 1; Fig. 3e-f). All data have been derived from the LEVITUS World Ocean Atlas 1994 (http://ingrid.ldgo.columbia.edu/SOURCES/.LEVITUS94/). Mean annual and seasonal values of all parameters have been calculated for 1° latitude and longitude square blocks (Conkright et al., 1994; Levitus et al., 1994; Levitus and Boyer, 1994b).

In contrast to DCA, CCA determines the position of the species optima and samples directly along gradients of inferred (environmental) variables. The perpendicular projection of a species or sample point to an inferred variable gives the position of the optimum of that species or sample on the variable.

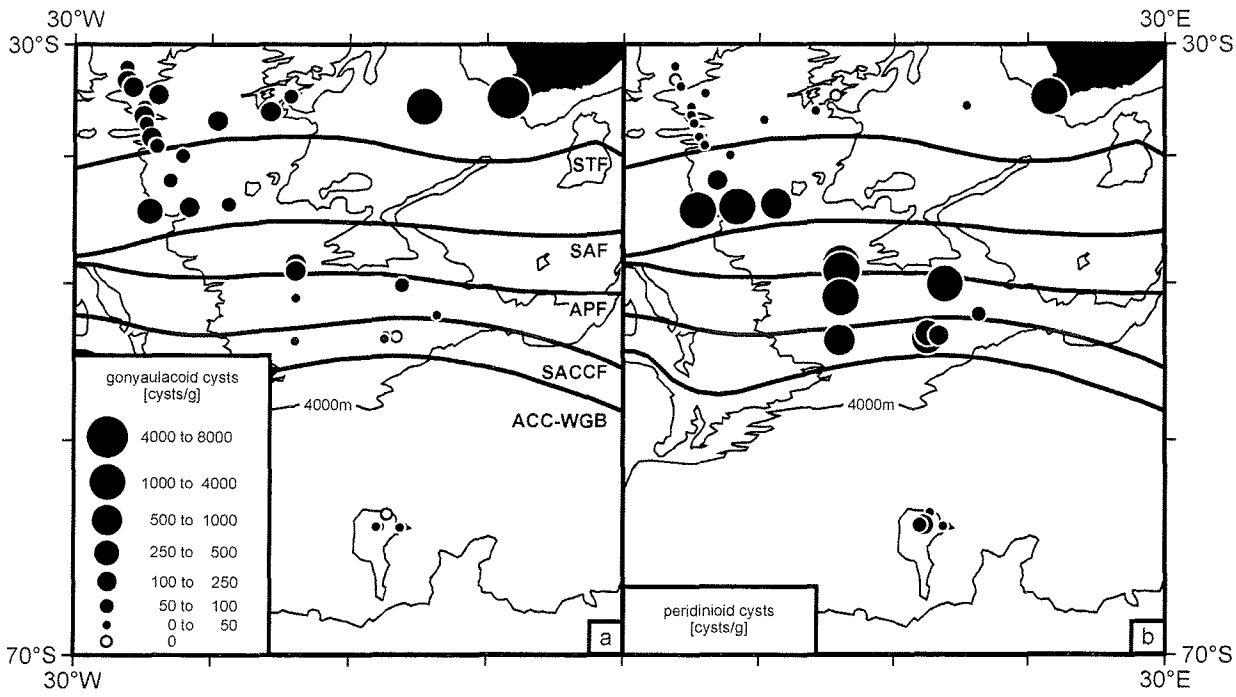

Fig. 4. Absolute abundance maps of gonyaulacoid (a) and peridinioid (b) dinocysts in cysts per gram of sediment.

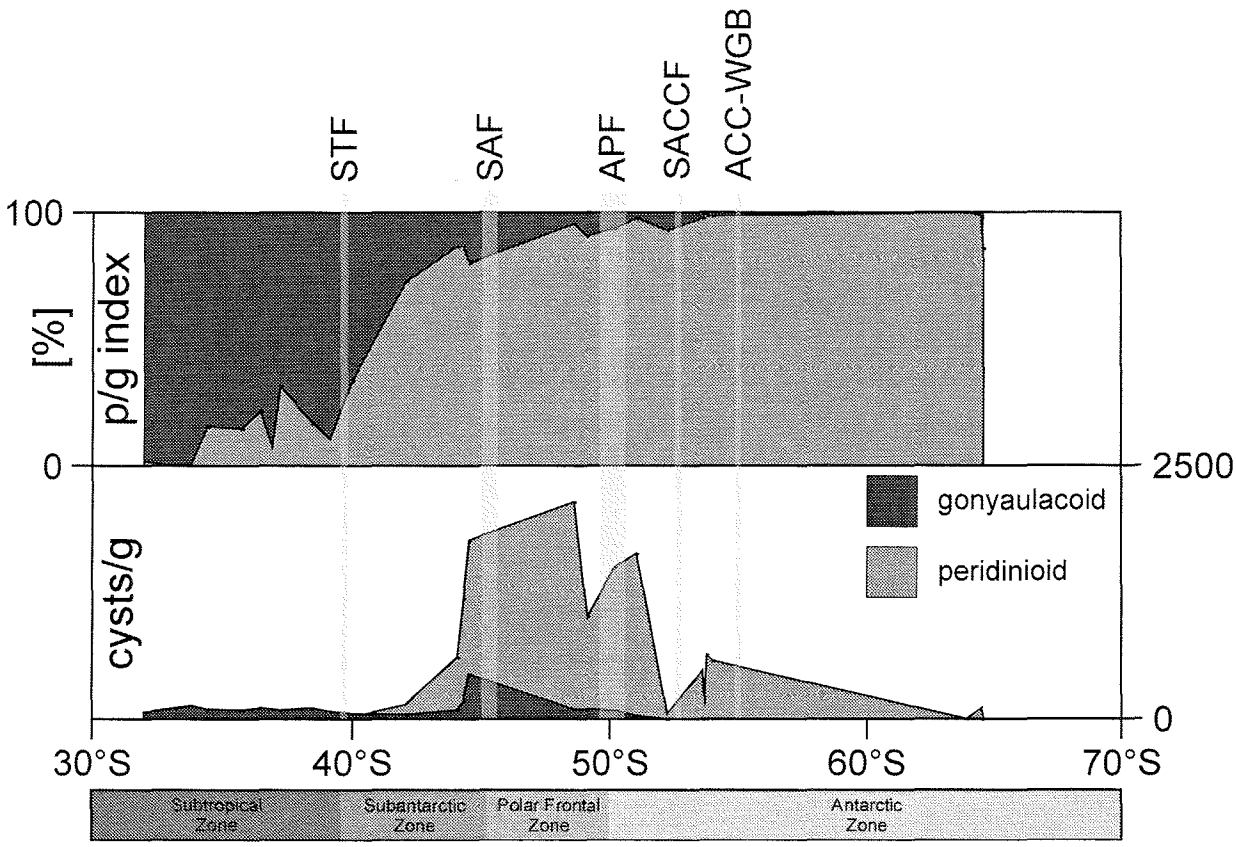

Fig. 5. Index between peridinioid and gonyaulacoid cysts (p/g index) as well as the absolute abundance of the two cyst groups in cysts per gram plotted against the meridional position of the samples (without the two Cape Basin samples GeoB2011-1 and PS2230-1).

Results

General distribution of dinoflagellate cysts

The analysis of the 32 surface samples shows a roughly latitudinal distribution pattern of dinocyst species across the fronts of the southern South Atlantic Ocean. Cysts of the orders Gonyaulacales and Peridiniales, in the following referred to as gonyaulacoid and peridinioid cysts respectively, make up the dinocyst assemblages in all analysed samples. It is striking that the total cysts per gram of sediment increases significantly in the open ocean samples from the Subtropical Front southwards with highest numbers in the Polar Frontal Zone between the Subantarctic Front and the Antarctic Polar Front, and then decreases south of the APF to lowest values in the Weddell Sea (Figs. 4 and 5). The gonyaulacoid cysts show highest values north of the STF, whereas the peridinioid cysts occur in high numbers south of this front.

Subtropical Zone

The samples of the Subtropical Zone can be divided into open ocean samples from the mid-Atlantic Ridge and one neritic sample off South Africa. The gonyaulacoid cyst species show relatively constant low values of not more than 140 cysts/g in the open ocean north of the STF. The cyst association in this area is dominated by the *Impagidinium* species, i.e. *I. aculeatum*, *I. variaseptum* and *I. paradoxum* (Fig. 6b, c, d), and to a lesser extent *I. patulum*, *I. strialatum* and *I. sphaericum* (Fig. 7a, b, c). North of the front, a few cysts of *Impagidinium pallidum* can also be observed (Fig. 7d). *Nematosphaeropsis labyrinthus* (Fig. 8b) and the cysts of *Protoceratium reticulatum* (Fig. 8a) also represent a prominent part of the association. Although *Pyxidinopsis reticulata* forms a small part of the association, it shows relatively higher abundances north of the STF compared to the regions at the front and south of it (Fig. 9d). A few specimens of *Bitectatodinium tepikiense* occur north of the STF. North of the STF, cysts of heterotrophic dinoflagellates are nearly absent with maximum values of around 40 cysts/g (mainly cysts of *Protoperidinium* spp.; Fig. 10a).

In comparison, the near coastal sample (GeoB2230-1) shows high numbers of peridinioid and gonyaulacoid species (Fig. 4). Cysts of *P. reticulatum* and *Spiniferites* spp. form more than 80% of the total assemblages (Fig. 8a, d). *Protoperidinium* spp. and *Echinidinium* spp. cysts dominate the peridinioid assemblage (Fig. 10a, d).

Subtropical Front

The dinocyst association changes markedly at the STF. Beside high percentages of *Impagidinium* cysts, *N. labyrinthus* forms about 20% of the association and cysts of *P. reticulatum* about 18% (Fig. 8a, b). The other gonyaulacoid species seem to play only a minor role at the STF.

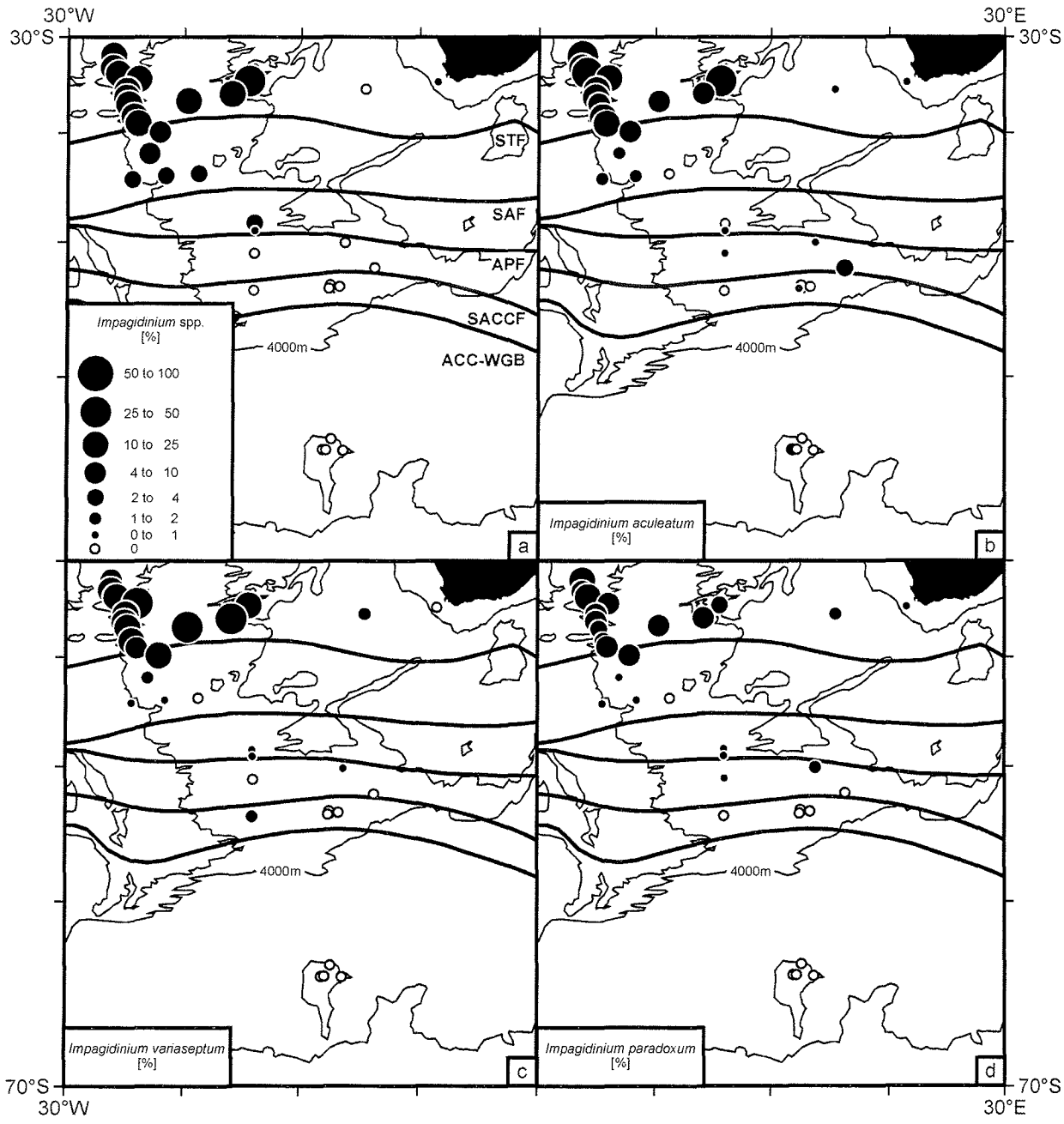

Fig. 6. Relative abundance maps of the cysts *Impagidinium* spp. (a), *Impagidinium aculeatum* (b), *Impagidinium variaseptum* (c) and *Impagidinium paradoxum* (d).

The peridinioid cysts still occur in low numbers, but it is remarkable that the samples proximately north and south of the STF contain two different types of "round browns", light brown coloured specimens and dark brown coloured specimens (see also the systematic section in Appendix A).

Subantarctic Zone

The assemblage composition in the Subantarctic Zone changes from an association dominated by gonyaulacoid species to one dominated by peridinioid species (Fig. 4). The gonyaulacoid cyst abundance in the Subantarctic Zone at the mid-Atlantic Ridge, although low south of the STF, with

values around 60 cysts/g, shows higher values of up to 450 cysts/g north of the SAF. Within the gonyaulacoid species, the assemblage changes from one dominated by *Impagidinium* to one dominated by *N. labyrinthus*.

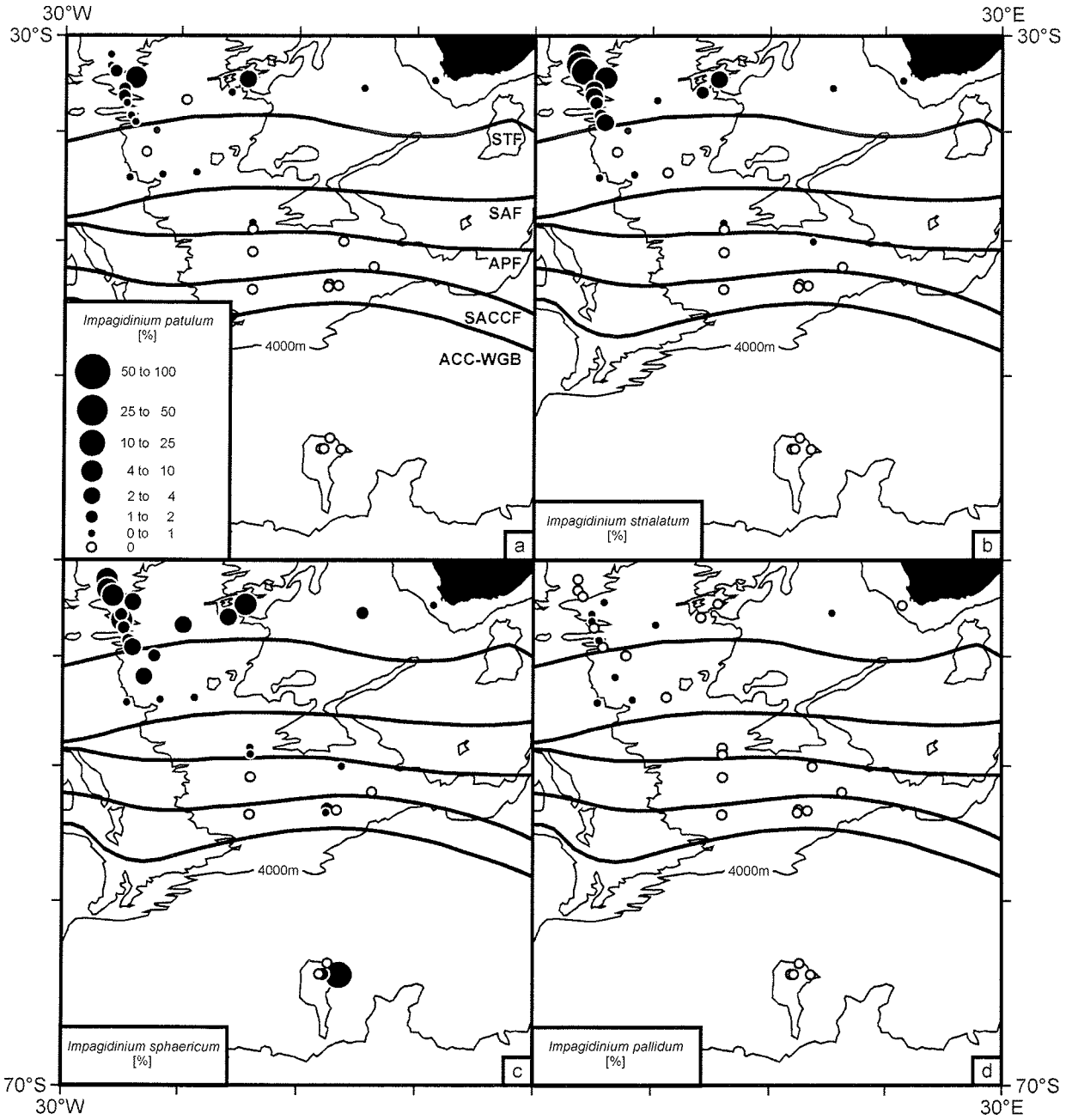

Fig. 7. Relative abundance maps of the cysts *Impagidinium patulum* (a), *Impagidinium strialatum* (b), *Impagidinium sphaericum* (c) and *Impagidinium pallidum* (d).

A similar trend is observed in the peridinioid dinocyst concentrations with values from around 30 cysts/g in the north to 1777 cysts/g in the southern SAZ (Fig. 4). The peridinioid cyst diversity increases southward. Within the SAZ, low amounts of *Selenopemphix antarctica* (Fig. 10c) and *Cryodinium meridianum* gen. nov. sp. nov. (Fig. 10b) are present.

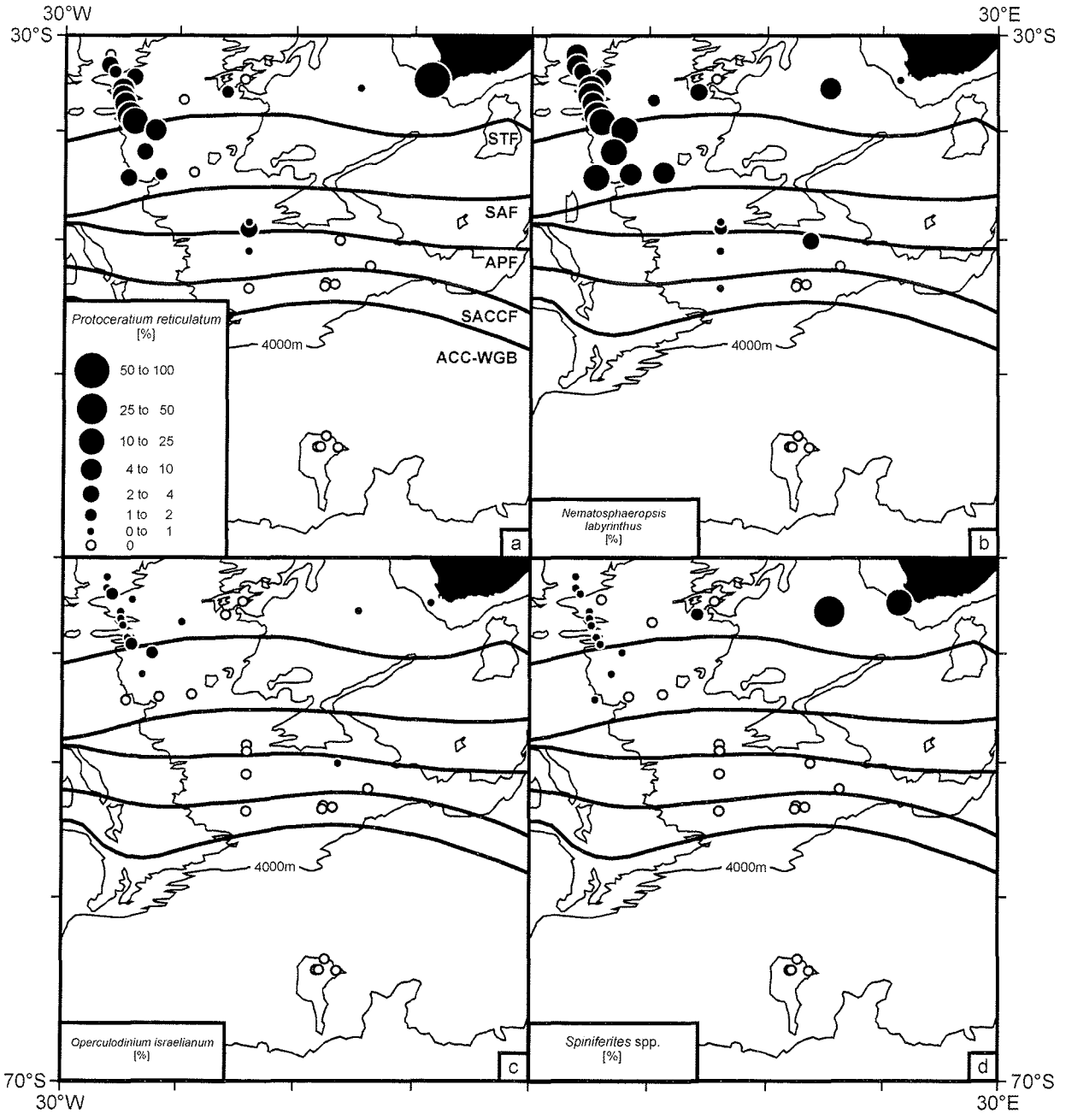

Fig. 8. Relative abundance maps of the cysts *Protoceratium reticulatum* (a), *Nematosphaeropsis labyrinthus* (b), *Operculodinium israelianum* (c) and *Spiniferites* spp. (d).

Polar Frontal Zone and Antarctic Zone

In the Polar Frontal Zone between the Subantarctic Front and the Antarctic Polar Front, as well as in the region south of the APF, gonyaulacoid cysts are few in number and no *Spiniferites* species were found (Fig. 8d).

Peridinioid cysts of *Protoperidinium* spp., *S. antarctica* and *C. meridianum* dominate the cyst assemblages between the SAF and the ACC-Weddell Gyre Boundary. At the APF, the dominance within the peridinioid cyst assemblage shifts from *Protoperidinium* spp. to *S. antarctica.*

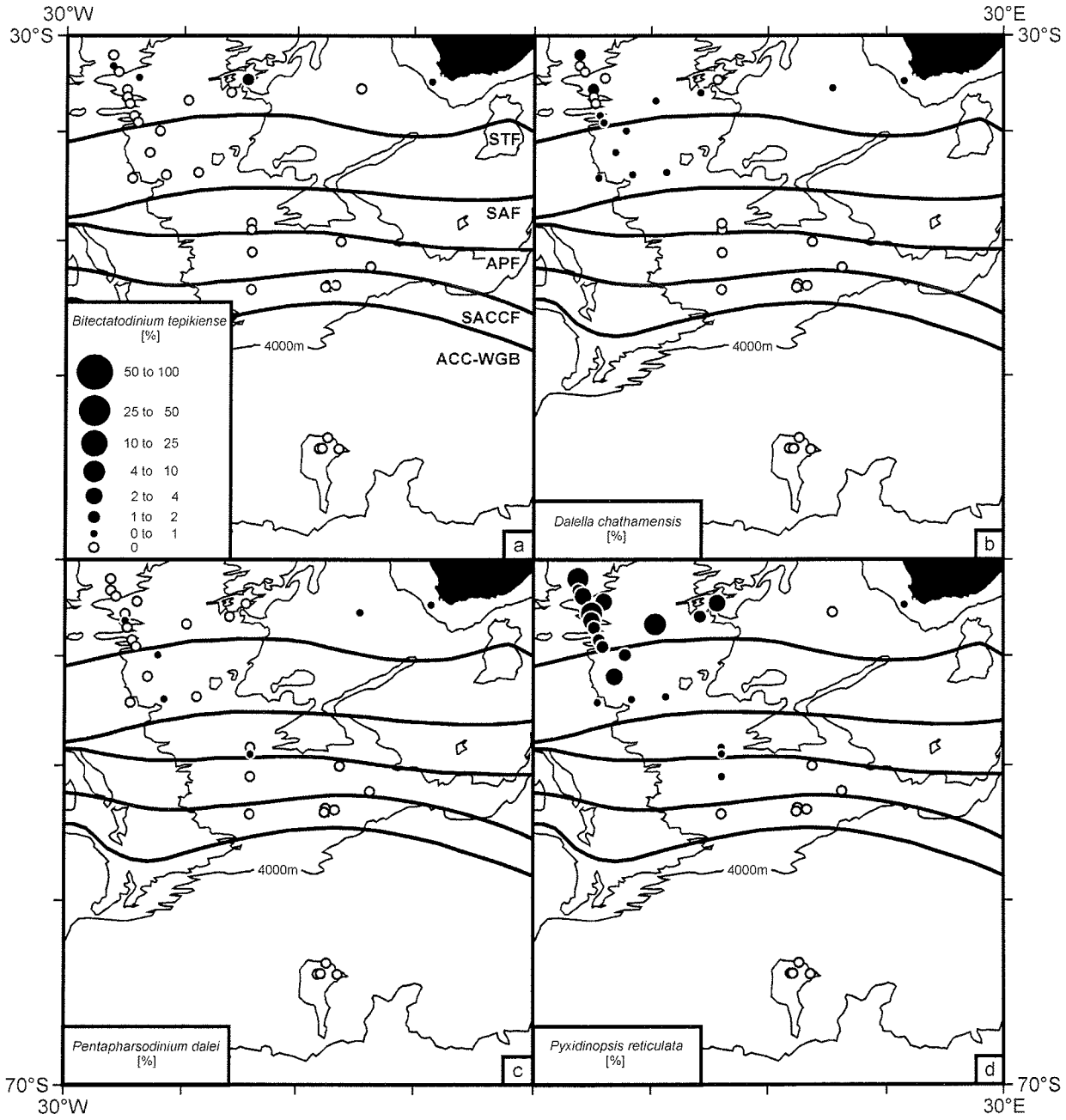

Fig. 9. Relative abundance maps of the cysts *Bitektatodinium tepikiense* (a), *Dalella chathamensis* (b), *Pentapharsodinium dalei* (c) and *Pyxidinopsis reticulata* (d).

The cyst assemblage at the Maud Rise in the Weddell Gyre is mainly composed of a few *Impagidinium* specimens together with *S. antarctica* and a few cysts of *Protoperidinium* spp. and *C. meridianum*.

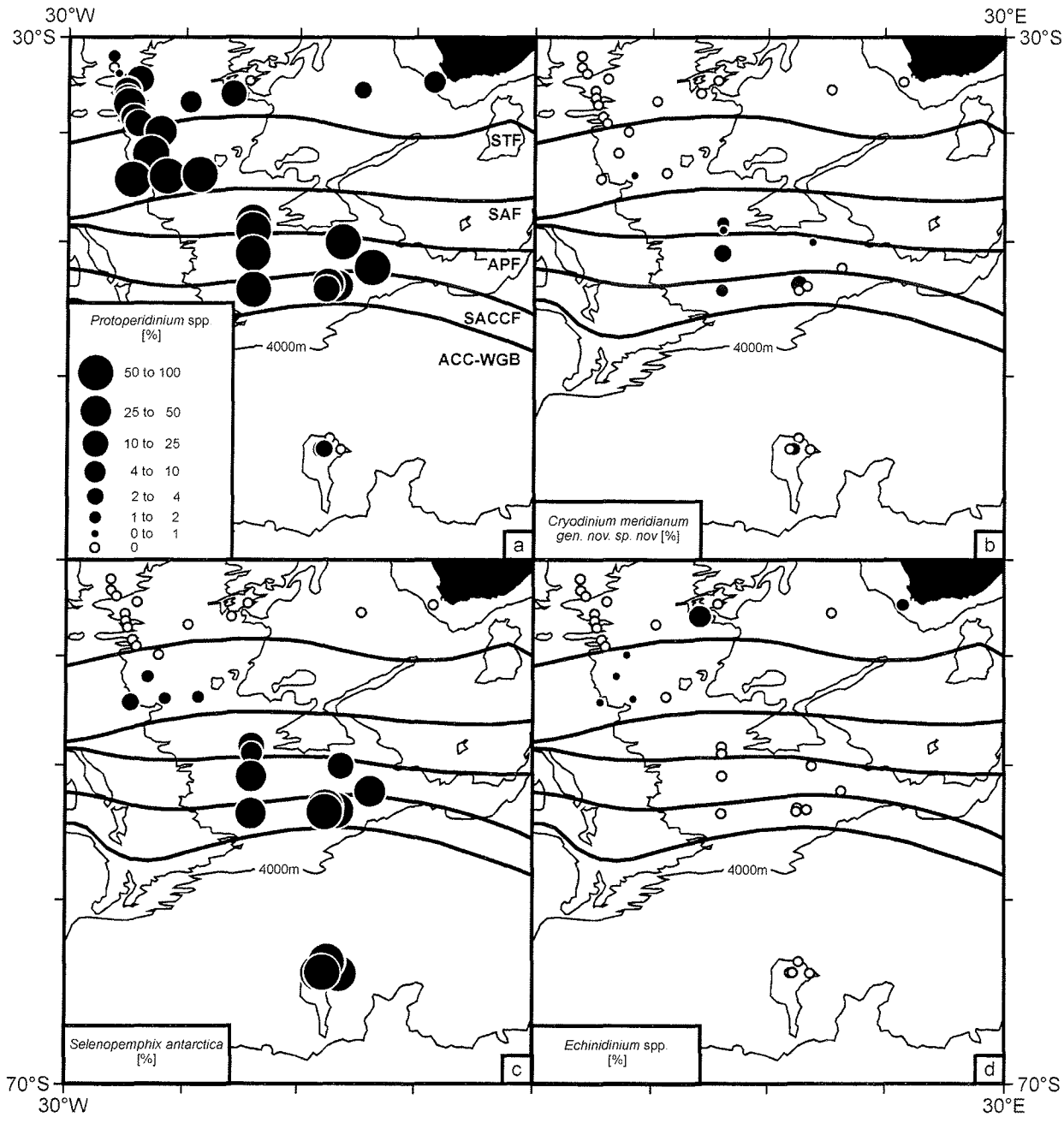

Fig. 10. Relative abundance maps of the cysts *Protoperidinium* spp. (a), *Cryodinium meridianum* gen. nov. sp. nov. (b), *Selenopemphix antarctica* (c) and *Echinidinium* spp. (d).

Statistical analyses

The DCA reveals a gradient with a length of 4.3 sd on the first DCA axis, indicating an unimodal distribution of the cyst species. 77.2% of the variance in the data set can be explained by the first DCA axis, whereas the second DCA axis with a length of 1.919 sd explains only 8.8% of the variance. Based on the statistical results, three dinocyst groups can be recognised (Fig. 11):

1. an association composed of *Protoceratium reticulatum* cysts, *Spiniferites* species, cysts of *Protoperidinium pentagonum* and *Echinidinium* cyst species;

2. an association of *Impagidinium* species together with *Nematosphaeropsis labyrinthus*, *Pyxidinopsis reticulata*, *Operculodinium israelianum* and *Dalella chathamensis*; and

3. an association composed of *Protoperidinium* cyst species, *Cryodinium meridianum* gen. nov. sp. nov, *Selenopemphix antarctica*, *Bitectatodinium tepikiense* and *Impagidinium sphaericum*.

Comparison with the positions of the samples along the first DCA axis (Fig. 12) indicates that association 1 is characteristic for near coastal samples, association 2 for the open ocean environment north of the Subtropical Front, and association 3 for the regions of the Antarctic circumpolar Current and the Weddell Sea. The sample positions in the DCA plot nearly reflects the real distribution pattern of the samples in the Southern Ocean (Fig. 12). The meridional distribution of the samples is mainly correlated with the gradient on the first axis. The CCA reveals high covariance between the environmental parameters of temperature, salinity and nutrients. Therefore, no clear correlation between cyst distribution, assemblage composition and one specific environmental parameter could be calculated with the available data. However, amongst the 6 tested parameters, sea-surface winter temperature seems to explain the greatest amount of variance in the cyst distribution (Tab. 3).

Table 3. Significances of sea surface water variables used in the CCA.

Variable Significance

Marginal Effects [a]		**Conditional Effects** [b]		
Variable	**Lambda 1**	**Variable**	**Lambda 1**	**P-value**
SSWT	0.73	SSWT	0.73	0.005
SSST	0.72	SSWS	0.39	0.005
NO_3^-	0.72	SSST	0.31	0.005
PO_4^{3-}	0.71	SSSS	0.12	0.005
SSSS	0.68	NO_3^-	0.06	0.025
SSWS	0.66	PO_4^{3-}	0.05	0.070

[a] Marginal effects represent the amount of variance explained by the variable, uncorrected for covariance.

[b] Conditional effects represent the amount of variance explained by one particular variable only (i.e. the unique effect of the variable on the species composition). The P-value indicates the significance of the variable (at the 5% significance level, $P \leq 0.05$).

NO_3^-	: mean annual sea surface nitrate concentration
PO_4^{3-}	: mean annual sea surface phosphate concentration
SSSS	: mean sea surface summer salinity
SSST	: mean sea surface summer temperature
SSWS	: mean sea surface winter salinity
SSWT	: mean sea surface winter temperature

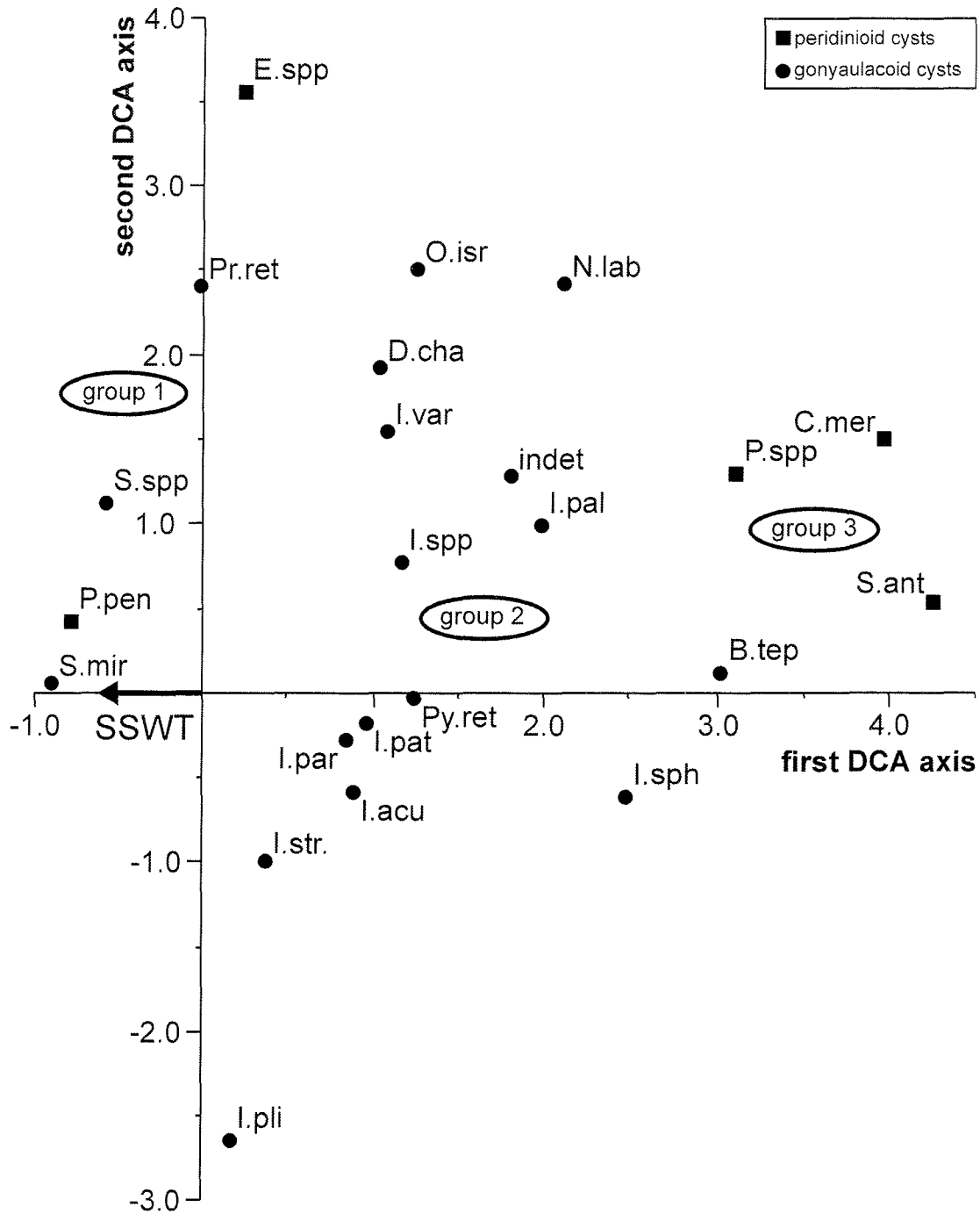

Fig. 11. Results of the DCA showing variance in the species distribution. The first axis explains 77.2 % of the variance and is most likely related to environmental parameters such as sea surface temperature, salinity and/or nutrient concentration (see text for further explanation). Abbreviations: B.tep: *Bitectatodinium tepikiense*; C.mer: *Cryodinium meridianum* gen. nov sp. nov.; D.cha: *Dalella chathamensis*; E.spp: *Echinidinium* spp.; I.acu: *Impagidinium aculeatum*; I.par: *Impagidinium pallidum*; I.pal: *Impagidinium paradoxum*; I.pat: *Impagidinium patulum*; I.pli: *Impagidinium plicatum*; I.sph: *Impagidinium sphaericum*; I.spp: *Impagidinium* spp.; I.str.: *Impagidinium strialatum*; I.var: *Impagidinium variaseptum*; indet: indetermined species; N.lab: *Nematosphaeropsis labyrinthus*; O.isr: *Operculodinium israelianum*; Pr.ret: *Protoceratium reticulatum*; P.pen: *Protoperidinium pentagonum*; P.spp: *Protoperidinium* spp.; Py.ret: *Pyxidinopsis reticulata*; S.ant: *Selenopemphix antarctica*; S.mir: *Spiniferites mirabilis*; S.spp: *Spiniferites* spp.; SSWT: sea surface winter temperature.

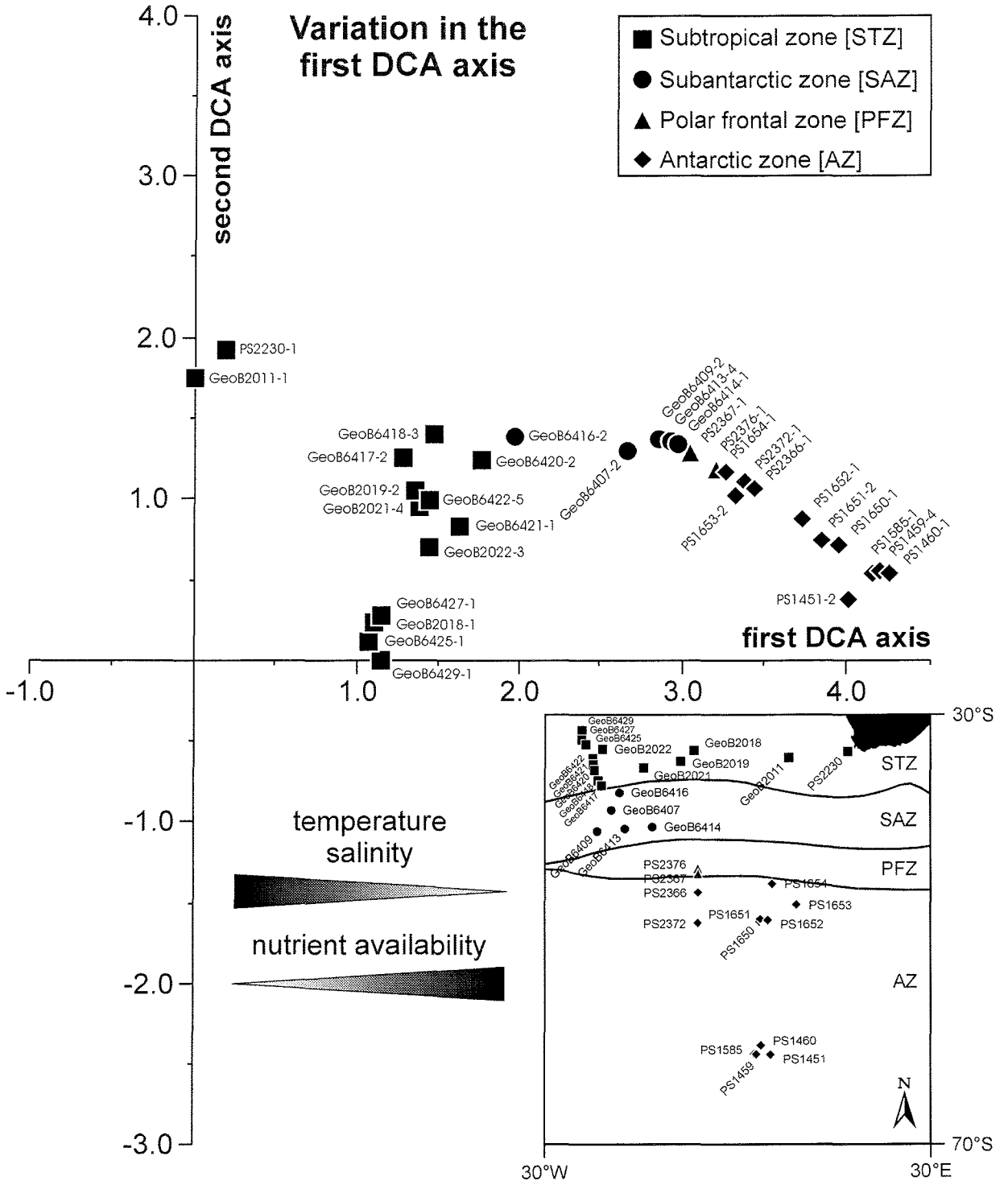

Fig. 12. The variance in sample distribution shown by the first DCA axis shows a strong correlation with the parameters sea surface temperature, salinity and nutrient concentration (see text for further explanation).

Discussion

Besides the inherent biological process of cyst production, oceanographic processes such as transport, erosion, resedimentation, dilution and preservation may influence and alter the assemblage compositions found in surface sediment samples.

Transport

Organic-walled dinocysts behave like silt particles in the water column (Anderson et al., 1985). The Southern Ocean is an area of large water volume transport by both the high velocity, upper level currents of the ACC (Peterson and Stramma 1991) and fast bottom water currents, especially below the Weddell Gyre (Pudsey, 1992). Sediment particles sinking through the water column are prone to lateral transport as well as post depositional relocation by bottom currents (Frank et al., 1996). Although large influence of sediment erosion and redeposition can be excluded in the observed areas due to the absence of reworked dinocysts older than the Quaternary in the surface sediment, reworking of Quaternary sediments cannot be excluded due to similar dinocysts occurring in Quaternary glacials and interglacials.

The dinocysts show sharply defined boundaries in their associations exactly at the oceanic fronts. It is evident that *Impagidinium* cysts occur in higher concentrations north of the Subtropical Front; south of it they are nearly absent. In contrast, peridinioid cysts occur in high numbers only between the Subantarctic Front and the Antarctic Polar Front. These distributions are comparable to the relationship between assemblage compositions and the Southern Ocean frontal system described by Harland et al. (1998) and Marret and de Vernal (1997). Furthermore, the neritic sample (PS2230-1) in the Subtropical Zone does not contain typical species of subtropical oceanic environments, such as *I. variaseptum*, or of subpolar and polar regimes, such as *S. antarctica*. Vice versa, typical neritic species of the genus *Spiniferites* are highly abundant offshore South Africa (Fig. 8d) but are only present in one other sample north of the STF. Such a clear distribution pattern would be unlikely if transport was a major influence in cyst distribution patterns. Therefore, we assume no large influence of lateral transport within the dinocysts assemblages. Major changes in the dinoflagellate cyst association are, however, observed in sediments characteristically half a degree north of the major Southern Ocean fronts (Fig. 5). Studies on the dinoflagellate distribution in surface waters of the Southern Ocean revealed a higher abundance of cyst-producing species south of the STF and APF (Klaas, 1997; Barange et al., 1998; Eynaud et al., 1999). Assuming that dinocyst distribution changes thus occur directly south of the oceanic fronts, we should take into account a slight meridional northward shift of the dinocyst deposition with respect to their corresponding motile stages. This may be due to the subduction of denser surface water masses to the south of an oceanic front below the lighter waters to the north of it (Lutjeharms and Valentine, 1984; Bathmann et al., 1997).

Preservation

The different oxygen concentrations of deep and bottom water masses (Fig. 2) may influence the dinocyst assemblages through the post-depositional degradation of organic matter (Prahl et al., 1997). Zonneveld et al. (1997) have shown a species-dependent susceptibility of organic-walled dinocysts to aerobic degradation. Oxygen-enriched deep and bottom waters are especially corrosive for the thin, brown walls of peridinioid cysts. Transparent walls of gonyaulacoid cysts, such as those of the genus *Impagidinium*, seem to be more resistant against corrosion (Zonneveld et al., 2001b).

We observed very low concentrations of dinocysts in two samples of the Maud Rise (PS1451-2 and PS1460-1), influenced by oxygen-rich Weddell Sea Deep Water and Weddell Sea Bottom Water (Fig. 2a). The relative abundance of *I. sphaericum* in the sample PS1451-2 is very high (Fig. 7c) compared to the assemblages of the two adjacent samples (PS1459-1 and PS1585-2). These adjacent samples, deposited at shallower depths under the influence of less corrosive Circumpolar Deep Water, show more then ten times higher concentrations of dinocysts. Therefore, we assume an alteration of the dinocyst assemblage at the Maud Rise, especially due to enhanced decay of peridinioid cysts in samples influenced by oxygen-rich deep and bottom waters.

Nevertheless, we could not find any other signs for increased degradation of dinocysts in oxygen-rich deep waters in the whole area north of the ACC-Weddell Gyre Boundary. We thus assume that, with the exception of the southernmost samples, ecological processes rather than aerobic degradation control cyst distribution changes in the Southern Ocean.

Cyst production

Subtropical Zone

In this study, mainly gonyaulacoid cysts (more than 16 different species) were discovered in relatively high numbers in the Subtropical Zone, which is characterised by nutrient-depleted Subtropical Water. Photo-autotrophic gonyaulacoid dinoflagellates are found nowadays in the more stable, predictable and nutrient-poor environments (Harland et al., 1998). They are capable of surviving adverse conditions, as long as they get enough sunlight. Therefore, they can prosper in the oligotrophic regions of the open ocean.

In the STZ, the assemblage of gonyaulacoid species is dominated by *Impagidinium* species. All *Impagidinium* species seem to show a similar distribution, although the most prominent species, *I. variaseptum,* has contrarily been described by Marret and de Vernal (1997) as a species with an affinity to outer-neritic environments compared to the two other prominent *Impagidinium* species, *I. aculeatum* and *I. sphaericum*. The latter two species have been described as oceanic, with temperate to tropical affinities (Edwards and Andrle, 1992). *Pyxidinopsis reticulata* seems to prefer a similar environment to the temperate, oceanic *Impagidinium* species because of its co-occurrence.

In contrast to the gonyaulacoid cysts, the cysts of peridinioid dinoflagellates are rarely present in the STZ. These heterotrophic dinoflagellates take advantage on environments with high nutrient content which encourages increased diatom populations upon which the heterotrophic dinoflagellates mainly feed (Harland et al., 1998). Thus, the low numbers of peridinioid cysts in the warm, oligotrophic area north of the STF may be the result of low food supply (e.g. diatoms). This assumption is supported by the statistical analysis. Due to the positioning of mostly all peridinioid cysts on the right hand side of the first DCA axis (Figs. 11 and 12), an affinity to high nutrient availability is suggested and hence availability of prey species.

The higher numbers of *Protoperidinium* cysts in the vicinity of the front suggest more favourable conditions there compared to the oligotrophic regime, which may be due to the slightly increased nutrient concentrations at the front and consequently higher abundances of primary and secondary producers (Barange et al., 1998).

Subtropical Front

The Subtropical Front, a band of turbulent water movement, is characterised by an abrupt temperature drop compared to the STZ. Here, the dinocyst assemblage is composed of lower numbers of *Impagidinium* species together with higher numbers of the cosmopolitan species *Nematosphaeropsis labyrinthus* and cysts of *Protoceratium reticulatum*. The latter two are thought to be highly tolerant species with an affinity for transitional areas between oceanic and neritic environments (Edwards and Andrle, 1992; Dale, 1996). Therefore, this assemblage shift is most probably related to the transition from oligotrophic, stable, stratified surface water masses of the STZ to the turbulent, higher nutrient regime of the STF (Eynaud et al., 1999).

Compared to other Antarctic dinoflagellate studies (Marret and de Vernal, 1997; Harland et al., 1998), the almost complete absence of *Bitectatodinium tepikiense*, *Dalella chathamensis* and cysts of *Pentapharsodinium dalei* (Fig. 9) is remarkable. According to Dale (1996), *B. tepikiense* is characteristic for the transition from temperate to subpolar regimes in the Northern Hemisphere, especially in frontal structures. Therefore, we would expect this species to occur in higher numbers at the STF. However, *B. tepikiense* occurs in low numbers only in a few samples distally north of the STF, whereas its appearance south of the STF is limited to only one cyst. Therefore, this species seems to react differently in similar environments of both hemispheres. Marret and de Vernal (1997) suggested that *I. variaseptum* and *D. chathamensis* may be characteristic for the Southern Hemisphere. In their study, they show highest relative abundances of *I. variaseptum* in the subtropical domain and of *D. chathamensis* in the subantarctic domain. In our study, *I. variaseptum* shows a similar distribution. However, contrary to its occurrence in few numbers south of the APF in the western Atlantic sector of the southern Ocean (Harland et al., 1998) *D. chathamensis* is not observed south of the SAF in the eastern Atlantic sector (Fig. 9b). This might be attributed to transport from the Pacific Ocean to the western Atlantic sector through Drake Passage by high velocity currents.

Subantarctic Zone

The Subantarctic Zone south of the STF is rather oligotrophic, which is reflected by low diatom abundances in the surface waters (Eynaud et al., 1999) and in the surface sediments (Zielinski and Gersonde, 1997). The dinocyst assemblage reflects these circumstances with an association similar to that found north of the STF.

Further southward in the SAZ, a significant change in assemblage composition from a gonyaulacoid- to a peridinioid-dominated association is observed, coinciding with much higher concentrations of both cyst groups. Furthermore, an increase of peridinioid species diversity is found. Studies on diatom distribution in the same area reveal a change from the low nutrient environment of the SAZ to a nutrient-rich, high primary production regime in the Polar Frontal Zone with highest abundances of diatoms at the SAF and further southwards (Zielinski and Gersonde, 1997). The corresponding higher cyst concentrations of heterotrophic species, together with their higher diversity, may be due to this change to surface water masses dominated by silicious organisms, which form a favourable prey for heterotrophic dinoflagellates (Froneman and Perissinotto, 1996; Klaas, 1997; Harland et al., 1998). In our study, this environmental change is expressed by the change of the peridinioid/gonyaulacoid index [p/g index = peridinioid cysts/g / (peridinioid cysts/g + gonyaulacoid cysts/g)], comparable to the p/g ratio used by Harland et al. (1998) as a proxy indicator for productivity. Within the Subantarctic Zone, the index changes gradually from gonyaulacoid-dominated to peridinioid-dominated (Fig. 5). In the observed area, this index thus seems to be useful in revealing oceanographic changes especially between the STF and SAF, and hence could be of future use in reconstructing the Late Quaternary dynamics of the frontal system.

Nevertheless, not only the increase in abundance of prey alone but also a change in the types of organisms forming the prey may be of importance for the occurrence of specific heterotrophic dinoflagellates. Harland and Pudsey (1999) investigated the distribution of dinoflagellate cysts and diatoms species in sediment traps of the Southern Ocean. In their study, they show predominance of *S. antarctica* in Weddell Sea traps, which coincides with high abundances of well-preserved sea ice diatoms. In contrast, traps of the Bellingshausen Sea and Scotia Sea contain mainly cysts of *Protoperidinium* spp. and large amounts of well-preserved oceanic diatoms. Hence, further studies are necessary to reveal the relationships between heterotrophic dinoflagellates and their prefered prey.

The spiny cysts of *Echinidinium* spp. are well known from modern sediments of upwelling areas of the Arabian Sea (Zonneveld, 1997) and the subtropical southeastern South Atlantic Ocean (Zonneveld et al., 2001a). Because of their pressumed protoperidinioid affinity, their low occurrence in samples of the oligotrophic, open ocean environment (Fig. 10d) is not surprising. The lack of *Echinidinium* spp. in samples south of the SAF may suggest a temperature dependence to tropical and temperate areas.

The assumption that temperature of the surface waters is another major factor controlling the dinoflagellate distribution in the Southern Ocean in addition to the nutrient concentration is supported

by the statistical analysis. Due to the generally uniform and latitudinally changing distribution pattern of oceanographic characteristics such as surface temperature, salinity and nutrient distribution (Fig. 3), the DCA of relative dinocyst abundances reveals only one significant controlling gradient in meridional direction (Fig. 12). Thus, the grouping of the different dinocyst species along this axis may be caused by their dissimilar temperature tolerance ranges in addition to the variations in nutrient supply. Groups 1 and 2, mainly containing gonyaulacoid species (Fig. 11), show a high affinity to the warm neritic and open ocean subtropical regimes, respectively, whereas the third group, mainly composed of heterotrophic species, seems to be restricted to the cold, high productivity areas of the subpolar regime.

Polar Frontal Zone and Antarctic Zone

At the Antarctic Polar Front, the surface water environment changes once again due to the transition from Subpolar Surface Water to Antarctic Surface Water. In the Polar Frontal Zone north of the APF and in the northern Antarctic Zone between the APF and the ACC-Weddell Gyre Boundary, we found only a few *Impagidinium* specimens as well as *P. reticulata*, cysts of *P. reticulatum* and *N. labyrinthus*. The latter two were not observed further southward in the AZ beyond the ACC-WGB.

Studies on dinocyst distributions in the North Atlantic Ocean have revealed that only a few species occur in areas with sea-surface temperatures around freezing point, as it may also be the case at the ACC-WGB and further southwards. Only *Impagidinium pallidum*, *Impagidinium sphaericum*, *Spiniferites elongatus*, cysts of *Protoperidinium* spp. and *Pentapharsodinium dalei* occure in high latitude areas of winter sea-ice cover in the Northern Hemisphere (de Vernal et al., 1994; de Vernal et al., 1997; Rochon et al., 1999). Therefore, the cold Antarctic Surface Water of the Antarctic Zone seems to exceed the temperature tolerance spectrum of *N. labyrinthus* and *P. reticulatum*, as well as most of the other gonyaulacoid cysts. These cysts possibly reflect the transition from the permanently ice-free AZ to the cold surface waters near the maximum winter sea-ice boundary (Fig. 1).

Only *I. variaseptum* and *I. sphaericum* are found in the southern AZ, a region of seasonal ice cover. According to Edwards and Andrle (1992), *I. sphaericum* possesses a broad temperature range with a tolerance for cold-temperate environments, which would explain its wide-spread occurrence from the subtropical region southwards into the subpolar region. Furthermore, the distributions reflect a certain amount of tolerance which few *Impagidinium* species have for seasonal ice cover. This is supported by studies in high latitude areas of the North Atlantic Ocean (Rochon et al., 1999). However, the low abundance of *I. pallidum* is remarkable. Harland et al. (1998) pointed out its presence in many samples of the Weddell Sea and Scotia Sea, with low absolute concentrations but with high relative abundances. Marret and de Vernal (1997) described the distribution of this species in the Pacific sector of the Southern Ocean as abundant in the Antarctic domain to common in the Subtropical domain. The cause of its limitation to some subtropical and subantarctic samples, together with its absence in antarctic samples, is still unclear.

In contrast, the concentrations of *Cryodinium meridianum* gen. nov. sp. nov., cysts of *Protoperidinium* spp. and *S. antarctica* are extremely high within the PFZ and AZ. In general, the appearance of peridinioid cysts in their highest numbers, especially in the PFZ, may be due to the high phytoplankton abundances in these areas, especially along oceanic fronts separating water masses (Bathmann et al., 1997). This is supported by Froneman and Perissinotto (1996), who pointed out a strong co-variance of protozooplankton, which includes heterotrophic dinoflagellates, with phytoplankton abundance in the Southern Ocean.

Amongst the peridinioid dinocysts, *C. meridianum* seems to be endemic within a narrow distribution range between the APF and the ACC-Weddell Gyre Boundary. Its highest abundance occurs distally off the fronts of this region. Only one specimen of this species is found further southwards at the Maud Rise. Beyond the observed areas, paratabulated "round browns" have not been discovered in the Southern Ocean yet.

Focusing on the changes in concentration and in particular, the relative abundance of cysts of *Protoperidinium* spp., it becomes obvious that the distribution of *Protoperidinium* spp. (with *P. conicoides* as its most prominent member) is highest between the SAF and the APF, and than decreases slightly towards the ACC-WGB. In oceanic regions of the North Atlantic Ocean, the distribution of cysts of *Protoperidinium* spp. suggests high tolerance for a large temperature and salinity range and sea-ice cover, but a greater dependence on food supply (Rochon et al., 1999). The diatom occurrence in the Southern Ocean is at its maximum within the opal belt between the SAF and the northern part of the Antarctic Zone, which is seasonally covered by sea-ice (e.g. Zielinski and Gersonde, 1997). In the studied area, the maximum winter sea-ice border and the ACC-Weddell Gyre Boundary are nearly congruent. The distribution of cysts of *Protoperidinium* spp. in the observed area is thus associated with the region of highest bioproductivity.

In contrast, the peridinioid cysts of *S. antarctica*, characteristic for the Southern Hemisphere, show higher numbers south of the APF and have a maximum abundance between the APF and the ACC-WGB. More significantly, their relative abundance increases southwards to a maximum at the Maud Rise. This suggests a large tolerance for polar environments of seasonal ice cover and/or low temperatures. On the other hand, its high abundance south of the APF may also be due to the seasonal growth in phytoplankton stock (Eynaud et al., 1999) related to an upwelling-associated increase in trace metals, especially iron (Bathmann et al., 1997). However, there is no evidence for a direct influence on heterotrophic dinoflagellate distribution by melting ice of the marginal ice zone (Bathmann et al., 1997).

Nevertheless, the ratio between cysts of *Protoperidinium spp.* and *S. antarctica* seems to be a useful method to determine the location of the Antarctic Polar Front in the Southern Ocean. There is not enough data in this study to make assumptions about the location of the ACC-Weddell Gyre Boundary, but dinoflagellate cysts seem to possess the potential to solve such questions.

Conclusion

The analysis of 32 surface sediment samples of the Southern Ocean (eastern Atlantic sector) between the Subtropical Front and the Weddell Gyre revealed a clearly distinguishable distribution pattern of organic-walled dinoflagellate cysts in relation to the water masses and frontal features of the Antarctic Circumpolar Current. Cysts of the photo-autotrophic, oceanic *Impagidinium* species are highly abundant north of the Subtropical Front. South of the STF, gonyaulacoid species capable of tolerating unpredictable environments, i.e. *Nematosphaeropsis labyrinthus* and cysts of *Protoceratium reticulatum*, seem to indicate the transition from Subtropical Surface Water to Subantarctic Surface Water. Cysts of heterotrophic dinoflagellates, such as *Protoperidinium* spp. and *Selenopemphix antarctica*, dominate the assemblages in the phytoplankton-rich water masses from the Subantarctic Front to the south. Cysts of *Protoperidinium*. spp. seems to be more characteristic for the environment around the Antarctic Polar Front, whereas *S. antarctica* increases in number south of the APF towards the boundary between the ACC and the Weddell Gyre. A newly discovered dinoflagellate cyst species, *Cryodinium meridianum* gen. nov. sp. nov., shows a relatively endemic distribution pattern between the APF and the ACC-Weddell Gyre Boundary. At the Maud Rise, a region of seasonal sea-ice cover, cysts of *S. antarctica* are present in low numbers, but with relative abundances of up to 100%, showing this species' high tolerance for low temperatures and for sea-ice cover.

The distribution of dinoflagellate cysts in the Southern Ocean compared to environmental parameters of the upper water column, suggests a general dependancy on surface water temperature and nutrient distribution, which is in turn reflected by the abundance of primary producers such as diatoms. The characteristic distribution patterns of individual cyst species may be useful for the reconstruction of palaeoenvironmental and/or palaeoceanographic changes, such as frontal shifts of the STF and the APF, in late Quaternary time series. Therefore, the dinocyst assemblage of the Southern Ocean possess a large potential for the use of transfer functions.

Acknowledgements

We thank everyone in the working group of Historical Geology and Palaeontology at Bremen University for their general assistance and discussion. Annemiek Vink is thanked for English corrections. Furthermore, we thank Hannes Grobe of the Alfred Wegener Institut for supporting the sample selection (sample data is available in the PANGAEA-Data Base: http://www.pangaea.de/home/oesper/). Finally we thank the referees Fabienne Marret and Rex Harland for their helpful comments on this manuscript. This research was funded by the Deutsche Forschungsgemeinschaft through the special research project Sonderforschungsbereich 261 "Der Südatlantik im Spätquartär: Rekonstruktion von Stoffhaushalt und Stromsystemen". This is SFB 261 contribution number 339.

Appendix A. Taxonomy

The dinoflagellate cyst species observed in this study of 32 surface sediment samples of the Southern Ocean (Atlantic sector) are listed below in alphabetical order. Type material and dinoflagellate cysts shown on plates I-III are stored at the Geosciences Collection of the University of Bremen.

Division DINOFLAGELLATA (Bütschli, 1885) Fensome et al., 1993
Subdivision DINOKARYOTA Fensome et al., 1993
Class DINOPHYCEAE Pascher, 1914
Subclass PERIDINIPHYCIDAE Fensome et al., 1993
Order GONYAULACALES Taylor, 1980
Suborder GONYAULACINEAE (Autonym)
Family GONYAULACACEAE Lindemann, 1928
Subfamily CRIBROPERIDINIOIDEAE Fensome et al., 1993
Genus ***Operculodinium*** Wall, 1967
Operculodinium israelianum (Rossignol, 1962) Wall, 1967 (Plate II, 7-9)
Genus ***Protoceratium*** Bergh, 1881a in Fensome et al., 1993
Protoceratium reticulatum (Claparède and Lachmann, 1859) Bütschli, 1885 (Plate II, 5 and 6)

Within the cysts of *Protoceratium reticulatum,* a large morphological variation was observed. The specimens vary in process shape, process length, and most often in the structure of the distal endings of the processes. Because of the large morphologic variation, a clear distinction between *Operculodinium israelianum* and cysts of *P. reticulatum* was often difficult. The taxon *O. israelianum,* on the other hand, contains different morphotypes with normal processes (var. long) and those with reduced process length (var. short). The predominant morphotype of the observed area possesses reduced processes (Plate II, 7-9).

Subfamily GONYAULACOIDEAE (Autonym)
Genus ***Bitectatodinium*** Wilson, 1973
Bitectatodinium tepikiense Wilson, 1973
Genus ***Dalella*** McMinn and Sun, 1994
Dalella chathamensis McMinn and Sun, 1994
Genus ***Impagidinium*** Stover and Evitt, 1978
Impagidinium spp. indet.

The taxon *Impagidinium* spp. represents a group of different species rather than a clearly determined single morphotype, including *Impagidinium* specimens with an unclear relation due to bad preservation or with unidentifiable species characteristics.

Impagidinium aculeatum (Wall, 1967) Lentin and Williams, 1981 (Plate I, 1-3)
Impagidinium pallidum Bujak, 1984
Impagidinium paradoxum (Wall, 1967) Stover and Evitt, 1978 (Plate I, 4-6)
Impagidinium patulum (Wall, 1967) Stover and Evitt, 1978
Impagidinium plicatum Versteegh and Zevenboom, 1995
Impagidinium sphaericum (Wall, 1967) Lentin and Williams, 1981 (Plate I, 7-9)
Impagidinium strialatum (Wall, 1967) Stover and Evitt, 1978 (Plate II, 1 and 2)
Impagidinium variaseptum Marret and de Vernal, 1997 (Plate I, 10-12)
Genus ***Nematosphaeropsis*** Deflandre and Cookson, 1955
Nematosphaeropsis labyrinthus (Ostenfeld, 1903) Reid, 1974 (Plate II, 3-4)
Genus ***Spiniferites*** Mantell, 1850
Spiniferites spp. indet.

Because of their low occurrence in the observed area, all specimens belonging to the genus *Spiniferites*, including *S. bulloides*, *S. elongatus*, *S. mirabilis*, *S. pachyderma* and *S. ramosus*, are grouped in *Spiniferites* spp.

Subfamily uncertain
Genus ***Pyxidinopsis*** Habib, 1976
Pyxidinopsis reticulata McMinn and Sun, 1994 (Plate II, 10-12)

Order PERIDINIALES Haeckel, 1894

Suborder PERIDINIINEAE (Autonym)
Family PERIDINIACEAE Ehrenberg, 1831
Subfamily CALCIODINELLOIDEAE Fensome et al., 1993
Genus ***Pentapharsodinium*** Indelicato and Loeblich III, 1986
Pentapharsodinium dalei Indelicato and Loeblich III, 1986

Family PROTOPERIDINIACEAE Bujak and Davies, 1998
Subfamily PROTOPERIDINIOIDEAE (Autonym)

Genus ***Cryodinium*** gen. nov.

Type: *Cryodinium meridianum* gen. nov. sp. nov.

Etymology: Greek, *cryos* (cold) in reference to the first discovery of this genus in sediments of the Southern Hemisphere subpolar region.

Diagnosis: Sphaeroidal protoperidinioid cysts with an intercalary archeopyle formed by the loss of the two paraplates 1a and 2a. Surface smooth or granular to scabrate and brown in colour. Single layered wall with low sutures reflecting a peridinioid tabulation pattern of 4′, 3a, 7′′, 3c, 5′′′, 2′′′′.

Discussion: Spheroidal, brown cysts with smooth or slightly granulated single or double layered walls are known to be produced by dinoflagellates of the genus *Protoperidinium,* which is defined by the tabulation of 4′, 2-3a, 6-7′′, 3c, 5′′′, 2′′′′ plus a transitional cingular-sulcal plate (Balech, 1974). *Cryodinium* gen. nov. fulfils these criteria, but as its cyst-theca relation is presently unknown, we decided to erect a new fossil genus (see later discussion on *Cryodinium meridianum* gen. nov. sp. nov.).

Some modern "round brown" cyst species reflect a peridinioid tabulation pattern as evidenced by the shapes of their hexagonal archeopyles, including cysts of *Protoperidinium avelanum* and *Protoperidinium conicoides* (Balech, 1974). However, they are clearly distinguishable from cysts of *Cryodinium* by their lack of sutures that reflect a paratabulation. This is also the case for the species of *Brigantedinium*, which is a fossil genus of round, brown cysts related to *Protoperidinium* species. *Brigantedinium* species as well reflect no paratabulation pattern besides the archeopyle (Read, 1977). Other paratabulated round brown cysts known from modern sediments include *Protoperidinium americanum*, *Zygabikodinium lenticulatum* and members of the genus *Dubridinium* (Loeblich and Loeblich, 1970; Reid, 1977; Lewis and Dodge, 1987). However, the pale brown cysts of *P. americanum* reflect tabulation pattern only through the shape of the archeopyle with other tabulation-like features due to gentle folding (Lewis and Dodge, 1987). *Z. lenticulatum* has an tabulation pattern 3′, 2a, 7′′, 3c, 5′′′, 1′′′′ reflected by thin sutures and has an archeopyle formed by rupture along a suture between the precingular and cingular plate series(Loeblich and Loeblich, 1970; Bujak and Davies, 1983). This is in contrast to *Cryodinium* which has four apical plates and an archeopyle formed by the loss of two intercalary paraplates. *Dubridinium* is most unlikely to be related to *Cryodinium*, since it is cavate and the paratabulation is restricted to the reflection of the cingulum only (Reid, 1977).

Cryodinium may be related to the Cretaceous "round brown" genus *Trithyrodinium*, defined by a symmetrical 3I archeopyle and no paratabulation-reflecting sutures (Evitt, 1985). However, this is

in contrast to the 2I archeopyle and the paratabulation-reflecting sutures of *Cryodinium*. Therefore, specimens of *Cryodinium* are the first "round brown" cysts with a fully reflected paratabulation on the epicyst and hypocyst and a 2I archeopyle to be found in modern sediments.

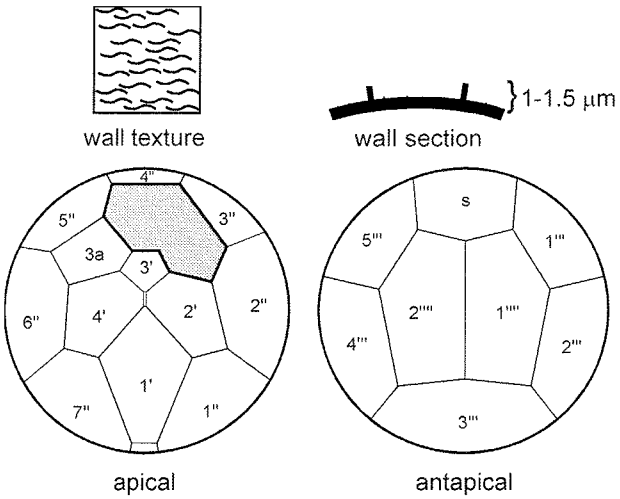

Fig. 13. Line drawing of the new species *Cryodinium meridianum* gen. nov. sp. nov. The apical view shows a peridinioid plate pattern with a 2i archaeopyle (plates 1a and 2a).

Cryodinium meridianum gen. nov. sp. nov. (Fig. 13; Plate III, 1-9)

Holotype: GSUB M1, Sample PS2376-2/1 (England Finder coordinates K35/3)

Paratype: GSUB M2, Sample PS2366-1/4 (England Finder coordinates U42/2)

Repository: Geosciences Collection of the University of Bremen

Type location: The Antarctic Circumpolar Current at the Antarctic Polar Front, westward of the Greenwich Meridian.

Etymology: Latin, *meridianus* (southerly) in reference to the first discovery of this species in higher latitudes of the Southern Hemisphere around the Greenwich Meridian.

Diagnosis: Protoperidinioid cyst with a peridinioid tabulation pattern fully reflected by low sutures. Sphaeroidal, proximate, brown cyst comprised of an autophragm with scabrate texture. Tabulation pattern: 4′, 3a, 7′′, 3c, 5′′′, 2′′′′ with an ortho-style first apical plate and a 2I-archeopyle (1a and 2a) with a hexagonal 2a-plate.

Description: The strongly pigmented brown cysts are sphaeroidal in shape with a single layered, thin wall (~1 µm). The wall surface is weakly to moderately scabrate with a paratabulation reflected by sutures of low septa (1-1.5 µm). Occasionally gentle folding is visible and appears to subdivide the paraplates. The intercalary archeopyle is formed by the seperation of a single operculum consisting of two paraplates, which is sometimes attached but is usually absent.

Dimensions: Range in maximum diameter is 30 (39) 49 µm. Sutures are 1-1.5 µm heigh. Number of specimens measured is 8.

Remarks: The cysts are seldomly well preserved. Most of the specimens are crushed, flattened or torn. The reflection of the paratabulation varies from prominent to nearly absent but the typical wall texture of this species is always present.

Discussion: *Cryodinium meridianum* is related to the genus *Protoperidinium*, which includes the majority of modern peridiniinean species (Bujak and Davies, 1983), from its paratabulation pattern. Due to its three intercalary plates, *C. meridianum* would fit into the sub-genus *Protoperidinium* (Bujak and Davies, 1983). *C. meridianum* is most likely produced by a *Protoperidinium* species with ortho-style 1′ and hexa-style 2a paraplates.

Genus ***Protoperidinium*** (Bergh, 1881) Balech, 1974
Protoperidinium spp. indet.

"Round, brown" cysts of *Protoperidinium* are grouped together in *Protoperidinium* spp. as it is frequently impossible to recognise the archeopyle type and consequently to identify on species level. Some of the samples contain two different types of "round browns". Both morphotypes are clearly distinguishable by their pigmentation; one morphotype is typically medium to dark brown in colour, whereas the other one is light brown to beige in colour. Both morphotypes include cysts with an archeopyle similar to that of *Protoperidinium conicoides* (Plate III, 12). However, due to the unknown cause of this phenomenon, both light brown and dark brown cysts were included in *Protoperidinium* spp.

Protoperidinium conicoides (Paulsen, 1905) Balech, 1974 (Plate III, 12)
Genus ***Selenopemphix*** (Benedek, 1972) Head, 1993
Selenopemphix antarctica Marret and de Vernal, 1997 (Plate III, 10 and 11)

Subfamily uncertain
Genus ***Echinidinium*** Zonneveld, 1997
Echinidinium spp. indet.

Because of their low occurrence in the observed area, all spiny, brown cysts of the genus *Echinidinium*, including *E. aculaeatum*, *E. delicatum*, *E. granulatum* and *E. transparantum*, were grouped within *Echinidinium* spp.

Plate I

Images of common *Impagidinium* cysts of the South Atlantic Ocean (line bars represent 10 µm).

1. *Impagidinium aculeatum.* Ventral view (internal).
2. *Impagidinium aculeatum.* Cross section.
3. *Impagidinium aculeatum.* Dorsal view (external).
4. *Impagidinium paradoxum.* Ventral view (internal).
5. *Impagidinium paradoxum.* Cross section.
6. *Impagidinium paradoxum.* Dorsal view (external) with 3′′ archaeopyle.
7. *Impagidinium sphaericum.* Ventral view (external).
8. *Impagidinium sphaericum.* Cross section.
9. *Impagidinium sphaericum.* Dorsal view (internal).
10. *Impagidinium variaseptum.* Ventral view (internal).
11. *Impagidinium variaseptum.* Cross section.
12. *Impagidinium variaseptum.* Dorsal view (external).

Plate I

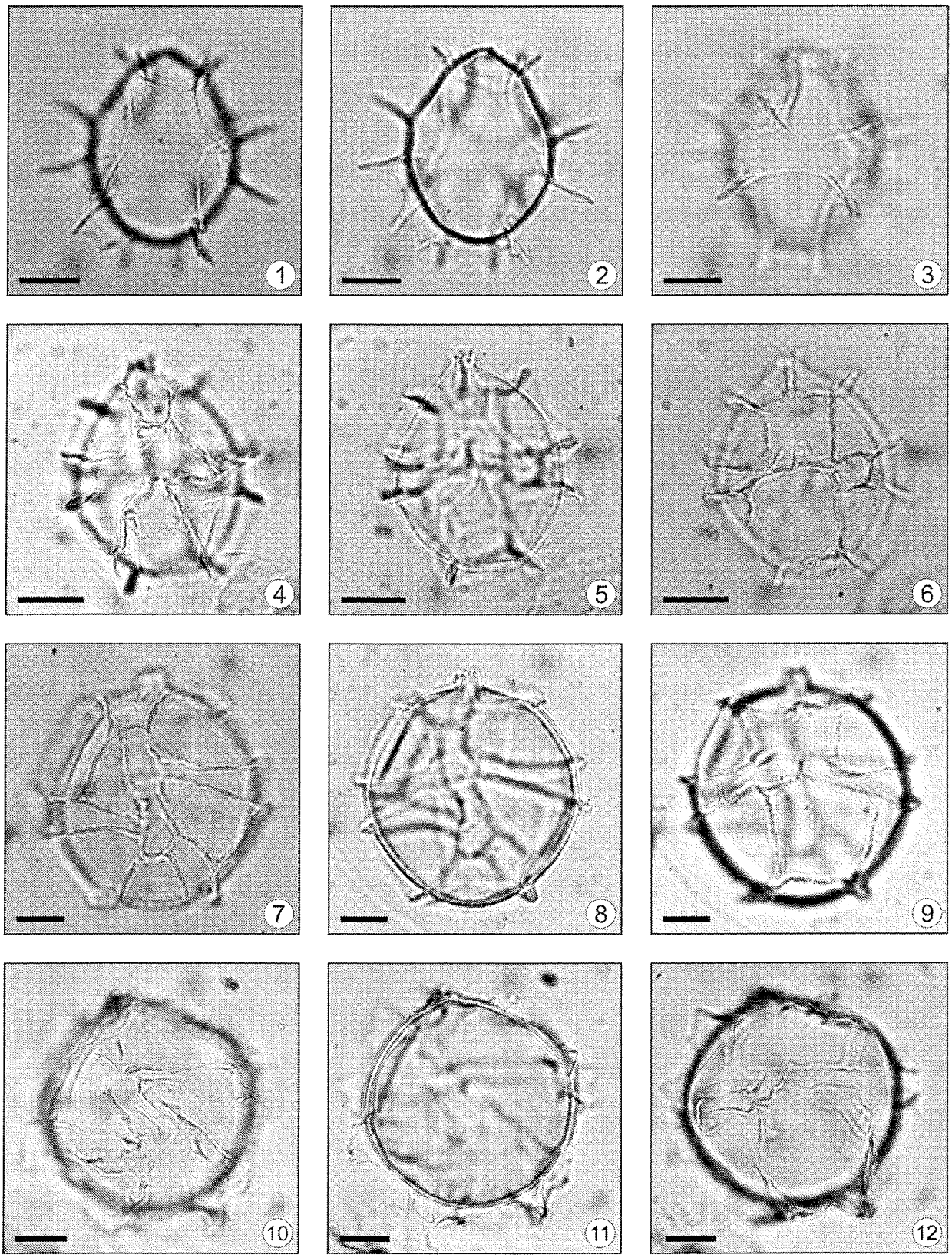

Plate II

Images of common gonyaulacoid cysts of the Antarctic Circumpolar Current (line bars represent 10 μm).

1. *Impagidinium strialatum.* Dorsal view (external) with 3'' archaeopyle.
2. *Impagidinium strialatum.* Cross section.
3. *Nematosphaeropsis labyrinthus.* Dorsal view (external).
4. *Nematosphaeropsis labyrinthus.* Cross section.
5. *Protoceratium reticulatum.* Dorsal view (external) with archaeopyle.
6. *Protoceratium reticulatum.* Cross section.
7. *Operculodinium israelianum* var. short. Ventral view (internal).
8. *Operculodinium israelianum* var. short. Cross section with reduced short processes.
9. *Operculodinium israelianum* var. short. Dorsal view (external) with 3'' archaeopyle.
10. *Pyxidinopsis reticulata.* Ventral view (internal).
11. *Pyxidinopsis reticulata.* Cross section.
12. *Pyxidinopsis reticulata.* Dorsal view (external) with archaeopyle.

Plate II

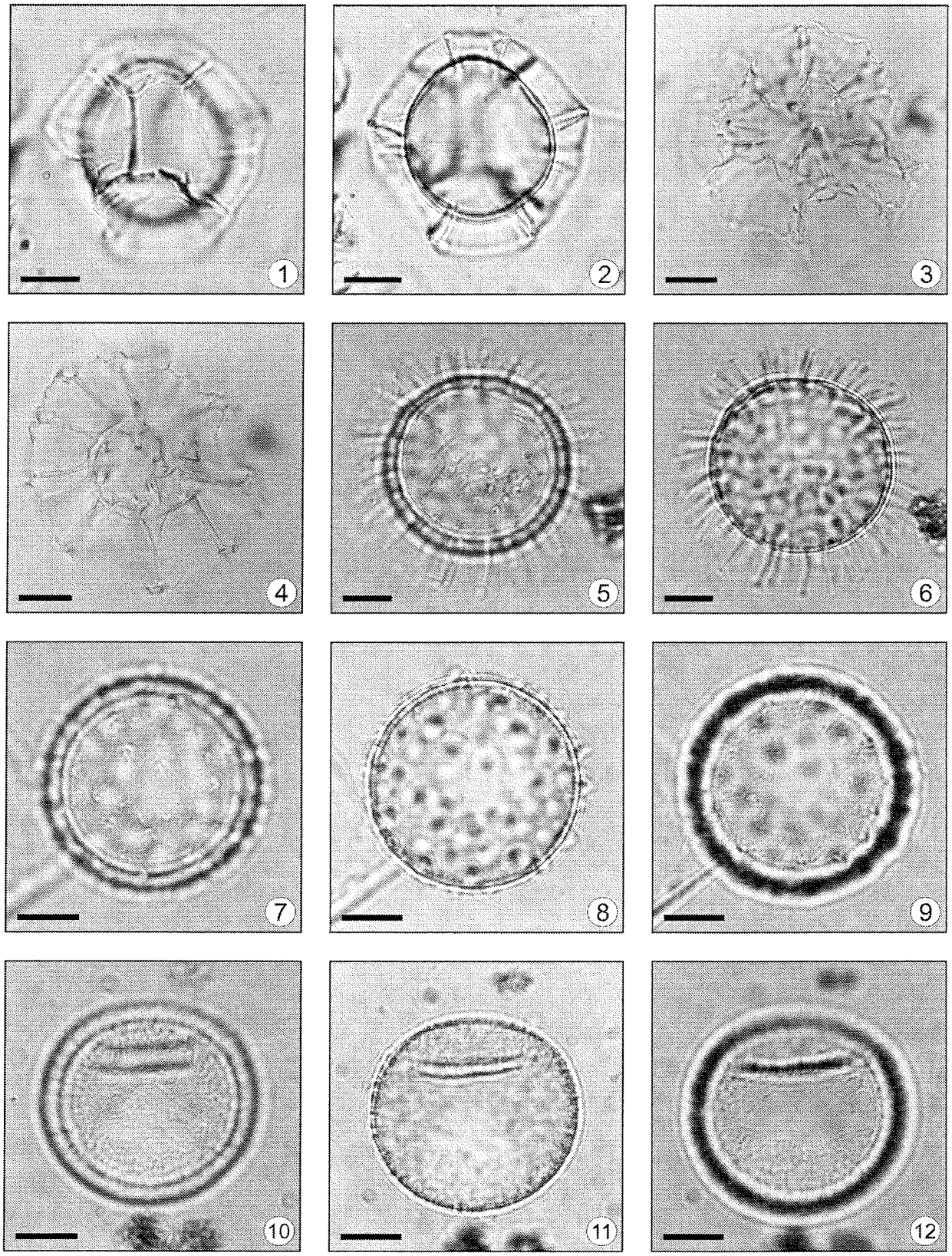

Plate III

Images of the new species *Cryodinium meridianum* gen. nov. sp. nov. and common peridinioid cysts of the Antarctic Circumpolar Current (line bars represent 10 μm).

1. *Cryodinium meridianum*. Holotype. Dorsal view (internal) with 2i archaeopyle.
2. *Cryodinium meridianum*. Holotype. Cross section.
3. *Cryodinium meridianum*. Holotype. Ventral view (external).
4. *Cryodinium meridianum*. Apical view (internal) with 2i archaeopyle.
5. *Cryodinium meridianum*. Cross section.
6. *Cryodinium meridianum*. Antapical view (external).
7. *Cryodinium meridianum*. Dextral view (internal).
8. *Cryodinium meridianum*. Cross section.
9. *Cryodinium meridianum*. Sinistral view (external).
10. *Selenopemphix antarctica*. Apical view.
11. *Selenopemphix antarctica*. Apical view with 1i archaeopyle.
12. *Protoperidinium conicoides*. Dorsal view with 1i archaeopyle.

Plate III

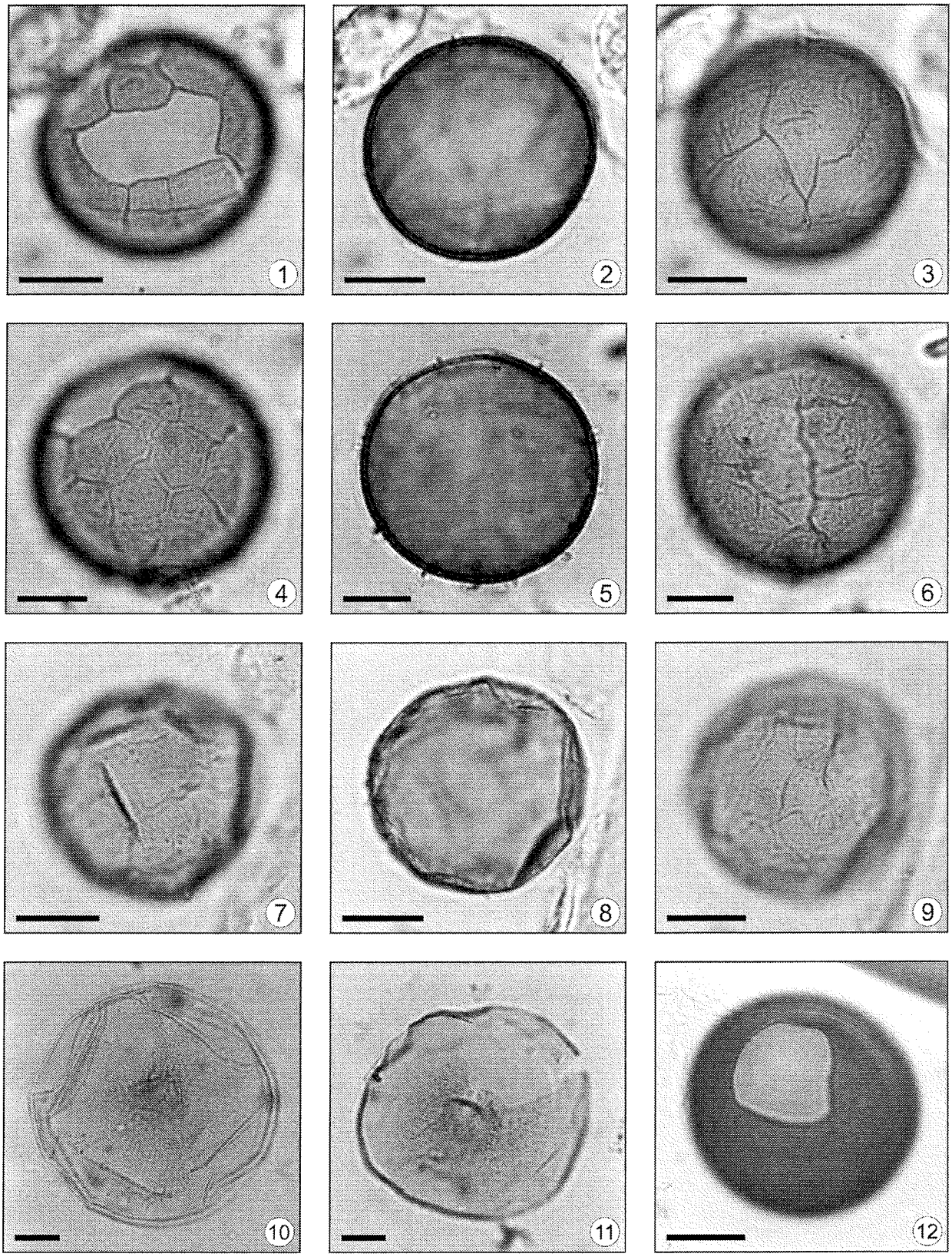

3. Palaeoceanography of the Late Quaternary Agulhas Current (South Atlantic Ocean) based on organic- and calcareous-walled dinoflagellate cysts, pollen and spores

Oliver Esper[1], Gerard J.M. Versteegh[2], Karin A.F. Zonneveld[1] and Helmut Willems[1]

[1]*Universität Bremen, Fachbereich 5 – Geowissenschaften, Postfach 330 440, D-28334 Bremen, Germany*

[2]*Netherlands Institute of Sea Research (NIOZ), P.O. Box 59, 1790 AB Den Burg, Texel, The Netherlands*

Abstract

During the last decades it has become increasingly apparent that climatic change is greatly influenced by changes in the ocean current systems, notably, the global thermohaline circulation. To understand the causes and effects of variations in the thermohaline circulation, it is necessary to study its past variability as well as its causes, preferably for key areas that are essential for sustaining the thermohaline circulation, such as the eastern South Atlantic Ocean.

Here we reconstruct the varying influence of the Agulhas Current, the South Atlantic Current and the Antarctic Circumpolar Current on the eastern South Atlantic Ocean for the last 160,000 years on the basis of dinoflagellate cysts, pollen and spores present in sediment core GeoB 3603-2. This core is derived from the south-eastern Cape Basin offshore South Africa, where the Agulhas Current enters the Atlantic Ocean. Our analyses reveal strong orbital forcing on the heat exchange between the Indian Ocean and the South Atlantic Ocean during the Late Quaternary. Accumulation rates of organic-walled dinoflagellate cysts indicate a dominant precessional forcing on palaeoproductivity with high productivity at times of high seasonal contrast. Calcareous dinoflagellate cysts indicate stratified, oligo- to mesotrophic conditions at times of low seasonal contrast, notably during the glacial Terminations. Additionally, periodicities on a sub-Milankovitch scale as well as modulations of the primary frequencies suggest complex interactions between the subtropical region around Africa and the high latitudes.

Keywords: dinoflagellate cysts, pollen and spores, Agulhas Current, Cape Basin, orbital forcing, palaeoceanography

Introduction

During the last decades it has become apparent that changes in the global ocean current systems greatly influence climate. One of the important oceanic features is the global thermohaline circulation, which transports cold, saline deep water from the northern hemisphere to the south and in return carries southern hemisphere warm surface waters via the South Atlantic Ocean to the northern hemisphere, thereby positively influencing the climate of the northern continents (Gordon, 1986). To understand the causes and effects of variations in the interhemispheric heat flux, it is necessary to have

detailed information on past changes in ocean circulation and their origin, notably for those key areas that seem critical for sustaining the thermohaline circulation, such as the eastern South Atlantic Ocean. Here, the southern tip of Africa forms a bottle-neck for the transport of warm, saline Agulhas Current (AgC) surface water from the Indian Ocean to the Atlantic Ocean and as such plays an important role in balancing the flow of North Atlantic Deep Water to the southern hemisphere (Gordon, 1986). The position of the AgC is the result of a complex interplay between local currents and atmospheric forcing and its evolution through time is presently poorly understood. One of the major forces influencing the oceanographic system is thought to be the periodic variation in solar insolation, the so called Milankovitch forcing (Imbrie et al., 1992). Studies on the tropical and subtropical eastern South Atlantic Ocean and the rain record of South Africa for the last 200 kyr indicate high precessional influence on the atmospheric and oceanic circulation (McIntyre et al., 1989; Schneider, 1991; Pether, 1994; Partridge, 1997). South hereof, in the eastern Atlantic Sector of the Southern Ocean, obliquity seems to be primarily related to environmental change (Brathauer and Abelmann, 1999). As the AgC is located in between these two areas, interferences between precessional-driven and obliquity-driven environmental change are expected, resulting in sub-Milankovitch climate variability (Little et al., 1997). At present it is, however, not clear to what extent such interference affects the AgC at Milankovitch and sub-Milankovitch scales.

Studies carried out in the southern and south-eastern South Atlantic Ocean have shown that organic-walled dinoflagellate cysts are useful indicators for reconstructing the palaeoenvironment and the palaeoceanography (Zonneveld et al., 2001; **Chapter 2**). The calcareous dinoflagellate cysts appear to reflect calm, stratified environmental conditions of the upper water column (Höll et al, 1998; Höll et al., 1999; Vink et al., 2000; Zonneveld et al., 2000; **Chapter 4**) whereas pollen and spores provide terrestrial information. Studies on the Mediterranean Sea and the North and South Atlantic oceans (Versteegh, 1994; Versteegh, 1997; Dupont et al., 1998; Höll and Kemle-von Mücke, 2000) have demonstrated the applicability of organic-walled dinoflagellate cysts, pollen and spores for tracing environmental changes aligned with the orbital forcing on the surface water productivity.

Here, we use organic- and calcareous-walled dinoflagellate cysts (dinocysts) as well as pollen and spores in order to obtain information on past oceanographic systems of the south-eastern South Atlantic Ocean and their possible orbital forcing over the last two glacial/interglacial cycles. This is done on the basis of a sediment core (GeoB 3603-2) located at the nexus of the three oceans surrounding South Africa (Fig. 1).

Present-day meteorology and oceanography

Climate of South Africa

Generally, the South African climate is determined by the position and strength of the subtropical anticyclones, the South Atlantic High (SAH) and the Indian Ocean High (IOH), as well as

by a continental pressure field sited above South Africa (Fig. 2), which varies from a well-developed low during summer to a weak high during winter. (Shannon, 1985). Nowadays, the Cape region is influenced by the westerly wind system with its depressions, reaching the continent during winter (Shannon, 1985) resulting in a Mediterranean-like climate: relatively dry, hot summers are followed by cool, wet winters with precipitation caused by westerly cyclonic disturbances. The westerlies prevent westward dust flux. Only during the short temporal formation of a large high above South Africa in autumn and winter, the wind direction can be westwards to south-westwards (the so called Berg-wind conditions). At these occasions, katabatic wind events may occur that are strong enough for large-scale dust transport up to 150 km offshore (Shannon 1985).

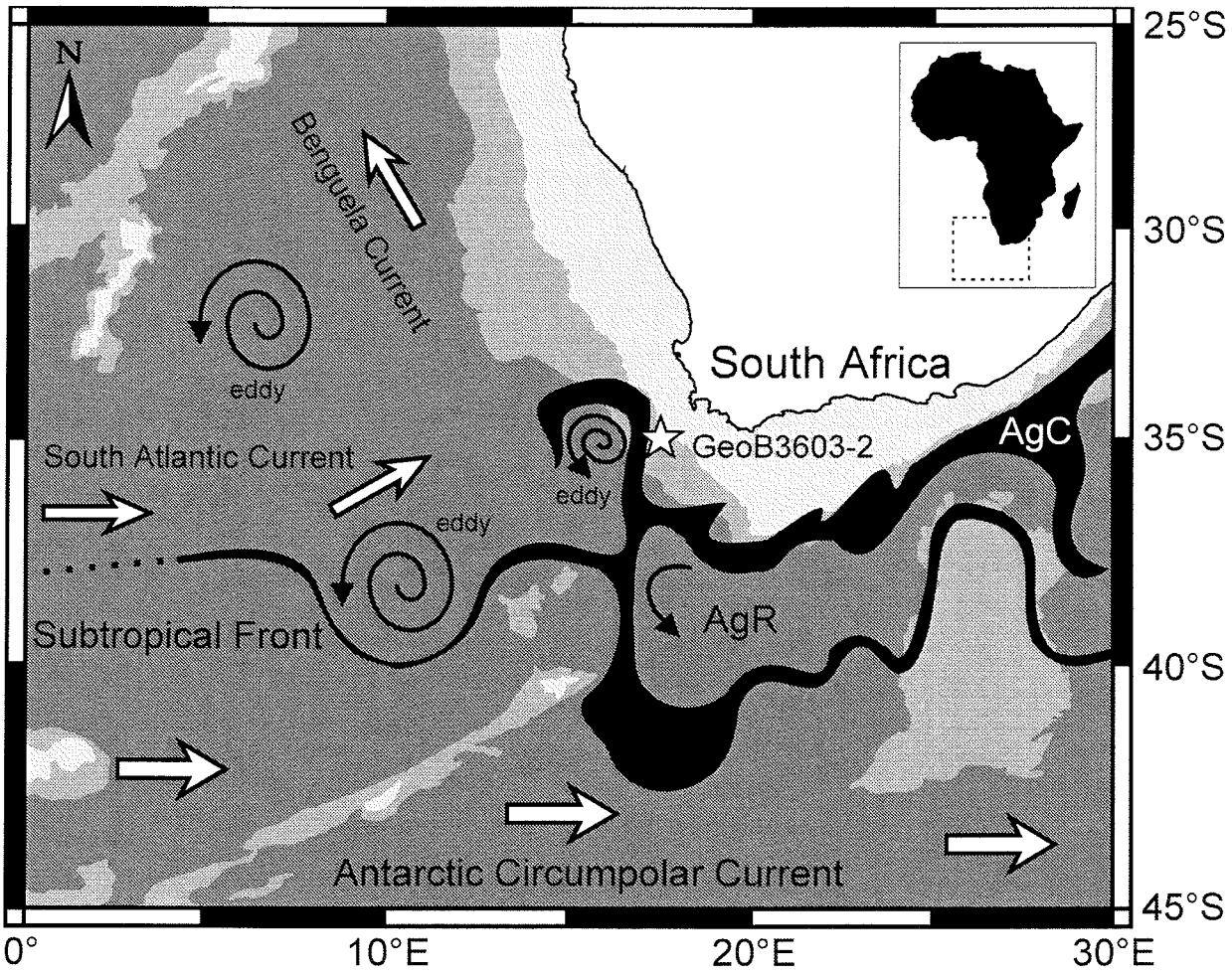

Fig. 1. Present-day oceanography of the Agulhas Retroflection area south of Africa (after Lutjeharms, 1996). The south-westward meandering Agulhas Current (AgC) retroflects into the Agulhas Return Current (AgR), whereby a small amount of Agulhas water invades the South Atlantic Ocean in the form of large, anticyclonic eddies, shed at the retroflection, and filaments between the eddy cores and the South African subcontinent. The position of sediment core GeoB 3603-2 is indicated by an asterisk.

The regions north of the small "Mediterranean" belt are under the control of the subtropical anticyclones throughout the year, resulting in a dry desert climate (Gasse, 2000). The prevailing winds influencing the south-western Cape region nowadays are predominately directed north-westward (alongshore) or north-eastward (inshore), depending on the strength of the SAH and the pressure

variations above South Africa. The wind field offshore western South Africa is controlled by the SAH, resulting in the south-east trade winds.

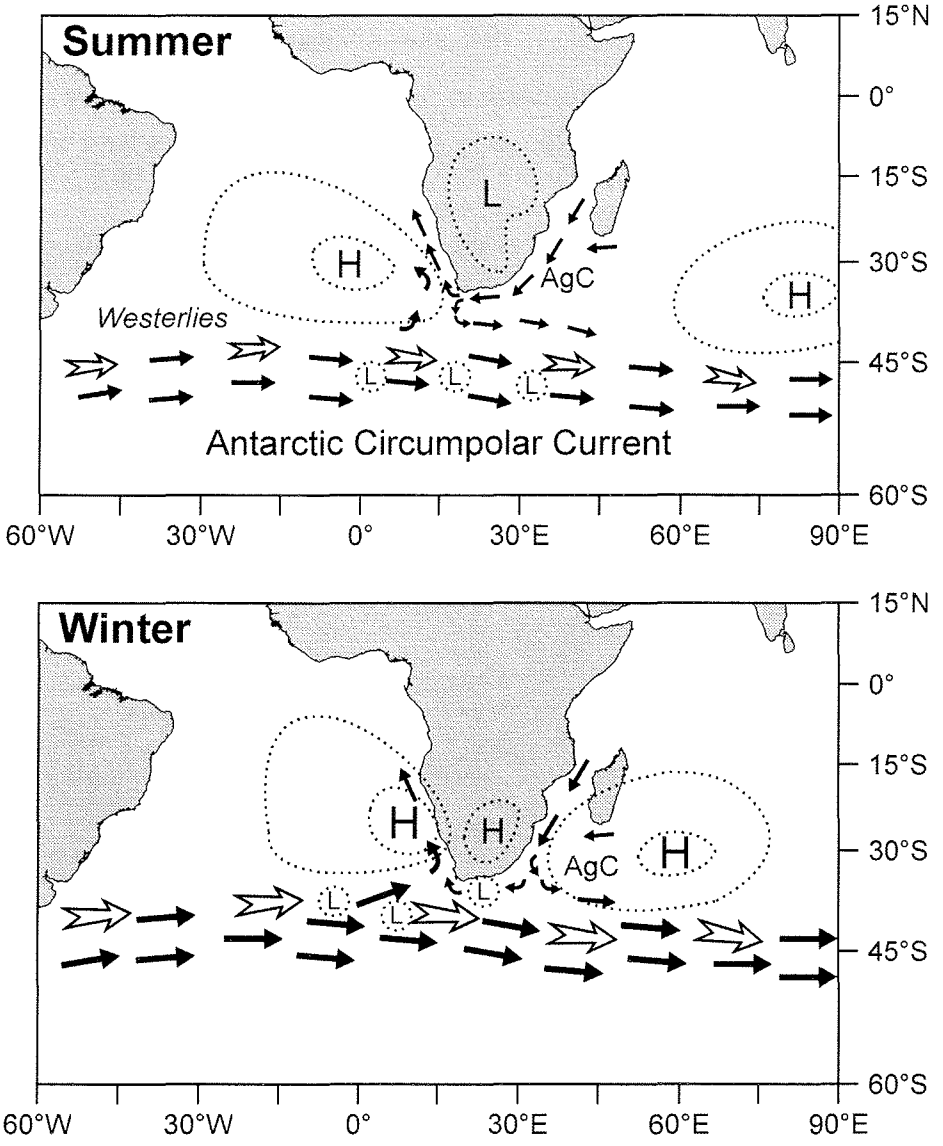

Fig. 2. Seasonal variations of the main atmospheric features above the Indian and South Atlantic oceans and the main surface currents surrounding South Africa (after Shannon, 1985 H: high pressure; L: low pressure; solid arrows indicate surface currents, open arrows indicate westerly winds).

Hydrography of the south-eastern Cape Basin

The hydrography of the south-eastern South Atlantic Ocean, off the Cape of Africa, is characterised by the interaction of three major currents: the Antarctic Circumpolar Current (ACC), the South Atlantic Current (SAC) and the Agulhas Current (AgC; Fig. 1).

South of the SAC and the AgC, cold, nutrient–rich subpolar water of the ACC circulates. This multibanded current is driven by the westerlies (Fig. 2) and is separated from the subtropical environments to the north by the Subtropical Front (STF; Peterson and Stramma, 1991).

The SAC transports temperate, nutrient-poor thermocline water from the oligotrophic areas of the South Atlantic Ocean to the Cape Basin. Off the Cape of Africa part of this current joins the AgC to form the source of the Benguela Current (BC; Stramma and England, 1999).

Wind driven upwelling of colder, nutrient-rich subsurface and intermediate waters occurs in the southern part of the Benguela upwelling area off Cape Agulhas and off the Cape Peninsula (Shannon, 1985). The intensity of these upwelling cells is related to the strength and position of the south-eastern trade winds which are controlled by the position of the SAH (Fig. 2).

The most complex of the three currents is the AgC, which transports warm and saline surface water and central water of the Indian Ocean to the region off southern South Africa (Gordon et al., 1992) where it has a strong influence on the environment and the climate of the region (Lutjeharms and de Ruijter, 1996).

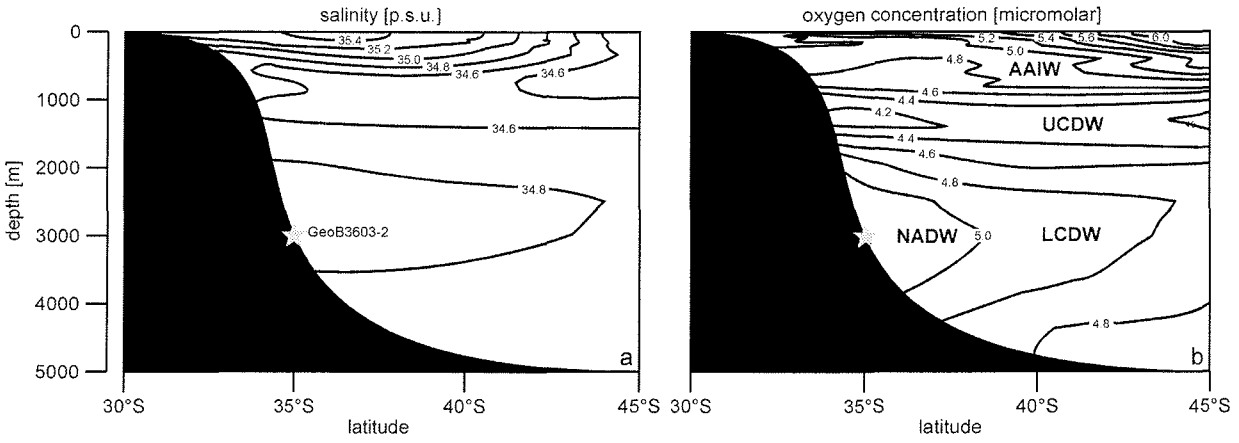

Fig. 3. N-S hydrographic section at 17° E showing the salinities and the oxygen concentrations of distinct water masses at the South African continetal slope (intermediate and deep water masses after Stramma and England; AAIW: Antarctic Intermediate Water; LCDW: Lower Circumpolar Deep Water; NADW: North Atlantic Deep Water; UCDW: Upper circumpolar Deep Water). The position of core GeoB 3603-2 is indicated by an asterisk.

The Agulhas Retroflection

The lower part of the AgC consists of oxygen-rich Indian sector Antarctic Intermediate Water, oxygen-depleted Upper Circumpolar Deep Water, and oxygen-rich North Atlantic Deep Water (Fig. 3; de Ruijter et al., 1999). The major part of these water masses is redirected at the Agulhas Retroflection and returns to the Indian Ocean. A small part of the AgC enters the South Atlantic Ocean either in the form of highly energetic anticyclonic eddies or as a small filament between the core of the eddies and the cape of South Africa (Lutjeharms and van Ballegooyen, 1988). Eddy and filament waters are further transported northward through the South Atlantic Ocean by the South Atlantic Gyre and the BC. At present, the large, anticyclonic eddies form the main means of transport of AgC water into the South Atlantic Ocean. These eddies are shed at the Agulhas Retroflection (Gordon, 1986) which at present is positioned more or less at the western edge of the shelf region south of Africa, known as the Agulhas Bank. On the Agulhas Bank a strong thermocline is established during austral summer due to high insolation combined with the influx of warm Indian Ocean surface water, whereas during winter

a cold, well mixed upper water column prevails (Schumann et al., 1995). It is assumed that the volume transport of the AgC determines the path and the position of the Agulhas retroflection and, therefore, the frequency of eddy shedding (Lutjeharms and van Ballegooyen, 1984; Ou and de Ruijter, 1986). An increase in AgC velocity, caused by intensified South Indian Ocean trade winds, forces an early retroflection south-east of the tip of Africa with a resulting return of most of the warm water back to the Indian Ocean whereas a weak AgC is able to penetrate more westward into the South Atlantic Ocean. The westward shifted retroflection would favour the eddy shedding into the South Atlantic Ocean and, therefore, higher volume transport of warm water could take place. In the course of the spawning process, a cold wedge of the Subtropical Front protrudes northward and cuts off the retroflection loop (Lutjeharms and van Ballegooyen, 1988). As a result of the shedding process an influx of colder subpolar water into the region south of the Cape takes place (Lutjeharms and van Ballegooyen 1988).

Besides the South Indian Ocean trade winds, the retroflection shift and Agulhas water influx are controlled by the position of the STF (McIntyre at al., 1989; Pether, 1994). During austral summer the STF, boundary between the AgC system and the SAC to the north and the ACC to the south, is assumed to be located south of Africa at a relatively poleward position (Fig. 2). Because of the southward shift of the front, the influx of AgC water is enabled. According to Ffield et al. (1997), the AgC volume transport is seasonally changing with slightly increased transport during March and September (equinoxes) due to a stronger subtropical gyre, whereas the AgC may be weakened during June and December (solstices). Lowest volume transport is observed during austral summer. Therefore, during austral summer the poleward shifted STF together with the reduced volume transport of the AgC would favour the westward protrusion of the Agulhas Retroflection and consequently force the increase of warm water influx to the South Atlantic Ocean by eddies and filaments. This situation coincides with an increase of upwelling in the southern Benguela (Weeks and Shillington, 1994) and, therefore, increased advection of warm Indian Ocean water to the tip of Africa (Pether, 1994).

The upwelling regime of the Benguela has its average southern border at Cape Point, but occasionally it stretches farther east to Cape Agulhas, reaching the Agulhas Retroflection area (Lutjeharms and Stockton, 1987). The upwelling activity of the Cape region is related to a higher frequency of easterly to south-easterly alongshore winds caused by the south-eastward ridging of the SAH during the austral summer (Schumann et al., 1995). Consequently, the resulting enhanced summer upwelling leads to nutrient-rich surface water in the eastern Cape Basin. A special situation may occur during "El Niño" like events. An unusual northward migration of the SAH together with the westerly wind belt during austral summer is thought to result in less summer upwelling due to a decrease in easterly winds, consequently leading to high sea surface temperatures and lower nutrient concentrations (Schumann et al, 1995). In contrast, during austral winter the equatorward back shifting STF aligned with the northward replacement of the westerly belt could force the AgC to early

retroflection and less warm water influx to the South Atlantic Ocean (Fig. 2). This further leads to stronger SE trade winds in the northern Benguela coinciding with decreased upwelling in the southern Benguela (Weeks and Shillington, 1994). This situation would also change the environment in the eastern Cape Basin by increasing the influence of both the STF and the SAC waters.

Material and methods

Material

Gravity core GeoB 3603-2 was taken in the south-eastern Cape Basin (position: 35°08´S, 17°33´E) at a depth of 2840 m (Bleil et al., 1996). 100 samples, 2 cm^2 of wet sediment each, were taken every 5 cm for the organic-walled dinocyst, pollen and spore analyses. For the calcareous dinocyst analysis 48 samples of 1 cm^2 wet sediment were taken (Fig. 4). The sampled interval of the core covers oxygen isotope stage 6.4 (162 kyr B.P. after Martinson et al., 1987; kyr B.P. means 1000 years before present) upwards. The stratigraphy is based on the oxygen isotope analysis of the benthic foraminifer *Cibicidoides wuellerstorfi* (**Chapter 4**).

Preparation and identification methods

For the analysis of the organic-walled dinocysts, pollen and spores content, the weighted material was treated with HCl (10%) to dissolve carbonate, neutralised (KOH 10%), treated with HF (40%) to dissolve silica and neutralised (KOH 40%). The organic-walled dinocysts, pollen and spores were cleaned ultrasonically, sieved over a 20 µm mesh, concentrated, mounted on a microscopic slide with glycerine jelly and sealed with paraffin wax (see **Chapter 2**).

For calcareous dinocyst analysis, the weighted material was suspended in tap water and sieved over a 75 µm sieve. The remaining particles were split by wet sieving into a 75 µm to 20 µm fraction and a 20 µm to 5 µm fraction. The particles of the two fractions were mounted on microscopic slides and sealed with SPURR´s resin (**Chapter 4**).

For counting a light microscope was used (400x and 1000x magnification). Slides were counted entirely for each sample. When slides contained less than 200 specimens, additional slides were counted. For the calcareous dinocyst identification polarised light was used in addition (Janofske, 1996). The nomenclature of the identified dinocysts follows Fensome et al. (1993), Zonneveld (1997) and Williams et al. (1998), for further taxonomical information see **Appendix A**.

Two groups of pollen and spores were established, one containing all bisaccate pollen and the other containing all non-bisaccate pollen and spores. Below, we will refer to the organic-walled dinocysts, pollen and spores as palynomorphs.

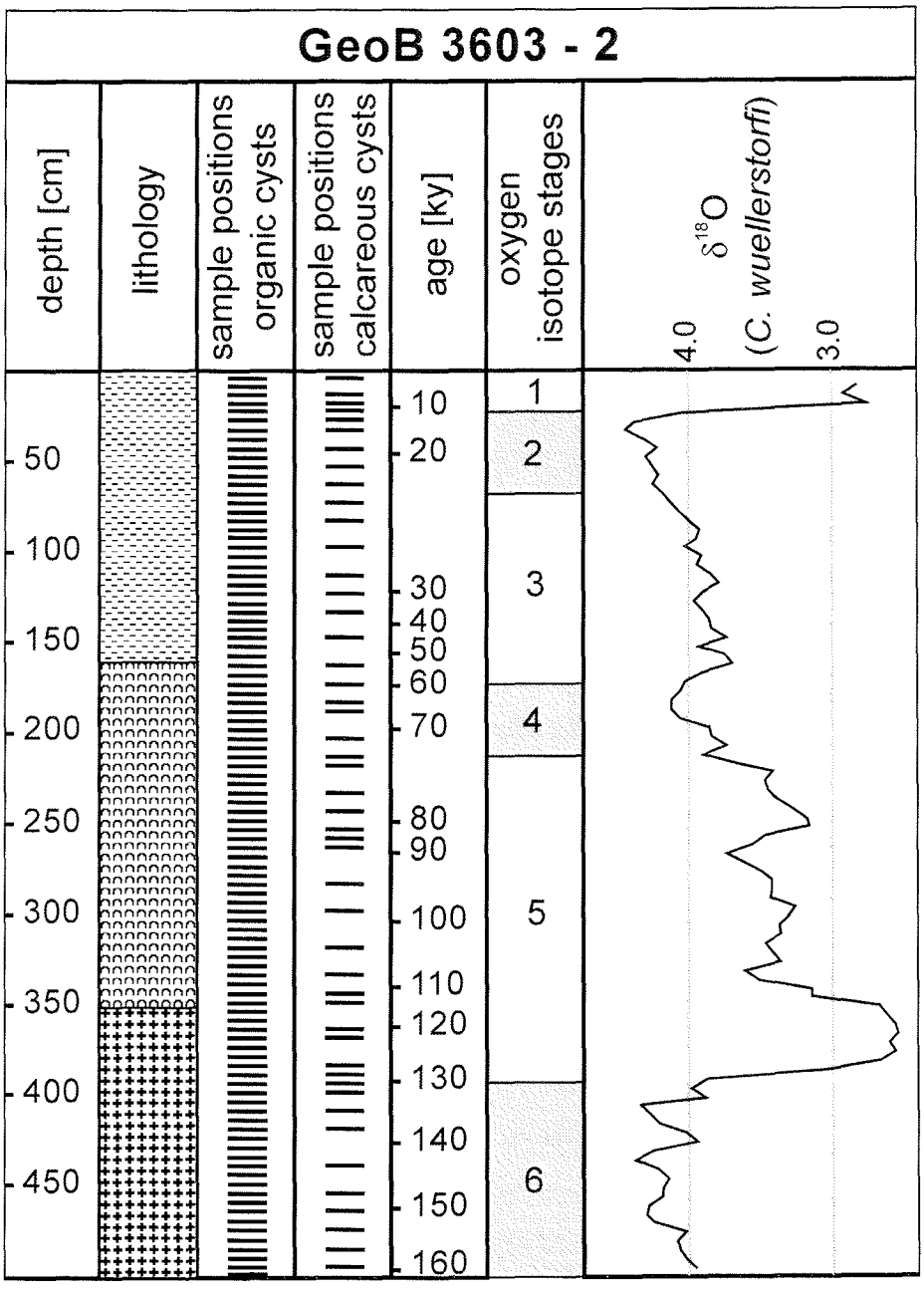

Fig. 4. Sample positions for the organic-walled and calcareous dinoflagellate cyst analysis, lithology, and stratigraphy of sediment core GeoB 3603-2 (after Wefer et al., 1996; **Chapter 4**).

Data processing

The counting results were transformed to values of palynomorphs and calcareous dinocysts per gram dry sediment using the following equations:

$$\text{palynomorph/g} = [(C \times \text{m.f.})/\text{d.w.}] \quad (1)$$

$$\text{calcDino/g} = [(C \times \text{m.f.})/\text{d.w.}]_{20\text{-}75\mu m} + [(C \times \text{m.f.})/\text{d.w.}]_{5\text{-}20\mu m,} \quad (2)$$

where C is the number of counted specimens in one or more slides; m.f.: multiplication factor (sample volume divided by slide containing volume); d.w.: dry weight of the sediment. The indices in (2) indicate the two fractions counted for the calcareous dinocysts.

For further analyses, accumulation rates (AR: in specimens cm^{-2} ka^{-1}) for all palynomorphs and calcareous dinocysts, were calculated:

$$AR = \text{TYPE/g} \times \text{DBD} \times \text{SR}, \quad (3)$$

where TYPE/g is the number of palynomorphs per gram dry sediment (palynomorph/g) or calcareous dinocysts per gram dry sediment (calcDino/g), DBD is dry bulk density in gram per cubic centimetre and SR is the sedimentation rate of each sample in centimetre per thousand years.

In addition, indices between single palynomorph and dinocyst groups were calculated using the following equation:

$$\text{INDEX (group1 / group2)} = \text{AR (group1)} / [\text{AR (group1)} + \text{AR (group2)}] \quad (4)$$

These indices are used to eliminate factors common to all cyst groups and reveal other processes influencing the assemblages.

Multivariate analyses and spectral analysis

To reveal relationships between the organic-walled dinocyst species within the analysed time series, the accumulation rates have been analysed with Detrended Correspondence Analysis (DCA; Ter Braak and Smilauer, 1998). For further information on this technique see Versteegh and Zonneveld (1994). Due to their very rare appearance within the dinocyst assemblage, we excluded *Impagidinium pallidum*, *Impagidinium velorum* and *Spiniferites delicatus* from the analysis.

For the spectral analysis two methods were used within the ANALYSERIES software package:

1. the method after Blackman and Tukey (1958) for its high confidence of the results;
2. the maximum entropy method (e.g. Haykin , 1983) for its high resolution.

Power spectra were calculated for the normalised accumulation rates.

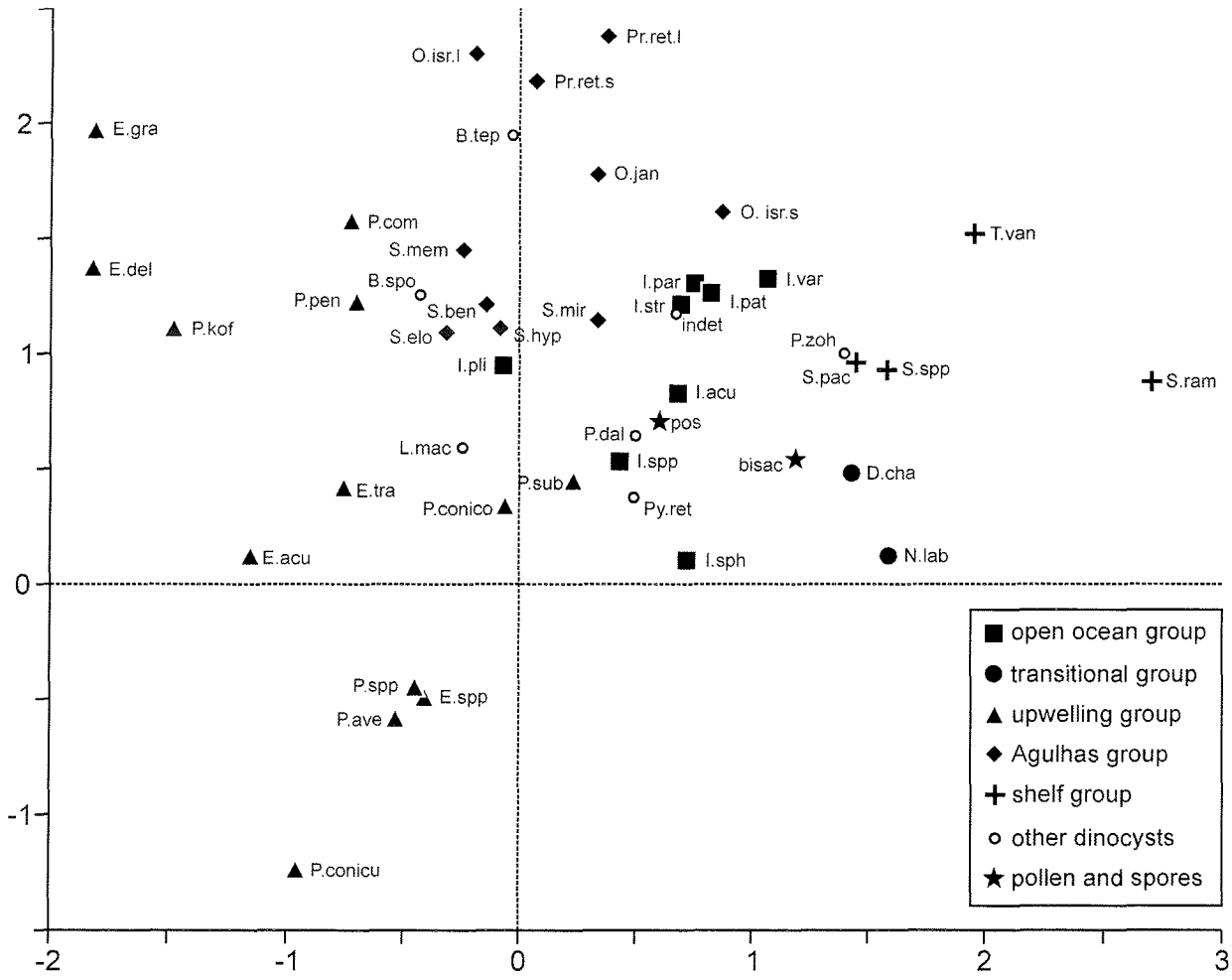

Fig. 5. Results of the Detrended Canonical Analysis on 100 sediment surface samples based on palynomorph accumulation rates. The first canonical axis represents 46% of the variance, its length of 2.36 sd suggests an unimodal distribution of the palynomorphs. The second canonical axis with a length of 2.11 sd represents 16% of the variance. Abbreviations: B.spo: *Bitectatodinium spongium*; bisac: bisaccate pollen; B.tep: *Bitectatodinium tepikiense*; D.cha: *Dalella chathamensis*; E.acu: *Echinidinium aculeatum*; E.spp: *Echinidinium delicatum*; E.gra: *Echinidinium granulatum*; E.spp: *Echinidinium* spp.; E.tra: *Echinidinium transparantum*; I.acu: *Impagidinium aculeatum*; I.par: *Impagidinium pallidum*; I.pal: *Impagidinium paradoxum*; I.pat: *Impagidinium patulum*; I.pli: *Impagidinium plicatum*; I.sph: *Impagidinium sphaericum*; I.spp: *Impagidinium* spp.; I.str.: *Impagidinium strialatum*; I.var: *Impagidinium variaseptum*; indet: indetermined species; L.mac: *Lingulodinium machaerophorum*; N.lab: *Nematosphaeropsis labyrinthus*; O.isr.l: *Operculodinium israelianum* long; O.isr.s: *Operculodinium israelianum* short; O.jan: *Operculodinium janduchenei*; P.dal: *Pentapharsodinium dalei*; P.kof: *Polykrikos kofoidii*; P.zoh: *Polysphaeridium zoharyi*; pos: pollen and spores; Pr.ret.l: *Protoceratium reticulatum* long; Pr.ret.s: *Protoceratium reticulatum* short; P.ave: *Protoperidinium avellana*; P:conico: *Protoperidinium conicoides*; P.conicu: *Protoperidinium conicum*; P.pen: *Protoperidinium pentagonum*; P.spp: *Protoperidinium* spp.; P.sub: *Protoperidinium subinerme*; Py.ret: *Pyxidinopsis reticulata*; S.hyp: *Spiniferites hyperacanthus*; S.mem: *Spiniferites membranaceus*; S.mir: *Spiniferites mirabilis*; S.pac: *Spiniferites pachydermus*; S.ram: *Spiniferites ramosus*; S.spp: *Spiniferites* spp.; T.van: *Tuberculodinium vancampoae*.

The spectral analysis may reveal the first order response of the palynomorph and dinocyst associations to environmental changes forced by the variation in the orbital parameters precession of the equinoxes (19-kyr and 23-kyr bands), obliquity (41-kyr band) and eccentricity (100-kyr band). However, besides the linear response on the Milankovitch frequencies, multiples and combination tones of the Milankovitch frequencies originating from non-linear transformations in the response chain of insolation, climate and sedimentation can occur (von Dobeneck and Schmieder, 1999). In the

case of combination tones, a first frequency (carrier frequency) modulated by at least one second frequency (modulating frequency) can be detected (Yiou et al., 1994; Rial and Anaclerio, 2000). Thus, besides the carrier frequency ω_c the spectral analysis could also trace sidebands of $\omega_c - \omega_m$ and $\omega_c + \omega_m$ as well as multiples of this (Tab. 1). The frequency modulation (fm) of the response signal is represented by the following equation:

$$fm(signal) = \sin [2\pi \omega_c t + \phi_c + \beta \sin (2\pi \omega_m t + \phi_m)], \quad (5)$$

where ω_c is the carrier frequency and ω_m is the modulating frequency, ϕ_c and ϕ_m are the phases of the carrier and modulator, respectively, and β is called the index of modulation and is equal to $\Delta\omega_{max} / \omega_m$ where $\Delta\omega_{max}$ is the maximum frequency deviation (after Rial and Anaclerio, 2000).

Tab. 1. Main periods and major sidebands resulting out of a carrier frequency (ω_c) modulation by a second and/or third frequency (ω_m).

modulation formular	frequency	period/sideband
$\omega_c 1$[1]	0,053	19,0
$\omega_c 2$[2]	0,043	23,0
$\omega_c 3$[3]	0,024	41,0
$\omega_c 1+\omega_m 2$	0,096	10,4
$\omega_c 1-\omega_m 2$	0,009	109,3
$\omega_c 1+\omega_m 3$	0,077	13,0
$\omega_c 1-\omega_m 3$	0,028	35,4
$\omega_c 2+\omega_m 3$	0,068	14,7
$\omega_c 2-\omega_m 3$	0,019	52,4
$\omega_c 1+\omega_m 2+\omega_m 3$	0,121	8,3
$\omega_c 1+\omega_m 2-\omega_m 3$	0,072	13,9
$\omega_c 1-\omega_m 2+\omega_m 3$	0,034	29,8
$\omega_c 2-\omega_m 1+\omega_m 3$	0,015	65,6

[1] $\omega 1$: precession of the equinoxes
[2] $\omega 2$: precession of the equinoxes
[3] $\omega 3$: obliquity

Dinoflagellate cyst groups

Based on the results of the Detrended Correspondence Analysis of the organic-walled dinocysts content of the assemblages (Fig. 5) and the study of the organic-walled dinocyst distribution in eastern South Atlantic Ocean surface sediments focused on their ecological affinities, resulting in four dinocyst groups (Zonneveld et al., 2001), five groups of organic-walled dinocysts were established by splitting the Southern Benguela group of Zonneveld et al. (2001) in two groups. Species with no clear relationship to the prominent members of the concerning groups of Zonneveld et al. (2001) were excluded. Their combined relative abundance never exceeds 14.5% of the total assemblage. The ecological affinities of the single species described below are mainly based on sediment surface studies of the northern hemisphere (Rochon et al., 1999), the Benguela area

(Zonneveld et al., 2001) and the southern South Atlantic Ocean (**Chapter 2**). The new groups contain the following taxa:

1. Open ocean group (*oce*): all *Impagidinium* species.

Impagidinium species generally have been described as oceanic, with a broad thermal tolerance (Harland et al., 1998) and temperate to tropical affinities (e.g. Edwards and Andrle, 1992). In addition, *I. sphaericum* is assumed to tolerate even the cold waters of high latitudes (Rochon et al., 1999). For the Benguela area Zonneveld et al. (2001) also supposed an oligotrophic affinity of *Impagidinium* species. This is supported by a study carried out in the central South Atlantic Ocean, where relatively high numbers of *Impagidinium* species, especially *I. aculeatum*, *I. paradoxum* and *I. variaseptum*, occur in an oligotrophic area north of the Subtropical Front (**Chapter 2**). High accumulation rates of the *oce*-group are used here to indicate influence of open ocean conditions. However, recent results have shown that in comparison to the other species *oce*-group species are extremely resistant against aerobic degradation (Zonneveld et al., 2001; Zonneveld and Versteegh, pers. comm.). Their high relative abundance might, therefore, be the result of selective preservation rather than higher productivity in these environments. Sediment trap studies have shown that although these species tolerate oligotrophic conditions, increased cyst production occurs when surface water nutrient conditions are enhanced (e.g. Zonneveld and Brummer, 2000). Accumulation rates of these species are, therefore, not influenced by aerobic organic matter degradation but rather reflect past productivity.

2. Transitional group (*tra*): *Nematosphaeropsis labyrinthus* and *Dalella chathamensis*.

Nematosphaeropsis labyrinthus is found to be rather cosmopolitic with a wide range of temperature and salinity tolerance (Rochon et al., 1999). However, besides its high ecological tolerance this species is thought to have an affinity to transitional areas between oceanic and neritic environments (Edwards and Andrle, 1992; Dale, 1996; **Chapter 2**). For *Dalella chathamensis*, **Chapter 2** showed a relatively restricted distribution north and south of the STF in the central South Atlantic Ocean. Therefore, we use accumulation rates of the *tra*-group as well as indices of the *tra*-group versus other gonyaulacoid cyst-groups as proxies for transitional/frontal water influence. *N. labyrinthus* and most probably also *D. chathamensis* are extremely resistant against aerobic organic matter degradation (Zonneveld et al., 2001).

3. Upwelling group (*upw*): all *Protoperidinium* species together with all *Echinidinium* species and *Polykrikos kofoidii*.

This ubiquitous group is assumed to tolerate a wide range of temperature and salinity (Rochon et al., 1999). It is composed of cyst species related to heterotrophic dinoflagellates which are assumed to feed mainly on phytoplankton, such as diatoms (e.g. Harland et al., 1998; **Chapter 2**). An increase

in the prey organisms would consequently be indicated by an increase in heterotrophic dinoflagellates and, therefore, in increased cyst abundance of the *upw*-group. Highest numbers of heterotrophic organic-walled cysts, such as the cysts of *Protoperidinium*, nowadays are associated with high bioproductivity areas, such as the Benguela upwelling system off south-west Africa (Zonneveld et al., 2001) and the nutrient-rich subantarctic and polar frontal zones of the Antarctic Circumpolar Current (**Chapter 2**). Both *Protoperidinium* and *Echinidinium* species are extremely sensitive to organic matter degradation and their accumulation rates might reflect differential preservation (Zonneveld et al., 2001).

4. Shelf group (*she*): *Spiniferites* spp., *Spiniferites pachydermus*, *Spiniferites ramosus*, *Tuberculodinium vancampoae*.

The species of this group, especially *S. ramosus*, are found in shelf-near to coastal environments with moderate to high water temperatures and high nutrient availability. In the region they are restricted to the South African shelf and the Agulhas Bank (Davey, 1971; Davey and Rogers, 1975). Therefore, an increased accumulation rate of the *she*-group is used as a sign for increased shelf water influence. These species are moderately resistant to aerobic organic matter degradation (Zonneveld et al., 2001).

5. Agulhas group (*agu*): *Protoceratium reticulatum*, *Operculodinium israelianum*, *O. janduchenei*, *Spiniferites bentorii*, *S. elongatus*, *S. hyperacanthus*, *S. membranaceus* and *S. mirabilis*.

Although *P. reticulatum* represents a cosmopolitic species with a wide temperature and salinity tolerance (e.g. Rochon et al., 1999), Davey (1971) showed that for the area concerned this species is related to the warm Agulhas Current. The other species of the *agu*-group are mainly associated with subtropical, warmer surface water conditions (Edwards and Andrle, 1992; Dale, 1996). Especially *S. mirabilis* is assumed to have a warm water affinity (e.g. Rochon et al., 1999). Therefore, an increase in the *agu*-group accumulation rate may reflect increased influence of warm, subtropical water. The species of the *agu*-group are moderately resistant against aerobic organic matter degradation (Zonneveld et al., 2001).

6. Pollen and spores group (*pos*): sum of all pollen and spores observed in the samples.

The pollen and spore signal in the ocean sediments obviously is a product of transport, either by wind or by rivers. Both mechanisms are feasible for the studied area.

7. calcareous dinoflagellate cysts.

The calcareous dinoflagellates occur in overwhelming numbers mainly in stratified, more oligotrophic environments without extreme temperature variations (Vink et al., 2000; Zonneveld et al.,

2000) and high accumulation rates can be used to identify such conditions in the upper water column (**Chapter 4**). The taxon *Sphaerodinella albatrosiana* is related to well stratified, less trophic, warm (sub)surface water masses and has its highest concentrations in the oligotrophic western equatorial South Atlantic Ocean (Vink et al., 2000; **Chapter 4**). *Sphaerodinella tuberosa* var. 2, in contrast, prefers stratified, more trophic, colder (sub)surface water masses and nowadays is found in higher numbers in the south-eastern South Atlantic Ocean (Zonneveld et al., 2000; **Chapter 4**). An index, based on both species, thus, may reflect the relative importance of oligotrophic water masses at the core location.

Results

DCA

The Detrended Correspondence Analysis reveals a gradient of 2.36 SD on the first DCA axis, indicating a rather unimodal distribution of the cyst species. 46% of the variance in the data set is explained by the first DCA axis. Most of the peridinioid cysts are found at the left side of the first DCA axis, whereas the gonyaulacoid cysts are plotted on the right side (Fig. 5). The second axis, which is not necessarily independent of the first axis, accounts for 16% of the variation.

Accumulation rates

Accumulation rates of all palynomorph groups except the *agu* and *she*-groups follow the austral summer insolation at 35°S (after Berger 1978a). This is most clearly for the *upw*-group which follows the insolation signal for seven out of the eight cycles present in the studied interval (Fig. 6). The *upw*-group shows notably high accumulation during glacial insolation maxima. The *agu*-group does not follow this general pattern. Its accumulation rates show peaks during glacial stage 6 (around 158 kyr B.P. and around 143 kyr B.P.) and during the late stage 5 (around 78 kyr B.P.). At the Last Glacial Maximum (LGM), increased values can be observed as well. During the Holocene, the *agu*-group shows the highest accumulation rates of the whole record. The *she*-group generally covaries with the other groups but has an anomalous peak at substage 5.3 (~96 kyr B.P.), mainly composed of *S. ramosus*. Due to this single event proper power spectrum analysis was impossible on the *she*-group.

Spectral analyses show significant power at the 23-kyr and 19-kyr precession frequency bands though the importance of these frequencies in the spectrum varies considerably for different groups (Fig. 7). The *upw*-group also shows significant power at the 41-kyr obliquity band whereas the *agu*-group is marked by significant power at the 100-kyr eccentricity band. Additionally, all groups show power at 'non-standard' frequencies (e.g. with power at about 53, 45, 37, 15 or 13 kyrs) arising from interference between the main orbital cycles (Table 1), notably precession and obliquity.

The calcareous dinocyst accumulation rates of the prominent species *T. heimii*, *S. tuberosa* var. 2 and *S. albatrosiana* also follow austral summer insolation. They differ mainly from those of the

organic-walled cysts (Fig. 11) in that they have a prominent maximum at Termination 2 (around 126 kyr B.P). An additional maximum for *T. heimii* occurred around substage 5.1 (79 kyr B.P.). At substage 1.1 only *T. heimii* shows an increase in accumulation rate again.

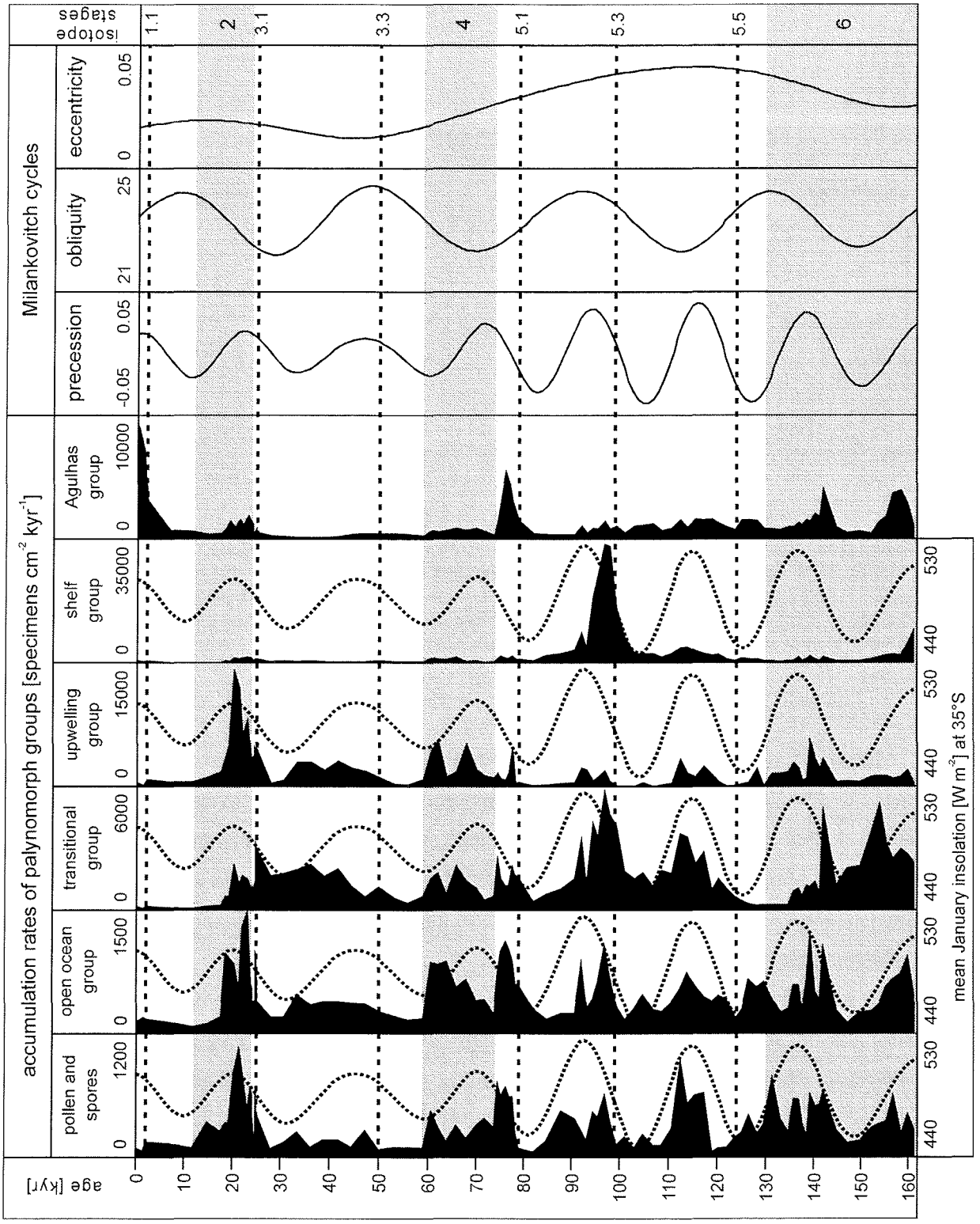

Fig. 6. Accumulation rates of organic-walled dinoflagellate cysts, pollen and spores in relation to the calculated mean January insolation (austral summer), the precession, the obliquity and the eccentricity at 35°S (after Berger, 1978a; stratigraphy for core GeoB 3603-2 in **Chapter 4**).

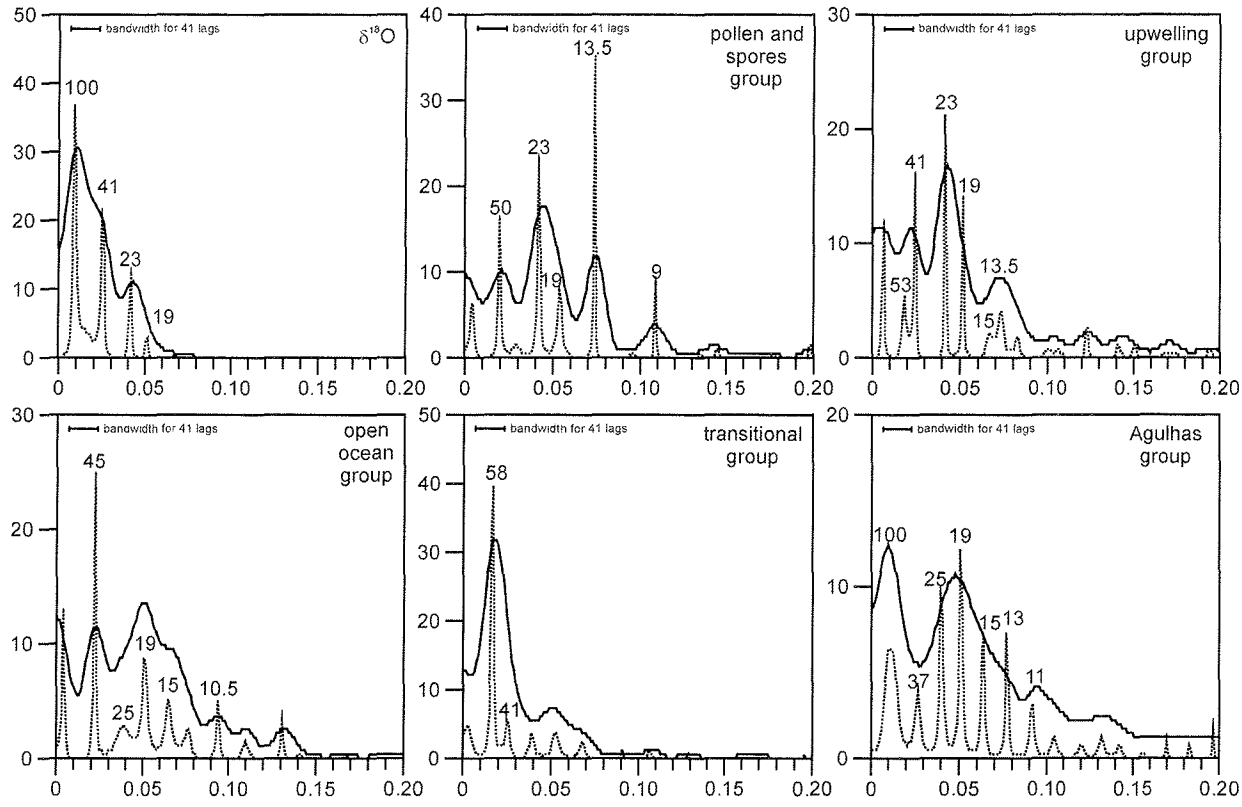

Fig. 7. Power spectral analysis of the $\delta^{18}O$ values of *Cibicidoides wuellerstorfi* and the palynomorph accumulation rates, calculated with the ANALYSERIES software package, using the method after Blackman and Tukey (1958; solid lines) with 41 lags, Tuckey window and a confidence interval at 80% given by $0.549 < DP/P < 2.957$, and the maximum entropy method (e.g. Haykin , 1983; dashed lines). The analysis revealed a strong precession signal (19-23 kyr) within the pollen and spores, the upwelling group, and the open ocean group as well as interference frequencies (for details see text).

Indices and relative abundances

All five indices which include the *upw*-group vary in the same way, indicating that changes in the *upw*-group dominate the variance in the palynomorph associations. High values occur at times of high austral winter insolation (Fig. 8) with maxima at times of highest winter insolation. Since precession is the dominant variable influencing winter insolation, these maxima coincide with minima in seasonal contrast. The spectral analysis of these five indices revealed power centred at 25-kyr for all but the *she/upw*-index (Fig. 10).

The remaining four indices which include the *tra*-group (for the *tra/upw* index see previous paragraph) also covary, suggesting that the *tra*-group is the next important variable influencing the palynomorph associations (Fig. 9). The highest values occur at Termination 2. During the early stage 5 (104 kyr B.P.) only *she/tra*-index and the *agu/tra*-index show a second slight increase. At the transition from stage 5 to stage 4 and around Termination 1, all four indices show also maxima. Spectral analysis shows significant power centred around 63-kyr and 28-kyr, more complex sidebands of the two precessional frequencies modulated by obliquity (Tab. 1) as well as low power at 41-kyr for the *pos/tra*-index, the *oce/tra*-index and the *agu/tra*-index. The *she/tra*-index in contrast shows clear

power at 111-kyr and 41-kyr (Fig. 10). The remaining indices based on the *she, agu and oce* groups only, did not reveal further interpretable information on additional variables influencing the dataset.

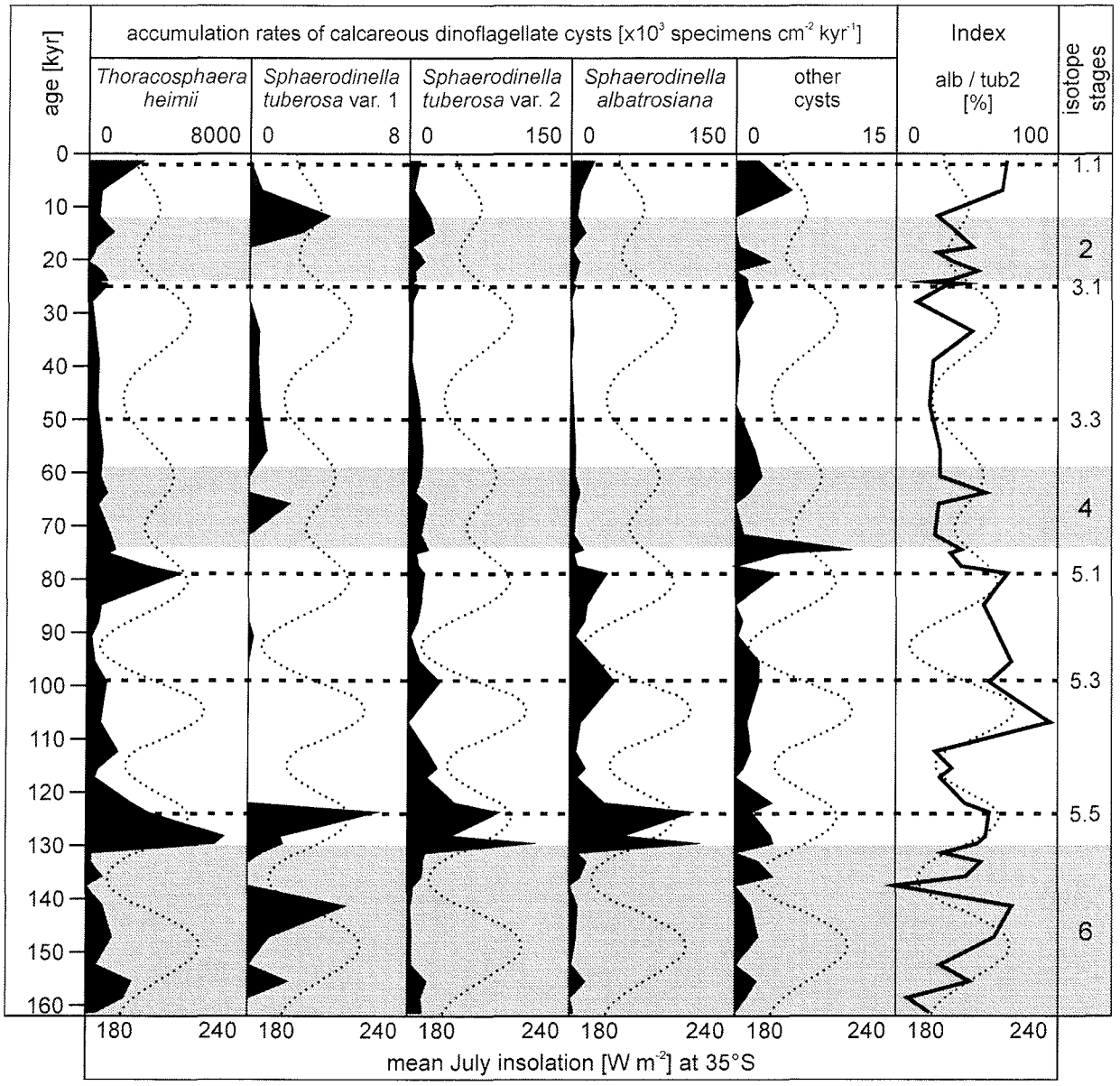

Fig. 8. Accumulation rates of calcareous dinoflagellate cysts, as well as the index of the calcareous dinoflagellate species *Sphaerodinella tuberosa* var. 2 with *Sphaerodinella albatrosiana*, in relation to the calculated mean July insolation (austral winter) at 35°S (after Berger, 1978a; stratigraphy in **Chapter 4**).

The index between S. *albatrosiana* and *S. tuberosa* var. 2 *(alb/tub2*-index*)* shows a clear periodicity following the maximum winter insolation at 35°S (Fig. 11). Highest values are reached during stages 5 and 1, more or less low values occur during stage 6 and lowest values are reached during stages 2-4.

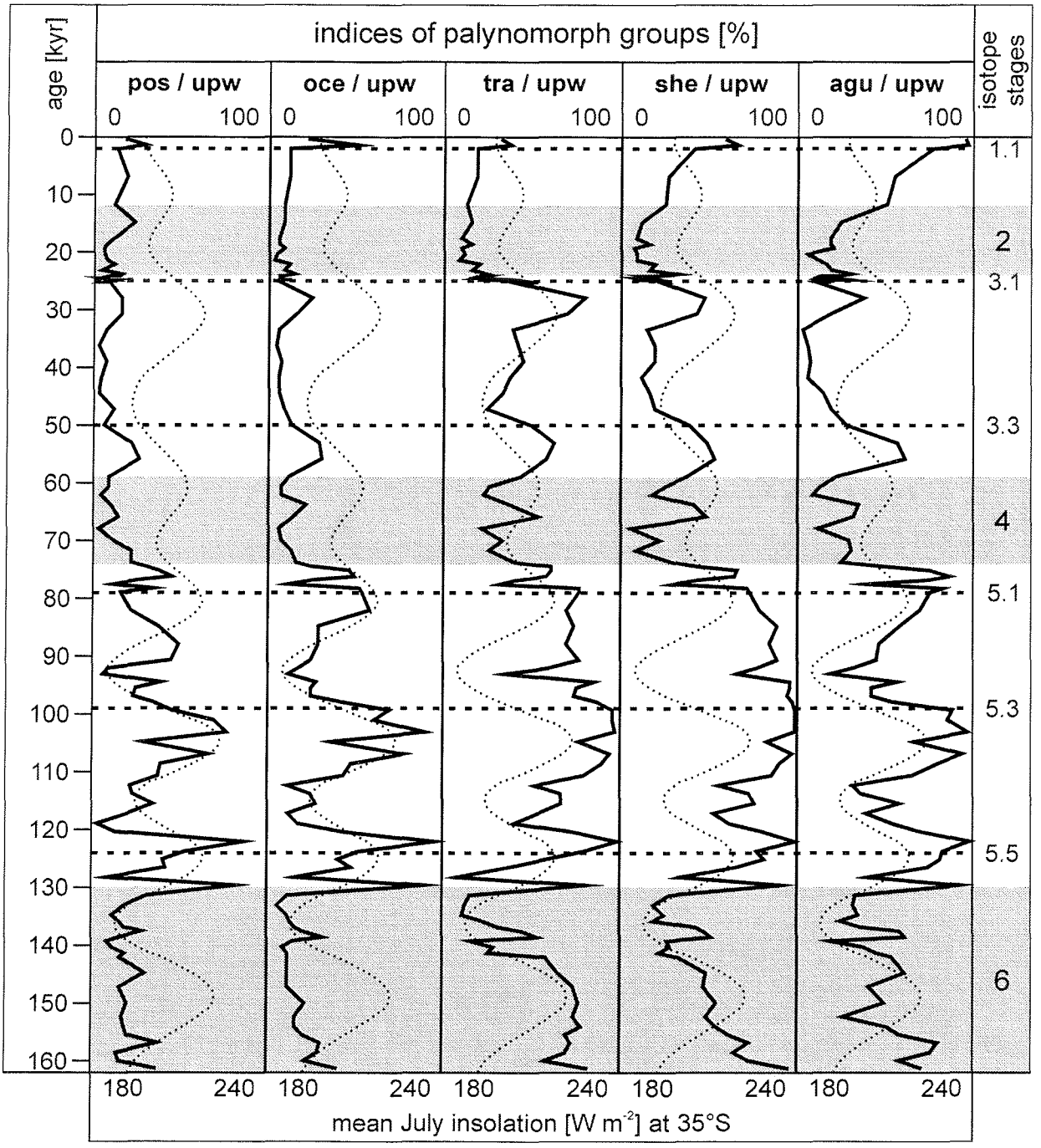

Fig. 9. Indices of the pollen and spores (*pos*), the open ocean group (*oce*), the transitional group (*tra*), the shelf group and the Agulhas group (*agu*) versus the upwelling group (*upw*) in relation to the calculated mean July insolation at 35°S (after Berger, 1978a; stratigraphy in **Chapter 4**).

Discussion

Marine environment

Dinocyst abundance as well as the assemblage composition depends on three main factors: transport, preservation and production. Each providing information on the palaeoenvironmental history of the region.

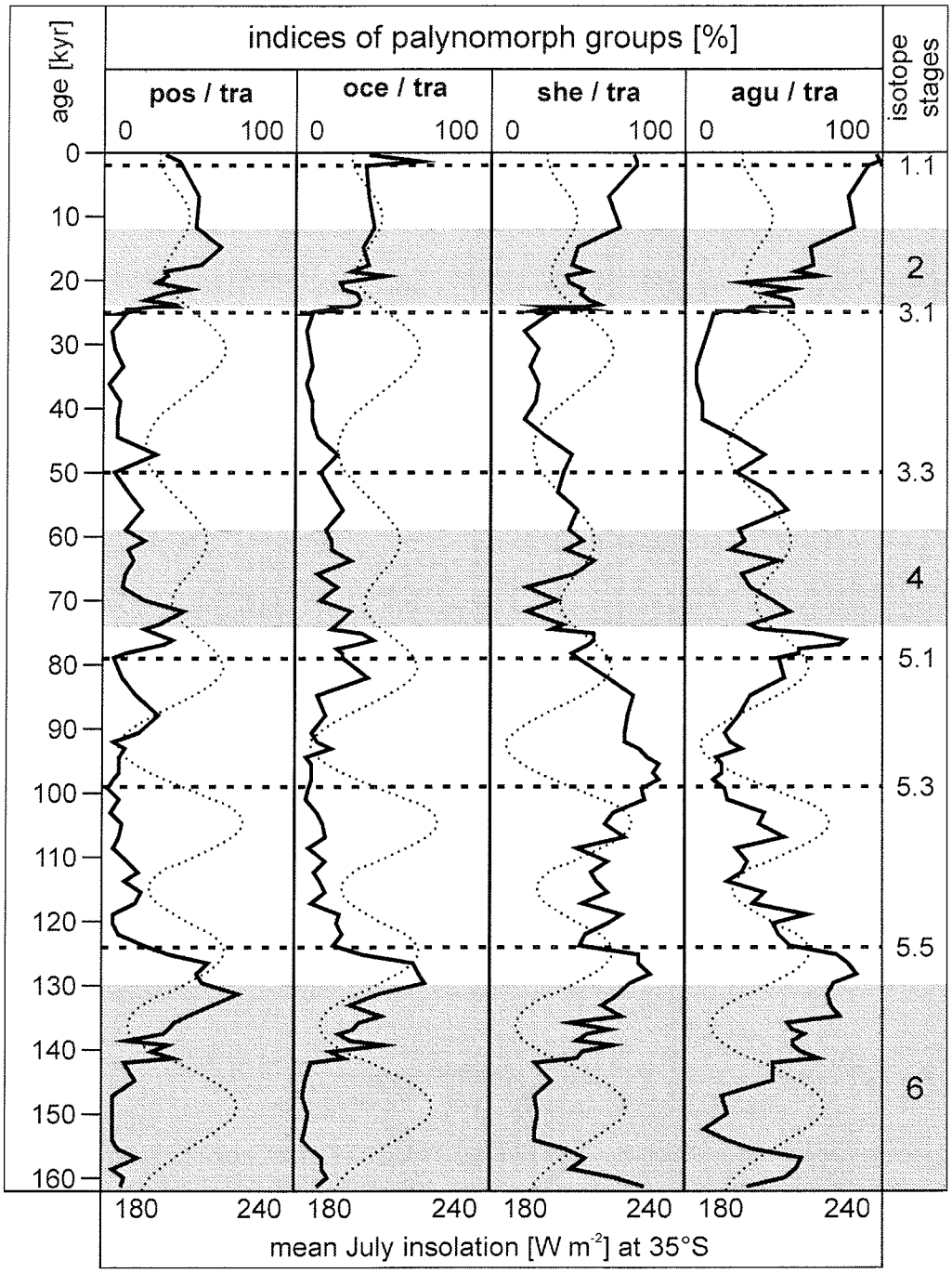

Fig. 10. Indices of the pollen and spores (*pos*), the open ocean group (*oce*), the shelf group (*she*) and the Agulhas group (*agu*) versus the transitional group (*tra*) in relation to the calculated mean July insolation at 35°S (after Berger, 1978a; stratigraphy in **Chapter 4**).

Transport

Due to their size, organic- and calcareous-walled dinocysts are behaving like silt particles and are therefore prone to lateral transport. The organic-walled dinocyst association is primarily composed of species belonging to subtropical environments. Cysts typically found in high numbers in the subantarctic and polar frontal zones of the Southern Ocean, such as *Selenopemphix antarctica* (**Chapter 2**), were not observed in the core sediments. Therefore, we assume no cross frontal transport of subpolar and polar dinocysts northwards to the core location.

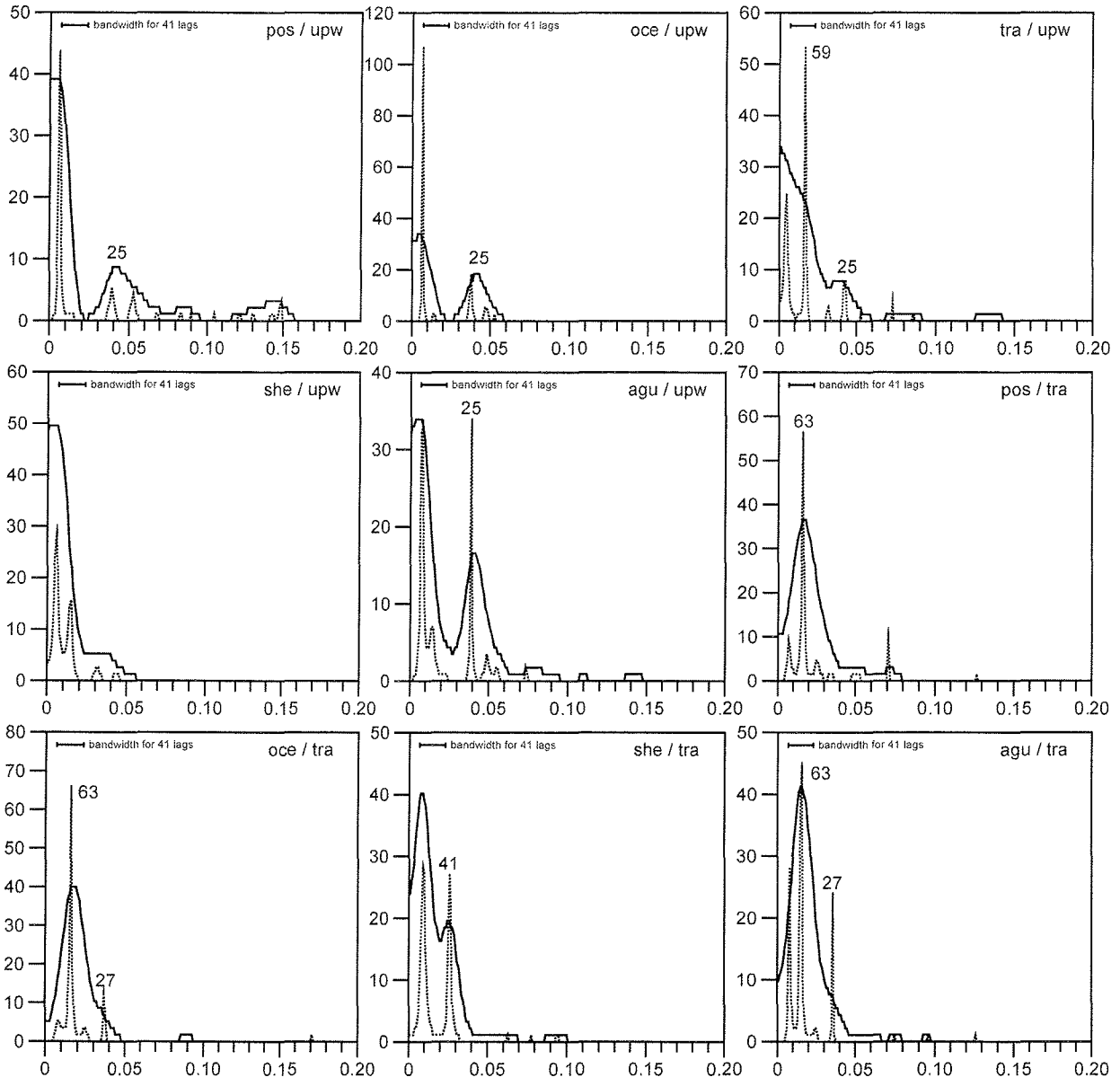

Fig. 11. Power spectral analysis of the palynomorph indices (Agulhas group: *agu*; open ocean group: *oce*; pollen and spores: *pos*; shelf group: *she*; transitional group: *tra*; upwelling group: *upw*), calculated with the ANALYSERIES software package, using the method after Blackman and Tukey (1958; solid lines) with 41 lags, Tuckey window and a confidence interval at 80% given by $0.549 < DP/P < 2.957$, and the maximum entropy method (e.g. Haykin, 1983; dashed lines).

The oceanic environment related *Impagidinium* species occur in relatively high numbers along the STF and also are present in the core sediments. They may have been transported to the core location from open ocean regions north of the STF by the South Atlantic Current. However, *Impagidinium variaseptum* which is prominent in the area near the STF (**Chapter 2**), is under-represented in the core sediments compared to the other *Impagidinium* species. Therefore, also transport via the SAC is considered insignificant.

Although Zonneveld et al. (2001) assumed *P. reticulatum* and *S. ramosus* to be autochthonous at the position of core GeoB 3603-2, Davey (1971) considers these to belong to the Agulhas Current and the south-western shelf of Africa, respectively. An increased inflow of the AgC, therefore, forms

another way to get large amounts of *P. reticulatum* at the core position. This could explain the extraordinary high number of *P. reticulatum* cysts observed in the core top sediments. An extension of Agulhas water onto the shelf may also cause transport of high amounts of *S. ramosus* from the shelf to the core position. The latter conditions might be responsible for the high numbers of these *Spiniferites* cysts around substage 5.3 (Fig. 5).

Based on the assemblage compositions of calcareous dinocysts of five sediment cores in the South Atlantic Ocean **Chapter 4** showed that the influence of transport on the calcareous dinocysts assemblage of core GeoB 3603-2 is insignificant.

Preservation

Recent studies have shown a high vulnerability of the brown *Protoperidinium* cysts to the process of organic matter degradation under oxygen availability in contrast to several transparent gonyaulacoid species, notably *Impagidinium* species which are extremely resistant (Zonneveld et al., 1997; Zonneveld et al., 2001). Like the organic-walled dinocysts, the pollen and spores are susceptible to degradation (Campbell, 1999). Studies carried out on Mediterranean sapropel S1 and the Madeira Abyssal plain F-turbidite indicate, that the preservation capacity of the pollen and spores is similar though somewhat higher than that of the P-cysts (Keil et al., 1994; Zonneveld and Versteegh, pers. comm.). In the case of a major influence of oxygen induced degradation on the dinocyst assemblage we expect different signals of P-cysts, pollen and spores compared to *Impagidinium* with notably reduced concentrations of the P-cysts, pollen and spores at times of increased bottom water oxygen availability. Nowadays, the southernmost extension of relatively oxygen-rich North Atlantic Deep Water reaches the core location, whereas during glacials the core position was bathed in less oxygenated Lower Circumpolar Deep Water (Bickert and Wefer, 1996). Therefore, if increased degradation on the P-cysts, pollen and spores took place, it may have happened during interglacials. Indeed we see lower accumulation rates of the *upw*-group during interglacials then during glacials (Fig. 6). However, the *oce*-group, which is extremely resistant against aerobic organic matter degradation (Zonneveld et al., 2001) shows the same accumulation rate pattern (Fig. 6). Sediment trap studies from vastly different marine environments such as the Gulf of Naples (Montresor et al., 1998), the Southern Ocean (Harland and Pudsey, 1999) and the Somali upwelling region (Zonneveld and Brummer, 2000) indicate increased production of *oce*-group species at times and sites with enhanced bioproductivity in surface waters. Consequently, accumulation rates of the *oce*-group may represent productivity.

The preservation of calcareous dinocysts mainly depends on the water pressure dependant carbonate dissolution, the carbonate ion concentration of the surrounding water mass and the pore water concentration of carbonate ions as a result of organic matter degradation (**Chapter 4**). For the location of core GeoB 3603-2, especially the position of the lysocline is important. It is linked to the mixing zone of carbonate ion supersaturated North Atlantic Deep Water and carbonate ion

undersaturated Lower Circumpolar Deep Water of which the latter reached the core location during the cooler intervals (Bickert and Wefer, 1996). Nevertheless, its influence was limited and we infer for the calcareous dinocysts a moderate preservation during glacials and interglacials and excellent preservation during the glacial Terminations 2 and 1 (**Chapter 4**).

Production of dinocysts

Having assessed the influences of transport and preservation on the dataset, most variance in the dataset can be considered to reflect local environmental change in the surface waters, as nutrient supply, water temperature, salinity, solar radiation, water movement, predation and diseases. We expect the environmental changes in the studied area to be expressed in the organic-walled and calcareous dinocyst accumulation rates and the assemblage composition as shown by the various indices.

According to the general theory of astronomical cycles (Berger, 1978b), we expect dominance of the precessional components for low and intermediate latitudes, whereas for time series of high latitudes dominance of the obliquity component is expected. Seen in this light, the dominance of the precession part of insolation variability for all palynomorph accumulation rates, and indices considered (except for the *agu*-group), suggests that the dataset is primarily influenced by low latitude orbital forcing (Fig. 7), with low accumulation rates during minima in precession (low austral summer insolation). However, also obliquity and eccentricity influences are present. The *oce* and *upw*-groups show power at the 41 kyr obliquity cycle (Fig. 7), whereas the amplitudes of the *pos* and *upw*-groups show significant power for the 100 kyr eccentricity component. Moreover, significant power occurs at frequencies resulting from interference of precession with obliquity and eccentricity.

We may suppose that the observed interference patterns reflect intrinsic environmental complexity, in the sense that environment at the site reflects the interference pattern of two or more systems driven by different orbital parameters.

Alternatively, individual taxa or groups of taxa may not reflect the environmental interference between orbital parameters but differ in the extent to which they reflect a given orbital forcing (e.g. precession for taxa indicating productivity and obliquity for taxa indicating temperature). In that case, the process of grouping taxa or, more likely, the calculation of indices may have generated the interference patterns. This however, does not take into account that the different orbital parameters still must be reflected in the dataset and thus in one way or another must have influenced the environment.

Finally, a primarily precession forced surface signal, which suffers from a postdepositional bottom-water induced diagenetic overprint forms another way to produce interference patterns. Firstly, since the bottom-water composition reflects high latitude (41 and 100 kyr dominated) processes and

secondly since the diagenesis will be selective. The high resistance to diagenesis of the *oce*-group makes this latter option the least likely one.

The observed strong precession influence disagrees with Flores et al. (1999), who suggested changes in the phytoplankton community to follow the classical 100-kyr saw-tooth shaped $\delta^{18}O$ curve, which reflects ice volume (or sea level) resulting from high latitude environmental change. This discrepancy is most easily attributed to the low resolution of that study. Therefore, we conclude that environmental changes in the region result from linear low latitude orbital forcing as well as from interference between both low and high latitude orbitally forced mechanisms.

Below we will discuss the orbital configurations and their corresponding environmental settings for the studied site and interval.

Marine environmental configurations

Glacials

We found high accumulation rates of almost all palynomorph groups indicating enhanced productivity to correlate with high austral summer insolation (high seasonal contrast) (Figs. 6,8). Two mechanisms could have increased productivity: (1) increased upwelling of nutrient-rich central and intermediate water or (2) an increased influence of the nutrient-rich subpolar waters due to northward movement of the STF. The relatively low accumulation rates of the *tra*-group, nowadays observed to be dwelling at the STF in the South Atlantic Ocean (**Chapter 2**), suggest no direct positioning of the STF at the core location during the LGM. Furthermore, the total lack of cold water species such as *S. antarctica* and *I. pallidum,* indicative for subantarctic surface water, suggests that influx of such waters into the Cape Basin is rather unlikely. Therefore, the organic-walled dinocyst assemblage must reflect nutrient-rich waters originating at the core location. At present increased upwelling occurs at this position during the austral summer. We, therefore, suggest higher summer productivity for glacials with high seasonal contrast. At the same time, the continuous presence of the AgC related *agu*-group and warm water related *she*-group provide evidence for a continuous inflow of warm Agulhas water. The same environment probably occurred during stage 4 and the late stage 6, despite the lower accumulation rates of the *upw*-group compared to stage 2. However, the mechanism responsible for the production of dinocysts related to the *upw*-group seem to be increased during stage 6 as well as stages 4-2.

This scenario of high productivity and a continuing inflow of warm Agulhas water is supported by Prell et al. (1980), who reconstructed the Indian Ocean circulation for the LGM. They postulated a slightly northward shift of the average STF position and assumed a generally cooler, probably shallower AgC with greater seasonal variation in intensity and temperature than today. For LGM summers they reconstructed a shallow poleward flowing AgC, whereas during LGM winters they postulate intensification of the current and outcropping of subtropical waters. As a consequence, only a minimum of Indian Ocean water would have rounded the tip of Africa and reached the Atlantic

Ocean during winter. The SAH would have had its northernmost position, causing strong Atlantic Ocean trade winds which, in turn, resulted in increased upwelling in the northern Benguela region. Our glacial scenario is also supported by Winter and Martin (1990) who suggested a rather stable mean position of the AgC during the last 150 kyr, based on coccolithophorid studies. Furthermore, they assumed a continues heat transfer from the Indian Ocean low latitudes to the high latitudes south of Africa with a retroflection close to its present-day position, even for the LGM. This is supported by the coccolithophorid based work of Flores et al. (1999), who pointed out that during the stages 2 to 4 and 6 no direct influence of subantarctic surface waters did occur and that no collapse of the retroflection had happened, despite their reconstruction of an eastward displacement of the Agulhas retroflection and therefore reduced influx of warm water, in coincidence with an increased influence of the STF close to the tip of South Africa. The present results reject the theory of McIntyre et al. (1989), who assumed a northward progradation of the STF up to the tip of Africa, resulting in the closure of the AgC influx and the increased influence of the Subpolar regime in the region south of Africa.

For the glacial summer situation some authors mentioned the possibility of conditions similar to that occurring nowadays during the so called "El Niño" events (e.g. Pether, 1994). The northward shifted SAH and the westerly wind belt would suppress the summer upwelling and enable the establishment of warm, less mixed surface water conditions. This would have coincided with an increased influx of warm Indian Ocean water caused by a weak and shallow AgC (Prell et al., 1980). A continuous influx of the AgC during the LGM summers could explain the slightly increased accumulation rates of the *agu*- and *she*-groups. However, this would not explain the low accumulation rates of the calcareous dinocysts during glacials, generally related to those warm and stratified conditions. Furthermore, such conditions would also prevent high production rates of especially the *oce*- and *upw*-groups through summer upwelling. Therefore, the assumption of "El Niño" like conditions at the core position during glacial summers of high seasonal contrast is not supported by the dinocyst accumulation rates.

In the frequency domain, the *upw*- and *oce*-groups are the only ones showing not only precession related spectral power but also strong obliquity power. This imposes high latitude influence on trade winds intensity and thus upwelling. At the same time, *agu*- and *tra*-groups do not allow for obliquity influences. The dinocyst signal may, thus, reflect dynamic, trophic, cold water conditions in the upper water column caused by enhanced upwelling and/or the northward progradation of the STF during glacial winter seasons. The strong obliquity signal modulating the dominant precession signal of the *oce*- and *upw*-group, may reflect the interference of the precessional dominated subtropical system, represented by the AgC, with the obliquity forced Southern Ocean via shifts of the STF.

Transitions

High accumulation rates of calcareous dinocysts occurred at the transitions from glacial stage 6 to interglacial stage 5 (Termination 2), at substage 5.1 and to a lesser degree at the transition from stage 2 to stage 1 (Termination 1), suggesting very warm, calm, stratified surface water probably resulting from a strong thermocline in the Agulhas Bank region during summer. This assumption is supported by the reduced influence of the *tra*-group on the palynomorph assemblage (Fig. 8), suggesting less dynamic conditions and reduced frontal influence at the core location. These peaks coincide with a reconstructed increase in surface water temperature (Schneider et al., 1999) as well as an increase in subtropical species of the warm water related radiolarian *Didymocyrtis tetrathalamus* and the warm water indicating foraminifera *Globigerinoides ruber* (Charles and Morley, 1988). The calcareous dinocyst peak around substage 5.1 seems to reflect a similar environmental setting and is also reflected by these radiolarian and foraminifera species, though to a lesser degree. Generally, calcareous dinocysts peaks occur at times of minimal precession in combination with a maximum in obliquity.

Interglacials

Also in interglacials we observed increased accumulation rates of the *oce*- and *upw*-group at times of maximum summer insolation (maximum seasonal contrast) in stage 5 and, to a lesser extent, in stage 3. At times of reduced *oce*-group accumulation rate an increase of the *tra*-group accumulation rate is observed. Its highest values occurring around 94 kyr B.P. are accompanied by an anomalous increase in accumulation rates of the *she*-group suggesting increased stratification. Although we observe generally increased values of dinocyst accumulation for interglacial times of high seasonal contrast as well, these observations may be due to a weaker response to summer upwelling, especially around 94 kyr B.P., aligned with increased intrusion of warm Agulhas water on the western shelf and transport of high values of *S. ramosus* to the core location. Furthermore, the influence of the *tra*-group on the palynomorph assemblage is increased at times of low *oce*-group accumulation, whereas its highest influence occurs at times of low obliquity (Fig. 6; Fig. 8).

Terrestrial environment

Production and transport of pollen and spores

Similar to the *oce*-group, the pollen and spores of core GeoB 3603-2 show high accumulation rates at times of maximum summer insolation and low accumulation rates when summer insolation was also low. The accumulation rate maxima coincide with maximum rainfall over south-eastern South Africa, inferred from the Late Pleistocene Pretoria Saltpan-record, with the exception of the blurred first 50 kyr of the Pretoria Saltpan-record (Partridge et al., 1997). Even the eccentricity modulated amplitudes of the inferred rainfall pattern and the pollen and spore accumulation rates agree

well with our results. The Pretoria Saltpan-rainfall exhibits dominant precessional variability in the atmospheric circulation consistent with the calculated changes in southern hemisphere summer insolation (Partridge et al., 1997). Therefore, we assume a periodic mechanism linked to the system responsible for the variation in the ocean currents surrounding South Africa. This could be the trade wind variations caused by orbitally forced shifts of the subtropical anticyclones of both the Indian and South Atlantic oceans.

Glacials

At times of high seasonal contrast the increased insolation during the glacial summer could locally have compensated for the global tendency towards cooler summers and enhanced winters. The high seasonal contrast could also have resulted in severe changes of the atmospheric circulation between the seasons, resulting in more frequent heavy winds and thunderstorms during winter.

For the LGM a shift in moisture transport from the Indian Ocean to the Atlantic Ocean is assumed, implying an extreme northward shift of the westerly wind belt up to at least 25°S (Gasse, 2000). This could have extended the "Mediterranean" belt northward, establishing a climate of harsh winters with increased precipitation caused by the westerly associated depressions. This is supported by the assumption of monsoon controlled increased rainfall in the Pretoria Saltpan at times of increased summer insolation (Partridge et al., 1997), leading to increased aquatic transport of pollen and spores. Increased precipitation may also have increased fluvial transport of pollen and spores into the Cape Basin. Therefore, the atmospheric circulation above South Africa may have become enhanced as well, resulting in strengthening of the ocean currents surrounding South Africa and consequently leading to the high accumulation rates of pollen and spores at the LGM.

Apart from increased aquatic transport aeolian transport is likely to be enhanced as well during glacial periods. Nowadays, Berg-winds (which form a mechanism for aeolian pollen transport into the Cape Basin) occur in autumn and winter when a strong high can develop above South Africa. Maybe, the extra glacial cooling of the South African inland plateau during winter favoured the development of such a high. If these westward blowing Berg-winds are responsible for increased pollen and spores transport to the Cape Basin during the LGM, the high pollen accumulation rates would imply a strong high above South Africa to be present more often. On the other hand, the northward shifted westerly wind belt may have reduced the development of such a high and thus also aeolian Berg-wind transport of pollen and spores into the Cape Basin. The northward shifted westerlies have been suggested to favour the occurrence of "El Niño" like conditions, associated with strong west wind and decreased rainfall (Schumacher et al., 1995). However, the organic-walled and calcareous dinocyst results indicate that "El Niño" like conditions are unlikely at times of high seasonal contrast. Irrespective the mechanism, aeolian or aquatic, pollen transport to the basin is likely to be enhanced during glacial periods.

Interglacials

With the exception of the aperiodical appearance of Berg-wind conditions, the main wind direction above South Africa nowadays varies mainly between north-westward alongshore directed, to north-eastward inshore. Therefore, only at times of the westward flowing Berg-wind conditions, a large aeolian pollen and spores transport to the south-eastern Cape Basin could have happened, although the Berg-winds nowadays mostly follow the river Berg north of the Cape Peninsula, which is well north of the core location, so that their influence may be considered to be not significant during interglacials.

As the Cape region experiences a Mediterranean-like climate aquatic transport during winter is possible too. Moreover, during so called "La Niña" events, the westerlies are shifted southward and easterly wind increase in strength (Schumacher et al., 1995). This could either increase aeolian transport or favour summer rainfall and, therefore, result in increased aquatic transport. However, on the basis of the very low accumulation rates of pollen and spores in the Holocene samples, we assume neither high aeolian transport nor increased aquatic transport for the interglacial climate optima. Nevertheless, the pollen and spores record of the stage 5 shows two large peaks of accumulation rates associated with periods of increased seasonal contrast. This suggests increased particle transport to the Cape Basin, probably due to an environmental winter setting analogous to that during glacial periods, or more frequent "La Niña" events during summer. This situation consequently would be at its maximum during interglacial conditions with high seasonality, which is reflected by high accumulation rates during early stage 5.

An integrated model on the Agulhas retroflection

The above leads to the establishment of a general model describing the connection between the Indian Ocean and the Atlantic Ocean in the Agulhas Retroflection area during Late Quaternary glacial/interglacial-cycles.

Glacials

Winters at times of high seasonal contrast (Fig. 12c). This configuration leads to an accelerated Antarctic Circumpolar Current driven by enforced westerlies and a STF at its most equatorward position but still south of Africa. During the cold glacial winters, strong Indian Ocean trade winds, caused by the westernmost position of the Indian Ocean subtropical high and controlled by the continental low, enhance the AgC, forcing it to an early retroflection east of the tip of South Africa and prevent Agulhas water to enter the South Atlantic Ocean. A coinciding equatorward movement of the STF and simultaneously northward protruding subpolar water wedges either increases the transport of more oceanic and frontal dinoflagellate species to the core location, or favours the production of dinoflagellates by nutrient-enhancement west of the Agulhas Bank, as reflected by the *tra-*, *oce-* and *upw*-groups.

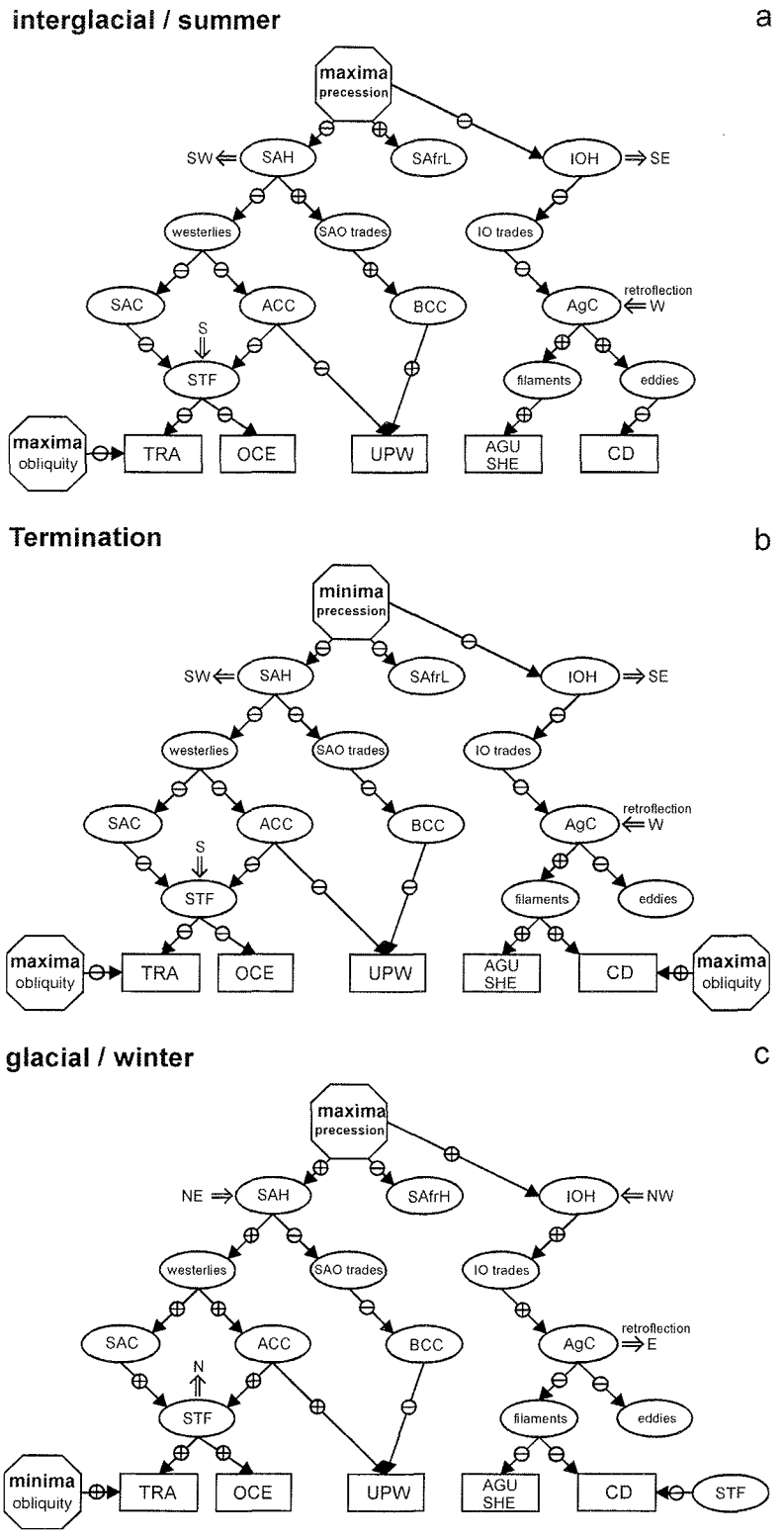

Fig. 12. Diagram of three settings of positive (+) or negative (-) influencing atmospheric and oceanic conditions in the south-eastern Cape Basin leading to environmental conditions favourable for dinoflagellate cyst (dinocyst) production. Setting (a) reflects the conditions prevailing nowadays in the Agulhas Retroflection region, setting (b) reflects conditions right after the glacial Terminations 2 and 1, and setting (c) reflects times of severe glacial winters (ACC: Antarctic Circumpolar Current; AgC: Agulhas Current; AGU: *agu*-dinocyst group; BCC: Benguela Coastal Current; CD: calcareous dinocyst group; IOH: Indian Ocean High; IO trades: Indian Ocean trade winds; OCE: *oce*-dinocyst group; SAC: South Atlantic Current; SAH: South Atlantic High; SAfrH: South African High; SAfrL: South African Low; SAO trades: South Atlantic trade winds; STF: Subtropical Front; SHE: *she*-dinocyst group; TRA: *tra*-dinocyst group; UPW: *upw*-dinocyst group).

Summers at times of high seasonal contrast. An equatorward shifted STF together with strong westerlies prevent the leakage of large amounts of oligotrophic AgC water into the South Atlantic Ocean. Furthermore, stronger SE trades alongshore South Africa favour summer upwelling in the southern Benguela. Increased nutrients and warmer surface water temperatures due to increased insolation consequently would lead to higher productivity as reflected by higher amounts of the *oce*-group.

During summers and winters at times of low seasonal contrast (Fig. 12d) relatively low, but less extreme temperatures and wind speeds would prevail in the Cape region. Strong, northward shifted westerlies and trade winds prevent large volume transport of the AgC, leading to less advection of warm water into the Benguela system and weak summer upwelling. The Cape Basin is under the influence of the STF, reflected by higher *tra*-group accumulation rates.

Terminations

During the last two Terminations (~130 kyr B.P.; ~12 kyr B.P.) there is minimal seasonal contrast. The region experiences cold summers and relatively warm winters. In combination with the simultaneous warming of the higher latitudes (obliquity maxima) and the poleward shift of the STF, this low seasonal contrast results in weaker summer trade winds and therefore weaker upwelling in the southern Benguela. A general weakening of the westerlies accompanied by weak Indian Ocean trade winds results in a less intensive AgC, enabling it to round the Cape and to intrude into the South Atlantic Ocean, explaining the deep thermocline resulting from increased influence of calm coastal currents as well as warm, nutrient depleted surface water of the AgC. Such an environment favours calcareous dinoflagellate production.

Interglacials

Summers at times of high seasonal contrast (Fig. 12a). The high seasonal contrast results in hot summers with a continental low and the Atlantic Ocean and Indian Ocean subtropical highs at their south-westernmost positions. This leads to southward shifted South Atlantic Ocean trade winds enhancing summer upwelling in the southern Benguela region and advection of Agulhas water. The weakened influence of the westerlies causes generally warm surface water conditions in the south-eastern South Atlantic Ocean. Eddy shedding has a higher frequency. The Agulhas Retroflection itself is nutrient-depleted and more stratified (Flores at al., 1999) and its increased influence on the core position, therefore, could establish an environment similar to that of the Agulhas Bank. This is reflected by the increase in abundance of the *agu*- and *she*-groups.

Winters at times of high seasonal contrast. A slightly equatorward shifted STF together with the also equatorward shifted and intensified westerly belt and strong trades of the Indian and Atlantic oceans strengthen the AgC and suppress its leakage into the South Atlantic Ocean. Decreased influx of

Agulhas water into the southern Benguela region leads to an environment less favourable for dinoflagellates.

During interglacial summers and winters at times of low contrast (Fig. 12b) intermediate temperatures and wind speeds prevail. Moderate westerlies and trade winds enable intermediate volume transport of the AgC with moderate advection of warm water into the Benguela system and less strong summer upwelling. Consequently, this situation leads to less productive surface water and decreased production of organic-walled dinocysts. In contrast, the production of calcareous dinocysts is favoured due to calm, stratified conditions.

Testing the model on a calcareous dinocyst-index

The *alb/tub2*-index (Fig. 11) might reflects a degree of stratification or temperature (Vink et al., 2000; **Chapter 2**). In the present core this would imply periodic changes in the influence of either (1) the stratified, nutrient-poor, warm Agulhas water or (2) cold, nutrient-rich waters from the southern and western sources or (3) upwelling at the core position. The index is low at times of low seasonality and increased at times of high seasonality. As we assumed the south-eastern Cape Basin to be highly controlled by both nutrient-rich cold water and nutrient-poor warm water surface currents we would expect periodic variations for the index of S. *albatrosiana* and *S.tuberosa* var. 2 similar to that of the organic-walled dinocysts. Furthermore, the index implies more influx of Agulhas water during stage 5 and 1 and colder, South Atlantic Ocean conditions during stages 6 and 2-4. This pattern is congruent to the indices of the palynomorph groups versus the *upw*-group (Fig. 7), confirming the hypothesis of warmer conditions during interglacials and colder conditions during glacials modified by insolation variations. This suggestion is supported by the results of Flores et al. (1999) and is in agreement with the work of Pether (1994). Thus, calcareous dinocysts seem to be a useful palaeoceanographic tool for indicating changes in (sub)surface water conditions and fit our model for the Agulhas Retroflection area controlled by precession and obliquity modulated variations in the insolation.

Conclusions

The analysis of the independent proxies of both organic- and calcareous-walled dinoflagellate cysts as well as pollen and spores in sediment core GeoB 3603-2, at the nexus between the cool South Atlantic Current, the cold Antarctic Circumpolar Current and the warm Agulhas Current, reflects a dynamic environment forced by Milankovitch and sub-Milankovitch components of the insolation. *Increased austral summer insolation* leads to enhanced production of organic-walled dinoflagellate cysts caused by either increased upwelling or by the influx of cold, nutrient rich, subantarctic surface water. *Low seasonal contrast* leads to conditions off the Cape Peninsula which are less favourable for organic-walled cysts producing dinoflagellates but are more favourable for the calcareous dinocysts

due to more stable, stratified, warmer surface water conditions which we attribute to increased transport of warm Indian Ocean water into the South Atlantic Ocean, especially during the last two major Terminations.

For *glacial periods with high seasonality*, increased aquatic transport of pollen and spores occurs, whereas for *interglacial periods with high seasonality* high pollen and spore accumulation rates are attributed to an increase in the frequency of extreme atmospheric conditions causing a combination of increased aeolian and aquatic transport.

Acknowledgements

All members of the working group of Historical Geology and Palaeontology of Bremen University are thanked for their general support and openness to discussion. We thank Annemiek Vink for critical discussion and English corrections and Nicole Zatloukal for technical support. This research was funded by the Deutsche Forschungsgemeinschaft through the special research project Sonderforschungsbereich 261 "Der Südatlantik im Spätquartär: Rekonstruktion von Stoffhaushalt und Stromsystemen". This is SFB 261 contribution number XXX.

Appendix A Taxonomy

organic-walled dinoflagellate cysts

42 species/morphotypes of organic-walled dinoflagellate cysts were recognised in core GeoB 3603-2. The taxonomy of subfamilies and higher taxonomic levels follows Fensome et al. (1993). The taxonomy of the organic-walled dinoflagellate cysts taxa cited in the current paper follows Williams et al. (1998). In general, the taxonomy for the motile dinoflagellates is used, except when application of motile names is not sufficient to differentiate the different cyst types. Cyst-theca relationships are discussed and listed in Head (1996).

Order PERIDINIALES Haeckel, 1894
Suborder PERIDINIINEAE (Autonym)
Family PERIDINIACEAE Ehrenberg, 1831
Subfamily CALCIODINELLOIDEAE Fensome et al., 1993
Genus *Pentapharsodinium* Indelicato and Loeblich III, 1986
Cyst of *Pentapharsodinium dalei* Indelicato and Loeblich III, 1986

Family POLYKRIKACEAE
Genus *Polykrikos* Bütschli, 1873
Cyst of *Polykrikos kofoidii* Chatton, 1914

Family PROTOPERIDINIACEAE Bujak and Davies, 1998
Subfamily PROTOPERIDINIOIDEAE (Autonym)
Genus *Protoperidinium* (Bergh) Balech, 1974
Cyst of *Protoperidinium* spp.
Cyst of *Protoperidinium avellana* (Meunier) Balech, 1974
Cyst of *Protoperidinium compressum* (Abe) Balech, 1974
Cyst of *Protoperidinium conicoides* (Paulsen) Balech, 1974

Cyst of *Protoperidinium conicum* (Gran) Balech, 1974
Cyst of *Protoperidinium pentagonum* (Gran) Balech, 1974
Cyst of *Protoperidinium subinerme* (Paulsen) Loeblich III, 1986

Subfamily uncertain:
Genus *Echinidinium* Zonneveld, 1997
Echinidinium spp.
Echinidinium aculeatum Zonneveld, 1997
Echinidinium delicatum Zonneveld, 1997
Echinidinium granulatum Zonneveld, 1997
Echinidinium transparantum Zonneveld, 1997

Order GONYAULACALES Taylor, 1980
Suborder GONIDOMACEAE Fensome et al., 1993
Family GONIODOMACEAE Lindemann, 1928
Subfamily HELGOLANDINIOIDEAE Fensome et al., 1993
Genus *Tuberculodinium* Wall, 1967
Tuberculodinium vancampoae (Rossignol) Wall, 1967

Subfamily PYRODINIOIDEAE Fensome et al., 1993
Genus *Polysphaeridium* Davey and Williams, 1966b
Polysphaeridium zoharyi (Rossignol) Bujak et al., 1980

Suborder GONYAULACINEAE (Autonym)
Family GONYAULACACEAE Lindemann, 1928
Subfamily CRIBROPERIDINIOIDEAE Fensome et al., 1993
Genus *Lingulodinium* Wall, 1967
Lingulodinium machaerophorum(Deflandre and Cookson) Wall, 1967

Genus *Operculodinium* Wall, 1967
Operculodinium israelianum (Rossignol) Wall, 1967
morphotype: *Operculodinium israelianum* long
Operculodinium israelianum short
Operculodinium janducheni Head et al., 1989

Genus *Protoceratium* Bergh, 1881
Protoceratium reticulatum (Claparède and Lachmann) Bütschli, 1885
morphotype: *Protoceratium reticulatum* long
Protoceratium reticulatum short

Subfamily GONYAULACOIDEAE (Autonym)
Genus *Bitectatodinium* Wilson, 1973
Bitectatodinium spongium (Zonneveld) Zonneveld and Jurkschat, 1999
Bitectatodinium tepikiense Wilson, 1973

Genus *Dalella* McMinn and Sun, 1994
Dalella chathamensis McMinn and Sun, 1994

Genus *Impagidinium* Stover and Evitt, 1978
Impagidinium spp.
Impagidinium aculeatum (Wall) Lentin and Williams, 1981
Impagidinium pallidum Bujak, 1984
Impagidinium paradoxum (Wall) Stover and Evitt, 1978
Impagidinium patulum (Wall) Stover and Evitt, 1978
Impagidinium plicatum Versteegh and Zevenboom, 1995
Impagidinium sphaericum (Wall) Lentin and Williams, 1981
Impagidinium strialatum (Wall) Stover and Evitt, 1978
Impagidinium variaseptum Marret and de Vernal, 1997
Impagidinium velorum Bujak, 1984

Genus *Nematosphaeropsis* Deflandre and Cookson, 1955
Nematosphaeropsis labyrinthus (Ostenfeld) Reid, 1974

Genus *Spiniferites* Mantell, 1850
Spiniferites spp.
Spiniferites bentorii (Rossignol) Wall and Dale, 1970
Spiniferites bulloides (Deflandre and Cookson) Sarjeant, 1970
Spiniferites delicatus Reid, 1974
Spiniferites hyperacanthus (Deflandre and Cookson) Cookson and Eisenack, 1974
Spiniferites membranaceus (Rossignol) Sarjeant, 1970
Spiniferites mirabilis (Rossignol) Sarjeant, 1970
Spiniferites pachydermus (Rossignol) Reid, 1974
Spiniferites ramosus (Ehrenberg) Mantel, 1854

Subfamily uncertain:
Genus *Pyxidinopsis* Habib, 1976
Pyxidinopsis reticulata McMinn and Sun, 1994

calcareous dinoflagellate cysts

Eight species/morphotypes of calcareous dinoflagellate cysts were recognised in core GeoB 3603-2. The taxonomy of subfamilies and higher taxonomic levels follows Fensome et al. (1993). The taxonomy of the calcareous dinoflagellate cysts taxa cited in the current paper is given in Keupp (1997), Keupp and Versteegh (1989), Keupp and Kohring (1993), Hildebrand-Habel et al. (1999) and Janofske (2000). Additionally, two morphotypes of *Sphaerodinella tuberosa* were distinguished: *Sphaerodinella tuberosa* var. 1 is composed of relatively large, block-like individual crystals which do not inter-finger with each other, whereas cysts of *Sphaerodinella tuberosa* var. 2 consists of smaller, roughly triangular-shaped, inter-fingering crystals.

Order THORACOSPHAERALES Tangen, 1982
Family THORACOSPHAERACEAE Schiller, 1930, emend. Tangen, 1982
Genus *Thoracosphaera* Kamptner, 1927
Thoracosphaera heimii (Lohmann) Kamptner, 1944

Order PERIDINIALES Haeckel, 1894
Family PERIDINIACEAE Ehrenberg, 1931
Subfamily CALCIODINELLOIDEAE Fensome et al., 1993
Genus *Calciodinellum* Deflandre, 1947
Calciodinellum operosum (Deflandre) Montresor et al., 1997

Genus *Sphaerodinella* Keupp and Versteegh, 1989
Sphaerodinella tuberosa (Kamptner) Hildebrand-Habel et al., 1999
morphotype: *Sphaerodinella tuberosa* var. 1
Sphaerodinella tuberosa var. 2
Sphaerodinella albatrosiana (Kamptner) Keupp and Versteegh, 1989

Genus *Orthopithonella* Keupp, 1984
Orthopithonella granifera (Fütterer) Keupp and Kohring, 1993

Genus *Scrippsiella* Balech ex Loeblich III emend. Janofske, 2000
Scrippsiella regalis (Gaarder) Janofske, 2000
Scrippsiella trochoidea (von Stein) Loeblich III, 1965 emend. Janofske, 2000

4. Reconstruction of palaeoceanographic conditions in the South Atlantic Ocean at the last two Terminations based on calcareous dinoflagellate cysts

Oliver Esper, Karin A.F. Zonneveld, Christine Höll, Britta Karwath, Holger Kuhlmann, Ralph R. Schneider, Annemiek Vink, Ilka Weise-Ihlo and Helmut Willems

Universität Bremen, Fachbereich 5 - Geowissenschaften, Postfach 330 440, 28334 Bremen, Germany

Abstract

Despite the increasing interest in the South Atlantic Ocean as key area of the heat exchange between the southern and the northern hemisphere, information about its palaeoceanographic conditions during transitions from glacial to interglacial stages, the so called Terminations, are not well understood. Here we attempt to increase this information by studying the calcareous dinoflagellate cysts (also referred to here as calcareous dinocysts) and the shells of *Thoracosphaera heimii* of five Late Quaternary South Atlantic Ocean cores. Extremely high accumulation rates of calcareous dinocysts at the Terminations might be due to a combined effect of better preservation and increased dinocyst production as a result of calm, oligotrophic conditions in the upper water column.

Low relative abundance of *Sphaerodinella albatrosiana* compared to *Sphaerodinella tuberosa* in the Cape Basin may be the result of the relatively colder environmental conditions in this region compared to the equatorial Atlantic Ocean, which shows a high relative abundance of *Sphaerodinella albatrosiana*.

Keywords: calcareous dinoflagellate cysts, palaeoceanography, Late Quaternary, glacial Terminations, South Atlantic Ocean

Introduction

In the last years the interest for palaeoceanographic changes in the South Atlantic Ocean and equatorial Atlantic Ocean in relation to glacial/interglacial cycles has increased significantly. This is due to the importance of the South Atlantic Ocean as a key area of heat transfer from the southern hemisphere to the northern hemisphere (Wefer et al., 1996a). It has been shown that past changes in ocean current patterns significantly influenced global climate and that changes of ocean chemistry may have had a great effect on primary production. Eventually, this may have led to changes in atmospheric composition, e.g. CO_2 concentration changes (Broecker, 1982).

In order to obtain insight into the relationship between oceanography and climatic change, detailed reconstructions are needed. Of special interest are times of large changes, such as transitions from glacials to interglacials. However, despite the increasing interest, reconstructions of the South

Atlantic Ocean are scarce, are mostly restricted to small regions, and often conflict each other. Furthermore, earlier studies have often dealt only with partial aspects of current dynamics in this area, such as ocean surface circulation (e.g. Kemle-von Mücke, 1994) or deep water circulation (e.g. Bickert and Wefer, 1996).

In this study, we want to enhance the current knowledge of the South Atlantic Ocean palaeoceanography by establishing a combined reconstruction of several areas representing different environments ranging from the south-eastern Cape Basin via the Guinea Basin to the western Brazil Basin, and comparing it with palaeoceanographic information of the South Atlantic Ocean which is already known (e.g. Howard and Prell, 1994; Bickert and Wefer, 1996; Curry, 1996; Mix and Morey, 1996; Wefer et al., 1996a). For these purposes, sediments of three gravity cores were investigated for calcareous resting cysts of dinoflagellates (also referred to here as calcareous dinocysts) and the calcareous shells of *Thoracosphaera heimii*. The results were compared to the results of two formerly published cores (Höll et al., 1999; GeoB 1105-4 and GeoB 2204-2). The sampled sites represent different oceanographic and environmental settings (Fig. 1a). They are located in (I) low- productivity areas of the south-eastern and northern Cape Basin, and the western Brazil Basin, and (II) the high productivity area of the Equatorial Divergence Zone upwelling system in the Guinea Basin and eastern Brazil Basin.

Dinoflagellates are unicellular, biflagellate algae with many different life strategies. They live in most aquatic environments and may possess a complex life cycle with a motile thecate stage and a fossilisable resting cyst stage. Besides the more well known dinoflagellates producing organic-walled cysts, a few authors have described some species of calcareous cysts and shells produced by dinoflagellates from coastal and neritic environments (Versteegh, 1993) and from open oceanic environments of subtropical to tropical regions (Kamptner, 1967; Wall and Dale, 1968; Müller, 1976). The calcareous cyst-producing species which are currently known are thought to be mainly autotrophic and might be important carbonate producers (e.g. Zonneveld et al., 1999).

Recent studies carried out in the tropical and southern Atlantic Ocean have shown the sensitivity of calcareous dinoflagellates for environmental changes during Late Quaternary times and therefore their applicability for palaeoceanographic reconstructions (Höll et al., 1998; Höll et al., 1999). Based on the comparison of calcareous cyst distribution in surface sediment samples of the South Atlantic Ocean with oceanic parameters such as temperature, salinity, and nutrients, a relationship between calcareous cyst production and more oligotrophic environments as well as temperature and salinity changes, has been demonstrated (Zonneveld et al., 1999; Vink et al., 2000; Zonneveld et al. 2000).

Present-day oceanography of the South Atlantic Ocean

One important component of the South Atlantic Ocean is the surface current system of the Subtropical Gyre (SG) (Fig. 1a). The eastern boundary of the SG is formed by the Benguela Ocean

Current (BOC). It is fed by warm surface waters of the Agulhas Current (AGC) originating in the Indian Ocean and a branch of the South Atlantic Current (SAC), the southern boundary current of the SG. Offshore South Africa, the waters of the BOC and SAC form the multiple-banded South Equatorial Current (SEC), which transports the water north-westwards in equatorial direction (Peterson & Stramma, 1991). Offshore NE Brazil, the SEC bifurcates into two branches: the Brazil Current (BC) which is redirected southwards and forms the western border of the SG, and the North Brazil Current (NBC), which retroflects off the coast of Guyana and partly flows back to the eastern Atlantic Ocean as the North Equatorial Counter Current (NECC). A second branch of the NBC carries the main part of the equatorial warm water north-westward. Waters of the SEC piling up off Brazil also flow back to the eastern South Atlantic Ocean as the South Equatorial Counter Current (SECC) (Gordon, 1986).

Other important features of the South Atlantic Ocean are the upwelling areas of the Equatorial Divergence Zone (EDZ) and the Benguela Coastal Current (BCC). At the EDZ, wind-driven water masses of the westward flowing SEC are diverted by the Coriolis Force to the north and south. This process causes upwelling of cold, nutrient enriched, deeper water and increased bioproductivity (e.g. Longhurst, 1993). The diverted water masses north and south of the equator are blocked by the NECC and SECC respectively and lead to the formation of two convergence zones (Peterson and Stramma, 1991). The wind driven upwelling of the BCC region off south-west Africa also leads to increased bioproductivity, forming one of the major high productivity regions of the world oceans (Shannon, 1985).

The intermediate water masses of the South Atlantic Ocean are formed by South Atlantic Central Water (SACW) and Antarctic Intermediate Water (AAIW). Beneath the SACW lies the AAIW. The latter one is of low salinity, has its origin at the Antarctic Convergence Zone, and fills up the South Atlantic Ocean between depths of 400 m and 1200 m (Reid, 1989).

The deep and bottom water masses consist of three main water masses: North Atlantic Deep Water (NADW), Circumpolar Deep Water (CDW), and Antarctic Bottom Water (AABW). Their spreading into the South Atlantic Ocean is determined by the structures of the six main ocean basins: the Brazil Basin, the Argentine Basin, the Guinea Basin, the Angola Basin, the Cape Basin, and the Agulhas Basin (Fig. 1b). Relatively warm, saline, oxygen-rich, nutrient depleted, and carbonate ion-saturated NADW has its origin in the polar regions of the northern hemisphere and flows southward. After crossing the equator above 3500 m water depth, it splits up into a western boundary current and a broad eastern branch with anticyclonic direction (Reid, 1989).

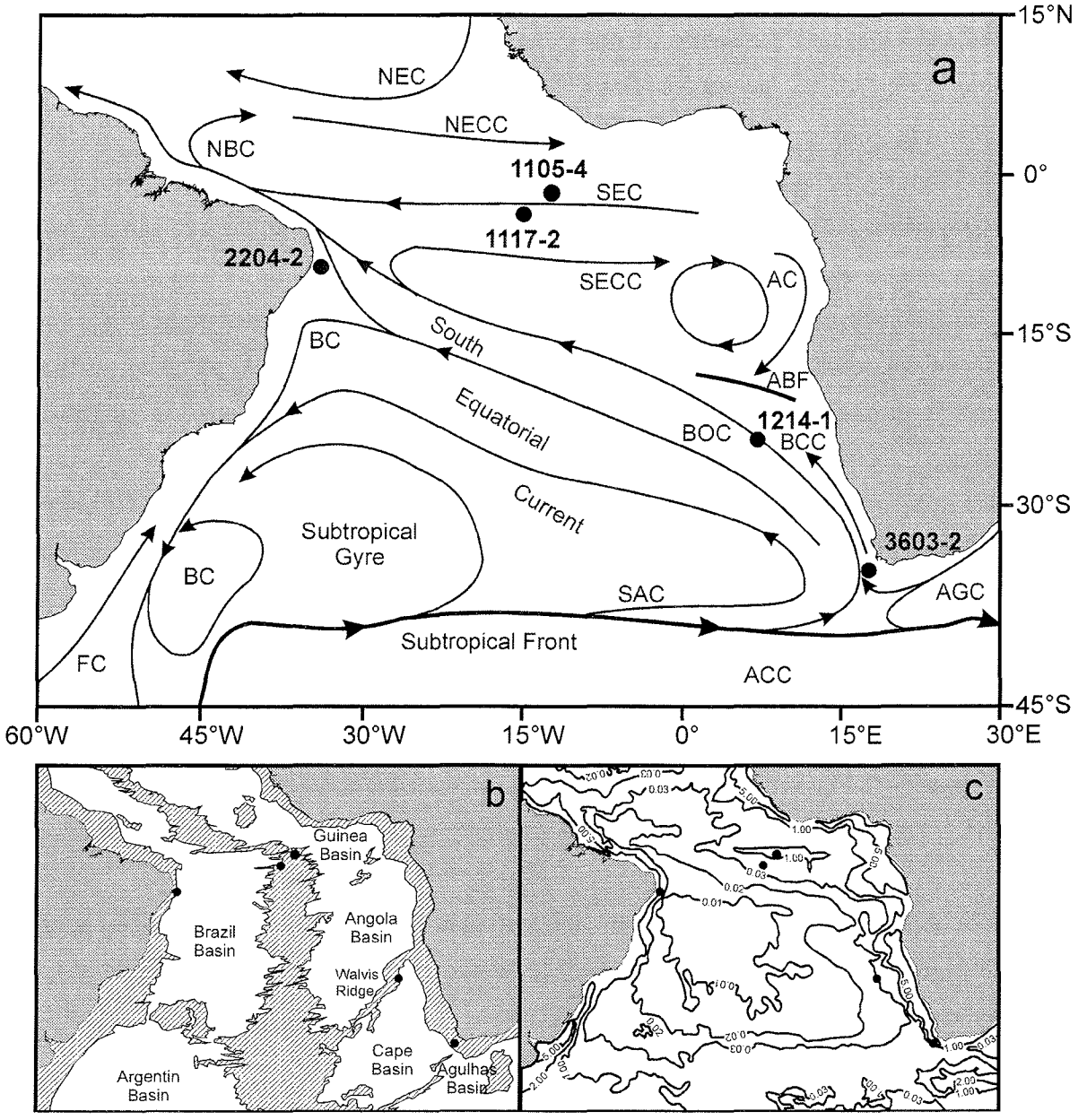

Fig. 1. a: Locations of GeoB cores and schematic summary of sea surface currents of the South Atlantic Ocean. AC: Angola Current; ACC: Antarctic Circumpolar Current; ABF: Angola-Benguela Front; AGC: Agulhas Current; BC: Brazil Current; BCC: Benguela Coastal Current; BOC: Benguela Ocean Current; FC: Falkland Current; NBC: North Brazil Current; NEC: North Equatorial Current; NECC: North Equatorial Counter Current; SAC: South Atlantic Current; SEC: South Equatorial Current; SECC: South Equatorial Counter Current (after Peterson and Stramma, 1991). **b:** Map of the South Atlantic Ocean depicting its basins (depth shallower than 4000m shaded). **c:** Productivity map based on chlorophyll *a* concentration of South Atlantic Ocean surface waters derived from Coastal Zone Color Scanner (CZCS) images of the Nimbus-7 satellite from the NASA Goddard Space Flight Center processing team (after Feldman et al., 1989). The chlorophyll-*a* concentration in milligram per cubic metre (mg/m^3) ranges from values below 0.1 mg/m^3 for oligotrophic oceanic areas to values higher than 5 mg/m^3 for high productivity areas.

The second large deep water mass is the relatively cold CDW and circulates between 50°S and 60°S around Antarctica in water depths of 500 m to 2500 m. On entering the South Atlantic

Ocean, CDW is split by NADW into an upper part (UCDW) and a lower part (LCDW). LCDW reaches the Agulhas and Cape Basins, filling them from the bottom up to a water depth of 4000 m (Reid, 1989). Extremely cold, low salinity and nutrient enriched AABW forms the deepest water mass of the western South Atlantic Ocean, which presently fills the Brazil Basin and Argentine Basin up to 4200 m water depth. The boundary between carbonate ion supersaturated NADW and undersaturated AABW or CDW defines the lysocline (Bickert, 1992; Le and Shackleton, 1992). It is the depth of initial carbonate dissolution. Depending on the weakness of the influx of AABW, the Guinea and Angola Basins are nearly completely filled with NADW.

Material

In this study we compared new material from three cores of the South Atlantic Ocean (GeoB 3603-2, GeoB 1214-1 and GeoB 1117-2; Fig. 1a) with that of two published cores from the eastern and western equatorial Atlantic Ocean (Höll et al., 1999; GeoB 1105-4 and GeoB 2204-2). The cores GeoB 3603-2, GeoB 1214-1, GeoB 1117-2, GeoB 1105-4, and GeoB 2204-2 were taken during RV METEOR cruises M 34/1, M 12/1, M 9/4, and M 23/3 (Wefer et al., 1989; Wefer et al., 1990; Wefer et al., 1994; Bleil et al., 1996).

We investigated the time interval containing the last two major glacial Terminations at the oxygen isotope stage transitions 2/1 (Termination 1: about 18-10 kyr B.P.) and 6/5 (Termination 2: about 133-122 kyr B.P.). The stratigraphy of the three eastern South Atlantic Ocean cores GeoB 1214-1, GeoB 1117-2, GeoB 1105-4 is based on oxygen isotope analysis of the benthic foraminifer *Cibicidoides wuellerstorfi* (Bickert and Wefer, 1996). For core GeoB 3603-2, oxygen isotope values of *C. wuellerstorfi* have been compared with the stacked oxygen isotope stratigraphy of Martinson et al. (1987). The stratigraphy of core GeoB 2204-2 is based on the planktic foraminifer *Globigerinoides sacculifer* (Dürkoop et al., 1997). Sample positions and lithology are given in Fig.2.

Methods

Samples of cores GeoB 1105-4, GeoB 1117-2 and GeoB 2204-2 were processed according to the method described in Höll et al. (1999). For core GeoB 3603-2 and core GeoB 1214-1 a new modified preparation method was used in order to obtain more accurate results in relative abundance and absolute counts of the calcareous dinocysts.

1 ml of wet sediment was dried overnight in an oven at 75°C. 500 mg of the material was mixed with 100 ml tap water (incl. a few drops of ammonia to keep the mixture alkaline) and agitated for 2 hours to loosen up the sediment particles. We did not use demineralized water, as the undersaturation of carbonate ions makes it corrosive against calcareous dinocyst walls and enhances dissolution. The mixture was placed in an ultrasone device for approximately 1 minute to break up the last remaining

sediment clusters and then sieved through a 75 µm sieve, to split larger particles such as foraminifers from the smaller calcareous dinocysts, with 3 litres of tap water. After a settling time of at least 24 hours, the excessive water in the beaker was carefully reduced to 500 ml by decantation. The rest of the water-sediment mixture was shaken up and sieved with another 500 ml of water over a 20 µm sieve into a 1000 ml glass beaker to separate the smaller shells of *T. heimii* from the larger calcareous dinocysts. The particles larger than 20 µm were brought with 15 ml of a 10% alcohol-water-ammonia mixture into a scaled glass test-tube. The particles smaller than 20 µm were left to settle in the beaker for 48 hours and were successively filtered through a 5 µm polycarbonate filter using a vacuum pump. The nearly dry filter was washed with 100 ml of the 10% alcohol-water-ammonia mixture, bringing the smaller 5-20 µm fraction into a scaled plastic storage beaker.

The mixture of both fractions were homogenised. After 5 sec, 50 µl and 100 µl for the larger and smaller fraction, respectively, were transferred to a glass slide and dried on a heating plate at 75°C. After that, the dry material was sealed with two drops of SPURR´s resin and placed in an oven overnight at 75°C to polymerise the resin. The slides of the larger than 20 µm fraction now contain the 600^{th} part of the calcareous dinocyst content of one gram of dried original material, whereas the 5-20 µm fraction slides contain the 2000^{th} part of the *T. heimii* content of one gram.

The material was analysed using a light microscope with polarised optics. The identification of the calcareous dinocysts is based on the polarization method of Janofske (1996). Taxonomical information are given in Appendix A. Whole slides were counted. When slides contained less than 200 specimens, additional slides were counted.

Due to the different preparation methods used to process the samples, the results of the five cores were not comparable in all terms. Tests carried out on cores Geo B 1105-4 and GeoB 2204-2, using the new preparation method, show large differences in the absolute abundance of calcareous dinocysts. This results in the overrepresentation of the *T. heimii* shells in comparison to the other calcareous dinocyst. However, samples processed with both methods are comparable in relative abundances of the calcareous dinocysts and in trends of calcareous dinocyst and *T. heimii* accumulation rates. The accumulation rates of calcareous dinocysts were calculated using the following equations:

$$\text{calcDino/g} = [(\text{C x m.f.})/\text{d.w.}]_{20\text{-}75\mu\text{m}} + [(\text{C x m.f.})/\text{d.w.}]_{5\text{-}20\mu\text{m}}, \quad (1)$$

where C is counted cysts in one or more whole slides, m.f. is multiplication factor (sample volume divided by slide volume), and d.w. is dry weight of the sediment measured at the beginning of the preparation.

$$\text{dinocyst accumulation rate (specimens/cm}^2\text{/kyr)} = \text{calcDino/g*DBD*SR}, \quad (2)$$

where calcDino/g is calcareous dinocysts per gram of dry sediment, DBD is dry bulk density in g/cm^3, and SR is sedimentation rate of each sample of the concerned core in cm/kyr.

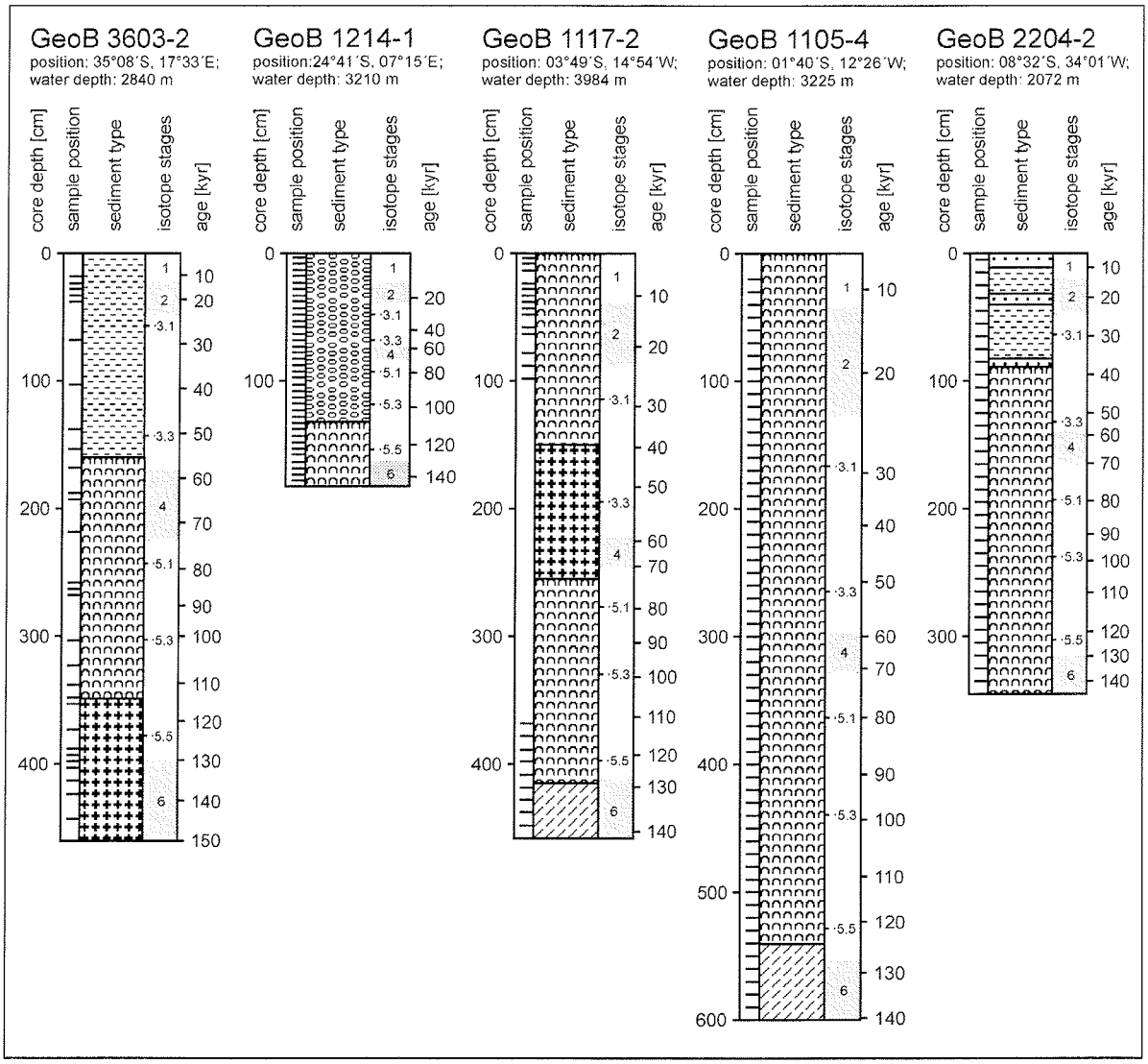

Fig. 2. Lithology and sample positions of the cores GeoB 3603-2, GeoB 1214-1, GeoB 1117-2, GeoB 1105-4 (ages of the latter three according to Bickert and Wefer, 1996) and GeoB 2204-2 (age according to Dürkoop et al., 1997).

Results

The calcareous dinocyst content of the five cores represents three environmentally different areas: (I) the south-eastern South Atlantic Ocean (Cape Basin), (II) the Equatorial Divergence Zone (Guinea and Brazil Basin) and (III) the western Tropical Atlantic Ocean (Brazil Basin).

The calcareous dinocyst-forming species *Sphaerodinella albatrosiana* (Kamptner) Keupp and Versteegh, 1989 (Plate I, 2 and 5), two morphotypes of *Sphaerodinella tuberosa* (Kamptner) Keupp and Versteegh, 1989 (Plate I, 7, 8, 10 and 11), *Calciodinellum operosum* Deflandre, 1947 (Plate I, 3 and 6), *Orthopithonella granifera* (Fütterer) Keupp and Kohring, 1993 (Plate I, 9 and 12), *Scrippsiella regalis* (Gaarder) Janofske, 2000, *Scrippsiella trochoidea* Balech ex Loeblich III emend. Janofske, 2000, and the shells of the vegetative, coccoid stage of *Thoracosphaera heimii* (Lohmann) Kamptner, 1927 (Plate I, 1 and 4) were found in almost all cores. In the course of this study we grouped the two morphotypes *S. tuberosa* var. 1 and *S. tuberosa* var. 2 into *S. tuberosa*.

Due to the different reproduction strategy (i.e. vegetative) and higher rate of reproduction of *T. heimii* in comparison to the other calcareous dinocysts (e.g. Tangen et al., 1982; Dale, 1992), a comparatively lower abundance of calcareous cysts in the upper water column and eventually in the sediment can be expected. Therefore, the accumulation rates of the shells of *T. heimii* were treated independently from those of the other calcareous dinocysts.

Among the other calcareous dinocysts, *S. albatrosiana* and *S. tuberosa* are dominant in the South Atlantic Ocean. *C. operosum*, *O. granifera*, *S. regalis* and *S. trochoidea* occur in low abundances only and are thereafter grouped as "other cysts".

The south-eastern South Atlantic Ocean and the Equatorial Divergence Zone

The calcareous dinocyst associations of the cores of the south-eastern (GeoB 3603-2; Fig. 3) and northern Cape Basin (GeoB 1214-1; Fig. 4) as well as the cores of the Equatorial Divergence Zone (EDZ; GeoB 1117-2, GeoB 1105-4; Fig. 5, 6) are dominated by *T. heimii*, *S. albatrosiana*, and *S. tuberosa*. The other cyst species always occur in low numbers. The ratio between *T. heimii* and the calcareous cysts is in average more than 50:1 in the Cape Basin and about 10:1 or less in the EDZ. Among the calcareous dinocysts, *S. tuberosa* dominates the association in the northern Cape Basin core and shows an equal occurrence to *S. albatrosiana* in the south-eastern Cape Basin core (Fig. 8). On the contrary, the calcareous cyst association of the EDZ is dominated by *S. albatrosiana* (Fig. 8). In both the Cape Basin and the EDZ region, *T. heimii*, *S. albatrosiana*, and *S. tuberosa* show low accumulation rates during the glacial maximum of stage 6 (135 ± 4.2 kyr B.P. (Martinson et al., 1987)), followed by prominent increasing values at Termination 2 with maximal values at event 5.5(123±2.4 kyr B.P.). After event 5.5 the accumulation rates decrease and are generally low during stages 5 to 3. At Termination 1 they increase again. The values at event 1.1of the northern Cape Basin core, as well as the cores in and off the EDZ, nearly reach those of event 5.5, whereas in the south-

eastern Cape Basin core only slightly increased values are observed.

The western Tropical Atlantic Ocean

The western core (GeoB 2204-2, Fig. 7) shows strongly oscillating values of the accumulation rates of *T. heimii*, *S. tuberosa* and the other cysts from stage 6 to stage 1. No clear trend can be observed. Only *S. albatrosiana* shows a pattern slightly similar to those of the other four cores. Its accumulation rate is quite low during stage 6, increases during Termination 2 and reaches its maximum shortly after event 5.5. Afterwards the value drops and remains low with a slight increase at stage 1. Highest values are achieved shortly after event 5.5. The ratio between *T. heimii* and the calcareous cysts is approximately 10:1. With the exception of event 5.5, *S. albatrosiana* shows only one fourth of the accumulation rates of *S. tuberosa* (Fig. 8).

Discussion

During the last years, more information about the ecology of calcareous cyst-producing dinoflagellates has become available. Studies on Recent distribution patterns in the South Atlantic Ocean, based on surface sediment samples, have suggested that they might have higher production rates in oligotrophic environments (Dale and Dale, 1992; Zonneveld et al., 1999; Vink et al., 2000; Zonneveld et al., 2000). Their affinity to oligotrophic conditions is also assumed for Late Quaternary time series, where Höll et al. (1998, 1999) pointed out a strong correlation between increased abundance of calcareous dinocysts and conditions of reduced productivity in the upper water column for the eastern and western equatorial Atlantic Ocean. Therefore, for cysts producing dinoflagellates, the capability was assumed to survive low nutrient concentrations, and produce large numbers of cysts in relatively stable and predictable environments affected by minimal seasonality.

Furthermore, several species seem to have differences in distribution pattern which are attributable to differences in cyst production in the overlying (sub)surface waters. For *T. heimii* and *S. albatrosiana*, Vink et al. (2000) pointed out a similar, mainly oceanic distribution in relatively cool, saline/dense and unstratified/oligotrophic waters of the western equatorial Atlantic Ocean. This is partly subscribed by Zonneveld et al. (2000), who showed negative correlations between *T. heimii* and *S. tuberosa* distributions and temperature and salinity in the central and eastern South Atlantic Ocean. They could positively correlate *S. albatrosiana* distributions with these two parameters. According to these studies, high production rates of calcareous dinocysts and *T. heimii* are most likely to occur under oligotrophic conditions in the upper water column. In addition, we expect an increase in abundance of *S. albatrosiana* compared to *S. tuberosa* in warm, higher salinity surface waters. Besides production, two main environmental processes may also have an affect on the abundance of calcareous dinoflagellate cysts, namely preservation and transport.

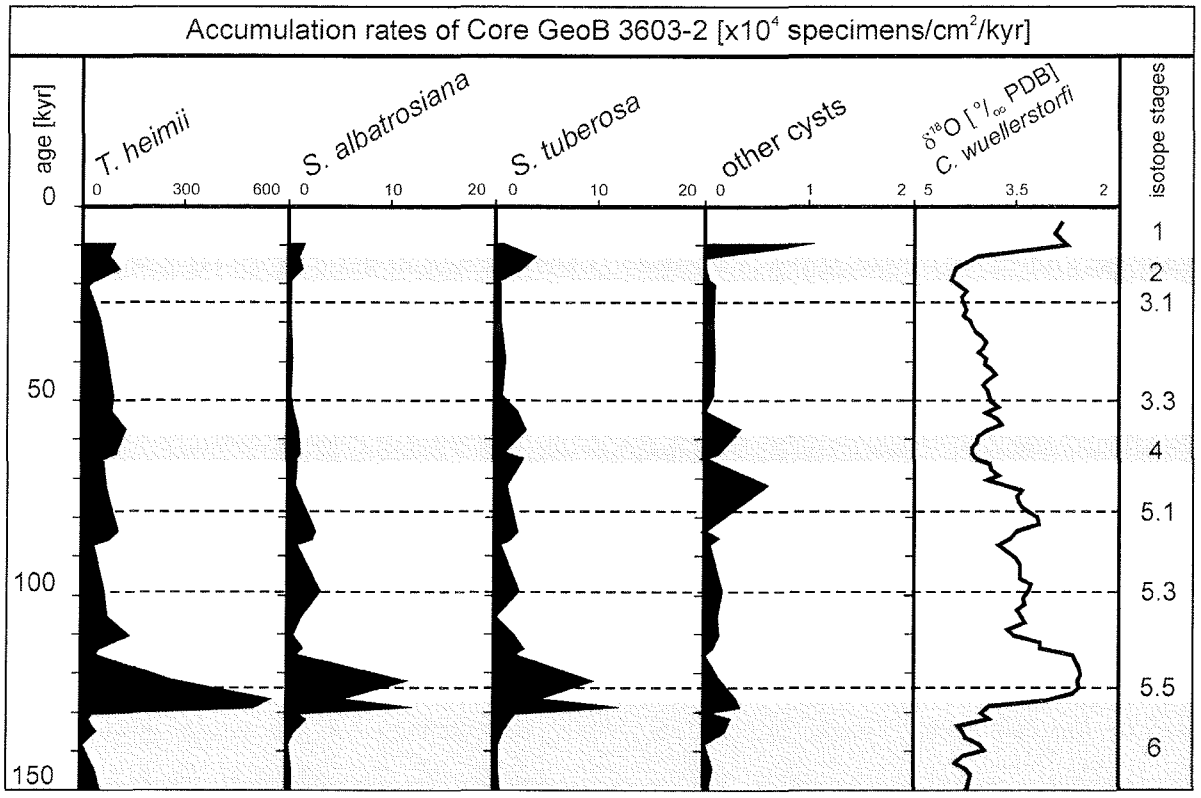

Fig. 3. Accumulation rates of the calcareous dinoflagellate cysts of core GeoB 3603-2 and oxygen isotope values of the benthic foraminifer *Cibicidoides wuellerstorfi*.

Transport

Due to their size, the calcareous cysts and shells produced by dinoflagellates behave as silt particles and are therefore susceptible to lateral transport by ocean currents (Anderson et al., 1985). However, there is no evidence for major influence of transport on the composition of the calcareous dinocyst associations and the accumulation rates in the studied cores. Namely the constant signals throughout all five cores could not be achieved solely through transport into the observed areas as all core positions are influenced by different current systems. This assumption is supported by Zonneveld et al. (1999), who compare calcareous dinocyst distributions in water samples, surface sediment samples, and two sediment cores of the South Atlantic Ocean. They point out a certain grade of vulnerability of secondary transport on calcareous cysts, but conclude a largely environmentaly determined distribution.

Preservation

Besides production and transport, calcareous dinoflagellate cyst accumulation rates could be influenced by preservation effects. Two processes inflicting dissolution on calcareous particles are well known from the world oceans: (I) the variation in the depth of the lysocline (Le and Shackleton, 1992), and (II) the influx and decay of organic matter, which increases the pore water carbonate ion concentration in sediments (Emerson and Bender, 1981; Jahnke et al., 1994).

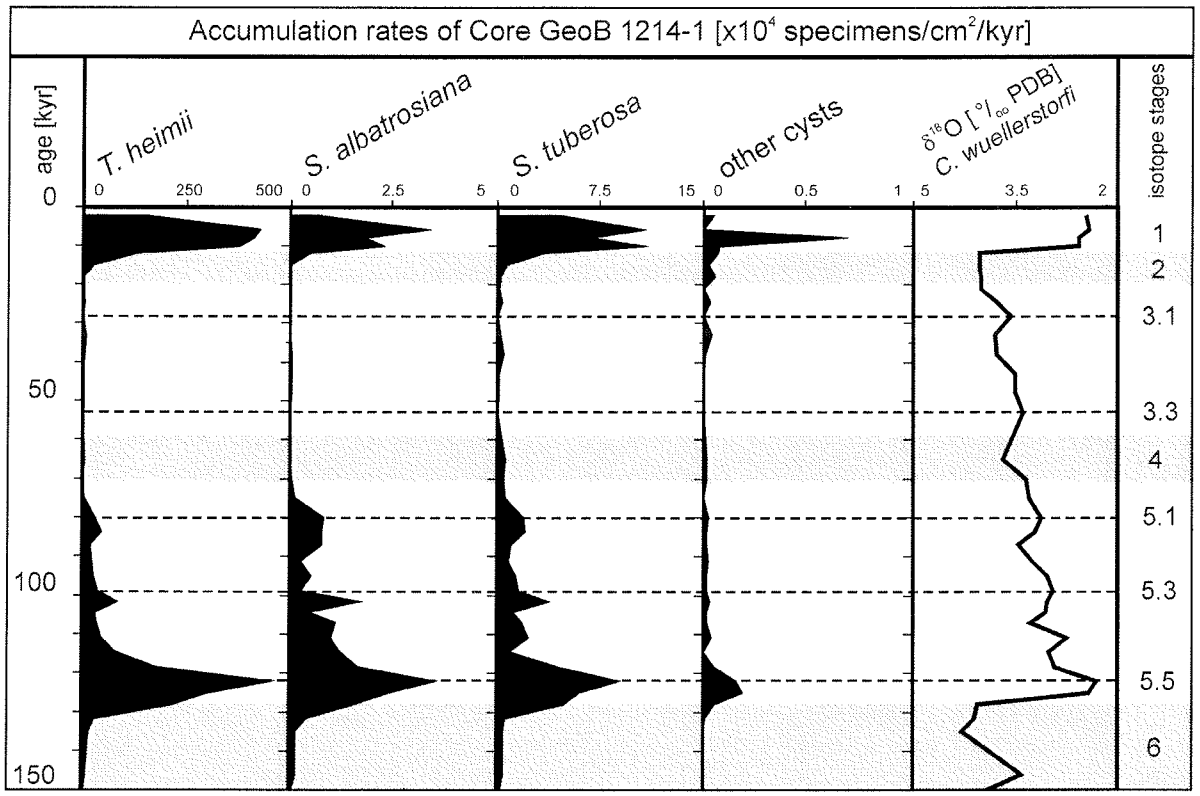

Fig. 4. Accumulation rates of the calcareous dinoflagellate cysts of core GeoB 1214-1 and oxygen isotope values of the benthic foraminifer *Cibicidoides wuellerstorfi* (after Bickert and Wefer, 1996).

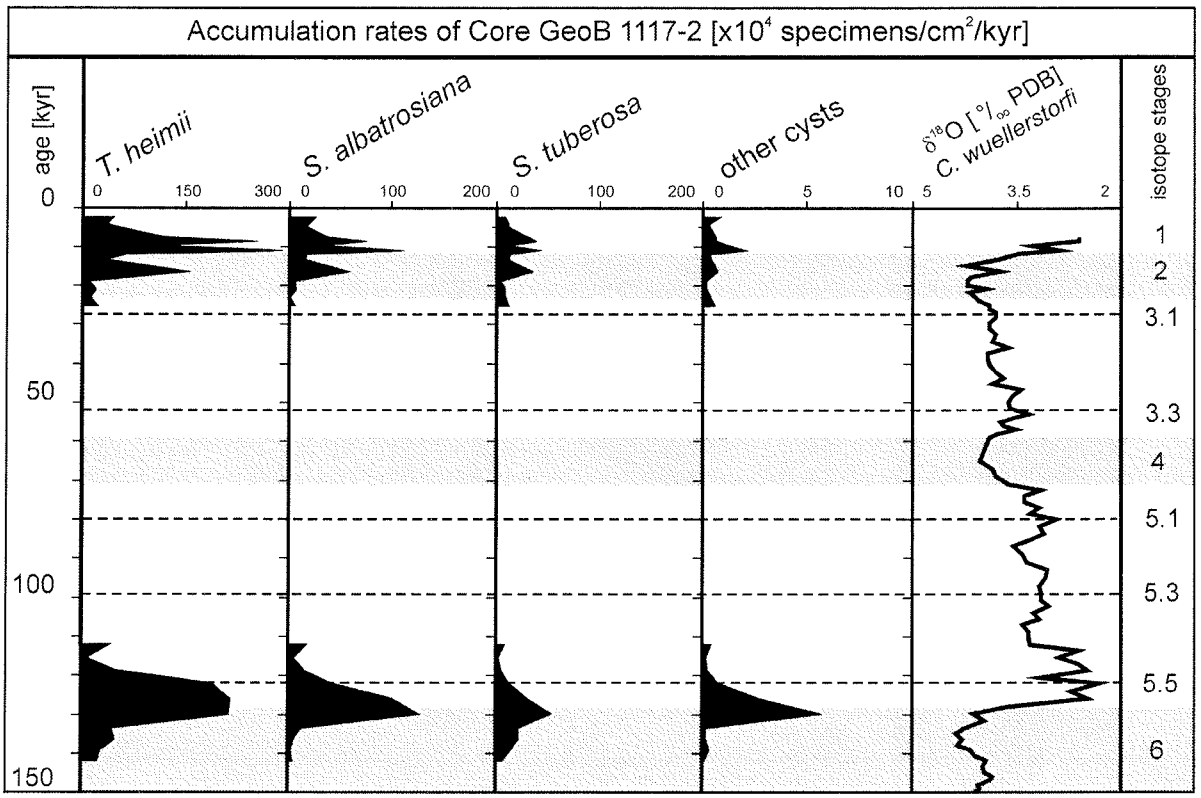

Fig. 5. Accumulation rates of the calcareous dinoflagellate cysts of core GeoB 1117-2 and oxygen isotope values of the benthic foraminifer *Cibicidoides wuellerstorfi* (after Bickert and Wefer, 1996).

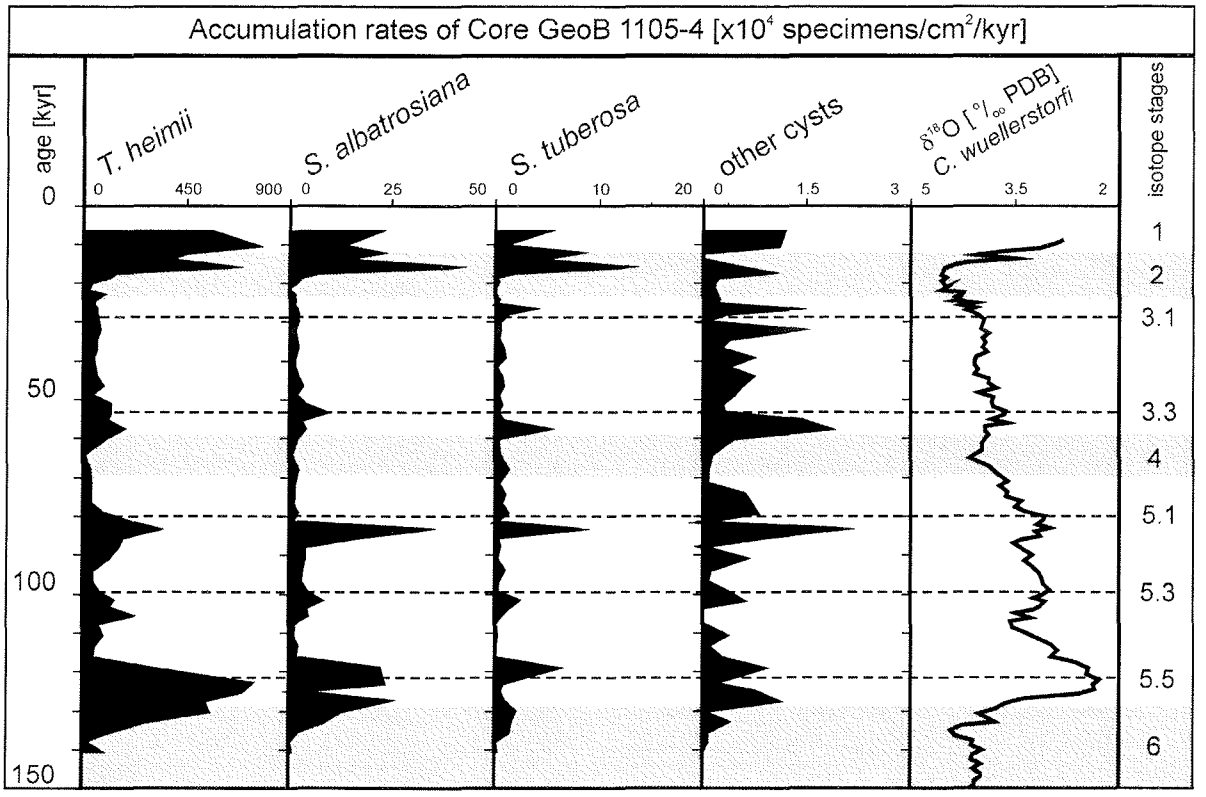

Fig. 6. Accumulation rates of the calcareous dinoflagellate cysts of core GeoB 1105-4 and oxygen isotope values of the benthic foraminifer *Cibicidoides wuellerstorfi* (after Bickert and Wefer, 1996).

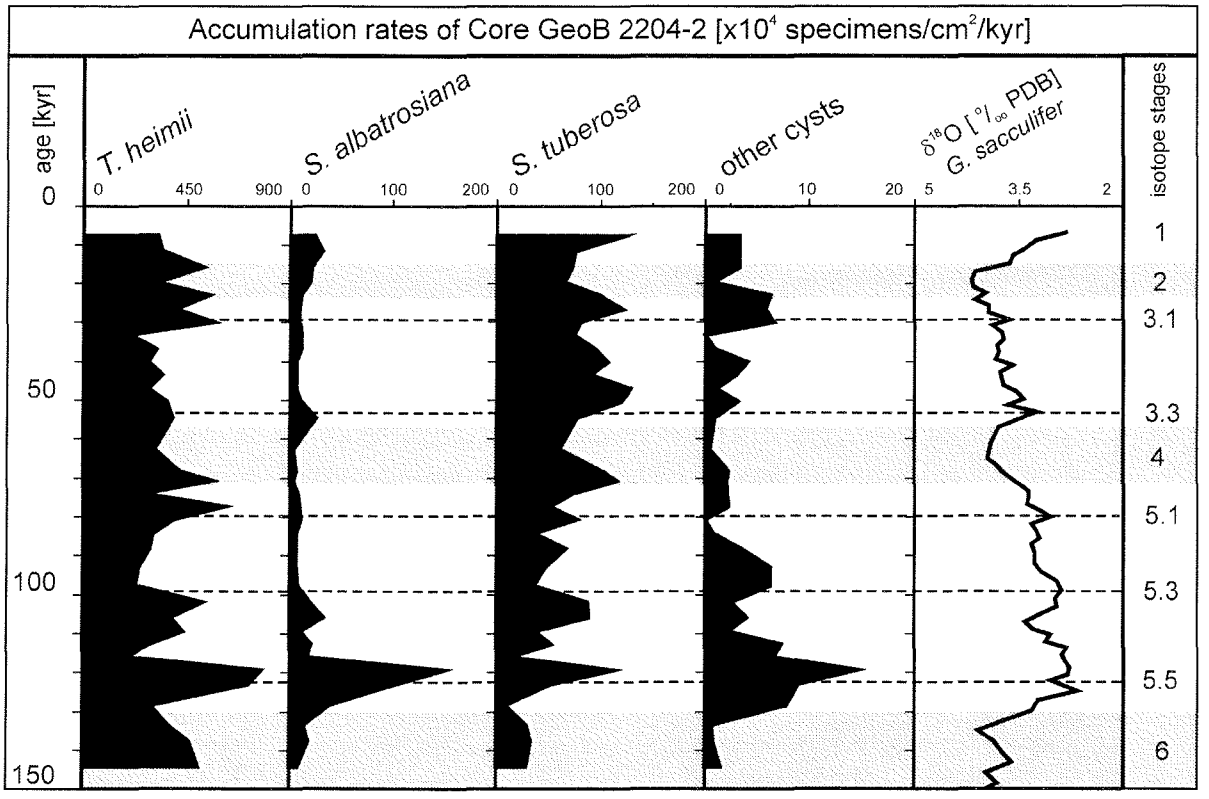

Fig. 7. Accumulation rates of the calcareous dinoflagellate cysts of core GeoB 2204-2 and oxygen isotope values of the planktic foraminifer *Globigerinoides sacculifer* (after Dürkoop et al., 1997).

Dissolution occurs mainly below the lysocline. It becomes critical below the calcium carbonate compensation depth (CCD). In the South Atlantic Ocean the water depth of the lysocline varies between the glacial/interglacial cycles. At present-day, the lysocline in the Cape Basin is linked with the mixing zone of carbonate ion supersaturated NADW and carbonate ion undersaturated LCDW at about 4000 m (Reid, 1989). In glacial times the production of NADW in the North Atlantic Ocean is thought to be decreased, thereby weakening or even cutting off the influx of less corrosive water to the southern ocean basins (Curry, 1996). This implies that, during glacials the LCDW dominated the Cape Basin rather than NADW and may have caused increased carbonate dissolution (Bickert and Wefer, 1996). If preservation changes through lysocline depth variations were the dominant influencing factor on calcareous dinocyst accumulation, we would expect low concentrations during glacials. Since we find comparable low values in glacials and interglacials in the cores GeoB 3603-2 and GeoB 1214-1 we assume, that varying carbonate dissolution as result of changing bottom water conditions had no major effect.

During interglacials the lysocline in the Brazil Basin is presumed to have a position at about 4000 m water depth (Bickert and Wefer 1996), whereas during glacials the lysocline is thought to be ascended to a depth of about 3200 m (Bickert and Wefer, 1996; Curry, 1996). Only the location of one core (GeoB 1117-2) is at nearly 4000 m depth, the two other equatorial Atlantic Ocean cores were taken from shallower depths of 3225m (GeoB 1105-4) and 2072m (GeoB 2204-2). Thus, dissolution through corrosive water may have occurred only at the deeper core position through influence of corrosive southern deep and bottom waters, as it has also been concluded by Höll et al. (1999). Since low accumulation rates of calcareous dinocysts in both glacial and interglacial intervals of core GeoB 1117-2 are observed, variations in the depth of the lysocline seem to have had minor effect on the calcareous dinocyst preservation only.

The second process influencing carbonate preservation, is the decay of organic matter at the sea floor, which can cause carbonate dissolution by reduction of carbonate ion concentration in the sediment pore water (Emerson and Bender, 1981; Jahnke et al., 1994). The rate of carbonate dissolution depends on the rate of organic matter production in the upper water column which, in turn, is related to nutrient concentration. We observe extremely high calcareous dinocyst accumulation rates at the Terminations in the Cape Basin and in the area of the Equatorial Divergence Zone. If this is the result of productivity related dissolution, decreased organic matter production would be expected to have taken place at the Terminations in comparison to glacials and interglacials. Nowadays, the AGC transports warm, low nutrient suprathermocline water with low chlorophyll-*a* concentrations from the Indian Ocean to the Cape Basin (Weeks and Shillington, 1994; Fig. 1c). This area is surrounded by the high productivity Benguela upwelling area in the north, which has its southernmost extension at the Cape Peninsula, and the high productivity Subtropical Front in the south (Shannon, 1985). Chlorophyll-*a* concentrations at the southermost core (GeoB3603-2) position

show intermediate values between those of the surrounding high productivity areas and the AGC. The warm Indian Ocean water is transported further northward via the Benguela and South Equatorial currents in equatorial direction. The northern Cape Basin may be influenced by upwelling through the westward drift of Benguela eddies composed of upwelled water under influence of the westward turning BOC (Diester-Haass, 1985). Furthermore, present-day weak Westerlies result in a shallow thermocline at the Walvis Ridge and lead to mesotrophic conditions in the upper water column at site GeoB 1214-1 as well. Reconstructions show that similar conditions prevailed during interglacial time intervals (Kemle-von Mücke, 1994).

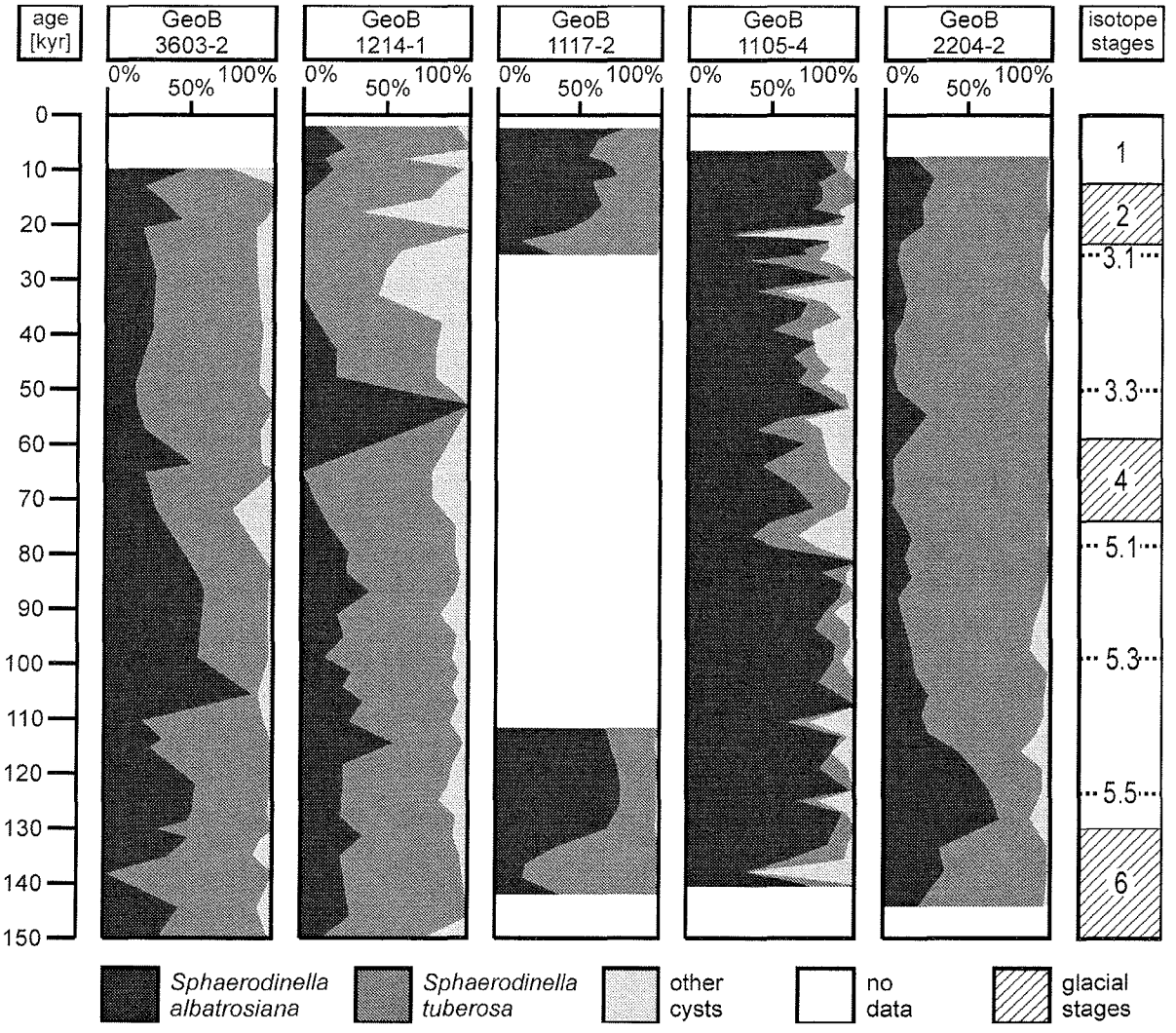

Fig. 8. Relative abundances of *Sphaerodinella albatrosiana*, *Sphaerodinella tuberosa*, and the other calcareous dinoflagellate cysts in relation to the oxygen isotope stages and events of the last 150 kyr (after Martinson et al., 1987).

For glacials, Winter and Martin (1990) reconstructed a slow down of the warm water influx from the Indian Ocean to the Atlantic Ocean via the AGC. Relatively more suprathermocline water from the Pacific Ocean is thought to have been transported into the South Atlantic Ocean via the so called "cold water way". The high productivity area of the STF might have migrated slightly

northwards during this times through a speed up of the SAC (Winter and Martin, 1990), influencing the southernmost core location. During present-day strong winters, Shannon (1985) showed southward progradation of the wind-driven Benguela upwelling influenced area. This may have taken place during glacials as well. Due to the strong SE-Tradewinds, resulting in the speed-up of currents, increased upwelling may have led to a shallow thermocline at the Walvis Ridge (site GeoB 1214-1). In combination with decreased influx of Indian Ocean water this could have caused cold, nutrient-enriched surface water, leading to high primary productivity.

For the Terminations, a large overturn has been assumed in the thermohaline circulation (Imbrie et al., 1992; Bickert and Wefer, 1996). The system possibly switched from the "cold water way", to the "warm water way" with increasing inflow of AGC water after a short period of calmness. As a result, the STF shifted back southward in the Agulhas region. Consequently, during the calm period, oligotrophic (sub)surface water conditions might have prevailed at the southernmost core position. For the Benguela system, Kemle-von Mücke (1994) pointed out possible deepening of the thermocline in the BOC caused by eastward progradiation of the SG at the Terminations. Eddie shedding at the westward turn of the BOC occurred to far northward to affect the southern Walvis Ridge (Diester-Haass, 1985). This would coincide with an increase in surface temperature due to the weakening of the cold water influx from the south and weakening of the coastal upwelling (Hart and Currie, 1960). Therefore, we would expect calmer, warmer, nutrient-depleted surface waters in the northern Cape Basin during the Terminations. This indicates that, relative to the present-day and glacial situations, extremely low productivity in the upper water column can be expected at both core positions that would have resulted in good preservation of carbonate during these intervals. As such, preservation could be an explanation for the observed extremely high cyst accumulation rates at the Terminations. Increased preservation during the Teminations has also been assumed for foraminifers (Diester-Haass, 1985; Howard and Prell, 1994). However, studies carried out on benthic foraminifers (Bickert, 1992) and coccoliths (Cepek, 1996) of Walvis Ridge core sediments, as well as planktic foraminifer studies in the Benguela area (Little et al., 1997), show no obvious dissolution effects. This is remarkable if productivity-related dissolution of carbonate would be the most important influencing factor. Thus, other factors might be of major influence as well.

Nowadays and during interglacials, a relatively weak SEC at the Equatorial Divergence Zone leads to weak equatorial divergence with moderate upwelling intensity and relatively stratified, less oligotrophic conditions above the location of core GeoB 1105-4. This is the result of a weaker zonal component of the SE trade winds coinciding with strong North African Monsoon caused by an increased pressure gradient between the ocean and North Africa (Mix and Morey, 1996). Considering that the core off the upwelling area (GeoB 1117-2) is located only 4°S of the equatorial divergence, the present-day upwelled waters from the EDZ descend at the approximate position of this core and cause convergence, coinciding with a deepening of the thermocline (Kemle-von Mücke, 1994).

Nevertheless, chlorophyll-*a* concentrations are comparable to those found at the Walvis Ridge (Fig. 1c).

During glacials, the more zonal SE trade winds, coinciding with a weaker Monsoon, accelerated the SEC, which may have caused increased equatorial upwelling at the EDZ (Mix and Morey, 1996). The upwelling area may have extended laterally to 7°S (Kemle-von Mücke, 1994), thereby affecting both core locations. As increased upwelling leads to higher nutrient concentrations in the surface water, this may have caused generally higher nutrient concentrations in the (sub)surface water, thus, leading to high primary production above the core positions.

For the Terminations, the changes from a strong to a weak Monsoon, coinciding with changes from a strong zonal component of SE trade winds to more meridional trade winds, may have caused a calm situation at the EDZ. Calmness in wind stress may have caused weakest oceanic currents with less upwelling intensity and lowest productivity in the equatorial region. Mix and Morey (1996) pointed out weakest upwelling at the EDZ during the global ice melting periods, which are actually the glacial Terminations. This indicates that extremely good preservation of carbonate during the Terminations could have occured at the EDZ as well, which is in convenience with our results. However, although changes in carbonate preservation seem to explain our dinocyst signals, studies on benthic and planktic foraminifer tests of the cores GeoB 1105-4 and GeoB 1117-2 as well as coccolith data of core GeoB 1117-2 show no dissolution effects (Bickert, 1992; Meinecke, 1992; Baumann et al., 1999). Therefore, it is questionable if productivity related dissolution is the only/major factor influencing the calcareous dinocyst accumulation rates.

Palaeoenvironmetal reconstructions of the region off north-east Brazil document extremely oligotrophic conditions in the upper water column for interglacial, glacial and transitional times (Houghton, 1991; Rühlemann, 1996). Consequently, extremely good preservation is expected in this region during the complete investigated interval. This is in agreement with our results that no obvious variation is observed in the calcareous dinocyst accumulation rates. Former observations on foraminifers and pteropods support this conclusion (Rühlemann, 1996; Gerhardt et al., 2000).

Production of calcareous cysts

Besides preservation effects, the accumulation rates of the calcareous dinocysts can also reflect cyst production. As discussed above, extremely calm, oligotrophic conditions could have occured in the studied areas at the Terminations. This would confirm the assumption made by Höll et al. (1998) and Höll et al. (1999), that calcareous dinocysts are produced in higher amounts under oligotrophic conditions. The high accumulation rates of the four eastern South Atlantic Ocean cores at the Terminations could imply increased production of cysts in these intervals. Therefore, we assume the extremely high accumation rates to be the result of a combined effect of production and good

carbonate preservation.

Temperature and salinity

The lower relative abundance of *S. albatrosiana* compared to *S. tuberosa* in the Cape Basin (Fig. 8) may be due to colder environmental conditions relative to that in the tropical Atlantic Ocean (Zonneveld et al. in press). Furthermore, the high relative abundance of *S. albatrosiana* in the EDZ compared to the Cape Basin (Fig. 8) may be due to fluctuations in surface temperature and salinity during glacial/interglacial cycles. As we mentioned earlier in this study, *S. albatrosiana* is assumed to be positively correlated with these parameters. This may reflect the increase in surface water temperature or salinity from glacials towards interglacials. This assumption is supported by Mix and Morey (1996), who reconstructed a shallow thermocline with colder surface waters during the glacials of the eastern tropical Atlantic Ocean in contrast to a deeper thermocline with warmer surface water during interglacials.

The comparison of the relative abundance of *S. albatrosiana* to *S. tuberosa* in the western equatorial Atlantic Ocean core shows a predominance of the latter during glacials and interglacials (Fig. 8). This may suggest decreased salinity compared to the eastern equatorial Atlantic Ocean rather than temperature changes, since minimal seasonal variations in sea surface temperatures are reconstructed for this region (Houghton, 1991). However, Dürkoop et al (1997) assumed minimal changes in salinity as well. Thus, the dominance of S. tuberosa in core GeoB 2204-2 can not be explained by changes in sea surface temperature and salinity.

Conclusions

The analysis of five gravity cores from the South Atlantic Ocean shows significantly high accumulation rates of calcareous dinocysts in the eastern South Atlantic Ocean at the Terminations 2 and 1. According to their relation to oligotrophic conditions in the upper water column, we assume calm, low-nutrient conditions during the Terminations from glacials to interglacials for the eastern South Atlantic Ocean core locations. Furthermore, we assume high dinocyst production rates coinciding with increased carbonate preservation as a result of low organic matter productivity related dissolution. The continually high accumulation rates of calcareous dinocysts at the western core position during the last two glacial/interglacial cycles leads to the assumption that no significant changes in the trophic conditions of the western tropical Atlantic Ocean occurred.

Low relative abundance of *S. albatrosiana* compared to *S. tuberosa* in the subtropical Cape Basin cores may reflect colder environmental conditions. At the Equatorial Divergence Zone, the high relative abundance of *S. albatrosiana* compared to *S. tuberosa* may be due to warmer sea surface temperatures compared to the Cape Basin.

Acknowledgements

We would like to thank Anne de Vernal and Jens Matthiessen for critical reading and correcting the manuscript. Furthermore, we thank Annemiek Vink for English corrections and the whole group of AG Willems for inspiring discussions. The data sets used in this paper are available in the PANGAEA data base (http://www.pangaea.de/home/oesper/). This study is carried out as part of the projects SFB 261:"Der Südatlantik im Spätquartär: Rekonstruktion von Stoffhaushalt und Stromsystem" and Graduiertenkolleg: "Stoffflüsse in marinen Geosystemen" (SFB 261 Contribution No. 290).

Appendix A. Taxonomic information

Eight species/morphotypes of calcareous dinoflagellate cysts were recognised in the observed sediment cores. The taxonomy of subfamilies and higher taxonomic levels follows Fensome et al. (1993). The taxonomy of the calcareous dinoflagellate cysts taxa cited in the current paper is given in Keupp (1997), Keupp and Versteegh (1989), Keupp and Kohring (1993), Hildebrand-Habel et al. (1999) and Janofske (2000). In addition, two morphotypes of *Sphaerodinella tuberosa* were distinguished: *Sphaerodinella tuberosa* var. 1 is composed of relatively large, block-like individual crystals which do not inter-finger with each other, whereas cysts of *Sphaerodinella tuberosa* var. 2 consists of smaller, roughly triangular-shaped, inter-fingering crystals.

Order THORACOSPHAERALES Tangen, 1982
Family THORACOSPHAERACEAE Schiller, 1930, emend. Tangen, 1982
Genus *Thoracosphaera* Kamptner, 1927
Thoracosphaera heimii (Lohmann) Kamptner, 1944

Order PERIDINIALES Haeckel, 1894
Family PERIDINIACEAE Ehrenberg, 1931
Subfamily CALCIODINELLOIDEAE Fensome et al., 1993
Genus *Calciodinellum* Deflandre, 1947
Calciodinellum operosum (Deflandre) Montresor et al., 1997

Genus *Sphaerodinella* Keupp and Versteegh, 1989
Sphaerodinella tuberosa (Kamptner) Hildebrand-Habel et al., 1999
morphotype: *Sphaerodinella tuberosa* var. 1
Sphaerodinella tuberosa var. 2
Sphaerodinella albatrosiana (Kamptner) Keupp and Versteegh, 1989

Genus *Orthopithonella* Keupp, 1984
Orthopithonella granifera (Fütterer) Keupp and Kohring, 1993

Genus *Scrippsiella* Balech ex Loeblich III emend. Janofske, 2000
Scrippsiella regalis (Gaarder) Janofske, 2000
Scrippsiella trochoidea (von Stein) Loeblich III, 1965 emend. Janofske, 2000

Plate I

Scanning electron microscope (SEM) and light microscope (LM) photographs of the calcareous dinoflagellate cyst species/morphotypes (line bars represent 10 μm).

1. and 4. *Thoracosphaera heimii* (SEM and LM).

2. and 5. *Sphaerodinella albatrosiana* (SEM and LM).

3. and 6. *Calciodinellum operosum* (SEM and LM).

7. and 10. *Sphaerodinella tuberosa* var. 1 (SEM and LM).

8. and 11. *Sphaerodinella tuberosa* var. 2 (SEM and LM).

9. and 12. *Orthopithonella granifera* (SEM and LM).

Plate I

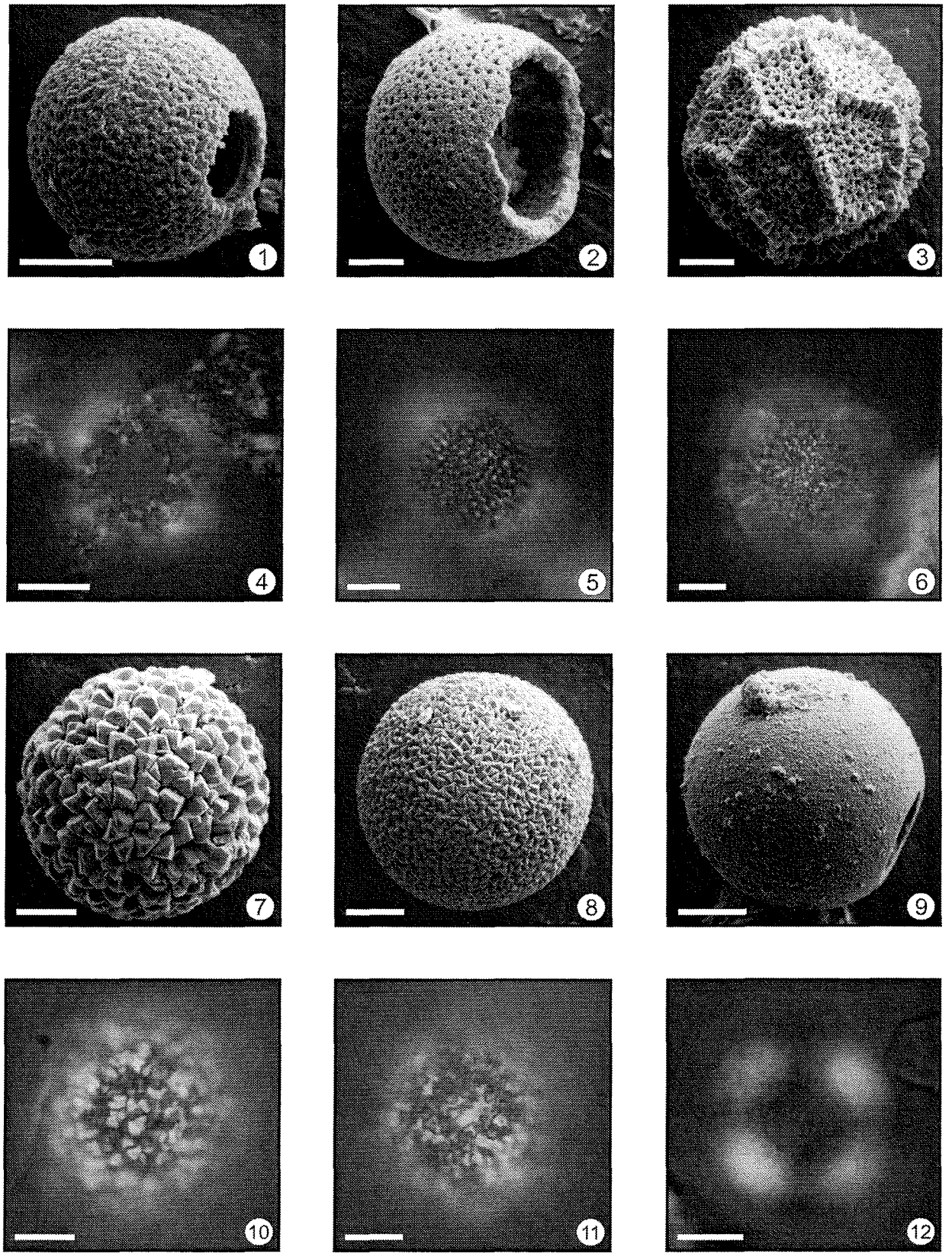

5. Palaeoceanography of the South Atlantic Ocean at the last two Terminations

Oliver Esper, Karin A.F. Zonneveld and Helmut Willems
Universität Bremen, Fachbereich 5 – Geowissenschaften, Postfach 330 440, D-28334 Bremen, Germany

Abstract

Nowadays, one of the most important oceanic circulation systems in sustaining the moderate climate of the northern hemisphere is the so called thermohaline circulation (THC). Within this current system, the southward flow of cold, saline North Atlantic Deep Water is balanced by cross-equatorial transport of southern hemisphere warm (sub)surface and intermediate waters via the South Atlantic Ocean. However, it is unclear how exactly the THC steered the climate during the Late Quaternary glacial/interglacial cycles. One of the questions is to what extend the source of the surface balance flow is the Indian Ocean; so called "warm water path". Besides this, a second major return path, carrying Antarctic Intermediate Water and Pacific waters, is assumed; so called "cold water path".

Information based on calcareous dinoflagellate cyst (dinocyst) accumulation rates of five previously published sediment cores of the South Atlantic Ocean and one new record derived from the Benguela upwelling area (GeoB1710-3) are compared to other palaeoceanographic proxies of the same cores or the same regions. Former studies assumed high calcareous dinocyst accumulation rates to reflect warm, stratified, less trophic surface water conditions. As maxima in calcareous dinocysts accumulation coincide with increased relative abundances of the tropical foraminifera *Globigerinoides ruber* (pink) and *Globigerinoides sacculifer* as well as with high surface water temperatures derived from alkenones in the eastern subtropical and equatorial South Atlantic Ocean, this implies generally weakened surface currents and reduced upwelling along the THC warm water path at the glacial Terminations. In coincidence with warm water influx from the Indian Ocean via the Agulhas Current during low seasonality caused by perihelion aligned with austral winters, this may have led to warm, saline, low-nutrient (sub)surface water in the eastern and equatorial South Atlantic Ocean. A reduced cross-equatorial transport via the North Brazil Current consequently may have led to southward recirculation of warm waters and the build-up of a heat depot in the South Atlantic Ocean subtropical region during the Terminations.

Keywords: Palaeoceanography, Calcareous dinoflagellate cysts, Glacial Terminations, Late Quaternary, South Atlantic Ocean

Introduction

In the last decades it has become apparent that large scale ocean circulation can have large impact on the world's climate via heat transfer (e.g. Wefer et al., 1996a). One of the most important

circulation systems is the so called thermohaline circulation (THC). Nowadays, large amounts of cold, saline deep water, produced in the North Atlantic Ocean, are transported to the southern hemisphere. In balance, warm tropical and subtropical (sub)surface and central waters are transported from the southern hemisphere across the equator to the North Atlantic Ocean, thereby positively influencing the climate of the northern continents (Gordon, 1986; Rahmstorf, 1996). Up to now it is, however, unclear how exactly the THC steered the climate during the Late Quaternary glacial/interglacial cycles. One of the main uncertainties is to what extend the source of the surface balance flow is the Indian Ocean; so called "warm water path". Besides this, a second major return path is assumed; so called "cold water path". Hereby, Antarctic Intermediate Water and Pacific surface waters enter the South Atlantic Ocean at the Drake Passage, cross the South Atlantic Ocean within the South Atlantic Current and join the Benguela Current offshore South Africa (Gordon et al., 1992). Whether the warm or the cold path contributes more to the return flow or even dominates it is still a debate (Gordon, 1986; Rintoul, 1991; Gordon et al., 1992; Nof and Van Gorder, 1999; Holfort and Siedler, 2001).

To reveal insight in this problematic, detailed information of the South Atlantic Ocean current system during the Late Quaternary is essential. Especially the last two major glacial Terminations are important due to the great impact of variations in the ocean circulation on hydrography and environment of the South Atlantic Ocean. To date, the main driving force on the south to north flowing currents of the South Atlantic Ocean are the south-eastern trade winds (Schneider, 1995; Wefer et al., 1996a; Schneider et al., 1999). The amount of volume transport as well as the strong upwelling of cold water in the eastern part of the South Atlantic Ocean is assumed to be mainly caused by strong zonal SE trades, at which strong eastern equatorial upwelling in addition is caused by weak monsoon intensity in combination with increased zonality of the SE trades (Mix and Morey, 1996; Little et al., 1997a).

Generally, increased warm water influx to the South Atlantic Ocean and transport further northward is assumed for interglacial periods. Vice versa, during glacials a more dominant "cold water path" combined with less influx of Indian Ocean water and generally stronger surface water circulation than during interglacials was reconstructed (McIntyre et al., 1989). Nowadays, contradicting reconstructions exist for the ocean circulation at the last Terminations. Arz et al. (1999) reconstructed a slow-down or even shut-down of the cross-equatorial heat transport during several times of the Termination 1, related to meltwater events of the northern hemisphere. Such meltwater events are also reconstructed for the Termination 2, assuming more or less similar conditions for both deglaciations (Lototskaya et al., 1998). Lototskaya and Gansen (1999) also assumed the establishment of a stable, stratified water column to be correlated with the Termination 2 in the North Atlantic Ocean. Highest sea-surface temperatures are assumed for the eastern South Atlantic Ocean based on alkenone temperature reconstructions (Kirst et al., 1999), implying either less input of cold waters via upwelling or increased warm water inflow of the warm water path. Based on the calcareous dinoflagellate cyst assemblage composition, less trophic, calm conditions for the south-eastern

subtropical and eastern equatorial South Atlantic Ocean surface currents at the Terminations is assumed (**Chapter 4**). In contrast, Kasten et al. (2001) assumed increased productivity during the Terminations based on anomalous barium concentrations at that times.

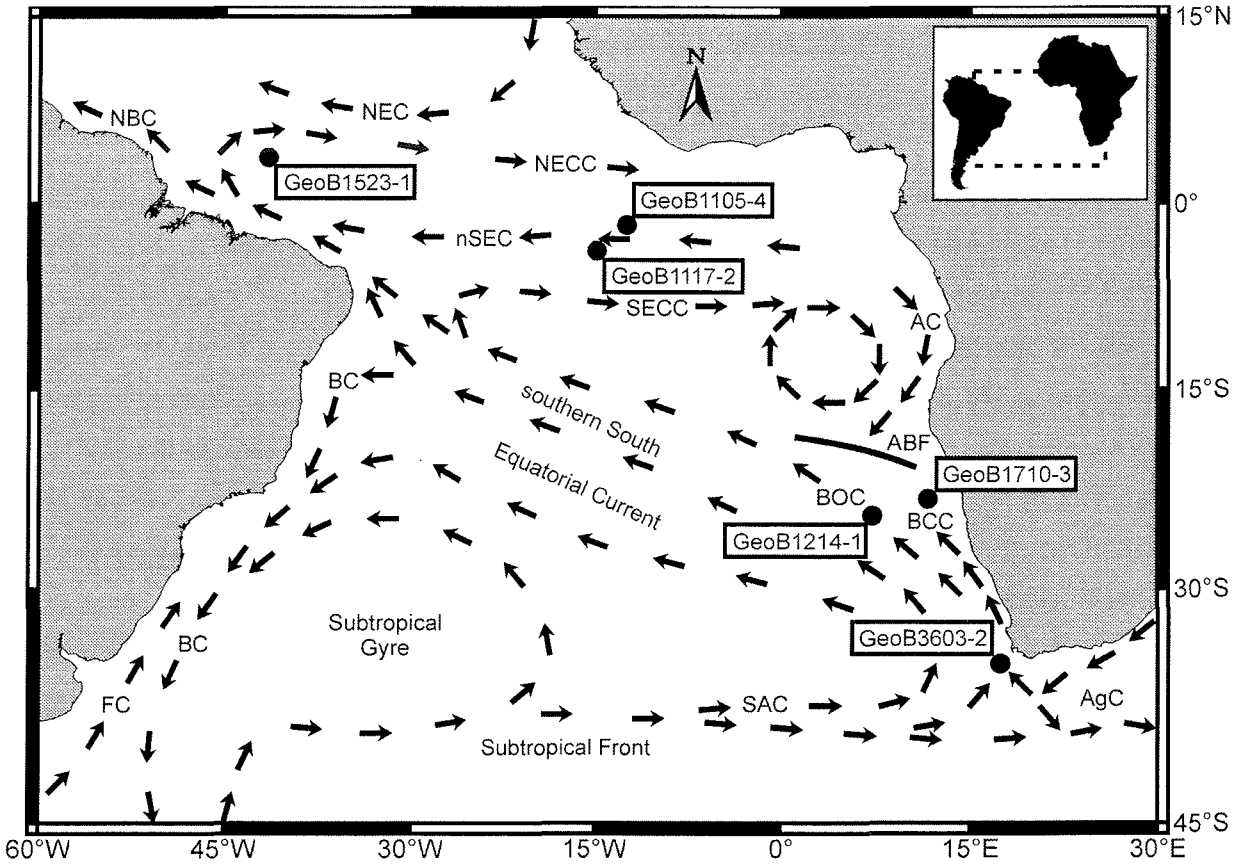

Fig. 1. Locations of the sediment cores and schematic summary of sea surface currents of the South Atlantic Ocean (after Peterson and Stramma, 1991; Stramma and Schott, 1999; AC: Angola Current; ACC: Antarctic Circumpolar Current; ABF: Angola-Benguela Front; AgC: Agulhas Current; BC: Brazil Current; BCC: Benguela Coastal Current; BOC: Benguela Ocean Current; FC: Falkland Current; NBC: North Brazil Current; NEC: North Equatorial Current; NECC: North Equatorial Counter Current; nSEC: northern South Equatorial Current; SAC: South Atlantic Current; SECC: South Equatorial Counter Current).

In this paper, we will show that calcareous dinoflagellate cyst (dinocyst) accumulation rates and planktic foraminifera relative abundances reflect orbital forced oceanic circulation changes related to the THC return flow. We show that warmer, more stratified conditions of the Benguela upwelling area and the Equatorial Divergence Zone occurred during Termination 2 and 1, related to decreased wind stress and reduced upwelling activity.

Oceanographic Settings

Main feature of the ocean surface circulation of the South Atlantic Ocean is the anticlockwise circulating Subtropical Gyre (Fig. 1; Peterson and Stramma, 1991). Its southern border is formed by the eastwards flowing temperate waters of the South Atlantic Current, which is bound southwards to the subpolar waters of the Antarctic Circumpolar Current by the Subtropical Front. Sources of the

South Atlantic Current are the Pacific Ocean beyond Drake Passage and the Falkland Current. Off Southwest Africa the South Atlantic Current joins the Agulhas Current, which transports tropical and subtropical warm, saline (sub)surface waters of the Indian Ocean in the form of large, anticyclonic eddies and filament water around the tip of Africa. The two currents form the source of the eastern border of the Subtropical Gyre, the Benguela Current. South of Walvis Ridge the mainly wind driven Benguela Current splits into a strictly northward flowing coastal current and a north-westward flowing ocean current. Driven by the south-eastern trade winds under the control of the South Atlantic Anticyclone, the Benguela Coastal Current forms the source of the nutrient–rich, high productivity Benguela upwelling area (Shannon, 1985). The less trophic Benguela Ocean Current on the other hand carries the warm Agulhas Current water further northwards across the Walvis Ridge and joins the westwards flowing South Equatorial Current, the northern boundary of the Subtropical Gyre. Off north-east Brazil the South Equatorial Current splits into the eastwards recirculating Equatorial Counter Current, the northwards flowing North Brazil Current and the southwards flowing Brazil Current, which forms the western boundary of the Subtropical Gyre. Within the eastern South Equatorial Current divergence takes place, forming the second most important high productivity area of the South Atlantic Ocean. The intensity of this divergence is driven by the zonal component of the south-eastern trade winds and the African monsoon. The North Brazil Current carries the warm, saline water across the equator and further northwards, finally reaching the mid-latitudes of the northern hemisphere, influencing the climate of the northern continents and balancing the southward flow of cold, high saline North Atlantic Deep Water produced in the northern hemisphere (Gordon, 1986).

Material and Methods

1. Core material

This study is based on a compilation of several previously published works on calcareous dinoflagellate cysts of six sediment cores from the eastern subtropical and equatorial South Atlantic Ocean, and one additional sediment core from the Benguela upwelling area (Tab. 1; Fig. 1). Gravity core GeoB 1710-3 was recovered in the northern Cape Basin off the Benguela upwelling area (23°25.9′S, 11°41.3′E), at a water depth of 2987 m (Schulz et al., 1992). 24 samples were taken for calcareous dinoflagellate cyst analysis (Fig. 2). Sample preparation has been done according to (**Chapter 4**). Due to the low abundance of calcareous dinocysts, 100 specimens on average have been counted for each sample. A number of 5 calcareous dinocyst species have been identified, following the taxonomy of Williams et al. (1997) and Janofske et al. (2000).

2. Methods

According to several studies on calcareous dinocyst distribution in South Atlantic Ocean sea surface sediments (Vink et al., 2000; Zonneveld et al., 2000) and Late Quaternary time series analyses

(Höll et al., 1998; Höll et al., 1999; Vink et al., 2000; **Chapter 3**; **Chapter 4**), high calcareous dinocyst accumulation rates are generally observed when a deep, stratified thermocline is present. In addition, *Thoracosphaera heimii* and *Sphaerodinella albatrosiana* are assumed to be related to well stratified, less trophic, warm (sub)surface water (Vink et al., 2000), whereas *Sphaerodinella tuberosa* var. 2 is assumed to be related to stratified, more trophic, colder (sub)surface water (Zonneveld et al., 2000; **Chapter 4**).

Table 1. Position and references for calcareous dinoflagellate cyst, planktic foraminifera and palaeotemperature records discussed in the text and shown in figures. The last column indicates different kinds of values showing maxima at the glacial Terminations 2 and 1.

Record	Position	Region	Reference	Type
GeoB1028-5	20°06′S, 09°11′E	Benguela Current	Schmidt, 1992	planktic foraminifera REL[1]
			Schneider et al., 1995	alkenone SST[2]
GeoB1031-4	21°53′S, 07°06′E	Benguela Current	Schmidt, 1992	planktic foraminifera REL[1]
GeoB1032-3	22°55′S, 06°02′E	Benguela Current	Schmidt, 1992	planktic foraminifera REL[1]
GeoB1105-4	01°40′S, 12°26′W	South Equatorial Current	Höll et al., 1998	calcareous dinocyst ACC[3]
			Schneider et al., 1996	alkenone SST[2]
GeoB1117-2	03°49′S, 14°54′W	South Equatorial Current	**Chapter 4**	calcareous dinocyst ACC[3]
GeoB1214-1	24°41′S, 07°15′E	Benguela Current	**Chapter 4**	calcareous dinocyst ACC[3]
GeoB1220	24°02′S, 05°18′E	Benguela Current	Schmidt, 1992	planktic foraminifera REL[1]
GeoB1523-1	03°50′N, 41°37′W	Brazil Current	Vink , 2000	calcareous dinocyst ACC[3]
GeoB1710-3	23°26′S, 11°42′E	Benguela Current	**Chapter 5**	calcareous dinocyst ACC[3]
			Kirst et al., 1999	alkenone SST[2]
GeoB3603-2	35°08′S, 17°33′E	Benguela / Agulhas Current	**Chapter 3**	calcareous dinocyst ACC[3]
			Schneider et al., 1999	planktic foraminifera REL[1] alkenone
			Schneider et al., 1999	SST[2]

[1] Relative abundance
[2] Sea surface temperature reconstruction
[3] Accumulation rates

Results

The analysis of the sediment core GeoB 1710-3 from late oxygen isotope stage 6 (145 kyr B.P.) up to the Recent revealed low abundances of calcareous dinocysts during the Late Quaternary and low species diversity. Only shells of *Thoracosphaera heimii* and cysts of *Sphaerodinella tuberosa* var. 2 and *Sphaerodinella albatrosiana* are abundant throughout the studied time interval. Very low calcareous dinocyst accumulation rates are increased significantly at the Terminations only (around 125 kyr B.P. and 12 kyr B.P.; Fig. 2). To a lesser extend, slightly increased accumulation rates were observed around interglacial substage 5.1. These three peaks occurred during times of low seasonal contrast, when perihelion is aligned with boreal summer/austral winter, and are associated with minima in precession and maxima in obliquity (Fig. 2).

The occurrence of the high calcareous cyst accumulation rates in core GeoB 1710-3 coincides with distinct calcareous dinocyst accumulation peaks observed in Late Quaternary sediments of the

Agulhas Current off South Africa (GeoB 3603-2; Fig. 3), the Benguela Ocean Current at Walvis Ridge (GeoB 1214-1; Fig. 3), the South Equatorial Current in vicinity of the Equatorial Divergence Zone (GeoB 1105-4 and GeoB 1117-2; Fig. 4) and the North Brazil Current (GeoB 1523-1; Fig. 4).

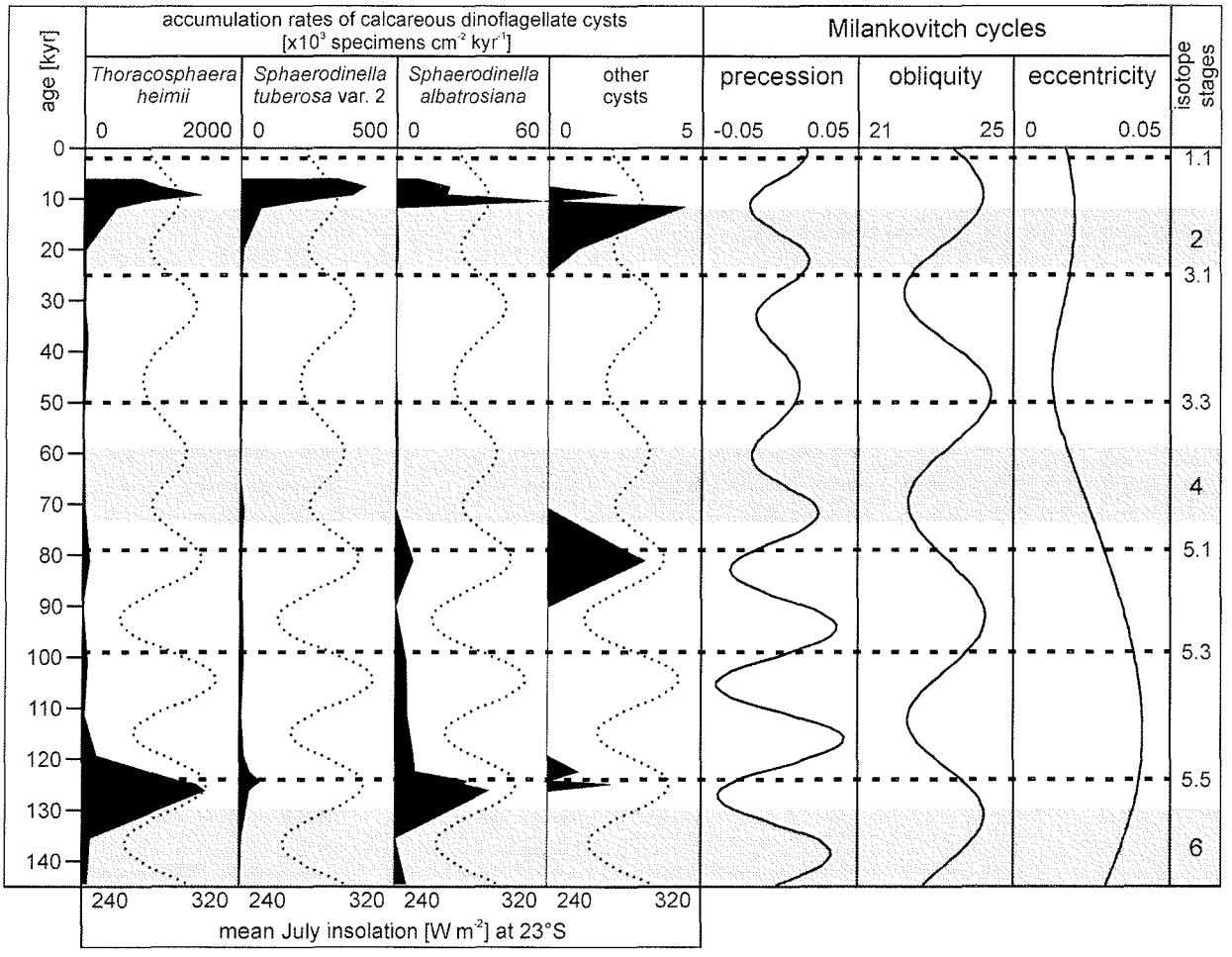

Fig. 2. Core GeoB 1710-3 calcareous dinoflagellate cyst accumulation rates in relation to the calculated mean July insolation (austral winter), the precession, the obliquity, and the eccentricity at 23°S (after Berger, 1978; stratigraphy after Schmiedl and Mackensen, 1997).

Discussion

In the eastern subtropical and equatorial tropical South Atlantic Ocean, high accumulation rates of calcareous dinoflagellate cysts are observed to occur more or less simultaneously in several different oceanic environments (Fig. 3 and 4). Calcareous dinocyst accumulation in these cores is thought to be mainly the result of cyst production in the upper water column (Höll et al., 1998; Höll et al., 1999; Vink, 2000; **Chapter 4**). For these cores neither large influence of cyst transport nor bad carbonate preservation was assumed at the Terminations 2 and 1 (Vink, 2000; **Chapter 4**). Quiet on the contrary, several studies in the eastern and tropical South Atlantic Ocean reconstructed excellent carbonate preservation during the glacial Terminations (e.g. Diester-Haass, 1985; Howard and Prell, 1994; Rühlemann et al., 1996). Similar results are observed for core GeoB 1710-3.

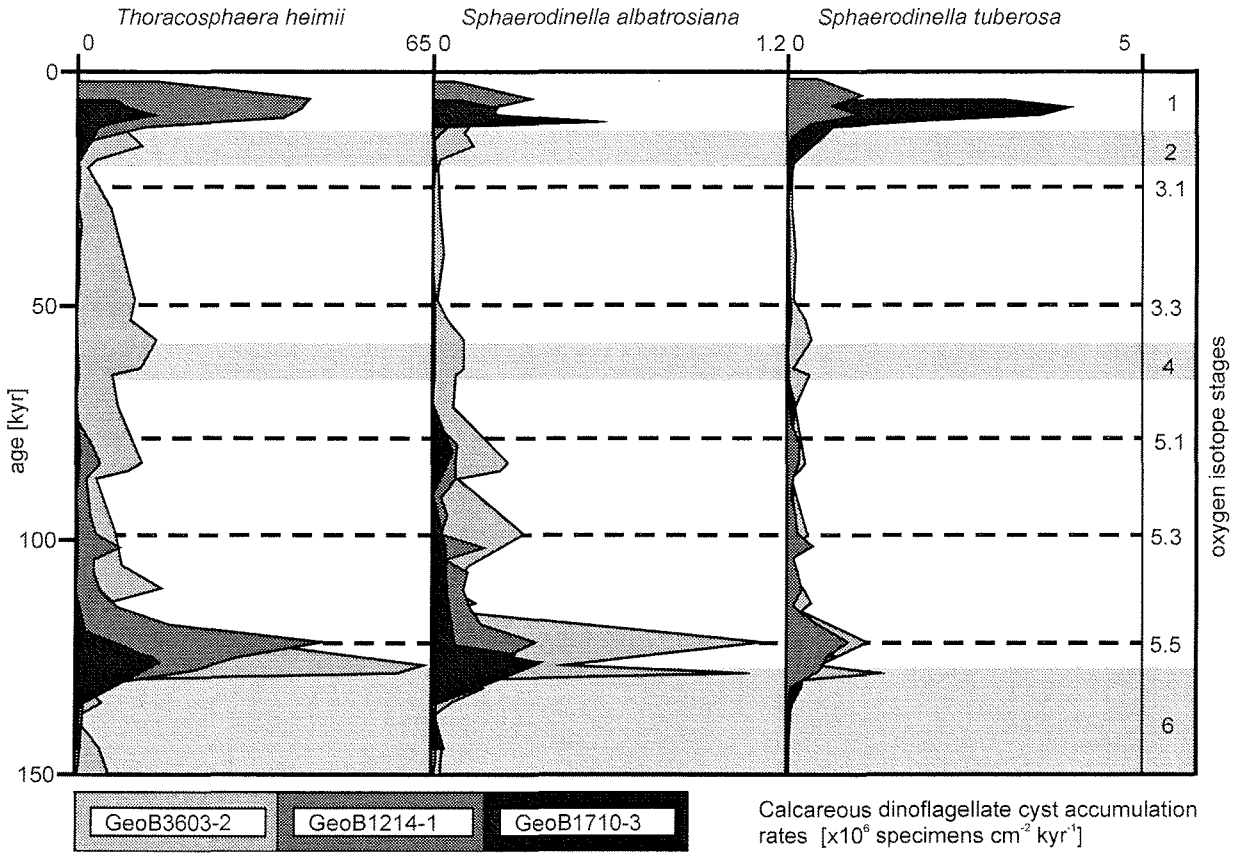

Fig. 3. Accumulation rates of *Sphaerodinella albatrosiana*, *Sphaerodinella tuberosa* var. 2 and *Thoracosphaera heimii* of the eastern subtropical Atlantic Ocean cores GeoB 3603-2, GeoB 1710-3 and GeoB 1214-1.

Since high calcareous dinocyst accumulation appears to be related to a deep, stratified thermocline and low nutrient availability in the surface water, the dinocyst peaks at the Terminations and to a lesser extend around oxygen isotope substage 5.1 suggest stratified, low trophic (sub)surface water conditions along the warm water path of the thermohaline circulation in the Benguela upwelling area in coherence with the oceanic conditions in the rest of the South Atlantic Ocean. In the following, we will discuss the oceanic processes possibly responsible for the establishment of such an environment in the South Atlantic Ocean.

Interbasin heat exchange

All sediment cores from the eastern subtropical and equatorial South Atlantic Ocean (Fig. 1) show an increase in accumulation rates of *T. heimii* and the calcareous cysts of *S. albatrosiana* and *S. tuberosa* var. 2 at times of initial deglaciation with highest values at times of high sea surface temperatures (Fig. 3, Fig. 4, Fig. 5; Schneider et al., 1999). In coincidence, an increase in relative abundance of the tropical foraminifera *Globigerinoides ruber* (pink) and *Globigerinoides sacculifer* in the Agulhas Current (Schneider et al., 1999) and in the Benguela Current at Walvis Ridge (Schmidt, 1992) is observed (Fig. 6).

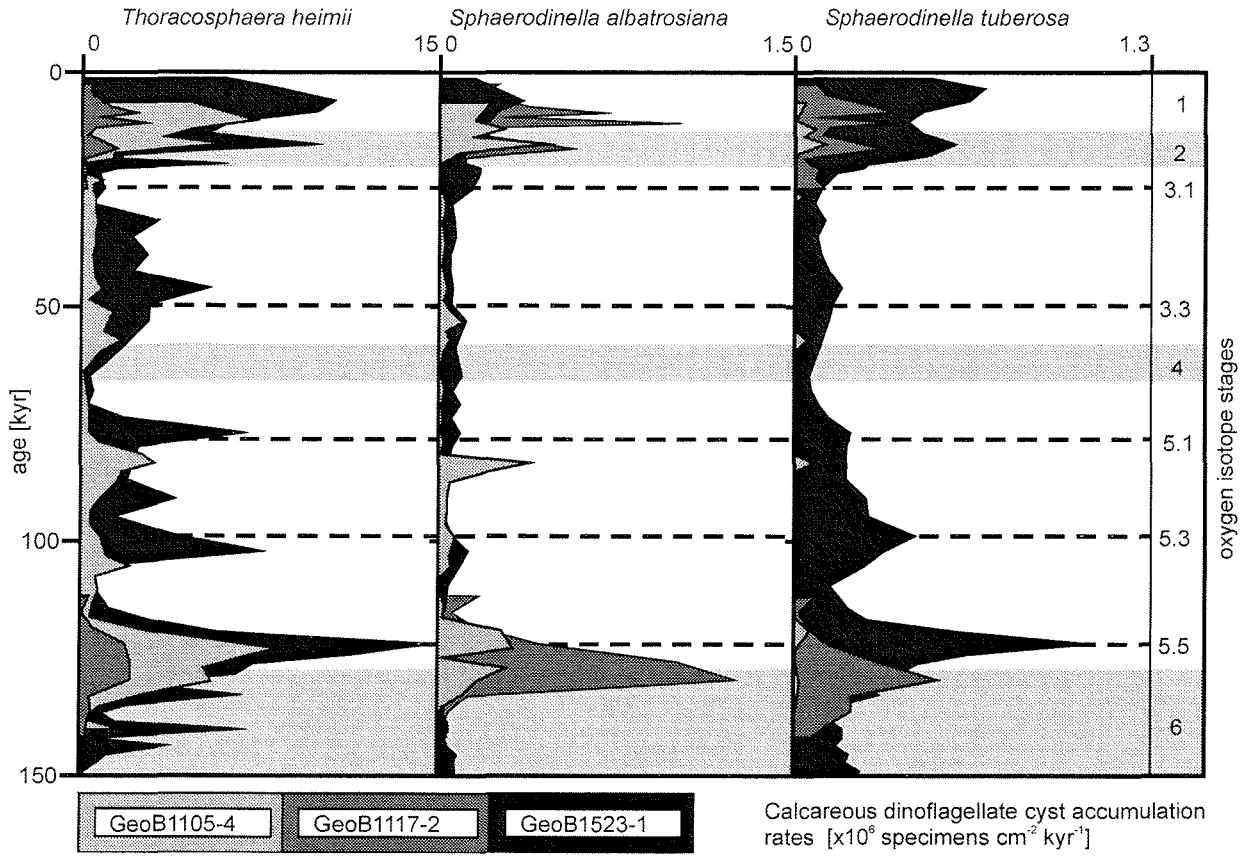

Fig. 4. Accumulation rates of Sphaerodinella albatrosiana, Sphaerodinella tuberosa var. 2 and Thoracosphaera heimii of the tropical Atlantic Ocean cores GeoB 1105-4, GeoB 1117-2 and GeoB 1523-1.

Due to several studies carried out on the distribution and ecological affinity of modern planktic foraminifera, the relative abundance of the tropical planktic foraminifera *G. ruber* (pink) and *G. sacculifer* reflects changes in sea surface temperatures (Ufkes et al., 1998; Ufkes et al., 2000). High relative abundance of the two species may be a sign of subtropical to tropical surface water temperatures due to the temperature optimum of *G. ruber* (pink) close to 27°C and *G. sacculifer* around 22°C (Mulitza et al., 1998a). Furthermore, *G. sacculifer* seems to tolerate low nutrient concentrations and might, therefore, reflect also less trophic conditions (Bijma et al., 1994; Bijma and Hemleben, 1994).

The foraminifera relative abundance at Walvis Ridge reflects a gradient from the rather cold Benguela Coastal Current to the warmer Benguela Ocean Current along the Walvis Ridge and implies warm and/or more stratified conditions at the Terminations (Schmidt, 1992). Thus, we assume for the Agulhas and Benguela currents a more stratified suprathermocline water column with less trophic, warmer water conditions than during the preceding glacials as well as the succeeding interglacial stages. This might be due to increased influx of warm, low-nutrient (sub)surface waters of the Indian Ocean to the Atlantic Ocean via the Agulhas Current and advection to the Benguela Current and/or the reduction in upwelling of cold, nutrient-rich central and intermediate waters along the western coast of South Africa and Namibia (Charles and Morley, 1988; McIntyre et al., 1989; Pether, 1994; **Chapter 3**).

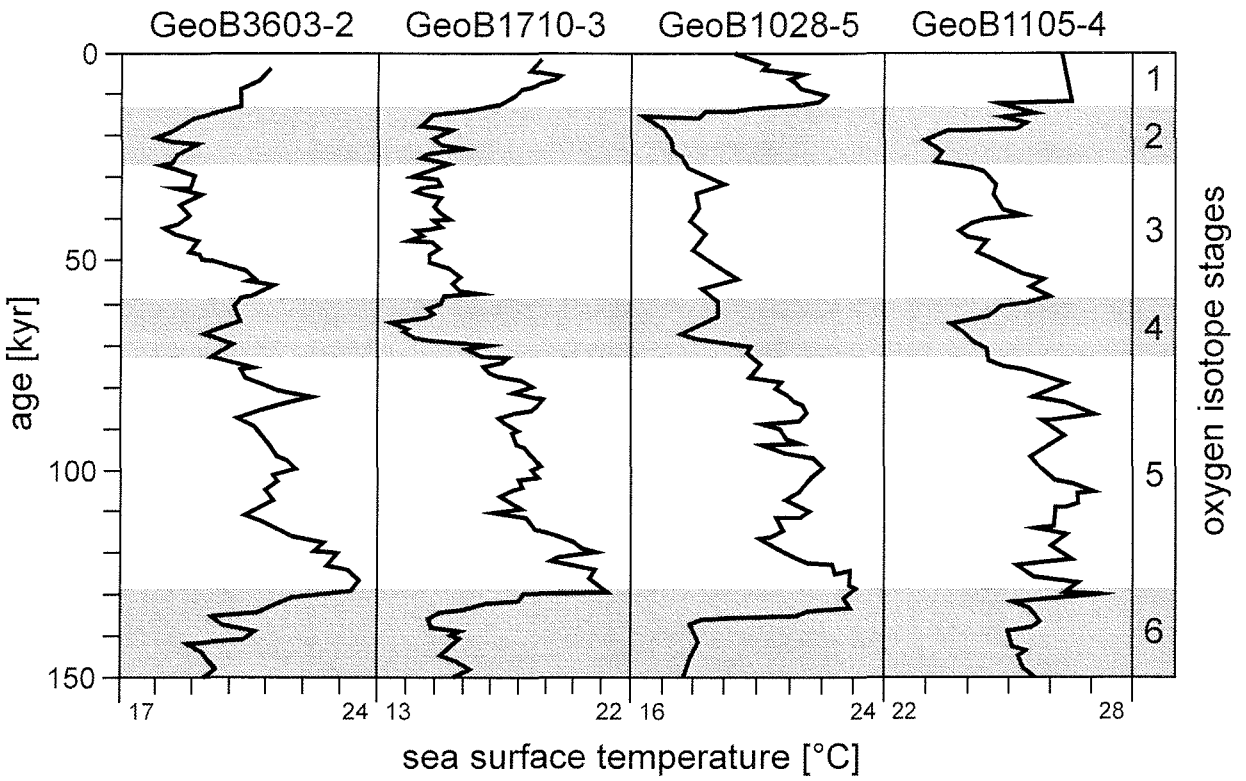

Fig. 5. Reconstructed sea surface temperatures of the eastern and equatorial South Atlantic Ocean based on alkenons (after Schneider et al., 1995; Schneider et al., 1996; Kirst et al., 1999; Schneider et al., 1999).

The input of Agulhas current and Agulhas Bank water into the southern Benguela is assumed to be at a maximum during interglacial summers under south-easterly winds, when the westerlies are shifted polewards south of Africa and the intensity of the circulation is reduced in the Indian Ocean (Pether, 1994; **Chapter 3**). This occurs especially when perihelion is aligned with boreal summer/austral winter, at times of high winter insolation in the Southern Hemisphere. In coherence with our observations, this constellation happened at both Terminations 2 and 1 as well as around substage 5.1.

Wind-driven upwelling

The second process influencing sea surface temperatures and nutrient concentrations is the upwelling of cold, nutrient-rich central and intermediate waters along the western coast of South Africa and Namibia. The upwelling process is caused by Ekman transport related to wind stress of the south-easterly trade winds. Especially the upwelling of cool water due to the advection of Antarctic Intermediate Water to the South Atlantic Central Water in the southern Benguela during late spring and summer negatively influences the sea surface temperatures (Dingle and Nelson, 1993). A reduction in upwelling intensity would lead to warmer (sub)surface water. Lower austral summer insolation during times of austral winter perihelion, together with deglacial warming at high latitudes, probably reduced the meridional temperature gradient and caused weaker SE trade winds (Pether, 1994). A reduction of summer upwelling in the Benguela would be the result. In addition, a

reduction of the intensity of thermal lows on the coastal plain during times of low seasonal contrast would result in less acceleration of the coastal wind and, therefore, in reduced upwelling.

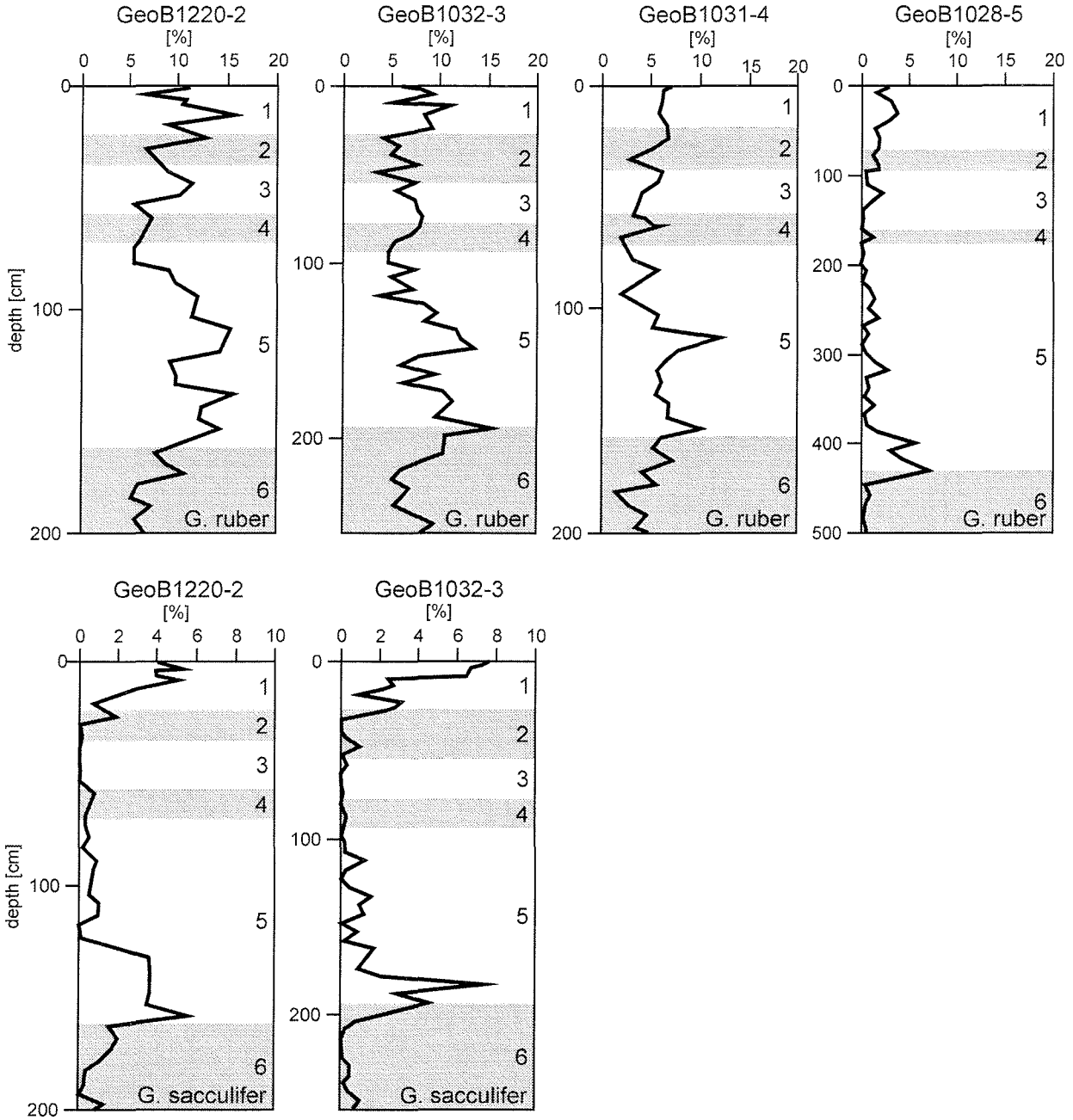

Fig. 6. Relative abundance of the planktic foraminifer *Globigerinoides ruber* (pink) and *Globigerinoides sacculifer* in sediment cores of the Walvis Ridge, eastern South Atlantic Ocean (after Schmidt, 1992).

For the northern Benguela upwelling, the zonality of the trade winds is of great importance. The zonality of the trade winds shows a strong 23-kyr periodicity that is almost in phase with the austral winter insolation (Schneider et al., 1995). Generally, an enhancement of upwelling intensity is aligned to times of increased trade wind zonality, coinciding with increased upwelling in the Angola Basin and along the Equatorial Divergence Zone (Little et al., 1997b). Thus, reduced upwelling may have occurred during times of meridional directed SE trade winds, when austral winter insolation was

at its maximum (Ufkes et al., 2000). Such orbital conditions occurred during the Terminations 2 and 1 and to a lesser extend around substage 5.1.

In the eastern Equatorial Atlantic, adjacent to the upwelling area of the Equatorial Divergence Zone, the calcareous dinocyst accumulation rates of cores GeoB 1117-2 and GeoB 1105-4 (Fig. 4) as well as the alkenone based SST reconstruction of GeoB 1105-4 (Fig. 5) again suggest less trophic, stratified, warm (sub)surface water conditions at the Terminations. During times of high summer insolation, e.g. times of high seasonality, the Equatorial Divergence is under the control of the zonal component of the SE trade winds and experiences decreased influence of monsoon winds. This results in enhanced upwelling. At the Terminations, the warming of Southern Ocean coinciding with a reduced thermal gradient above Africa due to highest insolation during the boreal summer leads to increased strength of the monsoon winds and to a weakening of the zonal component of the SE trade winds (McIntyre et al., 1989; Mix and Morey, 1996). This might have resulted in the observed decreased upwelling intensity as well as in decreased advection of cold Benguela water to the central Equatorial Atlantic Ocean coinciding with an increased advection of warm (sub)surface water of Indian Ocean origin (McIntyre et al., 1989; Mix and Morey, 1996; Schneider et al., 1996). Consequently, more stratified, warmer (sub)surface water above a deepened thermocline may have been the result.

Variations in thermocline depth

In the western equatorial Atlantic Ocean, a calcareous dinocyst record from the North Brazil Current (GeoB 1523-1) shows highest accumulation rates of calcareous dinocysts around the last two major glacial Terminations, but maxima in accumulation rates lag the peaks of the records from the eastern and south-eastern regions for a few thousand years (Fig. 4). As the region of the North Brazil Current nowadays is characterised by oligotrophic (sub)surface waters, the high calcareous dinocyst accumulation rates may reflect warm water conditions and a deep, stratified thermocline (Vink et al., 2000).

Largely inverse timing in palaeoproductivity for the western Equatorial Atlantic Ocean compared to the eastern and south-eastern regions is assumed (Rühlemann et al., 1996). An increase of upwelling related palaeoproductivity in the east, related to strengthening of zonal wind stress during times of high seasonality would coincide with a deepening of the thermocline and nutricline in the west, leading to more oligotrophic (sub)surface conditions. This may be the case in the cold substages of the last glacial/interglacial cycles (Rühlemann et al., 1996; Kinkel et al., 2000). Additionally, Mulitza et al. (1998) assumed that the nutrients were depleted only in the upper thermocline and enriched in deep waters during the cold substages. If calcareous dinoflagellate production is related only to oligotrophic conditions, this would have provided favourable conditions for calcareous cyst production. However, we do not observe increased accumulation rates during these times. This

suggests either less trophic level dependency of calcareous dinoflagellate production or deep-dwelling of these organisms.

Vice versa, during warm substages higher palaeoproductivity coinciding with a deep, stable thermocline was reconstructed for in the western equatorial Atlantic Ocean (Rühlemann et al., 1996; Mulitza et al., 1998). As we find high rates of dinocyst accumulation during these intervals, after all this might suggest rather nutrient affinity of calcareous dinoflagellate production. Vink et al. (2000), therefore, assumed for calcareous dinoflagellate production in the western Atlantic Ocean rather the establishment of a deep, stratified thermocline than an affinity to less trophic water conditions. Thus, the calcareous dinocysts peaks observed in the North Brazil Current may be caused by a deepening of the thermocline and warming of the suprathermocline water column.

Up to a certain point, the increased palaeoproductivity in the western Equatorial Atlantic Ocean at the Terminations would support the results of Kasten et al. (2001). They assumed high productivity of organic matter at the Terminations reflected by distinct peaks of excess barium and total degradation of the deposited organic carbon due to action of a oxidation front right after the Terminations. As no remains of organic organisms were found in higher concentrations in this specific intervals, the barium peaks may be attributed to carbonate producers as well. In addition, the degradation of organic matter in a low-productivity area would lead to increased carbonate dissolution (Jahnke et al., 1994), whereas Rühlemann et al. (1996) reconstructed good carbonate preservation for the Terminations 2 and 1. Thus, a relation of the barium peaks to carbonate producers is more likely than increased organic matter production. However, Kasten et al. (2001) neither attribute the barium production to specific biotic processes, nor do they exclude abiotic sources of the barium excess. Furthermore, no information is available on the barium content of calcareous cysts yet. Thus, a relation of the barium peaks with the simultaneously occurring high calcareous dinocyst accumulation rates can not be assumed.

For several times of the Termination 1, Arz et al. (1999) assumed slow-down or even shut-down of cross-equatorial (sub)surface water transport via the North Brazil Current due to a reduction in North Atlantic Deep Water production caused by freshwater events in the northern hemisphere. Thus, the warm South Atlantic Ocean Water may have been piled up in the western equatorial Atlantic Ocean, producing conditions favourable for calcareous dinoflagellates and tropical foraminifera. Most of the warm water, however, is assumed to return to the South Atlantic Ocean subtropics via the Brazil Current. At the end of such a freshwater event, the THC should have been reactivated, transporting large amounts of heat across the equator, forcing the deglaciation process in the northern hemisphere and finally leading to subsequent cooling of the southern hemisphere (Crowley, 1992).

Contrarily, conditions of reduced northward heat transport are assumed to have prevailed during the last glacial period as well, when stronger SE trades caused a pile-up and "push-back" of heat flow across the equator due to a strengthened retroflection of the North Brazil Current, leading to the accumulation and storage of warm and saline waters in the western subtropical Atlantic Ocean

(McIntyre and Molfino, 1996; Rühlemann et al., in press). Thus, either a weak North Brazil Current or a strong retroflection would have led to decreased cross-equatorial heat transport, causing anomalously high sea surface temperatures along the warm water return path and in the western subtropical Atlantic Ocean. However, this would have favoured the production of calcareous dinoflagellate cysts as well as tropical foraminifera not only during the observed intervals. As high accumulation peaks of calcareous dinocysts occur only at the warm substages, times of increased productivity in the western equatorial Atlantic Ocean, second to the warm, deep, stratified thermocline nutrient availability must play an important role in dinocyst production. Thus, the calcareous dinocyst record of the western Equatorial Atlantic Ocean reflects rather local changes in oceanography than can be compared to oceanographic conditions in the eastern subtropical and equatorial Atlantic Ocean at the Terminations (Vink, 2000).

Implications for the thermohaline circulation

Under the assumptions of insolation as a main driving force of the global thermohaline circulation return paths, perihelion aligned with austral winter, as it occurred at the last two glacial Terminations, would have enabled warm (sub)surface water transport from the Indian Ocean via the Agulhas Current into the South Atlantic Ocean and further northward up to the Equator via the Benguela Ocean Current and the South Equatorial Current. During these times, reduced upwelling in the Benguela region and in the Equatorial Divergence Zone would have led to decreased conversion of Antarctic Intermediate Water of the cold water path into South Atlantic Central Water. For several periods of the deglaciation, cross-equatorial transport is assumed to have been slowed-down due to a weak North Brazil Current (Arz et al., 1999), and warm (sub)surface water may have returned to the South Atlantic via the Brazil Current, recirculating in the subtropical gyre and possibly increasing its net heat budget. A slowed down THC may than be sustained by increased intermediate water outflow to the northern hemisphere. Thus, during the glacial Terminations 2 and 1, the cold water return path of the thermohaline circulation may have been the main flow balancing the reduced southward transport of North Atlantic Deep Water to the southern hemisphere.

Summary and Conclusions

The Late Quaternary record on calcareous dinoflagellate cysts of six sediment cores along the (sub)surface warm water return path of the THC in the Atlantic Ocean shows highest accumulation rates mainly at the last two glacial Terminations. These peaks coincide with increased relative abundances of tropical foraminifera and high surface water temperatures in the eastern subtropical and equatorial South Atlantic Ocean derived from alkenones. As calcareous dinocyst production is associated with the establishment of a stratified suprathermocline water column and low-nutrient tolerance, and secondary processes such as allochthonous transport and carbonate dissolution can be

excluded to be of large influence, this implies generally weakened surface currents along the THC warm water path. Decreased wind speed and a predominant meridional component of the south-eastern trade winds would have led to reduced upwelling in the Benguela and Equator Divergence regions. In coincidence with warm water inflow from the Indian Ocean via the Agulhas Current during times of low seasonality, this would have led to warm, saline, low-nutrient (sub)surface water in the eastern and equatorial South Atlantic Ocean. Reduction in cross-equatorial warm water transport and increased recirculation southward consequently would have led to the build-up of extremely warm, nutrient depleted (sub)surface water masses in the subtropics, finally intensifying the warm water conditions in the south-eastern South Atlantic Ocean.

Acknowledgements

We thank everyone in the working group of Historical Geology and Palaeontology at Bremen University for their general assistance. Furthermore, we thank Annemiek Vink and Gerard Versteegh for helpful discussions. Additionally, we thank Christian Harnach for laboratory work. The data presented in this paper is available in the PANGAEA data base (http://www.pangaea.de/home/oesper). The research was funded by the Deutsche Forschungsgemeinschaft through the special research project Sonderforschungsbereich 261 "Der Südatlantik im Spätquartär: Rekonstruktion von Stoffhaushalt und Stromsystemen". This is SFB 261 contribution number XXX.

Conclusions and prospects for future research

The eastern South Atlantic Ocean appears to be a highly dynamic region with several different environments. **Chapter 2** has shown that the subtropical central South Atlantic Ocean is characterised by dinoflagellate species known for there affinity to oceanic, oligotrophic environments. The region north of the Subtropical Front is dominated by *Impagidinium* species of high diversity. At the Subtropical Front, the cyst assemblage changes to increased numbers of the cosmopolitic species *Protoceratium reticulatum* and *Nematosphaeropsis labyrinthus*, associated with less numbers of oceanic cyst species. Further southward, at the Subantarctic Front, a more severe change in the organic-walled dinoflagellate cyst assemblage occurs. The cysts related to autotrophic species decrease in number and diversity, whereas a few cyst species related to heterotrophic dinoflagellates, such as the genus *Protoperidinium*, become dominant in highest numbers. This reflects the shift to the high-nutrient, cold water environment of the Antarctic Circumpolar Current. Thus, the organic-walled cyst producing dinoflagellates seem to be applicable tools to monitor the environmental changes in the Southern Ocean.

The environment of the subtropical eastern South Atlantic Ocean, on the other hand, represents a more complex connection of three oceans: the Atlantic Ocean, the Indian Ocean and the Southern Ocean. **Chapter 3** revealed a broad range of organic-walled dinoflagellate cyst species, related to high-nutrient, transitional and oceanic environments, to be characteristic for the Cape Basin. Furthermore, up to 8 calcareous dinoflagellate cyst species, dominated by *Thoracosphaera heimii*, *Sphaerodinella albatrosiana* and *Sphaerodinella tuberosa* var. 2, appear in highest numbers during specific time periods. The analysis of the sediment core GeoB 3603-2 revealed a complex system of linear and non-linear forcing on the environment of the Cape Basin, the gateway of warm, Indian Ocean (sub)surface water and cold, subpolar surface water to the South Atlantic Ocean. The calcareous- and organic-walled dinoflagellate cyst assemblages of core GeoB3603-2 reflect periodic productivity changes on a Milankovitch scale. Organic-walled dinoflagellate cysts are high abundant in times of high seasonal contrast, e.g. times of high austral summer insolation. This periodic change is reflected as well by the pollen and spores content of the observed sediment core. In addition, sub-Milankovitch frequencies in the power spectra of two dinoflagellate cysts groups, related to high nutrient environments and transitional environments, suggest interferences of the subtropical regime and the subpolar regime at the Subtropical Front. Calcareous dinoflagellate cysts, in contrast, show high numbers during times of low seasonal contrast, especially at the last two major glacial Terminations. Therefore, times of high seasonal contrast seem to favour surface water productivity due to upwelling, whereas times of low seasonal contrast seem to favour warm Indian Ocean water influx to the South Atlantic Ocean.

The comparison of variations in Late Quaternary calcareous dinoflagellate cyst assemblages at several locations in the South Atlantic Ocean, shown in **Chapter 4**, revealed a connection of the eastern South Atlantic Ocean by the (sub)surface return path of the thermohaline circulation. The similarity of the calcareous cyst distribution pattern at four locations of different environments, ranging from the more oligotrophic Walvis Ridge region to the upwelling regime of the Equatorial Divergence Zone, implies the establishment of stratified, less trophic conditions during glacial Terminations from the Cape Basin up to the equator. This assumption is supported in **Chapter 5** by additional information on the Late Quaternary calcareous dinocyst distribution in close vicinity of the Benguela upwelling area, as well as by the comparison of results based on calcareous dinocysts with distribution pattern of the warm water related planktic foraminifera *Globigerinoides ruber* (pink) and *Globigerinoides sacculifer*, and palaeotemperatures based on alkenones. The results suggest the establishment of warm, stratified, less trophic conditions in the entire eastern and equatorial South Atlantic Ocean along the thermohaline circulation return path at the Terminations 2 and 1.

For future research, the investigation of Late Quaternary environmental changes in the South Atlantic Ocean due to linear and non-linear forcing on Milankovitch and sub-Milankovitch scales could be of great importance to understand climatic change. The interferences of oceanic systems steered by the forcing of different dominant orbital and non-orbital parameters is not well understood yet. For example, it could be helpful to investigate the variations in dinoflagellate cyst assemblages within time series of the Southern Ocean to proof the dominance of obliquity rather than precession on high latitude insolation. In **Chapter 2** the organic-walled dinoflagellate cyst distribution is assumed to be front specific. Time series analyses of sediment cores nowadays positioned in vicinity of major fronts of the Southern Ocean may, in addition, provide information on the movement of the Subtropical Font, the Subantarctic Front and the Antarctic Polar Front during glacial/interglacial cycles. **Chapter 2** has also shown a possible use of the organic-walled dinoflagellate cyst distribution for temperature transfer functions in the eastern Atlantic sector of the Southern Ocean. To do so, the improvement of the distribution density of surface sediment sample analyses would be important.

In **Chapter 4** a certain influence of carbonate dissolution on the calcareous dinocyst preservation is assumed. Furthermore, a pilot study on the preservation of calcareous dinocysts, derived from Equatorial Atlantic Ocean sea-surface sediment samples of various depth, revealed alteration in the dinocyst wall structure depending on the water depth, may be related to diagenesis or dissolution (previously unpublished data). Another inportant field of future reseach could be, therefore, the estimation of dissolution vulnerability for several cyst species.

Acknowledgements

I wish to express my gratitude to Prof. Dr. Helmut Willems for giving me the possibility to do this dissertation, and his advice and support throughout the work. For her permanent encouragement, enthusiasm and unlimited dedication, and for teaching me to see beyond what is obvious, I am very grateful to my advisor Dr. Karin Zonneveld.

I would like to thank Sebastian Meier, Michael Streng and Jens Wendler, my office mates for the last four and a half years, along with Emma Eades, Christine Höll, Annemiek Vink and Ines Wendler, the so-called "Quaternary group", for the good fellowship and the comfortable atmosphere which made for a productive working climate. I am also grateful to Tania Hildebrandt-Habel for lively discussions not only concerning dinoflagellates, and Matthias Bork, Kai-Uwe Gräfe and Dorothea Janofske for many discussions providing me insight which greatly improved the quality of the dissertation. I also very much appreciate the stimulating discussions with Gerard Versteegh, who critically read much of this work and was always willing to help. Special thank is due to Erna Friedel for her permanent helpfulness not only in administrative matters. Hartmut Mai introduced me into the fascinating world of the scanning electron microscope. Anja Bammann, Angelika Freesemann, Anne Hübner, Monika Kirsch and Nicole Zatloukal are thanked for their laboratory and technical assistance as well as for the preparation of the ships cruises M41/2 and ANT-XVIII/5a. All members of the Division of Historical Geology and Palaeontology are thanked for providing me such a wonderful and hospitable company, making working in Bremen ever memorable.

I also sincerely thank my parents Hans-Werner and Hannelore Esper who have always been there for me. I am very sad that my father did not live to see me finishing this work.

The research was funded by the Graduiertenkolleg "Stoffflüsse in marinen Geosystemen" and by the Sonderforschungsbereich 261 "Der Südatlantik im Spätquartär: Rekonstruktion von Stoffhaushalt und Stromsystemen" at the Universität Bremen. Their financial support is greatly acknowledged.

References

Abelmann, A., Gowing, M.M., 1997. Spatial distribution pattern of living polycystine radiolarian taxa–baseline study for paleoenvironmental reconstructions in the Southern Ocean (Atlantic sector). Mar. Micropaleontol. 30, 3-28.

Abelmann, A., Brathauer, U., Gersonde, R., Sieger, R., Zielinski, U., 1999. Radiolarian-based transfer function for the estimation of sea surface temperatures in the Southern Ocean (Atlantic Sector). Paleoceanography 14 (3), 410-421.

Anderson, D.M., Lively, J.J., Reardon, E.M., Price, C.A., 1985. Sinking characteristics of dinoflagellate cysts. Limnol. Oceanogr. 30 (5), 1000-1009.

Arz, H.W., Pätzold, J., Wefer, G., 1999. The deglacial history of the western tropical Atlantic as inferred from high resolution stable isotope records off northeastern Brazil. Earth Planet. Sci. Lett. 167, 105-117.

Asmus, T., Frank, M., Koschmieder, C., Frank, N., Gersonde, R., Kuhn, G., Mangini, A., 1999. Variations of biogenic particle flux in the southern Atlantic section of the Subantarctic Zone during the late Quaternary: Evidence from sedimentary $^{231}Pa_{ex}$ and $^{230}Th_{ex}$. Marine Geology 159, 63-78.

Bakker, D.C.E, De Baar, H.J.W, Bathmann, U.V., 1997. Changes of carbon dioxide in surface waters during spring in the Southern Ocean. Deep-Sea Res. 44 (1-2), 91-127.

Balech, E., 1974. El genero "Protoperidinium" Bergh, 1881 ("Peridinium" Ehrenberg, 1841, partim). Revista del Museo Argentino de Ciencias Naturales "Bernardino Rivadavia", Hidrobiologia 4 (1), 1-79.

Barange, M., Pakhomov, E.A., Perissinotto, R., Froneman, P.W., Verheye, H.M., Taunton-Clark, J., Lucas, M.I., 1998. Pelagic community structure of the subtropical convergence region south of Africa and in the mid-Atlantic Ocean. Deep-Sea Res. I 45, 1663-1687.

Bathmann, U., Smetacek, V., De Baar, H., Fahrbach, E., Krause, G., 1994. The expedition Antarctis-X/6-8 of the research vessel *Polarstern* in 1992/93. Rep. Polar Res. 135, 236 pp.

Bathmann, U.V., Scharek, R., Klaas, C., Dubischar, C.D., Smetacek, V., 1997. Spring development of phytoplankton biomass and composition in major water masses of the Atlantic sector of the Southern Ocean. Deep-Sea Res. II 44 (1-2), 51-67.

Baumann, K.H., Cepek, M., Kinkel, H., 1999. Coccolithophores as indicators of ocean water masses, surface-water temperature, and paleoproductivity – Examples from the South Atlantic. In: Fischer, G., Wefer, G. (Eds.), Use of proxies in paleoceanography: Examples from the South Atlantic, Springer Verlag, Berlin, Heidelberg, pp. 117-144.

Berger, A.L., 1978a. Long-term variations of daily insolation and Quaternary climatic change. J. Atmos. Sci. 35, 2362.

Berger, A.L., 1978b. Long-Term variations of caloric insolation resulting from the Earth's orbital elements. Quat. Res. 9, 139-167.

Bickert, T., 1992. Rekonstruktion der spätquartären Bodenwasserzirkulation im östlichen Südatlantik über stabile Isotope benthischer Foraminiferen. Ber. Fachbereich Geowissenschaften Uni Bremen 27, 205 pp.

Bickert, T., Wefer, G., 1996. Late Quaternary deep water circulation in the South Atlantic: reconstruction from carbonate dissolution and benthic stable isotopes. In: Wefer, G., Berger, W.H., Siedler, G., Webb, D.J. (Eds.), The South Atlantic: present and past circulation. Springer, Berlin, Heidelberg, New York, pp. 599-620.

Bijma, J., Hemleben, C., 1994. Population dynamics of the planktic foraminifer *Globigerinoides sacculifer* (Brady) from the central red sea. Deep-sea Res. I 41 (3), 485-510.

Bijma, J., Hemleben, C., Wellnitz, K., 1994. Lunar-influenced carbonate flux of the planktic foraminifer *Globigerinoides sacculifer* (Brady) from the central red sea. Deep-sea Res. I 41 (3), 511-530.

Blackman, R. B., Tukey, J. W., 1958. The Measurement of Power Spectra From the Point of view of Communication Engineering, Dover Publications, New York, 190 pp.

Bleil, U., Brück, L., Frederichs, T., Haese, R., Hensen, C., Hilgenfeldt, C., Hoek, R., Hübscher, C., von Lom-Keil, H., Janke, A., Kreutz, R., Keenan, J., Little, M., Martens, H., Rosiak, U., Schmidt, W., Schneider, R.R., Segl, M., Spieß, V., Uenzelmann-Neben, G., Urbanek, H., Zühlsdorff, L., 1996. Report and preliminary results of METEOR-Cruise 34/1: Cape Town-Walvis Bay, 03.01.1996-26.01.1996. Ber. Fachbereich Geowissenschaften Uni Bremen 77, 129 pp.

Brathauer, U., Abelmann, A., 1999. Late Quaternary variations in sea surface temperatures and their relationship to orbital forcing recorded in the Southern Ocean (Atlantic sector). Paleoceanography 14 (2), 135-148.

Broecker, W.S., 1982. Glacial to interglacial changes in ocean chemistry. Progr. Oceanogr. 11, 151-197.

Broecker, W.S., Henderson, G.M., 1998. The sequence of events surrounding Termination II and their implications for the cause of glacial-interglacial CO2 changes. Paleoceanography 13 (4), 352-364.

Bujak, J.P., Davies, E.H., 1983. Modern and fossil Peridiniineae. Am. Assoc. Stratigr. Palynol. Contr. Series 13, 203 pp.

Campbell, I.D., 1999. Quaternary pollen taphonomy: examples of differential redeposition and differential preservation. Palaeogeogr., Palaeoclimatol., Palaeoecol. 149, 245-256.

Cepek, M., 1996. Zeitliche und räumliche Variationen von Coccolithophoriden-Gemeinschaften im subtropischen Ost-Atlantik: Untersuchungen an Plankton, Sinkstoffen und Sedimenten. Ber. Fachbereich Geowissenschaften Uni Bremen 86, 160 pp.

Charles, C.D., Morley, J.J., 1988. The paleoceanographic significance of the radiolarian *Didymocyrtis tetrathalamus* in eastern Cape Basin sediments. Palaeogeogr., Palaeoclimatol., Palaeoecol. 66, 113-126.

Conkright, M.E., Levitus, S., Boyer, T.P., 1994. World Ocean Atlas 1994 Volume 1: Nutrients. NOAA Atlas NESDIS 1. U.S. Department of Commerce, Washington, D.C. 150 pp.

Crowley, T.J., 1992. North Atlantic Deep Water cools the southern hemisphere. Paleoceanography 7, 489-497.

Curry, W.B., 1996. Late Quaternary deep circulation in the western Equatorial Atlantic. In: Wefer, G., Berger, W.H., Siedler, G., Webb, D.J. (Eds.), The South Atlantic: Present and Past Circulation, Springer-Verlag, Berlin, Heidelberg, pp. 577-598.

Dale, B., 1983. Dinoflagellate resting cysts: "benthic plankton". In: Fryxell, G.A. (Ed.), Survival strategies of the algae, Cambridge Univerity Press, Cambridge, pp. 69-136.

Dale, B., 1986. Life cycle strategies of oceanic dinoflagellates. UNESCO Technical Papers in Marine Science 49, 65-72.

Dale, B., 1992. Thoracosphaerids: Pelagic fluxes. In: Honjo, S. (Ed.), Dinoflagellate contribution to the Deep Sea, Ocean Biocoenosis Series 5, Woods Hole Oceanogr. Inst., Woods Hole, MA, pp. 33-43.

Dale, B., Dale, A.L., 1992. Dinoflagellate contribution to the Deep Sea. In: Honjo, S. (Ed.), Ocean Biocoenosis Series 5, Woods Hole Oceanogr. Inst., Woods Hole, MA, 75 pp.

Dale, B., 1996. Dinoflagellate cyst ecology: modeling and geological applications. Chap. 31. In: Jansonius, J., McGregor, D.C. (Eds.), Palynology: principles and applications. Vol. 3. Am. Assoc. Stratigr. Palynol. Found., Dallas, TX, pp. 1249-1275.

Davey, R.J., 1971. Palynology and palaeo-environmental studies, with special reference to the continental shelf sediments of South Africa. In: Farinacci, A., Matteucci, R. (Eds.), Proceedings of the Second Planktonic Conference, Roma 1970, Vol. 1, Technoscienza, Roma, pp. 331-347.

Davey, R.J., Rogers, J., 1975. Palynomorph distribution in Recent offshore sediments along two traverses off South West Africa. Mar. Geology 18, 213-225.

de Ruijter, W.P.M., Biastoch, A., Drijfhout, S.S., Lutjeharms, J.R.E., Matano, R.P., Pichevin, T., van Leeuwen, P.J. ,Weijer, W., 1999. Indian-Atlantic interocean exchange: Dynamics, estimation and impact. J. Geophys. Res. 104 (C9), 20885-20910.

de Vernal, A., Turon, J.-L., Guiot, J., 1994. Dinoflagellate cyst distribution in high-latitude marine environments and quantitative reconstruction of sea-surface salinity, temperature, and seasonality. Can. J. Earth. Sci. 31, 48-62.

de Vernal, A., Rochon, A., Turon, J.-L., Matthiessen, J., 1997. Organic-walled dinoflagellate cysts : Palynological Tracers of sea-surface conditions in middle to high latitude marine environments. GEOBIOS 30, 7, 905-920.

de Vernal, A., Hillaire-Marcel, C., 2000. Sea-ice cover, sea-surface salinity and halo-/thermocline structure of the northwest North Atlantic: modern versus full glacial conditions. Quat. Sci. Rev. 19, 65-85.

Devillers, R., de Vernal, A., 2000. Distribution of dinoflagellate cysts in surface sediments of the northern North Atlantic in relation to nutrient content and productivity in surface waters. Mar.

Geology 166, 103-124.

Diester-Haass, L. 1985. Late Quaternary Sedimentation on the eastern Walvis Ridge, SE Atlantic (HPC 532 and four piston cores). Mar. Geol. 65, 145-189.

Dingle, R.V., Nelson, G., 1993. Sea-bottom temperature, salinity, and dissolved oxygen on the continental margin off south-western Africa. S. Afr. J. Mar. Sci. 13, 33-49.

Dittert, N., Henrich, R., Carbonate dissolution in the South Atlantic Ocean: evidence from ultrastructure breakdown in *Globigerina bulloides*. Deep-Sea Res. I 47, 603-620.

Dürkoop, A., Hale, W., Mulitza, S., Pätzold, J., Wefer, G., 1997. Late Quaternary variations of sea surface salinity and temperature in the western tropical Atlantic: Evidence from □^{18}O of *Globigerinoides sacculifer*. Paleoceanography 12 (6), 764-772.

Edwards, L.E., Andrle, A.S., 1992. Distribution of selected dinoflagellate cysts in modern marine sediments. In: Head, M.J., Wrenn, L.H. (Eds.), Neogene and Quaternary Dinoflagellate Cysts and Acritarchs. Am. Assoc. Stratigr. Palynol. Found., Dallas, pp. 259-288.

Emerson, S., Bender, M., 1981. Carbon fluxes at the sediment-water interface of the deep-sea: calcium carbonate preservation. J. Mar. Res. 39 (1), 139-162.

Evitt, W.R., 1985. Sporopollenin dinoflagellate cysts, their morphology and interpretation. Am. Assoc. Stratigr. Palynol. Found. Editors, 333 pp.

Eynaud, F., Giraudeau, J., Pichon, J.-J., Pudsey, C.J, 1999. Sea-surface distribution of coccolithophores, diatoms, silicoflagellates and dinoflagellates in the South Atlantic Ocean during the late austral summer 1995. Deep-Sea- Res. I 46, 451-482.

Fahrbach, E., 1993. Zirkulation und Wassermassenbildung im Weddellmeer. Die Geowissenschaften 11, 246-253.

Feldman, G.C. et al., 1989. Ocean color: Availability of the global data set. Eos. Trans. AGU 70, 634-641.

Fensome, R.A., Taylor, F.J.R., Norris, G. Sarjeant, W.A.S., Wharton, D.I., Williams, G.L., 1993. A classification of living and fossil dinoflagellates. Micropaleontol. Spec. Publ. 7, 351 pp.

Ffield, A., Toole, J., Wilson, D., 1997. Seasonal circulation in the South Indian Ocean. Geophys. Res. Letters 24 (22), 2773-2776.

Flores, J.-A., Gersonde, R., Sierro, F.J., 1999. Pleistocene fluctuations in the Agulhas Current Retroflection based on the calcareous plankton record. Mar. Micropaleontol. 37, 1-22.

Frank, M., Gersonde, R., Rutgerd van der Loeff, M., Kuhn, G., Mangini, A., 1996. Late Quaternary sediment dating and quantification of lateral sediment redistribution applying $^{230}Th_{ex}$: a study from the eastern Atlantic sector of the Southern Ocean. Geol. Rundsch. 85, 554-566.

Froneman, P.W., Perissinotto, R., 1996. Microzooplankton grazing and protozooplankton community structure in the South Atlantic and in the Atlantic sector of the Southern Ocean. Deep-Sea Res. I 43, 703-721.

Funkhouser and Evitt, 1959. Preparation techniques for acid-insoluble microfossils. Micropaleontol. 5 (3), 369-375.

Fütterer, D., 1987. The expedition Antarctis-IV/3-4 of the research vessel *Polarstern* in 1985/86. Reports on Polar Research 33, 204 pp.

Fütterer, D., 1988. The expedition Antarctis-VI of the research vessel *Polarstern* in 1987/88. Reports on Polar Research 58, 267 pp.

Gasse, F., 2000. Hydrological changes in the African tropics since the Last Glacial Maximum. Quat. Sci. Rev. 19, 189-211.

Gerhardt, S., Groth, H., Rühlemann, C., Henrich, R., 2000. Aragonite preservation in Late Quaternary sediment cores on the Brazilian continental slope: Implications for intermediate water circulation. Int. Journ. Earth Sci. 88 (4), 607-618.

Gordon, A.L., 1986. Interocean exchange of thermocline water. J. Geophys. Res. 91 (C4), 5037-5046.

Gordon, A.L., Weiss, R.F., Smethie Jr., W.M., Warner, M.J., 1992. Thermocline and intermediate water communication between the South Atlantic and Indian oceans. J. Geophys. Res. 9 (C5), 7223-7240.

Harland, R., Pudsey, C.J., Howe, J.A., FitzPatrick, M.E.J., 1998. Recent dinoflagellate cysts in a transect from the Falkland Trough to the Weddell Sea, Antarctica. Palaeontology 41, 1093-1131.

Harland, R., FitzPatrick, M.E.J., Pudsey, C.J., 1999. Latest Quaternary dinoflagellate cyst climatostratigraphy for three cores from the Falkland Trough, Scotia and Weddell seas, Southern Ocean. Rev. Palaeobot. Palynol. 107, 265-281.

Harland, R., Pudsey, C.J., 1999. Dinoflagellate cysts from sediment traps deployed in the Belligshausen, Weddell and Scotia seas, Antarctica.- Mar. Micropaleontol. 37, 77-99.

Hart, T.J., Currie, R.I., 1960. The Benguela Current. Discovery reports XXXI, 123-298.

Haykin, S., 1983. Nonlinear Methods of Spectral Analysis. Springer-Verlag, Berlin, 2nd Edition.

Head, M., 1996. Modern dinoflagellate cysts and their biological affinities. In: Jansonius, J., McGregor, D.C. (Eds.), Palynology: principles and applications, Vol. 3. Am. Assoc. Stratigr. Palynol. Found., Dallas, TX, pp. 1197-1248.

Hill, M.O., Gauch, H.G.J., 1980. Detrended correspondence analysis: an improved ordination technique. Vegetatio 42, 47-58.

Höll, C., Zonneveld, K.A.F., Willems, H., 1998. On the ecology of calcareous dinoflagellates: The Quaternary eastern Equatorial Atlantic. Mar. Micropaleontol. 33, 1-25.

Höll, C., Karwath, B., Rühlemann, C., Zonneveld, K., Willems, H., 1999. Palaeoenvironmental information gained from calcareous dinoflagellates: The Late Quaternary eastern and western tropical Atlantic in comparison. Palaeogeogr., Palaeoclimatol., Palaeoecol. 146, 147-164.

Höll, C., Kemle-von Mücke, S., 2000. Late Quaternary upwelling variations in the eastern equatorial Atlantic Ocean as inferred from Dinoflagellate cysts, planktonic foraminifera, and organic carbon content. Quat. Res. 54, 58-67.

Holfort, J., Siedler, G., 2001. The meridional oceanic trasport of heat and nutrients in the South Atlantic. J. Phys. Oceanogr. 31, 5-29.

Holliday, N.P., Read, J.F., 1998. Surface oceanic fronts between Africa and Antarctica. Deep-Sea Res. I 45, 217-238.

Houghton, R.W., 1991. The relationship of sea surface temperature to thermocline depth at annual and interannual time scales in the tropical Atlantic. J. Geophys. Res. 96 (C8), 15173-15185.

Howard, W.R., Prell, W.L., 1994. Late Quaternary $CaCO_3$ production and preservation in the Southern Ocean: Implications for oceanic and atmospheric carbon cycling. Paleoceanography 9 (3), 453-482.

Imbrie, J., Boyle, E.A., Clemens, C.S., Duffy, A., Howard, W.R., Kukla, G., Kutzbach, J., Martinson, D.G., McIntyre, A., Mix, A.C., Molfino, B., Morley, J.J., Peterson, L.C., Pisias, N.G., Prell, W.L., Raymon, M.E., Shackleton, N.J., Toggweiler, J.R., 1992. On the structure and origin of major glaciation cycles, 1, Linear response to Milankovitch forcing. Paleoceanography 7(1), 701-738.

Jahnke, R.A., Craven, D.B., Gaillard, J.-F., 1994. The influence of organic matter diagenesis on $CaCO_3$ dissolution at the deep-sea floor. Geochim. Cosmochim. Acta. 58, 2799-2809.

Janofske, D., 1996. Ultrastructure types in Recent "calcispheres". Bull. Inst. océanogr. Monaco 14 (4), 295-303.

Janofske, D., 2000. *Scrippsiella trochoidea* and *Scrippsiella regalis* nov. comb. (Peridiniales, Dinophyceae): A comparison. J. Phycol. 36, 178-189.

Kamptner, E., 1967. Kalkflagellaten-Skelettreste aus Tiefseeschlamm des südatlantischen Ozeans. Ann. Nathist. Mus. Wien 71, 117-198.

Karwath, B., 2000. Ecological studies on living and fossil calcareous dinoflagellates of the equatorial and tropical Atlantic Ocean. Ber. Fachbereich Geowissenschaften, Universität Bremen 152, 175 pp.

Kasten, S., Haese, R.R., Zabel, M., Rühlemann, C., Schulz, H.D., 2001. Barium peaks at glacial terminations in sediments of the equatorial Atlantic Ocean-relicts of deglacial productivity pulses? Chem. Geol. 175, 635-651.

Keil, R.G., Hu, F.S., Tsamakis, E., Hedges, J.I., 1994. Pollen degradation in marine sediments as an indicator of oxidation of organic matter. Nature 369, 639-641.

Kemle-von Mücke, S., 1994. Oberflächenwasserstruktur und -zirkulation des Südostatlantiks im Spätquartär. Ber. Fachbereich Geowissenschaften Uni Bremen 55, 151 pp.

Kerntopf, B., 1997. Dinoflagellate distributin patterns and preservation in the equatorial Atlantic and offshore North-West Africa. Ber. Fachbereich Geowissenschaften, Universität Bremen 103, 137 pp.

Kirst, G.J., Schneider, R.R., Müller, P.J., von Storch, I., Wefer, G., 1999. Late Quaternary temperature variability in the Benguela Current system derived from alkenones. Quat. Res. 52, 92-103.

Klaas, C., 1997. Microprotozooplankton distribution and their potential grazing impact in the Antarctic Circumpolar Current. Deep-Sea Res. II 44 (1-2), 375-393.

Le, J., Shackleton, N.J., 1992. Carbonate dissolution: Fluctuations in the western Equatorial Pacific during the Late Quaternary. Paleoceanography 7 (1), 21-42.

Lemke, P., 1994. The expedition Antarctis-X/4 of the research vessel *Polarstern* in 1992. Rep. Polar Res. 140, 90 pp.

Levitus, S. and Boyer, T.P., 1994a. World Ocean Atlas 1994 Volume 2: Oxygen. NOAA Atlas NESDIS 2. U.S. Department of Commerce, Washington, D.C. 186 pp.

Levitus, S., Boyer, T.P., 1994b. World Ocean Atlas 1994 Volume 4: Temperature. NOAA Atlas NESDIS 4. U.S. Department of Commerce, Washington, D.C. 117 pp.

Levitus, S., Burgett, R., Boyer, T.P., 1994. World Ocean Atlas 1994 Volume 3: Salinity. NOAA Atlas NESDIS 3. U.S. Department of Commerce, Washington, D.C. 99 pp.

Lewis, J., Dodge, J.D., 1987. The cyst-theca relationship of *Protoperidinium americanum* (Gran & Braarud) Balech. J. Micropaleontol 6 (2), 113-121.

Lewis, J., 1991. Cyst-theca relationship in *Scrippsiella* (Dinophyceae) and related orthoperidinoid genera. Botanica Marina 34, 91-106.

Little, M.G., Schneider, R.R., Kroon, D., Price, B., Summerhayes, C.P., Segl, M., 1997a. Trade Wind forcing of upwelling, seasonality, and Heinrich events as a response to sub-Milankovitch climate variability. Paleoceanography 12 (4), 568-576.

Little, M.G., Schneider, R.R., Kroon, D., Price, B., Bickert, T., Wefer, G., 1997b. Rapid palaeoceanographic changes in the Benguela Upwelling System for the last 160,000 years as indicated by abundances of planktonic foraminifera. Palaeogeogr., Palaeoclimatol., Palaeoecol. 130, 135-161.

Loeblich Jr., A.R., Loeblich III, A.R., 1970. Index to the genera, subgenera and sections of the Pyrrhophyta, IV. J. Paleontol. 44, 536-543.

Löscher, B.M., De Baar, H.J.W., De Jong, J.T.M., Veth, C., Dehairs, F., 1997. The distribution of Fe in the Antarctic Circumpolar Current. Deep-Sea Res. II 44 (1-2), 143-187.

Longhurst, A., 1993. Seasonal cooling and blooming in tropical oceans. Deep-Sea Res. 40 (11/12), 2145-2165.

Lototskaya, A., Ziveri, P., Ganssen, G.M., van Hinte, J.E., 1998. Calcareous nannofloral response to Termination II at 45°N, 25°W (northeast Atlantic). Mar. Micropaleontol. 34, 47–70.

Lototskaya, A., Ganssen, G.M., 1999. The structure of Termination II (penultimate deglaciation and Eemian) in the North Atlantic. Quat. Sci. Rev. 18, 1641-1654.

Lutjeharms, J.R.E., Valentine, H.R., 1984. Southern Ocean thermal fronts south of Africa. Deep-Sea Res. 31, 1461-1475.

Lutjeharms, J.R.E., van Ballegooyen, R.C., 1984. Topographic control in the Agulhas Current system. Deep-Sea Res. 31 (11), 1321-1337.

Lutjeharms, J.R.E., 1985. Location of frontal systems between Africa and Antarctica: some preliminary results. Deep-Sea Res. 32, 1499-1509.

Lutjeharms, J.R.E., Stockton, P.L., 1987. Kinematics of the upwelling front off Southern Africa. In: Payne, A.I.L., Gulland, J.A., Brink, K.H. (Eds.), The Benguela and comparable ecosystems. S. Afr. J. Mar. Sci. 5, pp. 35-49.

Lutjeharms, J.R.E., van Ballegooyen, R.C., 1988. The Retroflection of the Agulhas Current. J. Phys. Oceanogr. 18, 1570-1583.

Lutjeharms, J.R.E., 1996. The Exchange of water between the South Indian and South Atlantic oceans. In: Wefer, G., Berger, W.H., Siedler, G., Webb, D.J. (Eds.), The South Atlantic: present and past circulation. Springer, Berlin, Heidelberg, New York, pp. 125-162.

Marret, F., de Vernal, A., 1997. Dinoflagellate cyst distribution in surface sediments of the southern Indian Ocean. Mar. Micropaleontol. 29, 367-392.

Matthiessen, 1995. Distribution patterns of dinoflagellate cysts and other organic-walled microfossils in Recent Norwegian-Greenland Sea sediments. Mar. Micropaleontol. 24, 307-334.

McIntyre, A., Ruddiman, W.F., Karlin, K., Mix, A.C., 1989. Surface water response of the equatorial Atlantic Ocean to orbital forcing. Paleoceanography 4 (1), 19-55.

McIntyre, A, Molfino, B., 1996. Forcing of Atlantic Equatorial and Subpolar millennial cycles by precession, Sciences 274, 1867-1870.

McMinn, A., Sun, X., 1994. Recent dinoflagellate cysts from the Chatham Rise, Southern Ocean, east of New Zealand. Palynology 18, 41-54.

Mix, A.C., Morey, A.E., 1996. Climate feedback and Pleistocene variations in the Atlantic South Equatorial Current. In: Wefer, G., Berger, W.H., Siedler, G., Webb, D.J. (Eds.), The South Atlantic: Present and Past Circulation, Springer-Verlag, Berlin, Heidelberg, pp. 503-525.

Montresor, M., Zingone, A., Marino, D., 1993. The calcareous resting cyst of *Pentapharsodinium tyrrhenicum* comb. nov. (Dinophyceae). J. Phycology 29, 223-230.

Müller, C., 1976. Nannoplankton-Gemeinschaften aus dem Jung-Quartär des Golfes von Aden und des Roten Meeres. Geol. Jb. D 17, 33-77.

Mulitza, S., Wolff, T., Pätzold, J., Hale, W., Wefer, G., 1998a. Temperature sensitivity of planktic foraminifera and its influence on the oxygen isotope record. Mar. Micropaleontol. 33, 223-240.

Mulitza, S., Rühlemann, C., Bickert, T., Hale, W., Pätzold, J., Wefer, G., 1998b. Late Quaternary $\delta^{13}C$ gradients and carbonate accumulation in the western equatorial Atlantic. Earth Planet. Sci. Lett. 155, 237-249.

Niebler, H.-S., Gersonde, R., 1998. A planktic foraminiferal tranfer function for the southern South Atlantic Ocean. Mar. Micropaleontol. 34, 213-234.

Nof, D., Van Gorder, S., 1999. A different perspective on the export of water from the South Atlantic. J. Phys. Oceanogr. 29, 2285-2302.

Orsi, A.H., Nowlin jr., W.D., Whitworth III, T., 1993. On the circulation and stratification of the Weddell Gyre. Deep-Sea Res. I 40 (1), 169-203.

Orsi, A.H., Whitworth III, T., Nowlin jr., W.D., 1995. On the meridional extend and fronts of the Antarctic Circumpolar Current. Deep-Sea Res. I 42 (5), 641-673.

Orsi, A.H., Johnson, G.C., Bullister, J.L., 1999. Circulation, mixing, and production of Antarctic Bottom Water. Progr. Oceanogr. 43, 55-109.

Ou, H.W., de Ruijter, W.P.M., 1986. Separation of an inertial boundary current from a curved coastline. J. Phys. Oceanogr. 16, 280-289.

Partridge, T.C., deMenocal, P.B., Lorentz, S.A., Paikers, M.J., Vogel, J.C., 1997. Orbital forcing of climate over South Africa: a 200,000-year rainfall record from the Pretoria Saltpan. Quat. Sci. Rev. 16, 1125-1133.

Peterson, R.G., Stramma, L., 1991. Upper-level circulation in the South Atlantic Ocean. Progr. Oceanogr. 26, 1-73.

Pether, J., 1994. Molluscan evidence for enhanced deglacial advection of Agulhas water in the Benguela Current, off southwest Africa. Palaeogeogr., Palaeoclimatol., Palaeoecol. 111, 99-117.

Pfiester, L.A., Anderson, D.M., 1987. Dinoflagellate reproduction. In: Taylor, F.J.R. (Ed.), The biology of dinoflagellates. Botanical Monographs 21, Blackwell Scientific Publications, Oxford, 611-648 pp.

Prahl, F.G., De Lange, G.J., Scholten, S. Cowie, G.L., 1997. A case of post-depositional aerobic degradation of terrestrial organic matter in turbidite deposits from the Madeira Abyssal Plain. Org. Geochem. 27 (3-4), 141-152.

Prell, W.L., Hutson, W.H., Williams, D.F., Bé, A.W.H., Geitzenauer, K., Molfino, B., 1980. Surface Circulation of the Indian Ocean during the Last Glacial Maximum, approximately 18,000 yr B.P. Quat. Res. 14, 309-336.

Pudsey, C.J., 1992. Late Quaternary changes in Antarctic Bottom Water velocity inferred from sediment grain size in the northern Weddell Sea. Mar. Geology 107, 9-33.

Rahmstorf, S., 1996. On the freshwater forcing and transport of the Atlantic thermohaline circualtion. Climate Dyn. 12, 799-811.

Reid, P.C., 1977. Peridiniacean and Glenodiniacean dinoflagellate cysts from the British Isles. Nova Hedwigia 29, 429-463.

Reid, J.L., 1989. On the total geostrophic circulation of the South Atlantic Ocean: Flow patterns, tracers, and transport. Progr. Oceanogr. 23, 149-244.

Rial, J.A., Anaclerion, C.A., 2000. Understanding nonlinear responses of the climate system to orbital forcing. Quat. Sci. Rev. 19, 1709-1722.

Rintoul, S.R., 1991. South Atlantic interbasin exchange. J. Geophys. Res. 96 (C2), 2675-2692.

Rochon, A., de Vernal, A., Turon, J.-L., Matthiessen, J., Head, M., 1999. Distribution of dinoflagellate cyst assemblages in surface sediments from the North Atlantic Ocean and adjacent basins and quantitative reconstruction of sea-surface parameters., Am. Assoc. Stratigr. Palynol Spec. Contr. Series. 35, 146 pp.

Rühlemann, C., 1996. Akkumulation von Carbonat und organischem Kohlenstoff im tropischen Atlantik: Spätquartäre Produktivitäts-Variationen und ihre Steuerungsmechanismen. Ber. Fachbereich Geowissenschaften Uni Bremen 84, 139 pp.

Rühlemann, C., Frank, M., Hale, W., Mangini, A., Mulitza, S., Müller, P.J., Wefer, G., 1996. Late Quaternary productivity changes in the western equatorial Atlantic: Evindence from ^{230}Th-normalized carbonate and organic carbon accumulation rates.

Rühlemann, C., Diekmann, S., Mulitza, S., Frank, M., in press. Late Quaternary changes of western equatorial Atlantic surface circulation and Amazon lowland climate recorded in Ceará Rise deep sea sediments, Paleoceanography.

Schmidt, H., 1992. Der Benguela-Strom im Bereich des Walfischrückens im Spätquartär. Ber. Fachbereich Geowissenschaften Uni Bremen 28, 172 pp.

Schmiedl, G., Mackensen, A., 1997. Late Quaternary paleoproductivity and deep water circulation in the eastern South Altantic Ocean: evidence from benthic foraminifera. Palaeogeogr., Palaeoclimatol., Palaeoecol. 130, 43-80.

Schneider, R.R., 1991. Spätquartäre Produktivitätsänderungen im östlichen Angola-Becken: Reaktion auf Variationen im Passat-Monsun-Windsystem und in der Advektion des Benguela-Küstenstroms. Ber. Fachbereich Geowissenschaften, Universität Bremen 21, 198 pp.

Schneider, R.R., Müller, P.J., Ruhland, G., 1995. Late Quaternary surface circulation in the east equatorial South Atlantic: Evidence from alkenone sea surface temperatures. Paleoceanography 10, 197-220.

Schneider, R.R., Müller, P.J., Ruhland, G., Meinecke, G., Schmidt, H., Wefer, G., 1996. Late Quaternary surface temperatures and productivity in the east-equatorial South Atlantic: Response to changes in trade/monsoon wind forcing and surface water advection. In: Wefer, G., Berger, W.H., Siedler, G., Webb, D.J. (Eds.), The South Atlantic: Present and Past Circulation, Springer-Verlag, Berlin, Heidelberg, pp. 527-551.

Schneider, R.R., Müller, P.J., Acheson, R., 1999. Atlantic alkenone sea-surface temperature records. In: Abrantes, F., Mix, A.C. (Eds.), Reconstructing ocean history: A windows into the future, Kluwer Academic, New York, pp. 33-55.

Schulz, H.D., Beese, D., Breitzke, M., Brück, L., Brügger, B., Dahmke, A., Dehning, K., Diekamp, V., Donner, B., Ehrhardt, I., Gerlach, H., Giese, M., Glud, R., Gumprecht, R., Gundersen, J., Henning, R., Hinrichs, S., Petermann, H., Richter, M., Sagemann, J., Schmidt, W., Schneider, R., Scholz, M., Segl, M., Werner, U., Zabel, M., 1992. Bericht und erste Ergebnisse über die Meteor-Fahrt M20/2 Abidjan–Dakar, 27.12.1991–3.2.1992. Ber. Fachbereich Geowissenschaften Uni Bremen 25, 173 pp.

Schumann, E.H., Cohen, A.L., Jury, M.R., 1995. Coastal sea surface temperature variability along the south coast of South Africa and the relationship to regional and global climate. J. Mar. Res., 231-248.

Sea Ice Climatic Atlas, 1985. Vol. 1, Antarctic. Prepared by Naval Oceanography Command Detachment, Asheville, NSTL, 131 pp.

Shannon, L.V., 1985. The Benguela Ecosystem Part I. Evolution of the Benguela, physical features and processes. Oceanogr. Mar. Biol. Ann. Rev. 23, 105-182.

Spieß, V., Abelmann, A., Bickert, T., Brehme, I., Coordes, R., Dehning, K., Dobeneck, T. v., Donner, B., Erhardt, I., Giese, M., Grigel, J., Haese, R., Hale, W., Hinrichs, S., Kasten, S., Laier, P., Oliveira, M. de, Rapp, R., Rogers, J., Petermann, H., Richter, M., Schmidt, A., Scholz, M., Skowronek, F., Zabel, M., 1994. Report and preliminary results of METEOR cruise M23/1 Capetown - Rio de Jeneiro, 4.2.1993 - 25.2.1993. Ber. Fachbereich Geowissenschaften Uni. Bremen 42, 139 pp.

Stramma, L., England, M., 1999. On the water masses and mean circulation of the South Atlantic Ocean. J. Geophys. Res. 104 (C9), 20863-20883.

Stramma, L., Schott, F., 1999. The mean flow field of the tropical Atlantic Ocean. Deep-sea Res. II 46, 279-303.

Tangen, K., Brand, L.E., Blackwelder, P.L., Guillard, R.R., 1982. *Thoracosphaera heimii* (Lohmann) KAMPTNER is a dinophyte: observations on its morphology and life cycle. Mar. Micropaleontol. 7, 193-212.

Taylor, F.J.R., 1987. General group characteristics; special features of interest; short history of dinoflagellate study. In: Taylor, F.J.R. (Ed.), The biology of dinoflagellates. Botanical Monographs 21, Blackwell Scientific Publications, Oxford, 1-23 pp.

Taylor, F.J.R., Pollingher, U., 1987. Ecology of dinoflagellates. In: Taylor, F.J.R. (Ed.), The biology of dinoflagellates. Botanical Monographs 21, Blackwell Scientific Publications, Oxford, 399-502 pp.

Ter Braak, C.J.F., Smilauer, P. (Eds.), 1998. Canoco 4. Centre for Biometry, Wageningen, 351 pp.

Toggweiler, J.R., Samuels, B., 1995. Effect of Drake Passage on the global thermohaline circulation. Deep-Sea Res. I 42 (4), 477-500.

Ufkes, E., Jansen, J.H.F., Brummer, G.-J., 1998. Living planktonic foraminifera in the eastern South Atlantic during spring: indicators of water masses, upwelling and the Congo (Zaire) River plume. Mar. Micropaleontol. 33, 27-53.

Ufkes, E., Jansen, J.H.F., Schneider, R.R., 2000. Anomalous occurrences of *Neogloboquadrina pachyderma* (left) in a 420-ky upwelling record from Walvis Ridge (SE Atlantic). Mar. Micropaleontol. 40, 23-42.

Versteegh, G.J.M., 1993. New Pliocene and Pleistocene calcareous dinoflagellate cysts from southern Italy and Crete. Rev. Palaeobot. Palynol. 78, 353-380.

Versteegh, G.J.M., 1994. Recognition of cyclic and non-cyclic environmental changes in the Mediterranean Pliocene: a palynological approach, Mar. Micropaleontol. 23 (2), 147-183.

Versteegh, G.J.M., Zonneveld, K.A.F., 1994. Determination of (palaeo-)ecological preferences of dinoflagellates by applying Detrended and Canonical Correspondence analysis to Late Pliocene dinoflagellate cyst assemblages of the south Italian Singa section. Rev. Palaeobot. Palynol. 84, 181-199.

Versteegh, G.J.M., Zevenboom, D., 1995. New genera and species of dinoflagellate cysts from the Mediterranean Neogene. Rev. Palaeobot. Palynol. 85, 213-229.

Versteegh, G.J.M., 1997. The onset of major Northern Hemisphere glaciations and their impact on dinoflagellate cysts and acritarchs from the Singa section, Calabria (southern Italy) and DSDP Holes 607/607A (North Atlantic). Mar. Micropaleontol. 30 (4), 319-343.

Vink, A., 2000. Reconstruction of Recent and Late Quaternary surface water masses of the western subtropical Atlantic Ocean based on calcareous and organic-walled dinoflagellate cysts. Ber. Fachbereich Geowissenschaften, Universität Bremen 159, 160 pp.

Vink, A., Zonneveld, K.A.F., Willems, H., 2000. Distribution of calcareous dinoflagellate cysts in surface sediments of the western equatorial Atlantic Ocean, and their potential use in palaeoceanography. Mar. Micropaleontol. 38, 149-180.

Vink, A., Zonneveld, K.A.F., Willems, H., 2001. Organic-walled dinoflagellate cysts in western equatorial Atlantic surface sediments: distributions and their relation to environment. Rev. Palaeobot. Palynol. 112, 247-286.

Vink, A., Rühlemann, C., Zonneveld, K.A.F., Mulitza, S., Hüls, M., Willems, H., in press. Shifts in the position of the North Equatorial Current and rapid changes in the western subtropical Atlantic during the Last Glacial. Paleoceanography.

von Dobeneck, T., Schmieder, F., 1999. Using rock magnetic proxy records for orbital tuning and extended time series analyses into the super- and sub-Milankovitch bands. In: Fischer, G., Wefer, G. (Eds.), Use of proxies in paleoceanography: Examples from the South Atlantic, Springer-Verlag, Berlin, Heidelberg, pp. 6001-633.

Wall, D., Dale, B., 1968. Quaternary calcareous dinoflagellates (Calciodinellideae) and their natural affinities. J. Paleontol. 42 (6), 1395-1408.

Wall, D., Dale, B., 1973. Paleosalinity relationships of dinoflagellates in the Late Quaternary of the Black Sea - a summary. Geoscience and Man 7, 95-102.

Wall, D., Dale, B., Lohmann, G.P., Smith, W.K., 1977. The environmental and climatic distribution of dinoflagellate cysts in Modern marine sediments from regions in the North and South Atlantic Oceans and adjacent seas. Mar. Micropalaeontol. 2: 121-200.

Weeks, S.J., Shillington, F.A., 1994. Interannual scales of variation of pigment concentrations from coastal zone color scanner data in the Benguela upwelling system and the Subtropical Convergence Zone south of Africa. J. Geophys. Res. 99 (C4), 7385-7399.

Wefer, G., Bleil, U., Schulz, H.D., Berger, W.H., Bickert, T., Brück, L., Claussen, U., Dahmke, A., Dehning, K., Djigo, Y.H., Hinrichs, S., Kothe, C., Krämer, M., Lücke, A., Mathias, S., Meinecke, G., Oberhänsli, H., Pätzold, J., Pflaumann, U., Probst, U., Reimann, A., Rostek, F., Schmidt, H., Schneider, R.R., Soltwedel, T., Spieß, V., 1989. Bericht über die METEOR-Fahrt M 9-4: Dakar-Santa Cruz, 19.2.1989-16.3.1989. Ber. Fachbereich Geowissenschaften Uni Bremen 7, 103 pp.

Wefer, G., Andersen, N., Bleil, U., Breitzke, M., Dehning, K., Fischer, G., Kothe, C., Meinecke, G., Müller, P.J., Rostek, F., Sagemann, J., Scholz, M., Segl, M., Thiessen, W., 1990. Bericht über die METEOR-Fahrt 12/1, Kapstadt - Funchal, 13.3.1990-14.4.1990. Ber. Fachbereich Geowissenschaften Uni Bremen 11, 66 pp.

Wefer, G., Beese, D., Berger, W.H., Buschhoff, H., Cepek, M., Diekamp, V., Fischer, G., Holmes, E., Kemle-von Mücke, S., Kerntopf, B., Lange, C., Mulitza, S., Otto, S., Plugge, R., Ratmeyer, V., Rühlemann, C., Schmidt, W., Schwarze, M., Wallmann, K., Zabel, M., 1994. Report and preliminary results of the METEOR-Cruise M 23/3: Recife-Las Palmas, 21.3-12.4.93. Ber. Fachbereich Geowissenschaften Uni Bremen 44, 71 pp.

Wefer, G., Berger, W.H., Bickert, T., Donner, B., Fischer, G., Kemle-von Mücke, S., Meinecke, G., Müller, P.J., Mulitza, S., Niebler, H.-S., Pätzold, J., Schmidt, H., Schneider, R.R., Segl, M., 1996a. Late Quaternary surface circulation of the South Atlantic: The stable isotope record and implications for heat transport and productivity. In: Wefer, G., Berger, W.H., Siedler, G., Webb, D.J. (Eds.), The South Atlantic: Present and Past Circulation, Springer-Verlag, Berlin, Heidelberg, pp. 461-502.

Wefer, G., Buschhoff, H., Carlsen, D., Dittert, N., Eggerichs, G., Flechsenhar, K., Giese, M., Gingele, F., Grieger, B., Henning, R., Klump, J., Kuhnert, H., Lamy, F., Laser, B., Meyer, A., Niewöhner, C., Ochsenhirt, W.-T., Pinck, A., Schmidt, A., Schmieder, F., Scholz, M., Schweinsber, S., Steinmetz, E., Vanicek, M., Willems, H., Wolff, T., Zenk, W., 1996b. Report and preliminary results of METEOR-Cruise M 34/3: Walvisbay-Recife, 21.02.-17.03.1996. Ber. Fachbereich Geowissenschaften Uni Bremen 79, 168 pp.

Wiebinga, C.J., de Baar, H.J.W., 1998. Determination of the distribution of dissolved organic carbon in the Indian sector of the Southern Ocean. Mar. Chem. 61, 185-201.

Williams, G.L., Lentin, J.K., Fensome, R.A.F., 1998. The Lentin and Williams index of fossil dinoflagellates: 1998 edition. Am. Assoc. Stratigr. Palynol. Contr. Series 34, 817 pp.

Winter, A., Martin, K., 1990. Late Quaternary history of the Agulhas Current. Paleoceanography 5 (4), 479-486.

Yiou, P., Ghil, M., Jouzel, J., Paillard, D., Vautard, R., 1994. Nonlinear variability of the climatic system from singular and power spectra of Late Quaternary records. Clim. Dynam. 9, 371-389.

Zielinski, U., Gersonde, R., 1997. Diatom distribution in Southern Ocean surface sediments (Atlantic sector): Implications for paleoenvironmental reconstructions. Palaeogeogr., Palaeoclimatol., Palaeoecol. 129, 213-250.

Zielinski, U., Gersonde, R., Sieger, R., Fütterer, D., 1998. Quaternary surface water temperature estimations: Calibration of a diatom transfer function for the Southern Ocean. Paleoceanography 13 (4), 365-383.

Zonneveld, K.A.F., 1997. New species of organic walled dinoflagellate cysts from modern sediments of the Arabian Sea (Indian Ocean). Rev. Palaeobot. Palynol. 97, 319-337.

Zonneveld, K.A.F., Versteegh, G.J.M., De Lange, G.J., 1997. Preservation of organic-walled dinoflagellate cysts in different oxygen regimes: a 10.000 year natural experiment. Mar. Micropaleontol. 29, 393-405.

Zonneveld, K.A.F., Höll, C., Karwath, B., Janofske, D., Kerntopf, B., Willems, H., 1999. Calcareous resting cysts as paleo-environmental tools. In: Fischer, G., Wefer, G. (Eds.), Use of proxies in

paleoceanography: Examples from the South Atlantic, Springer Verlag, Berlin, Heidelberg, pp. 145-164.

Zonneveld, K.A.F., Brune, A., Willems, H., 2000. Spatial distribution of calcareous dinoflagellate cysts in surface sediments of the Atlantic Ocean between 13°N and 36°S. Rev. Palaeobot. Palynol. 111, 197-223.

Zonneveld, K.A. F., Hoek, R.P., Brinkhuis, H., Willems, H., 2001. Geographical distributions of organic-walled dinoflagellate cysts in surficial sediments of the Benguela upwelling region and their relationship to upper ocean conditions. Progr. Oceanogr. 48, 25-72.

Zonneveld, K.A.F., Versteegh, G.J.M., de Lange, G.J., in press. Palaeo-productivity and post-depostional aerobic organic matter decay reflected by Eastern Mediterranean dinoflagellate cysts assemblages. Mar. Geol.